Chapter 14: Climate Phenomena and their Relevance for Future Regional Climate Change

Coordinating Lead Authors: Jens Hesselbjerg Christensen (Denmark), Kanikicharla Krishna Kumar (India)

Lead Authors: Edvin Aldrian (Indonesia), Soon-Il An (Korea), Iracema Cavalcanti (Brazil), Manuel de Castro (Spain), Wenjie Dong (China), Prashant Goswami (India), Alex Hall (USA), Joseph Katongo Kanyanga (Zambia), Akio Kitoh (Japan), James Kossin (USA), Ngar-Cheung Lau (USA), James Renwick (New Zealand), David Stephenson (UK), Shang-Ping Xie (USA), Tianjun Zhou (China)

Contributing Authors: Tercio Ambrizzi, Mark Baldwin, Michela Biasutti, Josephine Brown, Ping Chang, Clara Deser, David Enfield, Alessandra Giannini, Ashok Karumuri, Jeff Knight, Thomas Knutson, Ashwini Kulkarni,Victor Magnana, Gareth Marshall, Jan Polcher, Yun Qian, Izuru Takayabu, John Turner, Caroline Ummenhofer, Bin Wang, Chunzai Wang, Matthew Widlansky, Tim Woollings, Chidong Zhang

Review Editors: John Fyfe (Canada), Won-Tae Kwon (Korea), Kevin Trenberth (USA), David Wratt (New Zealand)

Date of Draft: 16 December 2011

Notes: TSU Compiled Version

Table of Contents

Executive Summary

[PLACEHOLDER FOR SECOND ORDER DRAFT: text from the Executive Summary of Chapter 11, WGI AR4 Second Order Draft; to be updated.]

[The climate phenomena and their relevance for regional climate change projections presented here are primarily based on four information sources (although not of equal weight in each region): global atmosphere-ocean climate models; downscaling techniques used to enhance regional detail; our level of physical understanding of the factors controlling regional responses; and recent climate change.

Global climate models remain the primary source of regional information on the range of possible future climates. Although some model deficiencies persist, a clearer picture of the robust aspects of regional climate change is emerging due to steady improvement in model resolution, the simulation of processes of importance for regional change, and the expanding set of model results available. Despite the progress, many aspects of regional climate change will remain uncertain as not all aspects of natural variability can be directly accounted for by a well-understood phenomenon as they are depicted in this chapter.

Methods to achieve regional details in projections have further matured since the IPCC WGI Fourth Assessment Report (IPCC, 2007b) and have been more widely applied. Research on the co-ordinated multi-model downscaling studies still lags that of equivalent GCM studies, and it remains an ongoing activity to develop probabilistic information on the distribution of possible climate responses and the sources of uncertainty, including the sensitivity to the global model input.

The growing insight into key physical processes that underlie regional climate responses and their representation in models increases confidence in the robust aspects of the model projections. A number of important themes have emerged:

- Warming generally increases precipitation gradients, and contributes to a reduction of rainfall in the subtropics and an increase in higher latitudes. Regions of large uncertainty in the precipitation response are often associated with boundaries between regions of robust increases and decreases, as there is little agreement between models on the accurate location of these boundaries.
- The poleward expansion of the subtropical highs, combined with the general tendency towards subtropical reduction in precipitation, creates especially robust projections of a reduction in precipitation on the poleward edges of the subtropics. Most of the regional projections of reductions in precipitation in the 21st century are associated with the land areas adjacent to these subtropical highs.
- Monsoonal circulations tend to weaken and yet result in increased precipitation, while the pattern of warming over the tropical oceans exerts strong control on precipitation changes within the tropics.

Previous chapters describe observed climate change on regional scales (Chapter 2) and compare model simulations with these changes (Chapter 11 and 12). In general, these comparisons are more useful for temperature than for precipitation, due to the smaller signal to noise ratio for the latter. For precipitation change there is a greater dependency on assessing model convergence in both global and downscaling models along with physical insights. Where there is lack of model convergence, further research into sources of model deficiencies is clearly needed before any robust conclusions can be reached. This lack of convergence especially in the tropics is highlighted, as the impacts of climate change may be large. Where there is near unanimity among models with good supporting physical arguments, as is typically the case for middle and higher latitudes, these factors encourage strong statements as to the likelihood of a regional climate change. However, these must be carefully weighed against the small sample of models, the lack of true independence among the models, and the absence, in many cases, of clear observational verification that this change is already occurring.]

The summary likelihood statements on projected change in climate phenomena are as follows:

Monsoon Systems

- Global monsoon precipitation is *likely* to strengthen in the 21st century with increase in its area affected and its intensity, while the monsoon circulation weakens. (Section 14.2.2)

Patterns of Tropical Convection

- Rainfall change over tropical oceans follows a 'warmer-get-wetter' pattern, increasing where the SST warming exceeds the tropical mean, and vice versa. (Section 14.2.3)
- Inter-hemispheric asymmetry in warming, such as that due to preferential cooling of the Northern Hemisphere under the influence of anthropogenic sulfate emissions, can affect the north-south SST gradients and the future behavior of ITCZ. (Section 14.2.3)
- The rainfall amount within the SPCZ and the area of the SPCZ are projected to increase. However, the eastern edge of the SPCZ region may experience reduced rainfall. (Section 14.2.3)
- Indications of the SACZ displacement southwards have been obtained in projections of future climate change. The future projections indicate increase of Sea Level Pressure at middle latitudes, as the Atlantic Subtropical High is displaced polewards, behavior that can be related to the positive trend of the AAO index and poleward shifting of the storm tracks (Section 14.2.3).

Northern Hemisphere Dipole Modes:
- There is robust evidence from climate model projections that increased greenhouse gas emissions will lead to a small positive trend in NAO. (Section 14.2.9)
- The amplitudes of the mean change in NAO vary substantially between climate model projections but these are generally small compared to natural year-to-year variations in NAO. (Section 14.2.9)
- There is growing evidence that the projected NAO trend is not the dominant cause of regional climate change in wintertime surface temperature over Europe and the Arctic. (Section 14.2.9)
- The NPO impacts winter air temperature and precipitation over much of western North America as well as Arctic sea ice in the Pacific sector. Climate model projections indicate no significant changes in the spatial or temporal characteristics of the NPO under greenhouse warming. However, the sensitivity of the NPO to tropical Pacific SST changes may be underestimated in the models, leading to uncertainty in the future NPO state. (14.2.9)

Tropical Pacific Mode
- Tropical Pacific atmospheric circulation of the twentieth century is *likely* to be weakening, while the different reconstructions of SST observation do not agree in the change in the east-west contrast of equatorial Pacific SST. The model projections broadly agree in more warming over tropical oceans than in the subtropics, owing to the difference in evaporative cooling but not in the change in the equatorial Pacific SST gradient. For this reason, it is hard to say whether El Nino is going to intensify or weaken. (Section 14.2.5)

Indian Ocean Mode
- The sea surface temperature warming is *likely* to be locally reduced over the eastern equatorial Indian Ocean during July-November, with decreased rainfall near Indonesia. The Indian Ocean dipole mode of interannual variability is *likely* to remain unchanged in amplitude but the negative skew of SST variability off Indonesia may weaken. The Indian Ocean response to ENSO may persist longer in time, strengthening ENSO's influence on summer rainfall and tropical cyclone activity over the Northwest Pacific and East Asia. (Section 14.2.6)

Tropical Atlantic Patterns
- The observed SST warming in the tropical Atlantic represents a reduction in spatial variations in climatology: the warming is weaker north than south of the equator; and the equatorial cold tongue weakens both in the mean and interannual variability. The *confidence* of the projections over the tropical Atlantic - both for the mean and interannual modes - *is low* because of large errors in model simulations of current climate. (Section 14.2.7)

Southern Annular Mode
- The observed trend toward a positive SAM phase is *likely* to continue in projections of 21st Century under further increases in greenhouse gases, but is *likely* to be counteracted by the recovery of stratospheric ozone, especially in southern summer. (Section 14.2.10)

Tropical Cyclone Extract
- Detection and attribution of trends as well as agreement among numerical simulations is compromised when the scale of focus is reduced from global to regional, but the influence of past and future climate change on tropical cyclones is *likely* to vary by region. Given the uncertainty of the homogeneity of

historic regional tropical cyclone records, there is *low confidence* in the fidelity of any reported regional trends in tropical cyclone activity on multidecadal timescales or greater. While projections under 21st century greenhouse warming indicate that it is *likely* that the global frequency of tropical cyclones will either decrease or remain essentially unchanged, concurrent with a *likely* increase in both global mean tropical cyclone maximum wind speed and rainfall rates, there is *lower confidence* in region-specific projections of frequency and intensity. Still, based on high-resolution modeling studies, the frequency of the most intense storms will *more likely than not* increase substantially in some basins under projected 21st century warming. (Box 14.3)

Extra Tropical Storms

- In the global average, changes in storm activity will *likely* be small compared to interannual variability. Some regional changes in activity can be of a comparable size to interannual variability, but there remains *little confidence* in these changes. It is *likely* that the storm track in the southern hemisphere will shift poleward in response to further anthropogenic forcing. According to current projections it is *more likely than not* that the North Pacific storm track will also shift polewards. The projections do not agree on a clear storm track shift in the North Atlantic, where there is *little confidence* in current models. Projected changes in cyclone intensity are weak, with *low to medium confidence*. (Box 14.4)

Summary likelihood statements on projected change in regional specific climate

Arctic

- The future evolution of temperature and sea ice in the Arctic on decadal time scales and longer will *very likely c*ontinue to be dominated by the signals of anthropogenic climate change. (Section 14.3.2)

North America

- Climate change in N America will *likely* be characterized by a loss of snowpack at high elevations, mid-continental summertime drying, and increasing precipitation over the northern third of the continent. (Section 14.3.3)

South America

- Precipitation increase over southeastern South America is *likely* as being inferred from multiple model simulations. Higher frequency of LLJ in future model projections is associated with increased moist flux from the Amazon Basin to the La Plata Basin, consistent with the precipitation increase in the southern regions. (Section 14.3.5).
- It is *likely* there will be an increase in extreme precipitation over La Plata basin region and decrease in central Amazonia and northern SA coast, as well as in number of extremes is projected for the last thirty years of 21st century. Number of consecutive dry days is *likely* to increase in Northeastern South America. (Section 14.3.5)

Europe

- It is *likely* that the intensity of precipitation in Northern Europe depend on the strength of the zonal flow. Hence, an increase in NAO is *likely* to increase both the number of wintertime storms heading into N. Europe and also increases the average intensity of precipitation per storm (Section 14.3.6)
- The patterns of projected precipitation change in summer season are coincident in all of the current climate model projections supporting with *moderate* to *high confidence* that a significant rainfall decrease across the entire Mediterranean region is *likely.* (Section 14.3.6)

Eastern Asia

- It is *very likely* that the termination of rainy season over Japan (Baiu) will delay, associated with El Niño-like tropical changes. (Section 14.3.9)

Southern Asia

- Indian Monson circulation is *likely* to weaken while the seasonal precipitation is *likely* to increase. There is also evidence from the observations and projections that the intensity of rain events is *likely* to increase while the number of rainy days during the monsoon season is expected to decrease. (Section 14.3.10)

Australia New Zealand

- A drying trend is *likely* to continue over southern Australia through the 21st century, and is *likely* to become evident over the north and east of New Zealand. Precipitation is *likely* to increase in the west of New Zealand in winter and spring. (Section 14.3.12)

Antarctica

- Total sea ice extent in the Antarctic has been increasing slowly in recent decades, but the trend is *likely* to reverse over coming decades, as continued warming comes to dominate the effects of increasing westerly winds over the southern oceans. (Section 14.3.13)

14.1 Introduction

Regional climates, including their mean state and variability, are the complex result of both local physical processes, and the non-local response to large-scale processes such as ENSO and other dominant modes of variability. This chapter will assess future regional climate change in the context of such processes by considering changes in *local phenomena* (e.g., convergence zones, jets, storm tracks, etc.) and *large-scale phenomena* described by well-known modes of variability. These phenomena determine regional climate by controlling the local energy and moisture balance in a region.

For example, the major monsoon systems where the movement of convergence zones over land leads to profound changes in local hydrological cycles. Monsoon systems are large-scale seasonal land-sea interaction phenomena that affect the lives and wellbeing of billions of people particularly in Asia, Africa, Australia, and the Americas. This chapter assesses current understanding of monsoonal behaviour in the present and future climate, how monsoon characteristics are influenced by the large-scale tropical modes of variability and their potential changes, and how the monsoons in turn affect regional extremes.

Specific modal phenomena of interest include the large-scale tropical "modes" of variability, such as ENSO, modes of variability affecting the mid-latitudes that are influenced by tropical variability, such as the PNA, and those that represent mid- and high-latitude dynamical variability, such as the NAO and the annular modes. We focus primarily on future changes in dominant modes known to be relevant for regional climate for which there is understanding of the underlying physical mechanisms.

Section 14.2 sets the scene by assessing recent climate research on monsoons, dominant modes of variability, and other phenomena known to be important for regional climate. Section 14.3 then uses these phenomena to interpret projected regional changes for regions defined in previous regional climate change assessments (IPCC, 2007a, 2007b). Unlike the regional assessment in AR4 (Christensen et al., 2007), this chapter will not provide assessed information about the detailed projected change at the regional scale, nor on the general quality of the methods used for providing down scaled regional information. For detailed spatial information on changes, we refer to the maps presented in the Atlas (Annex I).

14.1.2 Summary of Projections of Climate Phenomena in AR4

The assessment of regional climate projections in the Fourth Assessment Report (IPCC, 2007b) was largely restricted to General Circulation Model (GCM)-derived temperature with some limited precipitation statements and concentrated on a systematic assessment region by region. The present chapter is introducing a new way to assess regional climate changes as summarized above. Although little direct information was provided in AR4 about the role in controlling future regional climates, the information about the projected changes in climate phenomena themselves were assessed in Chapter 10 in AR4. In brief, the findings can be summarized as follows:

Mean Tropical Pacific Climate Change: Multi-model averages show a weak shift towards average background conditions which may be described as 'El Niño-like', with sea surface temperatures in the central and east equatorial Pacific warming more than those in the west, weakened tropical circulations and an eastward shift in mean precipitation.

El Niño: All models show continued El Niño-Southern Oscillation (ENSO) interannual variability in the future no matter what the change in average background conditions, but changes in ENSO interannual variability differ from model to model. Based on various assessments of the current multi-model data set, in which present-day El Niño events are now much better simulated than in the TAR, there is no consistent indication at this time of discernible changes in projected ENSO amplitude or frequency in the 21st century.

Monsoons: An increase in precipitation is projected in the Asian monsoon (along with an increase in interannual season-averaged precipitation variability) and the southern part of the west African monsoon with some decrease in the Sahel in northern summer, as well as an increase in the Australian monsoon in southern summer in a warmer climate. The monsoonal precipitation in Mexico and Central America is projected to decrease in association with increasing precipitation over the eastern equatorial Pacific through Walker Circulation and local Hadley Circulation changes. However, the uncertain role of aerosols in general, and carbon aerosols in particular, complicates the nature of future projections of monsoon precipitation, particularly in the Asian monsoon.

Sea Level Pressure: Sea level pressure is projected to increase over the subtropics and mid-latitudes, and decrease over high latitudes (order several millibars by the end of the 21st century) associated with a poleward expansion and weakening of the Hadley Circulation and a poleward shift of the storm tracks of several degrees latitude with a consequent increase in cyclonic circulation patterns over the high-latitude arctic and Antarctic regions. Thus, there is a projected positive trend of the Northern Annular Mode (NAM) and the closely related North Atlantic Oscillation (NAO) as well as the Southern Annular Mode (SAM). There is considerable spread among the models for the NAO, but the magnitude of the increase for the SAM is generally more consistent across models.

Tropical Cyclones (Hurricanes and Typhoons): Results from embedded high-resolution models and global models, ranging in grid spacing from 100 km to 9 km, project a likely increase of peak wind intensities and notably, where analysed, increased near-storm precipitation in future tropical cyclones. Most recent published modelling studies investigating tropical storm frequency simulate a decrease in the overall number of storms, though there is less confidence in these projections and in the projected decrease of relatively weak storms in most basins, with an increase in the numbers of the most intense tropical cyclones.
Mid-latitude Storms: Model projections show fewer mid-latitude storms averaged over each hemisphere, associated with the poleward shift of the storm tracks that is particularly notable in the Southern Hemisphere, with lower central pressures for these poleward shifted storms. The increased wind speeds result in more extreme wave heights in those regions.

[START BOX 14.1 HERE]

Box 14.1: What do we mean by Teleconnections, Modes of Variability, and Regimes?

This box defines key concepts used in climate science to describe the dominant spatio-temporal structure in a climate variable y(s,t) defined at different spatial locations s and times t.

Climate index
A univariate time series x(t) constructed from climate variables that provides an aggregate summary of the state of the climate system. For example, the difference between sea-level pressure in Iceland and the Azores provides one possible NAO index.

Climate pattern
A set of coefficients b(s) that depend on spatial location s obtained by "projection" of climate variables y(s,t) onto a *climate index* time series x(t). The projection is most easily done by linear regression (Baldwin et al., 2009).

Teleconnection
A statistical association between climate variables at widely separated spatial locations (i.e., further apart than the typical spatial decorrelation distance). Teleconnections are associations created by large-scale structures such as basin-wide coupled modes of ocean-atmosphere variability, Rossby wave-trains, mid-latitude jets and storm-tracks, etc.

Teleconnection pattern
Teleconnection patterns are *climate patterns* constructed by plotting a spatial map of correlations between variables at different spatial locations s and a variable at a given location s_0. In other words, the regression of y'(s,t) on index y'(s_0,t) where y'(s,t) is y(s,t) standardised to have zero mean and unit variance at each location.

Climate mode of variability
Underlying space-time structures with preferred spatial and temporal scales that can account for the main features of variability and *teleconnections* in climate variables at widely separated locations. Climate modes are generally assumed to be the product b(s)x(t) of a constant *climate pattern* b(s) and a *climate index* x(t)

that has zero time mean. The *climate* pattern b(s) can be obtained by regression of climate variables on a known index x(t) (e.g., the NAO spatial pattern defined using the Iceland and Azores sea-level pressure index). *Principal components* are often used to find the index that accounts for the most total variance (e.g., the NAM and SAM indices).

Climate regime
A state of the climate system that occurs more frequently than other nearby states due to either more persistence or more often recurrence. In other words, a cluster in climate state space that leads to a local maximum in the probability distribution

Empirical Orthogonal Functions (EOF)
The *climate pattern* b(s) obtained by regression of climate variables y(s,t) onto a *principal component* time series x(t). The principal component time series is the linear combination of climate variables at different locations that has maximum variance subject to certain normalisation constraints on principal component weights b(s). EOFs are non-linear functions of the covariance matrix and so are not simply related to *teleconnection patterns,* which are rows of the correlation matrix. Because of their maximum variance property, *principal components* are frequently used as climate indices (e.g., the Arctic Oscillation index is the principal component of sea-level pressures in the Northern Hemisphere).

[END BOX 14.1 HERE]

14.2 Climate Phenomena

14.2.1 Overview: Climate Phenomena and their Influence on Regional Climate

Regional climate[1] results from the complex superposition of several key processes:

- local ambient conditions caused by neighbouring regional systems present each year (e.g., monsoon circulations, tropical convergence zones, jets, etc.);
- local response to large-scale modes of variability (e.g., ENSO or NAO);
- global conditions determined by the general circulation of the atmosphere (e.g., the mean lower tropospheric temperature, the lapse rate, vertical humidity profile, etc.).

This chapter will assess the relevance of the first two processes in future regional climate change. Therefore, *climate phenomena* in this chapter are either *regional systems present each year*, or *dominant modes of variability.* Modes of variability, regimes, and other key concepts are summarised in Box 14.1.

The following subsections assess well-known phenomena that have strong impacts on regional climate. Each subsection briefly describes a climate phenomenon, the mechanisms for how it is likely to change in the future, and its relevance for explaining future regional climate change. The phenomena described here will form the basis for interpreting future regional climate change in Section 14.3. Other aspects of the phenomena are assessed elsewhere in this report: past variations (Chapter 2), climate model ability to simulate the phenomena (Chapter 9), and future climate model projections (Chapters 10-11).

Future regional climate is uncertain because each process is likely to change with climate change, and the processes can interact with one another. Climate phenomena are not independent and complex interactions between phenomena can occur e.g., trends in correlation between ENSO and NAO. Regional climate change results from one or more changes in the following factors:

1. *Ambient conditions* - the mean and variability of the ambient state may change (e.g., increase in surface temperature due to more radiative forcing);
2. *Response to modes of variability or regimes* - the local response to a mode or regime might change e.g., the teleconnection patterns of ENSO might displace eastward, increased humidity may amplify the regional influence of NAO in Europe, etc.;

[1] understood here to signify the whole probability distribution i.e., mean state and the variability including extremes.

3. *Mode amplitude distribution* - the probability distributions of the climate mode indices may change (e.g., shifts in the mean and/or variance, or more complex changes in shape);
4. *Regime probabilities* – the probability of being in certain regimes may change;
5. *Mode or regime structure* - the types and number of modes or regimes and their mutual dependencies may change e.g., different flavours of El Nino might emerge.

It is sometimes useful to interpret changes in mean regional climate in terms of changes in the modes of variability. However, it is necessary to quantify to what extent this is meaningful for future and past changes. It is not always possible to disentangle changes due to ambient conditions from changes in mode changes if both pathways give a similar regional response to changes in forcing. It is difficult to distinguish changes in modes of variability from trends in the mean in short noisy records of increasingly non-stationary climate. Box 14.2 presents a summary of the modes of variability covered in this chapter, and some of their known mechanisms and impacts.

Even if the change in a climate mode index does not contribute greatly to mean regional climate change, a climate mode still plays a very important role in regional natural variability. This is especially so for changes in the extremes of regional climate, which are likely to be sensitive to small changes in variance or shape of the distribution of the mode indices or the mode spatial patterns. It is therefore important to quantify how modes of variability might change in the future.

Individual climate modes and regimes require careful interpretation to avoid being physically misinterpreted (Monahan et al., 2009). However, a set of leading modes or regimes can provide a useful simplified basis for describing the state of the climate system. For example, a large fraction of Northern Hemisphere interannual variability can be reconstructed as linear combinations of the first two Empirical Orthogonal Functions (EOFs) of sea level pressure (approximately the NAM and the PNA) (Quadrelli and Wallace, 2004). Furthermore, four climate modes account for much of the variation in global atmospheric mass: the two annular modes (SAM and NAM), a global ENSO-related mode and a fourth mode related to the PDO, which in turn is closely related to ENSO and the PNA pattern (Trenberth et al., 2005). The linear paradigm uses a linear combination of mode indices (i.e., a sum of modes) to account for large fractions of variance in a local climate variable (Hurrell and Deser, 2010). However, there are alternative paradigms on how best to relate regional climate to large-scale patterns of variability. Whereas the linear paradigm is most useful for interpreting unimodal distributions, the non-linear regime paradigm considers the probability distribution of local climate variables to be a multi-modal mixture of distributions related to a discrete set of regimes (weather types). In the non-linear regime paradigm, regional climate has different distributions depending on which large-scale quasi-stationary state is currently active e.g., (Cassou and Terray, 2001; Monahan et al., 2001; Palmer, 1999). There is an ongoing debate by climate scientists on the strengths, weaknesses, and robustness of these different paradigms (Christiansen, 2005; Fereday et al., 2008; Stephenson et al., 2004).

[START BOX 14.2 HERE]

Box 14.2: Phenomena and their Role in the Climate System

Box 14.2, Table 1: Regional Climates = Effects of Major Characteristic Phenomena + Low-frequency Modes of Variability

Globe Latitude Belts	Major Characteristic Phenomena	Low-Frequency Climate Modes of Variability					Impacts	
		Fundamental Variability Modes	Main Physical Mechanisms	Time-Scales	Observed Trends	Derived Variability Modes	Regional Extreme Events	Future Trends
Extra-Tropics	H-L pressure systems Jet streams	NAM/NAO SAM	Mean flow-eddies interactions in upper-atmosphere	Intraseasonal Interannual	x-ref to observation chapter	PNA, NPO, EAP, PSA, BLC, CGT, ……?	Heat-waves Cold-air outbreaks	x-ref to CC chapter
	Storm-tracks	PDO[a] AMO[a]	Ocean dynamics &	Interdecadal Multidecadal	x-ref to observation		Droughts	

		IPO[a]	air-sea interactions		chapter		Floods	
Tropics	ITCZ Monsoons Tropical cyclones	ENSO[b] IOD[b]	Air-sea interactions	Interannual Interdecadal	x-ref to observation chapter	IOB, AMM, …..?	Droughts Floods	x-ref to CC chapter
		MJO[b]	Zonally propagating tropospheric waves	Intraseasonal	x-ref to observation chapter			

Notes:
(a) Also affect tropical latitudes
(b) Also affect extra tropical latitudes
Major Characteristic Phenomena: Determine the large-scale climate regime; are linked to the global circulation of atmosphere and ocean
Fundamental Variability Modes: Rely on their own physical mechanisms; have the highest amplitude in the regions where they are generated; can be modulated by interactions of other modes
Derived Variability Modes: Come out from the influence or interaction of other modes; have the highest amplitude wherever an amplifying interference between modes occurs; generally are phase-locked with the dominant original mode
Impacts: The modes of variability induce regional climate anomalies at diverse time-scales; when exceed certain thresholds in strength and/or permanence time can provoke extreme events such as droughts, floods, heat waves or cold spells that severely impact human activities and health.

Box 14.2, Table 2: Summary of impacts attributed to the fundamental modes of variability.

ENSO	Causes severe weather and significantly influences ecosystems, agriculture, freshwater supplies, and hurricanes worldwide
IOD	Associated with droughts in Indonesia, floods in East Africa, hot summers over Japan, and reduced rainfall over Australia
MJO	Modulate the intensity of monsoon systems around the globe and tropical cyclone activity in the Indian, Pacific and Atlantic Oceans, enhanced rainfall in Western North America, Northeast Brazil, Southeast Africa and Indonesia during boreal winter and Central America/Mexico and Southeast Asia during boreal summer.
NAM/NAO	Strong influence on the winter climate over the Euro-Atlantic and North Pacific sectors, modulating the intensity of mid-latitude storms and the occurrence of blocking events associated to cold air outbreaks and drought episodes. In summer contributes to anomalously warm and dry conditions over northern Europe.
SAM	Is associated with temperature anomalies over Antarctica, Australia, Argentina, Tasmania and the south of New Zealand and anomalously dry/wet conditions over southern South America, New Zealand, Tasmania, Australia and South Africa
PDO	Associated with widespread anomalies in the surface air temperature and precipitation over the entire North American continent and extratropical North Pacific.
AMO	Affects air temperatures and rainfall over much of the Northern Hemisphere, in particular, North America and Europe. It is associated with changes in African monsoon, the frequency of North American droughts and is reflected in the frequency of severe Atlantic hurricanes
IPO	Modulate high frequency ENSO rainfall teleconnections to Australia

Acronyms:
AMM: Atlantic Meridional Mode
AMO: Atlantic Multi-decadal Oscillation
BLC: Blocking
CGT: Circumglobal Teleconnection
EAP: East Atlantic Pattern
ENSO: El Niño-Southern Oscillation
IOB: Indian Ocean Basin
IOD: Indian Ocean Dipole
IPO: Interdecadal Pacific Oscillation
MJO: Madden-Julian Oscillation

NAM: Northern Annular Mode
NAO: North Atlantic Oscillation
PDO: Pacific Decadal Oscillation
PNA: Pacific North America
PSA: Pacific South America
SAM: Southern Annular Mode

[PLACEHOLDER FOR SECOND ORDER DRAFT: A synthesis figure to be produced to complement these tables. It is indented to show a global map marking all the phenomena and also including boxes showing the regions.]

[INSERT BOX.14.2, FIGURE 1 HERE]
Box 14.2, Figure 1: [PLACEHOLDER FOR SECOND ORDER DRAFT: A synthesis figure to complement the information about main phenomena that shows a global map marking all the phenomena and also boxes showing the regions to be used in Section 14.3.]

[END BOX 14.2 HERE]

14.2.2 Monsoon Systems

Monsoon systems represent the dominant variation in the climate of the tropics with profound local, regional, and global impacts. The fundamental driver of all the monsoon systems is differential solar heating of land and ocean due to seasonal migration of the sun and difference in thermal inertias of land and ocean that establish a land-sea temperature difference. This contrast, with the land being warmer than the surrounding ocean in summer, triggers a low-level flow of moisture from nearby oceans into the land; this moisture is the source of precipitation over monsoonal regions. As the monsoon season matures, latent heat released by convection high above the land surface helps to pull in additional moisture, maintaining the wet season. Due to the change of seasons the peak solar heating moves equatorward and then into the other hemisphere, so does the monsoon rainfall resulting in a winter monsoon.

The monsoon region is distributed globally over all tropical continents, and in the tropical oceans in the western North Pacific, eastern North Pacific, and the southern Indian Ocean (Wang and Ding, 2008). Monsoon affected region is, however, not uniform in historical record (Conroy and Overpeck, 2011), and can be modulated in the future. Examination of historical precipitation records over monsoon regions throughout the globe reveals a decreasing trend in the global land monsoon precipitation in the 1948–2003 period, with primary contributions from weakening of the summer monsoon systems in the Northern Hemisphere (Wang and Ding, 2006). For the 1979–2008 epoch, the fractional increase in monsoon area is greater than that in total precipitation, so that the ratio of these two measures (which serves as an index of the global monsoon intensity) exhibits a decreasing trend (Hsu et al., 2011a; Zhou et al., 2008). The observed trend in global monsoon precipitation over the East Asian land region is reproduced in CMIP3 model 20th century simulations under the observed anthropogenic forcing. However, the trend is much weaker in general. The global oceanic monsoon precipitation has increased since 1980, this positive trend is simulated by majority of CMIP3 models, though the models that do not include volcanic aerosols produce more significant positive trend. It is still difficult to detect observed change in global monsoon circulation from CMIP3 simulations and the models with finer resolution does not seem to produce better matching trend in tropical monsoon circulation (Kim et al., 2008).

Based on simulations of three high-resolution AGCMs, the future global monsoon area, precipitation and intensity are all projected to increase consistently among the models (Hsu et al., 2011b), see also Figure 14.1. The increase of the global monsoon precipitation is attributed to the increases of moisture convergence and surface evaporation, both of which are caused by the increase of water vapour in the air column, offset to a certain extent by the weakening of the monsoon circulation. Seasonal evolution of the thermal fields is associated with the transition of Asian summer monsoon. CMIP3 models project that the onset dates of the Asian summer monsoon over the Bay of Bengal, the Indochina peninsula and the South China Sea will delay by 5 to 10 days at the end of the 21st century under the SRES A1B scenario (Inoue and Ueda, 2011). This change might be related with delay of the reversal of upper-tropospheric meridional thermal gradient between over the Eurasian Continent and the north Indian Ocean. Further, uncertainties remain in the projections of the continental monsoon.

[INSERT FIGURE 14.1 HERE]

Figure 14.1: Changes in global monsoon area (GMA) under global warming. Difference of the GMA between the global warming and present-day simulations derived from the composite of five high-resolution model experiments, Red contours denote the composite GMA in the present-day simulations. Blue (orange) shading indicates the increase (decrease) of the GMA.

14.2.2.1 Indian Monsoon

Over India the summer monsoon (June-September) rainfall accounts for nearly 80% of the annual rainfall over most parts. It has been shown (Ramesh and Goswami, 2007) that the spatial and temporal extents of continental monsoon rainfall are changing (reducing) even though at larger scale the rainfall may not change, or even increase. Both Indian summer monsoon (or southwest: June-September) and winter monsoon (or northeast: October-December) exhibit variability at a wide spectrum of scales. The summer monsoon, in particular, is known to exhibit variations on weather scale to intra-seasonal, inter-annual, inter-decadal and longer time scales. The precipitation during the summer monsoon is characterized by a maximum along the monsoon trough extending to the northern Bay of Bengal and a secondary zone maximum south of the equator (between 0° and 10°S); these are also the seasonal locations of the inter-tropical convergence zone (ITCZ). Many earlier studies have noted intense intraseasonal oscillations (ISOs) in the summer monsoon, in the form of “active” and “break” spells, associated with fluctuations of the ITCZ and MJO. The most prominent (quasi) periodic ISOs of the Indian summer monsoon are those between 30 and 60 and between 10 and 20 days (or quasi biweekly). The ISO has characteristic patterns of rainfall, cloud and latent heating (Lau and Wu, 2010). The presence of the variability, especially the ISO, has significant influence on our ability to simulate and forecast monsoon.

The relationship between El Niño–Southern Oscillation (ENSO) and Indian summer monsoon rainfall is well known on interannual time scales. Warm ENSO events are associated with deficit monsoon rainfall and the cold events with excess rainfall in India. However, there are recent reports of weakening of relationship between ENSO and the Indian summer monsoon rainfall beginning around 1980 (Kumar et al., 1999). Ashok et al. (2001) attribute this weakening to the frequently occurring positive Indian Ocean Dipole events (Saji et al., 1999; Webster et al., 1999) in the last two decades of 20th century as a possible reason. Several other factors including natural decadal variability have been suggested as possible mechanism behind the weakening of the relationship. In contrast, a strengthening of the relationship between ENSO and the winter northeast monsoon covering south peninsular India and Sri Lanka is reported (Zubair and Ropelewski, 2006). Several land-based factors, such as the west Asian dust, Himalayan and Eurasian snow cover, also influence the Indian summer monsoon (Krishnamurti et al., 2010).

At longer time scales, there has been considerable investigation on relationship between decadal variability of Indian monsoon rainfall and SST forcing (Boschat et al., 2011; Kucharski et al., 2006). There are multiple lines of evidence that the Asian monsoon, and perhaps therefore the Indian monsoon as well, has undergone abrupt shifts and weakening in the past, giving rise to mega droughts (Cook et al., 2010; Meehl and Hu, 2006; Sinha et al., 2011).

Although the monsoon is a vigorous convective system, it may not be immune to anthropogenic forcing such as an increase of CO_2 (Sud et al., 2008). A majority of CMIP3 models have indicated an increase in the monsoon rainfall over the Indian region in the later part of 21st Century though the amount of increase varies from model-to-model and for different emission scenarios (Kumar et al., 2011b; May, 2011; Sabade et al., 2011). These studies indicate that the future increase in the monsoon rainfall is largely contributed by the increased availability of atmospheric moisture content without much of a change in the strength of monsoon circulation. The increase in monsoon rainfall is also reported to be happening despite an El Nino like pattern seen in the Pacific in future. However, studies of (Annamalai et al., 2007; Kumar et al., 2011b; Sabade et al., 2011) examining the monsoon rainfall and ENSO relationships in future using CMIP3 models do not indicate any perceptible change. But Annamalai et al. (2007) state that the results need to be taken with some caution because of the diversity in the simulation of ENSO variability in IPCC AR4 models.

Increase in the interannual variability of Indian Monsoon rainfall is projected in the future under different emission scenarios (Fu and Lu, 2010; Kumar et al., 2011b; Turner et al., 2007a). Recent studies are also suggestive of an extended monsoon season in the future (Kripalani et al., 2007b; Kumar et al., 2011b; Meehl et al., 2006).

However, uncertainties related to sensitivity of model resolution (Klingaman et al., 2011) and model biases (Levine and Turner, 2011) make definitive conclusions from model simulations difficult. Similarly, the aerosol concentration appears to affect the rainfall trends (Bollasina et al., 2011; Lau and Kim, 2010; Ramanathan and Carmichael, 2008) and the lack of explicit treatment of direct and indirect effects of aerosols in the current generation of coupled models can introduce some uncertainty in the future projections in this part of the world.

14.2.2.2 East-Asian Monsoon

East Asia is located leeside of the Tibetan Plateau between the Eurasian continent and the Pacific Ocean, and thus affected by humid southerly flow in summer and dry northerly cold air outbreak in winter. Early summer heavy rainfall events along the quasi-stationary Meyu-Changma-Baiu rain band and typhoons are unique features of this area, which is affected by large interannual variability such as ENSO. Understanding of climate change in the East Asian monsoon regions remains one of considerable uncertainty with respect to circulation and precipitation. The East Asian summer monsoon (EASM) has been weakening from the end of the 1970s which results in a tendency toward increased droughts in northern China and flood in Yangtze River Valley; this pattern is usually termed as “southern China flood and northern China drought” (Gong and Ho, 2002; Hu, 1997; Wang, 2001; Yu et al., 2004). The EASM weakening shows distinct three-dimensional structures with a tropospheric cooling trend over East Asia during July and August (Yu and Zhou, 2007). The cooling trend is most prominent at the upper troposphere around 300 hPa and is connected to northern hemisphere interdecadal climate change (Zhou and Zhang, 2009). Examinations on the long-term change of the EASM during the 20th century find no significant trends, indicating the pronounced weakening tendency of the EASM in recent decades is unprecedented (Zhou et al., 2009a). The EASM weakening since the end of 1970s is also evident in the atmospheric circulations. The western Pacific subtropical high, which controls the water vapour supply for monsoon rainfall, has extended westward and thus prevents the northward penetration of water vapour transport. In the upper level, the South Asian High has experienced a zonal expansion (Gong and Ho, 2002; Zhou et al., 2009b). The East Asian Subtropical Westerly Jet, which has a stronger impact on the Asian-Pacific climate (Zhang et al., 2006c), has enhanced south to its normal position (Yu and Zhou, 2007).

Whether the tropical ocean warming associated with the tropical interdecadal variability is resulted from natural variability remains unknown and thus the EASM change is also regarded as natural variability (Fu et al., 2009; Han and Wang, 2007). The anthropogenic factors including aerosol effect may contribute to modification of the Asian monsoon system. Analysis of wind data in China found that the surface wind speed associated with the East Asian monsoon has significantly weakened in both winter and summer during the past three decades. The monsoon wind speed is highly correlated with incoming solar radiation at the surface, which is very sensitive to aerosol loading (Xu et al., 2006). The dimming effect of aerosols (Qian et al., 2006; Qian et al., 2007) reduces the surface heating over land, and thus diminishes the temperature difference between land and ocean, and weakens the strength of the monsoon (Lau et al., 2008). The weakening of the East Asian monsoon system would be unfavourable for water vapour transport from south to north, prolonging the presence of the rain belt in the south, and thus exacerbating the trend of “southern flood and northern drought."

East Asian monsoon is connected to the western North Pacific monsoon through the teleconnection pattern (Pacific-Japan pattern) of convection. ENSO, which directly affects the convection activity over the western North Pacific region, thus indirectly influences the East Asian monsoon. Future projections of El-Niño like mean state changes in the tropical Pacific (i.e., eastward displacement of major rainfall area) favours prolonged East Asian summer rainfall season.

Under the A1B scenario, surface air temperature over East Asia is projected to increase significantly for both the middle and end of the twenty-first century, with larger magnitude over the north and in winter. There are also significant increases in rainfall in the twenty-first century under the A1B scenario, especially for the period 2070–2099 (Chen et al., 2011). . As far as the interannual variability is concerned, there are high probabilities for the future intensification of interannual variability of precipitation over most of China in both winter and summer (Chen et al., 2011; Lu and Fu, 2010b).

14.2.2.3 Indo-Australian Monsoon Including Maritime Continent

The Maritime Continent is located between the Asian and Australian continent, with monsoon rainfall generally peaking during the boreal winter. The annual cycle exhibit contrast between wet season in July-August and dry season in December-February (Aldrian and Susanto, 2003; Giannini et al., 2007) with high correlation of dry season with ENSO. The monsoon onset will experience substantial delay during extreme ENSO event. The monsoon indicates strong variability from diurnal to interannual and longer time scales. In fact, for the climate of the maritime continent, monsoon contributes to 72% of the total variances, while without monsoon signal ENSO contributes to 49.9% of variance and followed by decadal variability 8.29% (Aldrian and Djamil, 2008). The climate change projection over the region, therefore is particularly difficult due to substantial impact of ENSO. The understanding of future ENSO will be key of future climate over the region especially for the dry season. Since this area is located in the throughflow between two world major basins or between the Pacific and the Indian Oceans, thus the future role of the throughflow under climate change will also be important in characterizing the future monsoonal pattern. Aldrian et al. (2005) suggested the role of sea-air interaction over the region that drive the local monsoonal pattern. Naylor et al. (2007) suggest a decrease of precipitation in dry season (July-September), while increase of precipitation in wet season (April-June), which lead to shift of the monsoon annual pattern.

14.2.2.4 Western and North Pacific Monsoon

The western North Pacific summer monsoon (WNPSM) does not show any trend during 1950–1999. When forced by observed historical sea surface temperature, the interannual variability of the western North Pacific summer monsoon is reasonably reproduced (Zhou et al., 2009c). Since the late 1970s the overall coupling between the western North Pacific monsoon system and ENSO has become strengthened. The relationships between ENSO and the western North Pacific monsoon have become enhanced during ENSO's developing, mature, and decaying phases, overriding the weakening of the Indian monsoon–ENSO anti-correlation during the developing phase (Wang et al., 2008b). The WNPSM exhibits a peculiar seasonal change with stepwise transitions with rapid changes in precipitation at intervals of roughly one month from mid-May through mid-July through heat-induced teleconnection and air-sea interaction (Ueda et al., 2009), while the latest one in mid-July is related to the withdrawal of the Baiu rainy season around Japan. The CMIP3 models have difficulties in reproducing the stepwise eastward progress of convection, probably related to a poor SST distribution and poor representation of monsoon trough over the warm pool area in GCMs (Inoue and Ueda, 2009).

14.2.2.5 African Monsoon

The West African climate is dominated by the West African monsoon (WAM) system. The monsoon develops during northern spring and summer, with a rapid northward jump of the rainfall belt from along the Gulf of Guinea at 5°N in May-June to the Sahel at 10°N in July-August. The WAM brings the rainfall maxima to their northernmost location in August and then withdraws to the south afterward. The cross-equatorial gradient in tropical Atlantic SST influences the monsoon flow and moistening of the boundary layer, so that a colder northern tropical Atlantic induces negative rainfall anomalies. Warm anomalies in the Indian Ocean tend to increase vertical stability elsewhere, much like during the growth phase of ENSO, and induce subsidence and dry near-surface flow over north Africa (Hagos and Cook, 2008; Lu, 2009). It is unclear whether the uncertainty in future change in West African monsoon rainfall can be attributed to model biases in tropical Atlantic SST, most notably the failure to reproduce the climatological east-west gradient at the equator, to differences in the patterns of projected SST that influence the monsoon, or to the dominance of different processes, land or ocean based, in different models (Biasutti et al., 2008; Giannini, 2010; Xue and others, 2010). However, the CMIP3 ensemble simulates a more robust response during the pre-onset and the demise portion of the rainy season (Biasutti and Sobel, 2009; Seth et al., 2010b). Rainfall is projected to decrease during spring—implying a delay of about a week in the development of the mean rainy season; but to increase in fall—implying an intensification of late-season rains.

14.2.2.6 North America Monsoon System

The warm season precipitation in the southwestern USA and northern Mexico is controlled by the North American Monsoon System (NAMS) with a seasonal reversal of the prevailing winds over the Gulf of California. Many factors influence NAMS including interannual (ENSO) and decadal (PDO) climate variability (Cavazos et al., 2008). Future changes in these modes as well as mean tropical SST changes and land surface temperature changes are the key for future projections of NAMS.

Positive trends in NAMS have been detected, particularly in areas north of the "core" monsoon area of Arizona and western New Mexico (Anderson et al., 2010b). The CMIP5 simulations tend to show a reduction in precipitation in the core zone of the monsoon (Annex I), but this signal is not robust across models. Thus the evidence for current or future anthropogenic influence on NAMS is very limited. The observed relationship between the monsoon strength and SSTs in the Gulf of California (Mitchell et al., 2002b) suggest that greater confidence in future changes in NAMS may only come when this feature is better resolved by climate models.

14.2.2.7 South America Monsoon System (SAMS)

The main atmospheric characteristics of the SAMS onset are related to humidity flux from the Atlantic Ocean over northern South America and Amazonia region, eastward shifting of subtropical high, strong northwesterly moisture flux east of tropical Andes (Drumond et al., 2008) (Raia and Cavalcanti, 2008) and the establishment of an anticyclonic anomaly at high levels (Bolivian High). A review of SAMS recent studies is shown in Marengo et al. (2010a). The annual cycle of precipitation in the SAMS region is very well represented by CMIP3 models (Bombardi and Carvalho, 2009; Seth et al., 2011). Some CMIP3 models project precipitation increase in austral summer and a decrease in austral spring in the SAMS region, while less precipitation over central-east Brazil during the rainy season is indicated by others (Bombardi and Carvalho, 2009; Seth et al., 2011). A high-resolution global model projects precipitation increase over Amazonia region and central South America in DJF (Kitoh et al., 2011). Precipitation increase is also projected in this high-resolution model over northwestern Amazonia in MAM, and central-southeast in SON. In JJA, reduced precipitation is expected over parts of the continent, except over the extreme northwest SA, where the model projects rainfall increase. The humidity flux increase associated with circulation features of the SAMS is consistent with precipitation changes over the continent. The evaporation increases over the continent in DJF and MAM as well as in the Amazonia and southeastern South America in JJA and SON. Reduced evaporation is projected in parts of Northeast Brazil and southern Amazonia during the four seasons. Persistent precipitation increases in part of the La Plata Basin and over the northeastern sector of Amazonia Basin.

SAMS onset dates are reasonably simulated by AGCMs and CMIP3 models, but in southeastern Brazil there is large dispersion among model results (Bombardi and Carvalho, 2009; Liebmann et al., 2007). The rainy season duration is underestimated in some areas and overestimated in others. The median onset and demise in the future projections is similar to the 20th century or one pentad later in central monsoon region (Bombardi and Carvalho, 2009). Precipitation increase at the end of the monsoon cycle and reduced precipitation in the onset in central monsoon region (Seth et al., 2010b) could indicate a shifting in the lifecycle monsoon period. These changes were related to less moisture convergence in the austral spring and more convergence during summer. Similar changes of extended rainy and dry seasons were found in the global tropical regions (Seth et al., 2011). The warmer troposphere and increased stability due to global warming act as a remote mechanism to reduced precipitation of SAMS in the winter, while during summer, the local mechanisms, such as increased evaporation and decreased stability contribute to the increased precipitation. Both mechanisms seem to reduce precipitation during spring.

14.2.3 Patterns of Tropical Convection

Tropical convection is organized into long and narrow convergence zones, often anchored by SST structures. How tropical convection changes in a warmer climate depends on the spatial patterns of SST warming. In model experiments where spatially uniform SST warming is imposed, precipitation increases in these tropical convergence zones (Xie et al., 2010d), following the 'wet-get-wetter' paradigm (Held and Soden, 2006). In CMIP3 model projections of future climate, however, the patterns of precipitation change are not entirely attributable to this paradigm. Instead, rainfall change over tropical oceans follows a 'warmer-get-wetter' pattern, increasing where the SST warming exceeds the tropical mean and vice versa (Sobel and Camargo, 2011; Xie et al., 2010d). On the flanks of a convergence zone, rainfall may decrease because of the increased horizontal gradient in specific humidity and the resultant increase in dry advection into the convergence zone (Neelin et al., 2003). Robust patterns of SST change among CMIP3 models include the equatorial enhanced warming (Liu et al., 2005) and reduced warming in the subtropical Southeast Pacific. The former pattern causes the Pacific convergence zone to move toward the equator, while the latter weakens the convergence zone over the South Pacific.

14.2.3.1 Intertropical Convergence Zone (ITCZ)

The ITCZ exhibits variability at different spatio-temporal scales. A northern shift of ITCZ has been suggested as the trigger of abrupt shifts of Northern Hemisphere atmospheric circulation (Steffensen et al., 2008). Southward shifts of the Atlantic ITCZ, and its relation to Atlantic thermohaline circulation is indicated by CMIP/PMIP simulations (Stouffer et al., 2006).

Inter-hemispheric asymmetry in warming, such as that due to preferential cooling of the Northern Hemisphere under the influence of anthropogenic sulfate emissions (Ming and Ramaswamy, 2009), can affect the north-south SST gradients and the future behavior of ITCZ. Analysis of ship reports shows an increase in cloud cover in the central equatorial Pacific over the past six decades (Tokinaga et al., 2012a), which suggests a southward shift of the tropical rain band. Models forced by anthropogenic aerosols generally simulate such a southward displacement of tropical convection (Rotstayn and Lohmann, 2002). There is also some observational evidence (Mann and Emanuel, 2006a) that anthropogenic aerosols cooled the tropical North Atlantic over the twentieth century. (Broccoli et al., 2006; Chang et al., 2011; Cheng et al., 2007) noted that there is a secular trend in the tropical Atlantic interhemispheric gradient over the twentieth century, with the tropical South Atlantic warming faster than the tropical North Atlantic and with resulting implications for the Atlantic ITCZ, primarily due to increase in sulfate aerosol forcing.

Change in the inter hemispheric SST gradient and ITCZ shift can also result from atmospheric teleconnection mechanisms. Modeling studies have shown that cooling from the mid-to-high Northern Hemisphere can affect the northern tropics (Broccoli et al., 2006; Kang et al., 2008). Variations of the Atlantic meridional overturning circulation (AMOC) can affect the tropical Atlantic ITCZ (Chang et al., 2008; Cheng et al., 2007). The AMOC is quite sensitive to twentieth-century climate forcings in fully coupled models (Delworth and Dixon, 2006). Modelling studies suggest that simulation of AMOC, and hence shifts of ITCZ, is quite sensitive to processes like cloud feedback (Zhang et al., 2010).

Climate models play increasingly important roles in understanding the response to and influence of ITCZ in climate change. However, although most models reproduce the observed broad patterns of precipitation and year-to-year variability (Braconnot et al., 2007; Newton et al., 2006), many models (especially those without flux corrections) still show an unrealistic double-ITCZ pattern over the tropical Pacific (Dai, 2006; De Szoeke and Xie, 2008; Lin, 2007; Zhang et al., 2007b). Improvement of estimate of response of ITCZ and consequent impact on regional climate will also critically depend on representation of aerosol effects in models, especially with regards to their impacts on inter-hemispheric asymmetric warming (Kiehl, 2007; Ramanathan and Carmichael, 2008).

14.2.3.2 South Pacific Convergence Zone (SPCZ)

The South Pacific Convergence Zone (SPCZ; Vincent, 1994), (Widlansky et al., 2011) extends from tropical warm pool convection of the western Pacific in a southeastward direction towards the Southern Hemisphere mid-latitudes. The SPCZ contributes most of the yearly rainfall to the hydrological budgets of South Pacific island nations. On the regional scale, highest rainfall follows the seasonal migration of the warm pool and SPCZ, reaching greatest intensity during austral summer (DJF). The SPCZ has a pivotal role in the climate of the southwest Pacific, with trends and variability in temperature and rainfall falling into coherent regions to the north and south of the mean position of the SPCZ, and to the east and west of the dateline, separating the zonal and diagonal components of the SPCZ respectively, (e.g., Folland et al., 2003; Griffiths et al., 2003).

The position of the SPCZ varies on interannual to decadal time scales, shifting northeast and southwest in response to ENSO and the Interdecadal Pacific Oscillation (e.g., Folland et al., 2002; Vincent et al., 2011). Since the fourth assessment report, several studies (Lintner and Neelin, 2008; Takahashi and Battisti, 2007; Vincent et al., 2011; Widlansky et al., 2011) have made progress explaining physical mechanisms of SPCZ orientation and variability, associated with zonal and meridional SST gradients, trade wind strength, and subsidence over the eastern Pacific.

Based on CMIP3 simulations of the SRES A2 emissions scenario, in austral summer (DJF) the SPCZ is likely to continue to occupy a similar location to the present, in the western and central Pacific. The rainfall amount (mean and maximum) within the SPCZ is projected to increase in the majority of CMIP3 models, and the area of the SPCZ (if defined using a constant rainfall threshold) is projected to increase. Therefore, the region currently influenced by the SPCZ is likely (>66% of models agree) to experience increased wet season rainfall by the late 21st century. This is consistent with increased moisture convergence in a warmer climate.

Climate model projections show no consistent shift in the slope or mean latitude of the austral summer SPCZ through the 21st century. However, a large majority of models simulate a westward shift in the eastern edge of the SPCZ, with reduced rainfall to the east of ~150°W, associated with a modeled strengthening of the trade winds in the southeast Pacific and an increased zonal sea surface temperature gradient across the South Pacific (Brown et al., 2011; Timmermann et al., 2010a; Xie et al., 2010b). While the tropical overturning circulation is projected to weaken in a warmer climate, the increase in atmospheric moisture content leads to higher rainfall in the SPCZ.

There is little consistent change in modeled SPCZ response to La Niña in future projections, but the multi-model mean SPCZ response to El Niño has a more zonal orientation and is shifted towards the equator, relative to the mean 20th century position (A2 simulations, Brown et al., 2011). This implies that the typical SPCZ response to El Niño events in a warmer climate may be closer to the response to very strong events in the observed present day climate (cf., Vincent et al., 2011), or such extreme events may occur more frequently. However, only a subset of CMIP3 models are able to simulate the present-day spatial pattern and evolution of observed very strong El Niño events (Lengaigne and Vecchi, 2010).

14.2.3.3 South Atlantic Convergence Zone (SACZ)

The South Atlantic Convergence Zone (SACZ) is associated with intense rainfall over Southeastern Brazil in the warm season, causing floods in many places and land sliding in mountain areas. Weakening of this feature causes dry conditions in that region.

Results from 6 out of 10 CMIP3 models project a decreased precipitation in central and eastern Brazil, which is a region affected by the SACZ, in A1B scenario (Bombardi and Carvalho, 2009). The reduction is also suggested in another study, which projects a southward displacement of the SACZ and the Atlantic Subtropical High during SON and DJF (Seth et al., 2010b). The reduction is consistent with results from 9 models out of 18 from CMIP3 that indicated an increase of positive anomalous precipitation over southeastern South America (SESA) in the second half of 21st century compared to the first half (Junquas et al., 2011b). An opposite behavior is expected for SACZ region, as the dominant mode of austral summer precipitation variability over South America depicts a dipole pattern, with one center over SACZ region and other over SESA. Although the models represent the dipole pattern, the explained variance of the dominant precipitation mode is larger in the models than in observations. Pacific SST warming and strengthening of the PSA-like wavetrain in the second half of 21st century compared to the first half were discussed as the mechanisms related to the changes in the dipole pattern by Junquas et al. (2011b). Previous results in IPCC 2007 had shown an increase of precipitation over the SESA region in projections of future climate, but changes in the SACZ region were not clear.

Another important result from Seth et al. (2010b), also consistent with precipitation reduction in the SACZ region, is the intensification of northerly wind at low levels over South America in future projections, which could represent an increase in the Low Level Jet occurrences. Higher frequency of LLJ in future model projections was obtained by Soares and Marengo (2009). Increased moisture flux from the Amazon Basin to the La Plata Basin is consistent with the precipitation increase in the southern regions and a decrease in the SACZ.

14.2.3.4 Madden-Julian Oscillations (MJO)

The Madden-Julian Oscillation (MJO; Madden and Julian, 1994) is the dominant component of tropical intraseasonal (20–100 days) circulation variability. It consists of pairs of increased and suppressed convective activity (associated with positive and negative anomalies in precipitation, respectively), over areas of up to 20,000 km^2. Associated with the precipitation pattern is an east-west (zonal) overturning circulation with ascending motion in the active region and descending motion in the suppressed region. This convection-circulation coupled pattern propagates eastward along the equator normally from the Indian Ocean to the western and central Pacific at an average speed of ~5 ms^{-1} (Zhang, 2005). In boreal summer, there is a northward propagation of the MJO in conjunction with its eastward propagation (Lawrence and Webster, 2002). The MJO modulates tropical cyclone activity (Frank and Roundy, 2006), contributes to intraseasonal fluctuations of the monsoons (e.g., Maloney and Shaman, 2008), and modulates the ENSO cycle (Zhang and Gottschalck, 2002). The MJO also excite teleconnection patterns outside the tropics in both hemispheres (e.g., L'Heureux and Higgins, 2008; Lin et al., 2009).

Simulation and prediction of the MJO by GCMs have been a challenging problem (e.g., Lin et al., 2006), although progress has been made in recent years (Benedict and Randall, 2009; Zhang et al., 2006a). Poor simulations of the MJO by climate models is associated with the sub-grid scale physical processes that must be parameterized in models, such as cumulus convection and atmosphere-ocean energy exchange. Because of the close connections between the MJO and extreme events, the inability of climate models to properly simulate the MJO and its potential response to climate change seriously limits the application of these models to predict the statistics of extreme events in the future, especially in the tropics. Possible changes in the MJO in a future warmer climate have just begun to be explored (e.g., DeMott et al., 2012).

14.2.3.5 The Quasi-Biennial Oscillation (QBO)

The quasi-biennial oscillation (QBO) is a near-periodic, large-amplitude, downward propagating oscillation in zonal (westerly) winds in the equatorial stratosphere (e.g., Baldwin et al., 2001). The QBO is the largest jet in the atmosphere, and is evident in time series of the zonal mean zonal wind near the equator, which changes from strong easterlies to strong westerlies through each QBO cycle (approximately 28 months). It is driven by vertically propagating internal waves that are generated in the tropical troposphere (Plumb, 1977).

The QBO has significant effects on the global stratospheric circulation, in particular the strength of the northern stratospheric polar vortex as well as the extratropical troposphere (e.g., Boer, 2009; Garfinkel and Hartmann, 2011; Marshall and Scaife, 2009). These extratropical effects occur primarily in winter when the stratosphere and troposphere are strongly coupled (e.g., Anstey and Shepherd, 2008; Garfinkel and Hartmann, 2011).

It is presently unclear how the QBO will respond to future climate change related to greenhouse gas increase and recovery of stratospheric ozone. Climate models assessed in the AR4 did not simulate the QBO as they lacked the necessary vertical resolution (Kawatani et al., 2011). The two studies that have been completed since the AR4 (Giorgetta and Doege, 2005; Kawatani et al., 2011) gave conflicting results and neither focused on associated changes in surface climate.

14.2.4 ENSO

The El Niño-Southern Oscillation (ENSO) is a coupled ocean-atmosphere phenomenon naturally occurring at an inter-annual time scale. El Niño, originally named by Peruvian fishermen, means the Child Christ in Spanish and involves abnormal warming of tropical eastern-to-central Pacific sea surface temperature (SST), which leads to a weakening of zonal SST contrast between the tropical western Pacific, ‘warm pool’ and the tropical eastern Pacific ‘cold tongue’. It is closely linked to the atmospheric counterpart, the Southern Oscillation, named by Sir Gilbert Walker (Walker, 1923, 1924), indicating the surface pressure seesaw between Darwin and Island Tahiti or more comprehensively the equatorial zonal-overturning circulation, so-called ‘Walker circulation’. Later, El Niño and Southern Oscillation had been merged as ‘El Niño-Southern

Oscillation' that is grown by a positive feedback between the surface air pressure gradient and SST gradient in the zonal direction referring Bjerkness feedback (Bjerknes, 1966, 1969).

14.2.4.1 Tropical Pacific Mean State

Patterns of tropical Pacific SST change under global warming are uncertain. The strengthening of tropical Pacific west-east SST contrast during the twentieth century was reported in the reanalysis data (An et al., 2011; Cane et al., 1997; Hansen et al., 2006; Karnauskas et al., 2009) and in most of CMIP3 (An et al., 2011), which may be due to 'ocean dynamic thermostat' indicating the overcompensated upwelling cooling against the surface radiative warming (Cane et al., 1997; Clement et al., 1996; Seager and Murtugudde, 1997). However, the raw data without interpolation or the bias-corrected data and some models showed the opposite result (Deser et al., 2010a; Tokinaga et al., 2012b). It is hard to tell from observations how the zonal SST gradient has changed even during the recent several decades because of observational uncertainties associated with limited data sampling, changing measurement techniques and analysis procedures. The uncertainty in the eastern Pacific warming is also related to a complexity of the cold tongue formation, which involves the balance between surface heat flux by virtue of various atmospheric feedback processes and ocean dynamic process (DiNezio et al., 2009), the influence by the ocean eddies (An, 2008; Contreras, 2002; Moum et al., 2009), and the Atlantic warming (Kucharski et al., 2011) through the mechanisms of the Walker circulation across equatorial South America or inter-basin SST gradient and ocean dynamics (Rodriguez-Fonseca et al., 2009; Wang, 2006; Wang et al., 2009). The tropical Pacific's response to global warming has been suggested to be neither El Niño-like nor La Niña-like (Collins et al., 2010; DiNezio et al., 2009; Tung and Zhou, 2010) since the mechanisms for these changes are different from that of ENSO events – the Bjerknes feedback.

Apart from change in the zonal SST gradient, surface ocean warms more near the equator than in the subtropics in model projections (Gastineau and Soden, 2009; Liu et al., 2005) because of the difference in evaporative cooling (Xie et al., 2010b). Other oceanic changes include a basin-wide thermocline shoaling (Collins et al., 2010; DiNezio et al., 2009; Vecchi and Soden, 2007a), a weakening of the surface current, and a slight upward shift of the equatorial undercurrent (Luo and Rothstein, 2011). A weakening of tropical atmosphere circulation during the twentieth century has been documented in observational and reanalysis data (Bunge and Clarke, 2009; Karnauskas et al., 2009; Tokinaga et al., 2012b; Vecchi and Soden, 2007a; Vecchi et al., 2006; Yu and Zwiers, 2010; Zhang and Song, 2006) and in CMIP3 (Gastineau and Soden, 2009; Vecchi and Soden, 2007a). On the other hand, the intensification of tropical atmosphere circulation during the recent decades was reported in various observational and reanalysis data (Li and Ren, 2011; Liu and Curry, 2006; Mitas and Clement, 2005, 2006; Vecchi et al., 2006; Zhang et al., 2011).

14.2.4.2 Variance Changes over the Recent Decades

The amplitude modulation of El Niño at the decadal or even centennial timescales during the past was observed in reconstructed instrumental records (An and Wang, 2000; Gu and Philander, 1995; Mitchell and Wallace, 1996; Wang, 1995; Wang and Wang, 1996; Yeh and Kirtman, 2005) and in various proxy records (Cobb et al., 2003; Li et al., 2011c; Yan et al., 2011), and was also simulated by CGCMs (An et al., 2008; Wittenberg, 2009). The modulation was believed to relate to changes in the mean climate conditions of the tropical Pacific (An and Wang, 2000; Fedorov and Philander, 2000; Li et al., 2011c; Wang and An, 2001, 2002), which indeed occurred between the pre-1980s and the post-1980s (An and Jin, 2000; An and Wang, 2000; Fedorov and Philander, 2000; Kim and An, 2011). Since the 1990s the occurrence of Central Pacific El Niño event (Ashok et al., 2007; Kao and Yu, 2009; Kug et al., 2009; Yeh et al., 2009) and its intensity (Lee and McPhaden, 2010) have been increased (see Figure 14.2). The increasing trend in ENSO amplitude is also observed during the recent century (Li et al., 2011c), which claimed to be caused by global warming (Kim and An, 2011; Zhang et al., 2008a). However, the long-term CGCM simulations demonstrated that the decadal even centennial timescale modulations of ENSO could be generated without invoking change in any external forcing (Wittenberg, 2009; Yeh et al., 2011). The modulation could be resulted from the nonlinear process in the tropical climate system (Timmermann et al., 2003) or the interactive feedback between the mean climate state and ENSO (Choi et al., 2009b; Choi et al., 2011; Ye and Hsieh, 2008). Thus, it is uncertain whether the decadal modulation of ENSO that occurred during the recent decades is due to global warming or natural variability. Furthermore, due to the fact that the change in tropical mean condition under global warming is quite uncertain even during the past few decades (see Section 14.3.1.1.2), it is hard to say whether ENSO is going to intensify or weaken, but it is very likely that ENSO will not disappear in the future (Collins et al., 2010).

[INSERT FIGURE 14.2 HERE]

Figure 14.2: (a) Intensities of El Niño and La Niña events in the central equatorial Pacific (Niño4 region) and the estimated linear trends, which is 0.20(±0.18)°C/decade for El Niño and −0.01(±0.75)°C/decade for La Niña events. (b) Intensities of El Niño and La Niña events in the eastern equatorial Pacific (Niño3 region) and the estimated linear trends, which is 0.39(±0.71)°C/decade for El Niño and 0.02(±0.47)°C/decade for La Niña events. The uncertainty ranges reflect the 90% confidence intervals estimated from a Student's t-test. Note that the vertical scales start from ±0.3°C and that the scales are different for the Niño3 and Niño4 time series. (Lee and McPhaden, 2010)

14.2.4.3 Teleconnections

ENSO event causes severe weather and significantly influences ecosystems, agriculture, freshwater supplies, and tropical cyclone activity worldwide. The ENSO signal reaches all over the globe in a way of atmospheric waves called as 'atmospheric ENSO's teleconnection'. The global teleconnection pattern of ENSO depends on the wave and heating sources associated with the location and amplitude of SST anomaly, and wave pathway that is influenced by the atmospheric climate condition. The wave paths associated with ENSO are not limited within the troposphere but expanded in the stratosphere (Bell et al., 2009). The global warming scenario projections archived in CMIP3 showed a systematic eastward shift in both El Niño and La Niña teleconnection patterns over the Northern Hemisphere, which might be due to the eastward migration of tropical convection center associated with the expansion of the warm pool under global warming (Kug et al., 2010b; Muller and Roeckner, 2008). It is unclear whether the eastward shift of tropical convection is related to more occurrence of Central Pacific El Niño. Nevertheless, some CGCMs, which do not simulate more Central Pacific El Niño events in response to global warming, do not produce a significant change in the zonal shift of the convection (Muller and Roeckner, 2008; Yeh et al., 2009).

14.2.4.4 Different Flavours of El Niño

A distinct character of El Niño – the warming in the equatorial central Pacific sandwiched by anomalous cooling in the east and west – was documented earlier (Larkin and Harrison, 2005; Trenberth and Tepaniak, 2001). For the purpose of distinguishing from the conventional El Niño with the maximum warming in the eastern Pacific (Yeh et al.), this type of El Niño is referred to as the Date Line El Niño (Larkin and Harrison, 2005), El Niño Modoki (Ashok et al., 2007), Central Pacific El Niño (Kao and Yu, 2009) or warm pool El Niño (Kug et al., 2009) [hereafter, referred to Central Pacific (CP) El Niño] (Figure 14.3). CP El Niño basically has no basin-wide features and occurs rather episodically (Yu et al., 2010). Indices for CP El Niño introduced so far are mostly the weighted areal-averaged SST (Ashok et al., 2007; Ren and Jin, 2011; Yeh et al., 2009) or ocean subsurface temperature anomalies (Yu et al., 2011).

[INSERT FIGURE 14.3 HERE]

Figure 14.3: Leading EOF patterns of SST anomalies obtained from a combined EOF-regression analysis of Kao and Yu (2009) for (a) the eastern-Pacific type of El Niño and (b) the central Pacific type of El Niño. Contour intervals are 0.1 (Courtesy from Jin-Yi Yu).

The global impacts of CP El Niño are also different from those of conventional EP El Niño (Ashok et al., 2007; Kao and Yu, 2009), including monsoonal rainfall over China (Feng and Li, 2011; Feng et al., 2011a), over India (Kumar et al., 2006a) and over Australia (Ashok et al., 2007; Taschetto and England, 2009; Taschetto et al., 2009; Wang and Hendon, 2007), air temperature and rainfall in the United States (Mo, 2010), and typhoon activity in the western North Pacific (Guanghua and Chi-Yung, 2010; Hong et al., 2011; Kim et al., 2011). The influence of CP El Niño on Atlantic hurricanes may also be different from conventional EP El Niño (Kim et al., 2009), but it has been showed that the anomalous atmospheric circulation in the hurricane main development region during CP El Niño is similar to that during EP El Niño (Lee et al., 2010). Change in the impacts is possibly due to the change in the location of tropical atmospheric heating source (Hoerling et al., 1997; Kug et al., 2010a). For example, conventional EP El Niño leads to the Pacific North American (Muller and Roeckner) pattern, while CP El Niño may force the second EOF mode of the North Pacific sea level pressure called 'North Pacific Oscillation' (Di Lorenzo et al., 2010).

Some studies argued that more frequent occurrence of CP El Niño events during the recent decades is related to the tropical Pacific warming in the response to increased greenhouse gas forcing (Yeh et al., 2009). The tropical Pacific warming, especially "La Niña-like" response mainly in the surface but not in the subsurface (Collins et al., 2010), causes the relative intensification of the zonal advection of heat compared to the vertical advection. A heat budget analysis in the ocean mixed layer reveals that the zonal advection is a major dynamical feedback process in developing of CP El Niño and the anomalous surface heat flux in the decaying of CP El Niño (Kug et al., 2010c; Yu et al., 2010). On the other hand, Lee and McPhaden (2010) argued that the warming trend in the central-to-western Pacific was resulted from more intense CP El Niño events, but not the other way around. McPhaden et al. (2011) further showed that the future climate condition change associated with the increased occurrence of CP El Niño is not consistent with the observed climate condition that leads to more frequent occurrence of CP El Niño. Thus, whether the mean climate state change leads to more frequent emergence of CP El Niño or the other way around is not known yet. Moreover, the increase in the frequency of CP El Niño may be a manifestation of natural climate variability (Yeh et al., 2011). Some studies suggested that CP and EP El Niños are not different phenomena, but rather a nonlinear evolution of ENSO (Takahashi et al., 2011).

14.2.5 PDO, AMO and TBO

14.2.5.1 PDO

The "Pacific Decadal Oscillation" (PDO) refers to the leading Empirical Orthogonal Function (EOF) of monthly Sea Surface Temperature (SST) anomalies over the North Pacific (north of 20°N) from which globally-averaged SST anomalies have been subtracted (Mantua et al., 1997). It exhibits anomalies of one sign along the west coast of North America and of opposite sign in the western and central North Pacific. The PDO is closely linked to fluctuations in the strength of the wintertime Aleutian Low Pressure System, an index of which is the North Pacific Index (NPI) defined as the average sea level pressure over the region 30°–65°N, 160°E–140°W (Trenberth and Hurrell, 1994). Anomalous air-sea energy exchange associated with interannual variations in the NPI produce the spatial pattern of the PDO (Alexander, 2010; Deser et al., 2004; Schneider and Cornuelle, 2005). Oceanic processes such as vertical entrainment and gyre-scale adjustment to wind stress curl fluctuations via baroclinic Rossby waves contribute to the low-frequency temporal character of the PDO (Schneider and Cornuelle, 2005). The PDO is linked to a pattern of tropical Indo-Pacific SST anomalies that resembles ENSO but with a broader meridional scale (Deser et al., 2004; Mantua et al., 1997). In view of its connection to the tropical and South Pacific, the PDO has also been termed the "Inter-decadal Pacific Oscillation" (Power et al., 1999). The PDO is closely linked to winter temperature and precipitation anomalies over North America and northeastern Asia (Deser et al., 2004; Lapp et al., 2011; McCabe and Dettinger, 2002) as well as salmon production along the west coast of North America (Mantua and Hare, 2002; Mantua et al., 1997).

The PDO does not exhibit significant changes in spatial or temporal characteristics under greenhouse gas warming in most of the 24 coupled climate models used in AR4 (Furtado et al., 2011; IPCC, 2007b), although some of the models indicate a weak shift toward more occurrences of the negative phase of the PDO by the end of the 21st century (Lapp et al., 2011). However, given that the models strongly underestimate the PDO connection with tropical Indo-Pacific SST variations (Furtado et al., 2011; Lienert et al., 2011), the robustness of the PDO projections remains uncertain.

14.2.5.2 Atlantic Multidecadal Oscillation

14.2.5.2.1 What is the AMO and why is it important for regional climate change?

The Atlantic Multidecadal Oscillation (AMO) is the name given to multidecadal fluctuations superimposed on the rising trend apparent in the instrumental SST record throughout the North Atlantic Ocean. Area-mean North Atlantic SST shows variations with a range of about 0.4°C and warming of a similar magnitude since 1870. The AMO appears to have a quasi-periodicity of about 70 years, although the approximately 150-year instrumental record possesses only a few distinct phases – warm during approximately 1930–1965 and after 1995, and cool between 1900–1930 and 1965–1995. The phenomenon has also been referred to as 'Atlantic Multidecadal Variability' (AMV) to avoid the implication of temporal regularity. Along with secular trends and Pacific variability, the AMO or AMV is one of the principal features of multidecadal variability in the instrumental climate record.

The AR4 WG1 report already highlighted a number of important links between the AMO and regional climates. Subsequent research using observational and palaeoclimatic records, and climate models, has confirmed and expanded upon these connections, such as West African Monsoon and Sahel rainfall (Chang et al., 2008; Mohino et al., 2011; Shanahan et al., 2009), summer climate in North America (Curtis, 2008; Feng et al., 2011b; Fortin and Lamoureux, 2009; Hu and Feng, 2008; Seager et al., 2008) and Europe (Folland et al., 2009; Sutton and Hodson, 2007) and Atlantic major hurricane frequency (Zhang and Delworth, 2009b). Further, the list of AMO influences around the globe has been extended to include decadal variations in the Indian (Feng and Hu, 2008b; Goswami et al., 2006a; Kucharski et al., 2009a; Kucharski et al., 2009b; Li et al., 2008; Luo et al., 2011; Zhang and Delworth, 2009b) and East Asian (Wang et al., 2008b) monsoons, Mediterranean (Marullo et al., 2011) and South American climate (Chiessi et al., 2009), Pacific variability (Wang et al., 2011; Zhang and Delworth, 2007), regional Hadley and Southern Hemisphere circulations (Baines and Folland, 2007) and Alpine glaciers (Huss et al., 2010). The breadth of these effects further highlights the importance of the AMO in the instrumental period. If AMO variability continues into the future, it could be an important contributor to regional climate change over the next few decades in a wide range of regions. Assessing future AMO activity relates to the questions of whether it is a long-lived fluctuation or peculiar to the instrumental period, its physical origins and predictability.

14.2.5.2.2 What AMO variability is likely in the future?

The fact that palaeo-reconstructions of Atlantic temperatures trace AMO-like variability back before the instrumental era was noted in AR4 WG1. This has been confirmed by further analyses, although these suggest potential for intermittency in AMO variability (Saenger et al., 2009; Zanchettin et al., 2010). Control simulations of climate models run for hundreds or thousands of years also show long-lived Atlantic multidecadal variability. These lines of evidence suggest the likelihood that AMO variability will continue into the future, and no fundamental changes in the characteristics of North Atlantic multidecadal variability in the 21st century are seen in the CMIP3 models (Ting et al., 2011). Many studies have diagnosed a trend towards a warm North Atlantic in recent decades additional to that implied by global climate forcings (Knight, 2009; Polyakov et al., 2010). Given the apparent duration of AMO phases of approximately 30 years, this suggests that the AMO may peak in the early decades of the 21st century and then cool, regionally offsetting some of the effects of global warming (Keenlyside et al., 2008). Based on studies that have examined the regional effects of the AMO (see above), a future AMO decline could have effects that include further drying of the African Sahel, reduction of Indian monsoon rainfall, increased wet season rainfall in North East Brazil, wetter summers in central North America, drier summers in North Western Europe, and a possible reduction in major Atlantic hurricane activity. On the other hand, Atlantic temperatures may not follow such a reliably regular evolution, as hinted at by palaeo data and model simulations (Zanchettin et al., 2010). Physically-based initialised climate prediction systems (Smith et al., 2007) have the potential to predict the future AMO state independent of any knowledge of past periodicities. Models do indicate the potential for multidecadal predictability of North Atlantic temperatures (Boer and Lambert, 2008) and the meridional overturning circulation of the Atlantic Ocean (Msadek et al., 2010), which is strongly believed to be closely associated with the AMO. Real predictability currently appears to be more modest (Pohlmann et al., 2011), and it is not known whether improvements to models' treatment of the factors involved in proposed AMO mechanisms (see Ch. 9, sect. 5.3 for a discussion) would lead to reliable AMO forecasts for the coming decades.

14.2.5.2.3 Which other processes might be relevant for simulating AMO trends?

Evidence from palaeo data and multi-century unforced control simulations of many of the current climate models gives the strong impression that the AMO arises internally within the climate system. Estimates of the climate response to the suite of 20th century climate forcing factors included in CMIP3 also fail to show the observed AMO phases (Knight, 2009; Kravtsov and Spannagle, 2008; Ting et al., 2011), reinforcing this view. Recent work, however, has questioned whether the amplitude of forcing from indirect sulphate aerosol effects in CMIP3 is too low in the North Atlantic region (Chang et al., 2011). A more recent ensemble of forced 20th century runs, with a more sophisticated aerosol treatment, is able to reproduce more of the observed variability of the AMO (Booth et al., 2011). If aerosol changes have been responsible for part of the variability of the AMO, this also implies a role in its regional climate effects. As a result, the future state of many regional climates may depend more on changes in aerosols than previously considered.

14.2.5.2.4 What are the global implications of changes in the AMO?

Some similarity in the shape of the instrumental time series of global and northern hemisphere mean surface temperatures and the AMO has long been noted. Climate models possessing intrinsic AMO variability (Knight et al., 2005), and with observed 20th century North Atlantic variations imposed (Zhang et al., 2007a), produce a peak-to-peak effect of about 0.25˚C on northern hemisphere mean temperature, much less than the approximately 0.8˚C of observed warming since 1970. Analyses separating the AMO and climate change by statistical means, however, find a potentially larger fractional contribution of the AMO to the recent warming trend (DelSole et al., 2011; Wu et al., 2011b). This result is supported by a climate model simulation with an AMO transition imposed from its control simulation (Semenov et al., 2010). It is possible, therefore, that more of the recent global-scale warming arises from internal climate variability and less from changing climate forcings than might otherwise be expected. This would have implications for the detailed attribution of climate change and raises the possibility that the global effects of future AMO variability may be large enough to delay further greenhouse gas induced global warming (would depend on emission scenarios and GHG warming) for several decades.

14.2.5.3 Tropospheric Biennial Oscillation

[PLACEHOLDER FOR SECOND ORDER DRAFT]

14.2.6 Indian Ocean Modes

14.2.6.1 Mean State

Changes in the mean state of the tropical ocean-atmosphere coupled system affect regional climate in two important ways. First, spatial variations in SST warming shape changes in mean rainfall over tropical oceans, following the “warmer-get-wetter” pattern (Xie et al., 2010a). Second, the mean state change affects interannual variability by modulating ocean-atmospheric feedback and teleconnection.

The basin-mean SST of the tropical Indian Ocean (TIO) has risen steadily for much of the 20th century, especially since the 1950s. Coupled ocean-atmosphere GCMs generally simulate this SST trend very well under the observed radiative forcing (Alory et al., 2007), suggesting the forced nature of the trend. The SST increase over the North Indian Ocean is noticeably weaker than the rest of the basin since 1930s, a difference suggested due to reduced surface solar radiation by Asian brown clouds with important effects on Indian and African monsoons (Chung and Ramanathan, 2006) and Arabian Sea cyclones (Evan et al., 2011b). Results from atmospheric GCMs forced by observed SST indicate that the Indian Ocean warming contributes to the decrease in African Sahel rainfall (Du and Xie, 2008; Giannini et al., 2003) and the rise in the NAO index (Hoerling et al., 2004).

Over the equatorial Indian Ocean, instrumental observations are ambiguous about change in zonal SST gradient, but coral isotope records off Indonesia for 1858–1997 indicate a reduced SST warming and/or suppressed freshening of salinity (Abram et al., 2008), in support of an IOD-like pattern in SST. Historical ship measurements suggest an easterly wind change for the past six decades especially during July-October, a result consistent with a reduction (increase) of marine cloudiness in the east (west) (Tokinaga et al., 2012b). Indeed, rainfall shows a decreasing trend at many stations over the maritime continent. Consistent with the easterly change in surface wind, expendable bathythermograph (XBT) observations suggest a thermocline shoaling in the east. Ocean GCMs forced by atmospheric reanalyses, however, point to changes of opposite sign (Han et al., 2010). This discrepancy could be due to modest forced changes compared to natural variability and spurious change in reanalyses.

In many CMIP3 models, the response of the equatorial Indian Ocean to global warming is characterized by easterly wind change, with a shoaling thermocline (Du and Xie, 2008; Vecchi and Soden, 2007a) and reduced SST warming in the east (Figure 14.4). The change in zonal SST gradient, in turn, reinforces the easterly wind change, indicative of Bjerknes feedback in the TIO response to global warming (Xie et al., 2010a). While the deceleration of the Walker circulation occurs under global warming even in the absence of any change in zonal SST gradient (Held and Soden, 2006), models with strong Bjerknes feedback tend to produce an IOD-like zonal pattern with reduced SST warming and suppressed convection in the eastern equatorial Indian Ocean (Cai et al., 2011). This coupled pattern is most pronounced during July-November.

[INSERT FIGURE 14.4 HERE]

Figure 14.4: August-October changes in CM2.1 A1B: (a) SST (color CI=0.125°C) and precipitation (green/gray shade and white contours at CI=20 mm/month); (b) sea surface height (CI=1 cm) and surface wind velocity (m/s). [PLACEHOLDER FOR SECOND ORDER DRAFT: to be replaced with a CMIP5 RCP6.0 ensemble mean.]

14.2.6.2 Modes

SST over the tropical Indian Ocean exhibits two distinct modes of interannual variability (IAV), as extracted from an EOF analysis over the basin. The Indian Ocean basin (IOB) mode, explaining more than 30% of the total variance, features a nearly uniform structure while the Indian Ocean dipole (IOD) mode, explaining less than 15% of the variance, has a heavy loading in the eastern equatorial Indian Ocean off Sumatra and Java of Indonesia, with weaker anomalies of the opposite polarity over the rest of the basin. See recent reviews by (Schott et al., 2009) and (Deser et al., 2010b). Both modes, especially IOB, are significantly correlated with ENSO. IOB peaks in the boreal spring of the ENSO decay year while IOD peaks in the fall of the ENSO developing year.

14.2.6.3 Basin mode

The IOB mode forms in response to ENSO via the atmospheric bridge and surface heat flux adjustment (Alexander et al., 2002; Klein et al., 1999). Recent studies show that ocean dynamics and ocean-atmosphere interaction within the TIO basin are important for the long persistence of IOB (Du et al., 2009; Izumo et al., 2008; Wu et al., 2008). In the summer following El Nino, the persistent basin-wide SST warming induces robust atmospheric anomalies (Xie et al., 2009), known as the TIO capacitor effect that includes a weakened Northwest Pacific monsoon (Wang et al., 2003), suppressed tropical cyclone (TC) activity (Du et al., 2011) over the Northwest Pacific, and anomalous rainfall over East Asia (Huang et al., 2004).

For a 60-year period since 1950, the IOB mode intensified markedly across the 1970s, a change most pronounced in the summer following ENSO (Xie et al., 2010c). This interdecadal change in IOB explains the intensification of correlation between the Northwest Pacific summer monsoon and ENSO (Wang et al., 2008a), a change reproduced in atmospheric GCM simulations forced by observed SST (Huang et al., 2010). Observations along a busy ship track across the North Indian Ocean and South China Sea reveal another epoch of strong IOB variability during 1880–1910 in addition to the current epoch after the 1970s, and a lull for about 60 years in between (Chowdary et al., 2012). Both epochs of intensified IOB variability coincides with those of enhanced ENSO activity, suggesting the importance of the Pacific forcing.

How the IOB mode responds to global warming depends in part on how ENSO will change (Section 14.2.4). In an OAGCM, (Zheng et al., 2011) found that the IOB mode and its capacitor effect persist longer, through summer into early fall in global warming (Figure 14.5). This increased persistence may intensify ENSO's influence on Northwest Pacific tropical cyclones. It also suggests that the recent intensification of IOB variability may be partly due to global warming.

[INSERT FIGURE 14.5 HERE]

Figure 14.5: IOB persistence in the A1B projections by six CMIP3 models with good skills in the IOB simulation (Saji et al., 2006) he JAS(1) North Indian Ocean SST regression upon the Nino3.4 SST index in the 20th (1901–2000, blue bars) and 21st (2001–2100, brown bars) centuries. JAS(1) denotes the July-August-September season in the ENSO decay year. The IOB persistence increases in four and decreases in one model. [PLACEHOLDER FOR SECOND ORDER DRAFT: to be updated with CMIP5 RCP6.0 results.]

14.2.6.4 Dipole Mode

IOD develops in July-November and involves Bjerknes feedback among zonal SST gradient, zonal wind and thermocline tilt along the equator, much akin to ENSO in the Pacific (Saji et al., 1999; Webster et al., 1999). Besides inducing local precipitation over ocean, a positive IOD event (with negative SST anomalies off Sumatra) is associated with droughts in Indonesia, reduced rainfall over Australia, intensified Indian summer monsoon, floods in East Africa, hot summers over Japan, and anomalous climate in the extratropical Southern Hemisphere (Yamagata et al., 2004).

IOD variability is high around 1850, and after the 1970s (Abram et al., 2008). A major IOD event occurred in 2006, and the dipole mode index remains positive for 2007 and 2008. Such a prolonged IOD-like state is very rare, which, along with the increase in IOD activity since the 1970s, prompts the suggestion that global warming might be a culprit (Abram et al., 2008; Behera et al., 2008; Cai et al., 2009).

In CMIP3 models, the IOD variability remains nearly unchanged in global warming (Ihara et al., 2009) (Figure 14.6a) despite the easterly wind change that shoals the thermocline (Figure 14.6b) and intensifies thermocline feedback on SST in the eastern equatorial Indian Ocean. (Zheng et al., 2010) show that the global increase in atmospheric dry static stability weakens atmospheric response to zonal SST gradient, countering the enhanced thermocline feedback. On balance, IOD amplitude does not change much in amplitude in global warming simulations, suggesting that the recent intensification of IOD activity is part of natural variability.

One important property of IOD does change in global warming. IOD in the current climate is strongly skewed, with cold events off Indonesia much stronger than warm ones. This skewness originates from a deep thermocline in the equatorial Indian Ocean that is subcritical for thermocline/Bjerknes feedback. In global warming, the shoaling thermocline weakens the asymmetry in thermocline feedback between cold and warm events (Zheng et al., 2010) (Figure 14.6b). The strong skewness in the current climate and its projected decrease have important implications for IOD's climatic influences. In current climate, climate anomalies are pronounced only at the positive phase of IOD. They may become strong at the positive phase in a warmer climate.

[INSERT FIGURE 14.6 HERE]

Figure 14.6: IOD change between the 20th century (1901–2000, blue bars) simulations and 21st century (2001–2100, brown bars) A1B projections by 12 CMIP3 models: (a) standard deviation, and (b) skewness of the September-November IOD index of (Saji et al., 1999). The amplitude change is small and inconsistent among models, increasing in five and decreasing in seven. The skewness decreases in nearly all the models. [PLACEHOLDER FOR SECOND ORDER DRAFT: to be updated with CMIP5 RCP6.0 results.]

The change the mean state of the tropical Indian Ocean is likely to feature an IOD-like pattern during July-November, with reduced warming and suppressed rainfall in the eastern basin including Indonesia. Many CMIP3 models project such a pattern in response to increased GHG, with support from limited observations for the past six decades. Under global warming, the IOD mode of interannual variability is likely to remain unchanged in amplitude despite a shoaling thermocline in the mean state of the eastern equatorial Indian Ocean but the negative skew of SST variability off Sumatra may weaken as a result of the mean thermocline change. The projected change in the IOB mode needs systematic assessments using the CMIP3/5 multi-model ensemble. There are indications that in a warmer climate, the IOB mode persists longer following the decay of an ENSO event, strengthening ENSO's influence on summer rainfall and tropical cyclone activity over the Northwest Pacific and East Asia.

14.2.7 Tropical Atlantic Patterns

14.2.7.1 Mean state

Over the past century, the Atlantic has experienced the most pronounced and robust warming trend of all the tropical oceans (Deser et al., 2010a; Tokinaga and Xie, 2011). The warming pattern, captured as the leading mode of an empirical orthogonal function (EOF) analysis on the observed 20th century SST (Figure 14.7), shows a clear hemispheric asymmetry with stronger warming trends in the tropical South than North Atlantic, particularly in the east equatorial south Atlantic and off the coast of Angola. The associated time variation, which displays a well-defined warming trend superimposed on a multidecadal variation, is highly correlated with the globally averaged SST (r=0.9) and with the Atlantic Multidecadal Oscillation (AMO) index (0.7). The warming has brought detectable changes in atmospheric circulation and rainfall pattern in the region. In particular, the ITCZ has shifted southward and land precipitation has increased (decreased) over the equatorial Amazon, equatorial West Africa, and along the Guinea coast (over the Sahel) (Deser et al., 2010a; Tokinaga and Xie, 2011).

[INSERT FIGURE 14.7 HERE]

Figure 14.7: The leading EOF (left) of a gridded observed SST record from Hadley Centre sea ice and SST version 1 (HadISST1) data set (Rayner et al., 2003), which explains 36% of the SST variance, and the associated time series (right) normalized by its maximum absolute value (blue) overlaid by the globally averaged SST (red) and an AMO index derived by averaging the SST over the entire North Atlantic Ocean (green).

CMIP3 20th century climate simulations generally capture the warming trend of the basin-averaged SST over the tropical Atlantic. Majority of the models also seem to capture the secular trend in the tropical Atlantic SST interhemispheric gradient and, as a result, the southward shift of the Atlantic ITCZ over the past century (Chang et al., 2011). However, none of the models reproduces the intense warming trend observed off the coast of Angola, and only a few models simulate the significant warming trend in the east equatorial South Atlantic. Modeling studies show that the interhemispheric SST gradient is responsive to changes in the Atlantic Meridional Overturning Circulation (AMOC) (Chang et al., 2008; Cheng et al., 2007), and to anthropogenic aerosol cooling that is strong over the Northern Hemisphere (Biasutti and Giannini, 2006a; Ming and Ramaswamy, 2009; Rotstayn and Lohmann, 2002; Williams et al., 2001). A more recent study (Chang et al., 2011) , based on CMIP3 multi-model 20th century climate simulations, argues that at least half the observed trend in the interhemispheric SST gradient may be attributed to 20th century climate forcings.

CMIP3 model future climate projections under the A1B scenario show an accelerated SST warming over much of tropical Atlantic. Projections of the interhemispheric SST gradient change, however, are not consistent among the models. Many models display little or no hemispheric asymmetry in the future SST warming trend, and show little change in the position of the ITCZ (Breugem et al., 2006). Interestingly, a few models that exhibit the most significant displacement of the ITCZ project a northward shift of the ITCZ over the 21st century (Breugem et al., 2006), in contrast to the southward shift for the past decades. One explanation is that GHG increase dominates in the future over the anthropogenic aerosol effect, the latter possibly being responsible for the recent southward shift in the Atlantic ITCZ (Chang et al., 2011; Tokinaga and Xie, 2011). However, large uncertainties exist in the model-based projection because the climate models suffer severe bias problems in the tropical Atlantic (Chapter 9).

14.2.7.2 Meridional Mode

On decadal time scales, the interhemispheric SST variation emerges more clearly as a “dipole-like” pattern revealed by the 2nd EOF of the observed 20th century SST record (Figure 14.8). The mode is referred to as the Atlantic meridional mode (AMM) (Chiang and Vimont, 2004; Servain et al., 1999; Xie and Carton, 2004), and is considered as a dynamical mode intrinsic to the tropical ocean-atmosphere system (Chang et al., 1997). A thermodynamic feedback between surface winds, evaporation, and SST (WES) is fundamental to the existence of this class of coupled ocean-atmosphere modes (Chang et al., 1997; Xie and Philander, 1994). Despite the importance of the local air-sea feedback, AMM variability is strongly influenced by other modes of climate variability, particularly El Niño/Southern Oscillation (ENSO) and the North Atlantic Oscillation (NAO) (Chang et al., 2006).

Not much research has been done on the long-term variation of the AMM. An examination of the time series associated with the 2nd SST EOF suggests that the AMM amplitude appeared to modulate over multidecadal time scales during the past century (Figure 14.8). AMM activities were relatively strong in the early and late decades of the 20th century and weak in the mid century. Interestingly, this variation in AMM activity seems to coincide with the multidecadal modulation of ENSO in the tropical Pacific, raising the possibility that the two phenomena may be interrelated. Some recent studies suggest that the interhemispheric SST anomaly in the tropical Atlantic can alter ENSO strength in the tropical Pacific through an atmospheric bridge (Dong et al., 2006; Timmermann et al., 2007). Possibly because of model biases in simulating AMM (Chapter 9), the long-term variation of the AMM in the CMIP3 20th century climate simulations shows little consistency among the models. Only a few IPCC models capture the intensified AMM variability during the late decades of the 20th century, as shown in observations.

Many IPCC model simulations with the A1B emission scenario show insignificant changes in the SST variance associated with the AMM, resulting in a negligible change in the multimodel mean variances. However, the few models that give the best AMM simulation over the 20th century project a weakening in future AMM activity (Breugem et al., 2006), possibly due to the northward shift of the ITCZ (Breugem et al., 2007). At present, model projections of future change in AMM activity is considered highly uncertain because of the poorly simulated Atlantic ITCZ by the models. In fact, uncertainty in projected changes in Atlantic meridional SST gradient has been identified as an important source of uncertainty for regional climate projection surrounding the tropical Atlantic Ocean (Good et al., 2008). Several physical factors are likely to affect the future state of the AMM. One is the position of the Atlantic ITCZ, which affects the strength and duration of WES feedback (Breugem et al., 2006, 2007; Chang et al., 2006), and thus AMM variability. Other factors include future changes in ENSO and the NAO, both exerting a significant remote influence on the AMM. Understanding future changes in AMM bears important implications for extreme climate changes, such as hurricane, under global warming in the tropical Atlantic sector, as the AMM is tightly coupled with ITCZ and has a profound impact on the regional atmospheric circulation. Atlantic hurricane activity correlates highly to the AMM on both interannual and decadal time scales, and this AMM-hurricane relationship provides a dynamic framework for understanding the impact of climate variability/change on Atlantic hurricanes (Smirnov and Vimont, 2011; Vimont and Kossin, 2007).

[INSERT FIGURE 14.8 HERE]

Figure 14.8: Same as Figure 14.7, except for the 2nd EOF (left), which explains 14% of the SST variance. The associated time series (blue in right panel) is overlaid by a detrended interhemispheric SST gradient index derived by differencing the SSTs averaged in the two boxes shown in the left panel. The two time series are correlated at r=0.86. The yellow shade and black lines show the amplitude modulation of the PC time series using a 21-year moving window.

14.2.7.3 Atlantic Niño

On decadal time scales, the interhemispheric SST variation emerges more clearly as a “dipole-like” pattern revealed by the 2nd EOF of the observed 20th century SST record (Figure 14.9). The mode is referred to as the Atlantic meridional mode (AMM) (Chiang and Vimont, 2004; Servain et al., 1999; Xie and Carton, 2004), and is considered as a dynamical mode intrinsic to the tropical ocean-atmosphere system (Chang et al., 1997). A thermodynamic feedback between surface winds, evaporation, and SST (WES) is fundamental to the existence of this class of coupled ocean-atmosphere modes (Chang et al., 1997; Xie and Philander, 1994). Despite the importance of the local air-sea feedback, AMM variability is strongly influenced by other modes of climate variability, particularly El Niño/Southern Oscillation (ENSO) and the North Atlantic Oscillation (NAO) (Chang et al., 2006).

Not much research has been done on the long-term variation of the AMM. An examination of the time series associated with the 2nd SST EOF suggests that the AMM amplitude appeared to modulate over multidecadal time scales during the past century (Figure 14.9). AMM activities were relatively strong in the early and late decades of the 20th century and weak in the mid century. Interestingly, this variation in AMM activity seems to coincide with the multidecadal modulation of ENSO in the tropical Pacific, raising the possibility that the two phenomena may be interrelated. Some recent studies suggest that the interhemispheric SST anomaly in the tropical Atlantic can alter ENSO strength in the tropical Pacific through an atmospheric bridge (Dong et al., 2006; Timmermann et al., 2007). Possibly because of model biases in simulating AMM (Chapter 9), the long-term variation of the AMM in the CMIP3 20th century climate simulations shows little consistency among the models. Only a few IPCC models capture the intensified AMM variability during the late decades of the 20th century, as shown in observations.

Many IPCC model simulations with the A1B emission scenario show insignificant changes in the SST variance associated with the AMM, resulting in a negligible change in the multimodel mean variances. However, the few models that give the best AMM simulation over the 20th century project a weakening in future AMM activity (Breugem et al., 2006), possibly due to the northward shift of the ITCZ (Breugem et al., 2007). At present, model projections of future change in AMM activity is considered highly uncertain because of the poorly simulated Atlantic ITCZ by the models. In fact, uncertainty in projected changes in Atlantic meridional SST gradient has been identified as an important source of uncertainty for regional climate projection surrounding the tropical Atlantic Ocean (Good et al., 2008). Several physical factors are likely to affect the future state of the AMM. One is the position of the Atlantic ITCZ, which affects the strength and duration of WES feedback (Breugem et al., 2006, 2007; Chang et al., 2006), and thus AMM variability. Other factors include future changes in ENSO and the NAO, both exerting a significant remote influence on the AMM. Understanding future changes in AMM bears important implications for extreme climate changes, such as hurricane, under global warming in the tropical Atlantic sector, as the AMM is tightly coupled with ITCZ and has a profound impact on the regional atmospheric circulation. Atlantic hurricane activity correlates highly to the AMM on both interannual and decadal time scales, and this AMM-hurricane relationship provides a dynamic framework for understanding the impact of climate variability/change on Atlantic hurricanes (Smirnov and Vimont, 2011; Vimont and Kossin, 2007).

[INSERT FIGURE 14.9 HERE]

Figure 14.9: Same as Figure 14.7, except for the 3rd EOF (left), which explains 9% of the SST variance. The associated time series (blue in right panel) is overlaid by a detrended Atl-3 index derived by averaging the SST in the box shown in the left panel. The two time series are correlated at r=0.5. The yellow shade and black lines show the amplitude modulation of the Atl-3 index using a 21-year moving window.

14.2.8 PNA and PSA

14.2.8.1 Pacific-North American Pattern

The term 'Pacific-North American' (PNA) pattern was coined by Wallace and Gutzler (1981) to refer to a recurrent mode of atmospheric variability prevalent over the North Pacific and the North American land mass, particularly during the winter season. Variations in the strength and polarity of the PNA patterns are accompanied by prominent shifts in the jet stream and storm tracks over the Pacific and North American sectors, and thus exert notable influences on the temperature and precipitation in these regions on intermonthly and interannual periods (Nigam, 2003b).

Observational evidence presented by Horel and Wallace (1981) and others indicate that the PNA pattern is linked to ENSO events in the tropical Pacific. However, Straus and Shukla (2002) and Nigam (2003b) pointed out that the teleconnection pattern related to ENSO variability exhibits some notable differences from the PNA pattern.

More recent diagnoses (see review by Bronnimann (2007)) show that ENSO may impact European climate through modulation of the North Atlantic Oscillation (NAO), especially during late winter and early spring. The observational and model results reported by Li and Lau (2011) and (2012) illustrate that one possible mechanism for this connection is related to the ENSO-forced teleconnection pattern in the North Pacific-North American sector. Specifically, this response pattern is accompanied by systematic changes in the position and intensity of the storm tracks over that region. The transient disturbances along the storm tracks propagate farther eastward and reach the North Atlantic. The ensuing dynamical interactions between these storm track eddies and the local quasi-stationary circulation lead to changes in the NAO. In addition to tropospheric processes, Ineson and Scaife (2009) have demonstrated a stratospheric link between ENSO and NAO in late winter.

Stoner et al. (2009) have made a comprehensive assessment of the capability of 22 coupled atmosphere-ocean GCMs contributing to IPCC AR4 in replicating the essential temporal and spatial aspects of the observed PNA pattern. Their results indicate that a majority of the models overestimate the fraction of variance explained by the PNA pattern, and that the spatial characteristics of PNA patterns simulated in 14 of the 22 models are in good agreement with the observations.

14.2.8.2 Pacific South America Pattern

The Pacific South America pattern (PSA), is a teleconnection prominent on intraseasonal to interannual time scales and is a result of tropical-extratropical interaction. Anomalous convection in tropical Pacific triggers circulation anomalies in the upper troposphere, which propagate as Rossby wavetrains toward the extratropics and then towards the tropics again. The PSA has a similar configuration to the Pacific North American (PNA) pattern. An example of the PSA at the intraseasonal scale is shown in Figure 14.10. Along with the SAM, the PSA has been shown to influence the surface climate across the south Pacific, including the west Antarctic (Schneider et al., 2011). This pattern is associated with atmospheric circulation anomalies over South America and has influences on extreme precipitation over the continent. The observed precipitation dipole associated with enhancement or weakening of the South Atlantic Convergence Zone is supported by the anomalous circulation, which is part of PSA. Opposite phases of this wavetrain induce opposite anomalous circulation over South America and anomalous convection in the dipole centers. As this pattern is related to anomalies in tropical Pacific /Indonesia convection, changes in these anomalies due to global warming could change the intensity, frequency, phase and position of the present pattern, with impacts on South America precipitation. A multimodel analysis from CMIP3 shows intensification of this pattern in projections to the end of 21st century related to the increase in frequency and intensity of positive SST anomalies in equatorial Pacific, with influences on the precipitation dipole over South America (Junquas et al., 2011b).

[INSERT FIGURE 14.10 HERE]
Figure 14.10: PSA pattern obtained from the First EOF of meridional wind, filtered in the 30–90 days band, period of November to March.

Experiments simulating the AMOC weakening, with a coupled model shows an influence on the PSA center close to Antarctica, through anomalous SST in the tropical Pacific (Timmermann et al., 2010b). In these experiments, there is intensification of the negative PSA phase (low pressure anomaly close to Antarctica) and corresponding SST anomalies near Ross Sea and Antarctica Peninsula. Brandefelt and Källén (2004) suggested that the track of the PSA may become elongated eastwards as the climate warms. Ongoing studies are been developed to address the influence of global warming on this pattern.

14.2.9 Northern Hemisphere Dipole Modes: NAO, NAM, and NPO

This section presents an assessment of dipole modes in the Northern Hemisphere and their relevance to future regional climate change. The North Atlantic Oscillation and Northern Annular Mode are covered in Sections 14.2.9.1–4 and the North Pacific Oscillation is addressed in Sections 14.2.9.5–6.

14.2.9.1 What is the North Atlantic Oscillation and Why is it Important for Regional Climate Change?

The North Atlantic Oscillation is a long-established mode that accounts for a large fraction of climate variability in the Northern Hemisphere (Hurrell et al., 2003; J.W. et al., 2003; Wanner et al., 2001). The NAO captures variations in sea-level pressure between the Atlantic subtropical high and the low pressure region over Iceland and the Arctic. It is intimately related to the North Atlantic jet and storms that influence climate over Europe and the N. Atlantic ocean (Hurrell and Deser, 2009).

The NAO has being interpreted as part of a more global phenomena known as either the Arctic Oscillation (AO) (Thompson and Wallace, 1998) or the Northern Annular Mode (NAM) (Thompson and Wallace, 2000). The climate index associated with the NAM/AO is very similar to the NAO index but the spatial climate patterns differ considerably over the N. Pacific (Ambaum et al., 2001; Feldstein and Franzke, 2006). The NAM/AO is more zonally symmetric than the NAO and so resembles the annular vortex mode higher up in the stratosphere, and the Southern Annular Mode (see Section 14.2.10). For historical reasons, we shall refer to NAO, AO and NAM as NAO unless further distinction is required.

NAO is a very active area of scientific research. Since the publication of the 4th IPCC report in 2006, more than 2000 peer-reviewed articles were published, which include NAO/AO/NAM in either the title or abstract. Many of these articles are impact studies, where NAO provides an aggregate index for capturing past trends and variations in regional climate impacts over a vast geographical area e.g., Europe, N. Africa, and eastern N. America land regions the N. Atlantic and Arctic oceans. This section will not endeavour to review all these publications but will assess recent NAO studies that are most relevant for future regional climate change.

14.2.9.2 What do Climate Model Projections tell us About NAO in the Future?

Recent multi-model studies of NAO in the IPCC AR4 simulations (Hori et al., 2007; Karpechko, 2010; Zhu and Wang, 2010) confirm the positive response of NAO to greenhouse gas forcing noted in earlier studies reported in IPCC AR4 (Kuzmina et al., 2005; Miller et al., 2006b; Stephenson et al., 2006). The projected NAO trends are generally found to have small amplitude compared to the natural internal variations (Deser et al., 2011). There is considerable variation in the NAO response from individual climate models, which contributes to uncertainty in the regional climate change response (Karpechko, 2010). For example, one study found no significant NAO trends in two simulations with ECHAM4/OPYC3 (Fischer-Bruns et al., 2009), whereas another study found a strong positive trend in NAO in the ECHAM5/MPI-OM SRES A1B simulations (Muller and Roeckner, 2008). Model uncertainty in NAO response is a major source of uncertainty in regional climate change predictions, for example, in European precipitation changes due to anthropogenic emissions (Boe et al., 2009).

Some evidence has been found from IPCC AR4 models of the NAO being a preferred pattern of response to climate change (Gerber et al., 2008). Simpler theoretical arguments also suggest that the forced response should project strongly onto natural modes of variability such as the NAO (Ring and Plumb, 2007). However, this finding is not supported by a detailed examination of the vertical structure of the simulated global warming response (Woollings, 2008). Hori et al. (2007) noted that NAO variability remained constant in the SRES-A1B and 20th century scenarios and concluded that the trend in NAO is a result of an anthropogenic trend in the basic mean state rather than enhanced NAO variability. However, other research has shown that there is a significant coupling between the trend in the mean state and modes of variability such as NAO (Branstator and Selten, 2009).

Various modelling studies have investigated changes in the spatial pattern of NAO due to external forcing (Brandefelt, 2006; Choi et al., 2010; Fischer-Bruns et al., 2009). Individual model simulations have shown the spatial extent influenced by NAO decrease with greenhouse gas forcing (Fischer-Bruns et al., 2009), a positive feedback between jet and stormtracks that enhances a poleward shift in the NAO pattern (Choi et al., 2010), and changes in the NAO pattern but with no changes in the propagation conditions for Rossby waves (Brandefelt, 2006). One modelling study found a trend in the correlation between NAO and ENSO during the 21st century (Muller and Roeckner, 2006). Any changes in the structure of NAO and its association with other modes of variability are likely to have major consequences for the impact of NAO on regional climate change.

14.2.9.3 Which Other Processes are Expected to be Relevant for Simulating NAO Trends?

Several climate models have underestimated 20th century decadal trends in NAO (see Chapter 9, Section 9.5.3.2). Such underestimation can lead to reduced variability in projections of regional climate e.g., Arctic sea ice (Koldunov et al., 2010). The underestimation of NAO trends may be due to low sensitivity caused by missing or poorly represented processes in climate models such as stratosphere-troposphere interaction, external forcing due to solar and volcanic radiative forcing, sea ice-troposphere interaction, etc.

Recent observational and modelling studies have helped to confirm that the lower stratosphere plays an important role in explaining recent negative NAO winters and long term trends in NAO (Dong et al., 2011; Ouzeau et al., 2011; Scaife et al., 2005; Schimanke et al., 2011). This is further supported by evidence that seasonal forecasts of NAO can be improved by inclusion of the stratospheric QBO (Boer and Hamilton, 2008; Marshall and Scaife, 2010). Other studies have demonstrated that stratospheric water vapour changes during 1965–1995 had a substantial impact on model-simulated NAO and suggested that stratospheric water vapour could be a teleconnection mechanism for communicating tropical forcing to the extra-tropics (Bell et al., 2009; Joshi et al., 2006). It is therefore highly likely that the stratosphere-troposphere interaction has an important role to play in future changes of NAO (Scaife et al., 2011).

There is also growing evidence that solar forcing has an impact on NAO (Lockwood et al., 2010). Observational studies have found little imprint of solar and volcanic forcing on NAO from 1766–2000 (Casty et al., 2007) and a non-linear modulation of the stratospheric cooling effect on NAO (Kodera et al., 2008). A recent modelling study has found a negative NAO response to solar minima (Ineson et al., 2011). Summertime NAO was found to be lower in periods of solar maximum in the GISS climate model (Lee et al., 2008).

There is modelling evidence that loss of sea-ice in the Arctic and high-latitudes can lead to a substantial negative NAO response (Deser et al., 2010c; Kvamsto et al., 2004; Seierstad and Bader, 2009).

14.2.9.4 How is Future Regional Climate Expected to be Related to Changes in NAO?

NAO accounts for a large fraction of natural climate variability over Eurasia, the Arctic, N. America, and the Middle East (Hurrell, 1996). However, modelling studies have shown that NAO does not account for a large fraction of the future change in mean temperature or precipitation over Europe (Stephenson et al., 2006). A growing number of studies find that the increasing NAO trend plays a secondary role to local radiative and advective processes in future greenhouse gas warming of the Arctic (Semenov, 2007; Teng et al., 2006; Turner et al., 2007b). Changes in local ambient conditions can be equally (if not more) important as changes in climate modes for regional climate change e.g., orographic precipitation changes and NAO for future water availability in the Middle East (Hemming et al., 2010). Changes in land surface conditions have been found to be equally important in determining mean regional climate as are non-local effects from NAO and PNA (Findell et al., 2009).

Rather than NAO being a signal for regional climate change, NAO variability can be considered to be noise that confounds detection and attribution of anthropogenic changes. Studies have attempted to remove NAO effects before detection and attribution (Zhang et al., 2006b). Detection of regional surface air temperature response to anthropogenic forcing has been found to be robust to the exclusion of model-simulated AO and PNA changes (Wu and Karoly, 2007). Model projections of wintertime European precipitation have been shown to become more consistent with observed trends after removal of trends due to NAO (Bhend and von Storch, 2008).

Changes in regional climate extremes depend heavily on changes in variances as well as changes in the mean and so are likely to be strongly dependent on any changes in the variability of NAO and its regional teleconnections (Coppola et al., 2005; Scaife et al., 2008). Changes in the tails of the NAO index or in the NAO teleconnection patterns are likely to lead to large changes in regional extreme events. There is emerging evidence that NAO-precipitation teleconnection patterns have changed in the past (Hirschi and Seneviratne, 2010) and that the relationships are scenario-dependent in climate simulations (Vicente-Serrano and Lopez-Moreno, 2008).

14.2.9.5 What is the North Pacific Oscillation and Why is it Important for Regional Climate Change?

The Pacific basin analog of the NAO, the North Pacific Oscillation (NPO) is a prominent pattern of wintertime atmospheric circulation variability characterized by a meridional dipole in sea level pressure and geopotential height (Linkin and Nigam, 2008; Rogers, 1981; Walker, 1924). The NPO and its upper air signature, the West Pacific (WP) teleconnection pattern, are linked to north-south displacements of the Asian-Pacific jet stream and Pacific stormtrack. The NPO/WP substantially influences winter air temperature and precipitation over much of western North America as well as sea ice over the Pacific sector of the Arctic, more so than either ENSO or the PNA (Linkin and Nigam, 2008). The NPO/WP also affects the strength of the North Pacific Ocean gyre-scale circulation, with consequences for upper ocean temperature, salinity, nutrients, and marine biology (Ceballos et al., 2009; Cloern et al., 2010; Di Lorenzo et al., 2009). The NPO is an intrinsic mode of atmospheric circulation variability, analogous to the NAO. By affecting the strength of the Trade Winds, which subsequently alter sea surface temperatures over the subtropical Pacific, the NPO contributes to the excitation of ENSO events via the "Seasonal Footprinting Mechanism" (SFM) (Alexander et al., 2010; Anderson, 2003; Vimont et al., 2009). Some studies indicate that warm events in the central tropical Pacific Ocean may in turn excite the NPO/WP (Di Lorenzo et al., 2009).

14.2.9.6 What do Climate Model Projections tell us About the NPO in the Future?

The NPO does not exhibit significant changes in spatial or temporal characteristics under greenhouse warming in the 24 coupled climate models used in the Intergovernmental Panel on Climate Change (IPCC) Fourth Assessment Report (Furtado et al., 2011). However, although the models produce a realistic NPO spatial pattern under present-day GHG concentrations, many of them are unable to capture the observed linkage with the North Pacific Ocean gyre circulation and most fail to show a realistic connection between tropical central Pacific warm events and the NPO (Furtado et al., 2011).

14.2.9.7 Other Related Patterns of Variability

Single modes such as NAO or NPO provide only one-dimensional description of regional climate. Additional modes of variability such as the East Atlantic Pattern are required to provide a more complete description of the strength and position of the jets and stormtracks, and the resulting regional climate (Seierstad et al., 2007; Woollings et al., 2010). The East Atlantic Pattern is important for storminess and regional climate in western Europe (e.g., the Iberian peninsula, France, England) but it is still very uncertain as to how this and other patterns are likely to change in the future.

14.2.10 Southern Annular Mode

The SAM (Southern Annular Mode, also known as the Antarctic Oscillation or AAO) is the primary mode of atmospheric circulation variability in the southern extra-tropics, comprising synchronous pressure anomalies of opposite sign in mid- and high-latitudes, which are related to fluctuations in the latitudinal position and strength of the mid-latitude jet. When pressures are below (above) average over Antarctica the SAM is defined as being in its positive (negative) phase and the circumpolar westerly winds are stronger (weaker) than average. Associated with this, the storm tracks move poleward during the positive SAM and equatorward during the negative SAM. Although broadly annular in nature, hence its name, the spatial pattern of the SAM does include a significant non-annular component in the Pacific sector (Figure 14.11). SAM variability has a major influence on the climate of Antarctica, Australasia, southern South America and South Africa (e.g., Thompson et al., 2011 and references therein).

In the past few decades the SAM has shifted towards the positive phase in austral summer and autumn (e.g., Marshall, 2007), a change attributed primarily to the effects of ozone depletion and, to a lesser extent, the increase in greenhouse gases (e.g., Thompson et al., 2011). It is likely that these two factors will continue to be the principal drivers into the future, but as the ozone hole recovers they will be competing to push the SAM in different directions (Arblaster et al., 2011; Thompson et al., 2011), at least during summer, when ozone depletion has had its greatest impact on the SAM to date. The SAM is influenced by teleconnections to the tropics, primarily associated with ENSO (Carvalho et al., 2005; L'Heureux and Thompson, 2006). Changes to the tropical circulation, and to such teleconnections, as the climate warms could further affect SAM variability.

[INSERT FIGURE 14.11 HERE]

Figure 14.11: Left – the pattern of the positive SAM in the 500 hPa monthly height anomaly field (average height anomalies when the amplitude time series is +1 standard deviation). Positive contours are red, negative are blue and zero is black. The contour interval is 7.5 m. Right – the seasonal-mean amplitude of the SAM pattern, taken from station data (courtesy G. Marshall, British Antarctic Survey, www.nerc-bas.ac.uk/public/icd/gjma/newsam.1957.2007.txt). The black line illustrates the long-term trend.

The AOGCMs used for the AR4 projected an upward trend in the SAM in both summer and winter (Miller et al., 2006b), but those models generally had very poor simulations of stratospheric ozone, with some not including it at all while others kept it constant into the future rather than having a recovery. In addition, Arblaster et al. (2011) showed that there can be significant differences in the sensitivity of these models to CO_2 increases, which will impact their overall predicted trends in the SAM. Since the AR4 a number of chemistry-climate models (CCMs) have been run that have a fully interactive stratospheric chemistry, although unlike the AOGCMs they are usually not coupled to the oceans. The majority of these CCMs, which generally compare well to reanalyses (Gerber et al., 2010), indicate that during the 21st Century the current observed SAM changes are essentially reversed during austral summer (Perlwitz et al., 2008; Polvani et al., 2011; Son et al., 2008); that is the impact of the ozone recovery has a far greater effect on the SAM than further increases in greenhouse gases in this season. In winter weak positive trends in the SAM continue through the 21st Century.

While there is some certainty regarding the likely trends in the SAM, its role in determining future regional climate change is more problematic because its impact can vary significantly from seasonal to decadal timescales. For example, the correlation between the SAM and temperature at some Antarctic Peninsula stations changes sign between seasons (Marshall, 2007) while the effect of the SAM on regional Australian rainfall also changes markedly through the year (Hendon et al., 2007b). Further uncertainty results from decadal variability within SAM-climate relationships. Silvestri and Vera (2009) discussed such non-stationary impacts and emphasised broad-scale changes in the sign of the SAM-precipitation relationship over southern South America and the SAM-temperature relationship over Australia between 1958–1979 and 1983–2004.

Marshall et al. (2011) examined a regional change in the sign of a SAM-temperature relationship in part of East Antarctica. They demonstrated that changes in the phase and magnitude of the wave-number 3 pattern, superimposed upon the annular structure of the SAM, were responsible for the reversal. Using ice-core data they also showed that such changes occurred throughout the 20th Century and hence were likely to reflect internal natural variability rather than an anthropogenic forcing. Such changes in coastal Antarctica will impact the role of the SAM in driving the formation of Antarctic Bottom Water, a central component of the global thermohaline circulation (McKee et al., 2011). Others have shown that the impact of the SAM on Antarctic climate also depends upon how it interacts with other modes of circulation variability, such as those related to ENSO (e.g., Fogt and Bromwich, 2006).

14.2.11 Blocking

Atmospheric blocking is associated with persistent, slow-moving high-pressure systems over middle or high latitude regions disrupting the normal eastward progress of transient storm systems, and are often associated with long-lived extreme weather conditions (e.g., 2010 Russian heat wave, Dole et al., 2011). Blocking in the NH is concentrated over the eastern north Pacific, the eastern north Atlantic, and across central north Asia (Barriopedro et al., 2010; Tyrlis and Hoskins, 2008). Blocking in the SH tends to be concentrated over the southeast Pacific, and in a zonal wave three pattern with maxima near the Date Line and over the southern Atlantic and Indian Oceans (Renwick, 2005).

There are statistically significant relationships between blocking activity and the dominant large-scale climate patterns. In the NH NAO phase relates to preferred Atlantic blocking location (Luo et al., 2010; Woollings et al., 2008), negative (positive) PNA phase favours (suppress) blocks onset in North Pacific (Croci-Maspoli et al., 2007). ENSO or MJO tropical patterns influence NH blocking activity because their influence on the mid-latitude westerly waves (e.g., Cassou, 2008).

How the location and frequency of occurrence of blocking events evolves in future is critically important for understanding regional climate change (Buehler et al., 2011). Climate models tend to underestimate blocking frequency and intensity, although they generally capture preferred locations and seasonal distributions for blocking events. Hence, model projections of blocking activity in future must be treated with caution (Matsueda et al., 2010; Scaife et al., 2010). While future trends in NH and SH blocking frequency remain uncertain, it is likely that the overall frequency of blocking events will decrease (Barnes et al., 2011; Dong et al., 2008; Wiedenmann et al., 2002), while a trend towards increasing intensity is about as likely as not.

14.2.12 Miscellaneous, Harmattan, NPGO

[PLACEHOLDER FOR SECOND ORDER DRAFT]

14.3 Regional Change

14.3.1 Overview of Regional Concept

14.3.1.1 Aims of this Section

This section assesses projections in future regional climate and interprets them in terms of projected changes in the major *climate phenomena* presented earlier in this chapter. The following sections discuss projected regional climate change in continental-scale regions similar to those used for impacts in WG1 and 2 in AR4: Arctic, North America, Central America and Caribbean, South America, Europe and Mediterranean, Central Asia and North Asia, Middle East and Southern Asia, Southeast Asia, Australia and New Zealand, Pacific Islands, and Antarctica. Each section assesses projected changes in surface temperature and precipitation, and interprets the changes in terms of the key phenomena important for climate in that region. The sections refer to the appropriate graphical summaries of the CMIP5 projections presented in Annex I (the Atlas). Maps in Annex I show smaller homogeneous sub-regions similar to those initially proposed by Giorgi and Francesco (2000) and Giorgi et al. (2001) with minor modifications similar to Ruosteenoja et al. (2003). For completeness, quantitative summaries for changes in the sub-regions are provided in Table 14.1, (presently based on Table 11.1 in Christensen et al. (2007) but to be updated with CMIP5).

This assessment does not aim to be exhaustive for several reasons. Firstly, it mainly focuses on only two key variables: surface air temperature and precipitation and so cannot provide all the information required for subsequent impact studies e.g., hydrological impacts that require evapo-transpiration. Secondly, not all of the projected change in a region can be attributed to the *key* phenomena – other as yet unidentified phenomena are also likely to be important (see also 10.6.1, where attribution issues are discussed more thoroughly). Thirdly, only raw model projections are considered here and no attempt is made to downscale climate model output to match observations, although we also consider results from regional down scaling simulations, when this adds more detailed information to the physically based understanding of projected changes. Prediction uncertainty due to model error (discrepancy with observations) is beyond the scope of this chapter, which focuses on physical processes rather than downscaling for impact studies. The spread of the multi-model ensemble is given in Annex I but it should be noted that without accounting for model error, this is not an estimate of the prediction uncertainty in future observables.

14.3.1.2 Sources of Uncertainty in Regional Climate Change Projections

Regional climate change projections share the same sources of uncertainty as for global mean projections (see Chapters 8 and 12), but the relative importance differs. Firstly, sampling uncertainty due to natural variability is much larger for regional averages than for global means, which makes detection and attribution problematic at the regional scale (Chapter 10). Secondly, aerosol forcing becomes a more important source of uncertainty on regional scales because of the spatial inhomogeneity of the forcing and the response. Thirdly, land use/cover change becomes a larger driver on regional scales (DeFries et al., 2002). Finally, projections of regional climate change also involve additional uncertainty due to the use of a cascade of uncertainty through the hierarchy of models needed to generate local information (e.g., uncertainty due to choice of downscaling scheme i.e., which regional climate model is embedded in the same general circulation model). The relative importance of the sources of uncertainty depends on the variable being projected, for example, climate models agree more readily on the sign and magnitude of temperature changes than for precipitation changes (IPCC, 2007b).

[INSERT TABLE 14.1 HERE]

Table 14.1: Temperature and precipitation projections by the AR4 global models. Original Table 11.1 from AR4. [PLACEHOLDER FOR SECOND ORDER DRAFT: AR5 models will be summarized]. Averages over a number regions of the projections by a set of 21 AR4 global models for the A1B scenario. The mean temperature and precipitation responses are first averaged for each model over all available realizations of the 1980–1999 period from the 20C3M simulations and the 2080–2099 period of A1B. Computing the difference between these two periods, the table shows the minimum, maximum, median (50%), and 25% and 75% quartile values among the 21 models, for temperature in degrees Celsius and precipitation as a fractional change. Regions in which the middle half (25–75%) of this distribution is all of the same sign in the precipitation response are colored light brown for decreasing and light green for increasing precipitation. Signal-to-noise ratio for these values is indicated by first computing a consensus standard deviation of 20 year means, using those models that have at least 3 realizations of the 20C3M simulations. The signal is assumed to increase linearly in time, and the time required for the median signal to reach 2.88 times the standard deviation is displayed as an estimate of when this signal is clearly discernable. The probability of extremely warm, wet, and dry seasons is also presented, as described in the text (in Christensen et al. (2007)). For definitions of the regions see Giorgi et al. (2001). [To be considered for Supplementary Material.]

14.3.2 Arctic

Arctic climate is affected by three documented modes of climate variability: NAO, PDO, and the AMO. These modes all have their greatest temperature impact at the margins of the Arctic region. For example, the NAO index is positively correlated with temperatures in the northeastern Eurasian sector, and adjacent coastal Arctic, and negatively correlated with temperatures in the Baffin Bay and Canadian Archipelago, but exhibits little relationship with temperature in the central Arctic (Polyakov et al., 2003). The PDO, meanwhile, plays a large role in temperature variability of Alaska and the Yukon (Hartmann and Wendler, 2005), also being positive correlated with temperatures there, and the AMO is positively associated with SST as far north as the Barents Sea (Levitus et al., 2009). The significance of the NAO for Arctic climate may be more in its impact on sea ice through the associated surface wind field: Positive NAO anomalies result in detectable ice advection anomalies that would lead to ice thinning (Rigor et al., 2002). Other more Arctic-centric analyses have revealed atmospheric variability patterns unrelated to the NAO, PDO, or AMO, but directly linked to sea ice advection, thinning, and export out of the Arctic (Overland and Wang, 2005; Overland et al., 2008; Wu et al., 2006; Zhang et al., 2008b).

The AR5 models show an ensemble-mean surface air warming pattern that is very similar to previous generations of models, with greatest warming in fall and winter, less warming in spring, and very modest warming in summer (Annex I) [PLACEHOLDER FOR SECOND ORDER DRAFT: statements to be made more precise and quantitative]. The warming is much larger than in the tropics or mid-latitudes, exhibiting the so-called "polar amplification" pattern (see Box 5.1). These simulated anthropogenic seasonal warming patterns match qualitatively the observed warming patterns over the past six decades (AMAP, 2011). Pan-Arctic temperature reconstructions based on proxy records from lake sediments, ice cores, and tree rings reveal that the observed warming is also highly unusual, and that Arctic temperatures over the past few decades have been significantly higher than any temperatures seen during the past 2000 years (Kaufman et al., 2009). Finally, the warm temperatures have been sustained in pan-Arctic land areas affected by the NAO and PDO as described above, despite the fact that both the PDO and the NAO have trended negative over the past decade. The absence of a connection between overall Arctic warming and NAO variability is particularly well documented in the literature (Semenov, 2007; Turner et al., 2007b). Thus three factors all point towards a likely role for anthropogenic forcing in the warming of the Arctic region over the past few decades: The pattern match of anthropogenic and observed warming in the Arctic, the large magnitude of the warming compared with estimates of natural variability, and the difficulty in reconciling recent trends in known modes of natural variability with the observed warming trends. This indicates that the future temperature evolution of Arctic climate on decadal time scales and longer will likely continue to be dominated by the signals of anthropogenic climate change (e.g., see Atlas projections over the 21st century for AR5 models), as the levels of anthropogenic forcing rise still further.

The most conspicuous manifestation of a warming Arctic climate is the ongoing sea ice loss during all seasons, but most prominently in late summer. The AR5 models all project significant ice loss over the course of the 21st century (make more precise and refer to atlas). However, the AR4 models consistently under simulated the ice loss of recent decades (Stroeve et al., 2007), and the AR5 sea ice projections must undergo a similar evaluation before their credibility can be assessed. Attempts at more credible sea ice projections through bias correction of AR4 models indicate ice-free Arctic summers sometime in the next 30 to 80 years (Boé et al., 2009; Wang and Overland, 2009). Natural processes also strongly affect sea ice anomalies on interannual time scales in both positive and negative senses, including Arctic-centered atmospheric circulation anomalies (noted above), cloud variations (Kay et al., 2008), and ocean circulation (Smedsrud et al., 2008). Therefore, ice loss or gain in any particular year cannot be taken as an indication of a trend due to anthropogenic forcing, or lack thereof.

Another important manifestation of Arctic climate change is hydrologic cycle intensification. The AR5 models robustly project increased moisture flux convergence and precipitation in the pan-Arctic region over the 20th and 21st centuries (refer to Atlas and be more precise), as did their AR4 counterparts (Kattsov et al., 2007; Rawlins and Coauthors, 2010). Because of a dearth of quality precipitation data in the region, it is very difficult to assess whether precipitation trends over the past few decades also show an increase (ACIA, 2005). However, river gauge observations do show consistent runoff increases of approximately 10% in Eurasian and N. American rivers draining into the Arctic since about the mid-20th century (Richter-Menge and Overland, 2009). Since the observed increasing temperatures in pan-Arctic land areas would enhance evapotranspiration, this runoff increase must be driven by an even larger increase in precipitation. Thus the available observations are qualitatively consistent with the model projections of increasing precipitation and runoff into the Arctic. However, the AR4 models diverged widely in the quantitative details of projected Arctic hydrologic change (Holland et al., 2007), underscoring the lingering uncertainty in this dimension of the region's changing climate.

14.3.3 North America

N. American regional climate is mainly affected by four modes of variability: NAO, PNA, PDO, and the North American monsoon (NoAM). The NAO affects the eastern half of N. America during winter. Positive NAO brings warmer temperatures to this zone, and a shift of the storm track northward from the southeastern U.S. to southwestern Canada (Hurrell et al., 2003). Positive PNA also affects wintertime climate, and brings warmer temperatures to western Canada and Alaska, cooler temperatures to the southeastern U.S., and dry conditions to the eastern U.S. (Nigam, 2003a). Storm track disturbances over North America may link the PNA and NAO patterns (Li and Lau, 2011, 2012). The PDO is associated with N. American climate anomalies that resemble those of the PNA (Mantua et al., 1997; Nigam et al., 1999), though the PDO is associated with much longer time scale variability. Positive anomalies of the NoAM bring excess rainfall to the northern half of Mexico and much of the southwestern U.S. during summer (Gutzler, 2004). Tropical cyclones also have a significant impact on the Mexican and U.S. Gulf Coast and the U.S. Eastern seaboard. Atlantic SST and the modes shaping it (AMM and AMO) may affect the frequency and intensity of such disturbances (Emanuel, 2007; Goldenberg et al., 2001; Landsea et al., 1999; Smirnov and Vimont, 2011; Vimont and Kossin, 2007).

There are a number of features of a warming climate that are highly relevant to ongoing and future climate change in North America. The first is that the land is expected to continue to warm more than surrounding oceans (Chapter 2, Chapter 12, Annex I). The resulting change in the land/sea contrast has dynamical consequences, in particular an amplification of the subtropical anti-cyclones located over the North Pacific and Atlantic sectors, especially in summer. The warming has also been associated with a systematic decline in the North American snowpack (Brown and Mote, 2009; McCabe and Wolock, 2010), particularly in the late spring, when temperatures rise enough above freezing that warming ought to cause additional snowmelt (Kapnick and Hall, 2011). Changes in the western North American snowpack over the last 50 years of the 20th century exceed model estimates of trends expected to occur by change due to internal variability alone (Pierce et al., 2008), indicating that anthropogenic changes in snowpack may already be underway. Projected changes in snowpack are difficult to assess with the AR5 models because of poorly resolved topography in western North America. The warming over land is also projected to lead to a two to four fold increase in the frequency of heat waves over the course of the 21st century (Lau and Nath, 2012). Finally, the AR5 models robustly predict significant summertime drying throughout the continent due to systematically increasing temperatures and evaporation, similar to previous generations of models (Chapter 12, Annex I).

Anthropogenic climate change may also bring with it systematic changes in the precipitation distribution over North America. As with previous generations of models, projections by AR5 models generally indicate a poleward shift in wintertime storm activity over the continent. They robustly produce an increase in atmospheric moisture convergence and hence precipitation in the northern third of the continent (Annex I). This change is also consistent with model projections of positive NAO trends in response to increased concentrations of greenhouse gases diagnosed in IPCC AR4 (Hori et al., 2007; Karpechko, 2010; Zhu and Wang, 2010). Thus Canada and Alaska may stand to experience a substantial anthropogenic precipitation increase over the remainder of the 21st century.

Future climate simulations also robustly predict that the climate of western North America, particularly south of the U.S. Pacific Northwest, will experience a precipitation decrease throughout the 21st century due to the same poleward shift in the storm tracks (Annex I) and associated poleward expansion and intensification of the subtropical dry zones (Seager and Vecchi, 2010). There is also broad consistency in simulated anthropogenic patterns of hydroclimate change in western N. America and the patterns of hydroclimate change observed over the course of the 20th century (Barnett et al., 2008), including the distinct dry period over the past decade (Cayan et al., 2010). However, there is disagreement in the literature as to whether the recent observed changes have a magnitude large enough to be attributable to anthropogenic forcing (Das et al., 2009; Seager and Vecchi, 2010). Still, the fact that simulations of anthropogenic changes in western N. American hydroclimate show a pattern consistency among themselves and with observations suggests the region may be particularly vulnerable to future reductions in water resource availability. A key remaining uncertainty in future hydroclimate of the western N. America is the impact of anthropogenic changes in tropical Pacific SST, since the region exhibits a documented precipitation sensitivity to SST modes in the equatorial Pacific (Cayan et al., 1999; Findell and Delworth, 2010) through the PNA mode of variability; unfortunately global models do not provide consistent information regarding anthropogenic changes in the equatorial Pacific SST (Seager and Vecchi, 2010).

Across a zone stretching from eastern N. America to northern Mexico, implications of anthropogenic climate change for precipitation are even less clear. In the southeastern U.S., the AR5 projections suggest a modest future reduction in the atmospheric supply of water vapor (Annex I). However, there is considerable variation across the ensemble, and observed precipitation variations appear to be mostly natural in origin (Seager et al., 2009a). Anthropogenic signals in summertime precipitation in North America east of the Rockies are similarly incoherent across the AR5 models (Annex I), perhaps due to the fact that this precipitation arises mostly from unresolved convective processes (Ruiz-Barradas and Nigam, 2006, 2010). Positive trends in the NoAM have been detected, particularly in areas north of the “core” monsoon area of

Arizona and western New Mexico (Anderson et al., 2010a). The AR5 simulations tend to show a reduction in precipitation in the core zone of the monsoon (Annex I), but this signal is not robust across models. Thus the evidence for current or future anthropogenic influence on the NoAM is very limited. The observed relationship between the monsoon strength and SSTs in the Gulf of California (Mitchell et al., 2002a) suggest that greater confidence in future NoAM changes may only come when this feature is better resolved by climate models.

14.3.4 Central America and Caribbean

The annual cycle of Central America and Caribbean climate is the result of air–sea interactions over the Western Hemisphere warm pool (WHWP) in the tropical eastern north Pacific and the Intra Americas Seas (IAS) (Amador et al., 2006; Wang et al., 2007). As in many other regions, transient-mean flow interactions play a key role in the characteristics of the mean circulation. For instance, the Caribbean Low Level Jet (CLLJ) is a key element of summer climate over the region (Cook and Vizy, 2010) that along with the North Atlantic subtropical high (NASH) is controlled by the size and intensity of the WHWP. The complex topography over Mesoamerica imprints a contrasting spatial structure to precipitation between the windward and leeward coasts of Central America that is rarely captured by climate models. Most IPCC AR4 projections indicate a warmer and drier future climate for the IAS region. Some observational analyses point in this direction. For instance, Comarazamy and Gonzalez (2011) have found that increased easterly surface winds over Puerto Rico for the 1950–2000 time frame disrupts a pattern of inland moisture advection and convergence, increasing cloud base heights and reducing the total column liquid water content over high elevations. This combination of elements translates into a dramatic decrease in accumulated precipitation during the Early Rainfall Season (ERS, April-June).

Interdecadal climate variations in the Mesoamerican and Caribbean region should be considered when trends in precipitation are determined. Prolonged dry or wet periods in the region are related to the combined effect of the very low frequency variability of the Pacific and Atlantic oceans (Mendez and Magana, 2010; Mendoza et al., 2007; Seager et al., 2009b). The intensity of the CLLJ appears to be an important element for easterly wave activity over the Caribbean and consequently, in determining wetter or drier conditions over the Caribbean and Central America region (Mendez and Magana, 2010). Also, an anomalously large WHWP is associated with weakened low-level jets and increased rainfall over the Intra-Americas Sea (IAS), reduced moisture transports into the eastern North Pacific and eastern North America, plus increased relative humidity and decreased vertical wind shear (Wang et al., 2008c). The shear and relative humidity above the warm pool affect hurricanes transiting the region to landfalls in the Caribbean, Central America and the US. The tropospheric mechanism linking a large WHWP to its impacts is the so-called “Gill atmosphere” response to an off-equatorial warm anomaly.

When the Atlantic sector is thought of in terms of local SST forcing, most of the CMIP3 projections from AR4 don’t make sense. SSTs increase and the WHWP as defined presently is larger by 2100 AD. Yet, rainfall over the IAS is severely reduced (IPCC, 2007b), vertical wind shear over the TNA is increased and the relative humidity is decreased (Vecchi and Soden, 2007b). However, impacts on the Atlantic sector tropospheric environment are not solely attributable to the Atlantic sector SSTs but more to their relationship to the global tropical SSTs — in other words, the competition between the WHWP and the Indo-Pacific warm pool (Latif et al., 2007; Vecchi and Soden, 2007c). The AR4 models warm the North Atlantic considerably less than the Pacific due to a reduced Atlantic meridional overturning circulation (AMOC), such that the WHWP behaves like an anomalously small/cool warm pool within the global context. As a result, overall tropical cyclone (TC) activity decreases in embedded models that resolve TCs (Knutson et al., 2008). This may also have an important effect in reducing total precipitation in the region, in addition to arguments that the drying trend in the IAS region is consistent with the weakening of the meridional overturning circulation in the atmosphere (Held and Soden, 2006; Vecchi and Soden, 2007a).

There are only a few examples of dynamical and statistical downscaling covering the Mesoamerican region. The expected increase of temperature for the mid of the 21st century is between 2 and 3°C, depending on the region, the scenario and the model under consideration (Karmalkar et al., 2011; Rauscher et al., 2008; Vergara, 2007). Most downscaled versions of the GCMs project decreases in precipitation over most of Mexico but only a few have considered the role of key elements that result in regional climate Mesoamerica and the Caribbean (Karmalkar et al., 2011).

14.3.5 South America

South America undergoes influences of large-scale atmospheric and oceanic systems as well as of regional systems. Pacific (ENSO) and Atlantic (SST tropical gradient) have a role on interannual climate variability of several regions of this continent; teleconnections, like Pacific South America (PSA), Southern Annular mode (SAM), Indian Ocean Dipole (IOD), can be related to climate variability over South America. Blocking conditions over Pacific and Atlantic Oceans, Southern Hemisphere stationary waves and storm tracks have also a role on South America climate variability. In a regional scale, the South America Monsoon System (SAMS) is responsible for the rainy season in large areas of the continent; South Atlantic Convergence Zone (SACZ) and Atlantic Intertropical Convergence Zone (ITCZ) also affect precipitation in large areas of South America.

ENSO is one of the main sources of interannual variability over South America. Northeast Brazil is affected by droughts in El Nino and floods in La Nina, while large areas of La Plata basin have floods in El Nino and droughts in La Nina. The mechanisms of these influences during ENSO events are changes in the Walker circulation that affect tropical South America, and influences of wavetrains from tropical Pacific to South America that affect the southern and southeastern continent. There has been no consensus about the ENSO behaviour in the future, as discussed in (Coelho and Goddard, 2009). However, a reconstruction of ENSO events since 16th century indicated the increase in frequency of such events during the 20th century, likely related to anthropogenic forcing (Gergis and Fowler, 2009). Precipitation changes over South America projected by some models are consistent with El Nino influences, i.e., increase rainfall over southeastern and north-western South America and reduced over Northeast (Marengo et al., 2009).

Besides Pacific Ocean influences on South America, the tropical Atlantic SST anomalies also affect precipitation over northern and northeastern South America through the ITCZ position and intensity. Northeast Brazil, region with high temporal and spatial variability is frequently affected by droughts associated with the ITCZ anomalies. Tropical North Atlantic SST anomalies can be related to displacements of NAO centers, which change the atmospheric circulation and affect ITCZ position (Souza and Cavalcanti, 2009). The ITCZ shifting southwards due to increased aerosol over North Atlantic, which reduces the North Atlantic SST (Chang et al., 2011) and Atlantic thermohaline circulation (Stouffer et al., 2006) can affect precipitation over Northeast Brazil.

Precipitation over southeastern South America and southeastern Brazil is influenced by the Southern Annular Mode (Reboita et al., 2009; Vasconcellos and Cavalcanti, 2010). The mechanisms of these influences are related to changes in storm tracks, jet streams position and intensification of PSA anomalous centers by the SAM. The wavetrain over South America intensified by the influence of SAM on PSA, results in a cyclonic/anticylonic pair over the continent and a related precipitation dipole anomaly, responsible for extreme precipitation in the South Atlantic Convergence Zone (SACZ), as discussed in Vasconcellos and Cavalcanti (2010). The future projections indicate increase of Sea Level Pressure at middle latitudes of South Atlantic Ocean (Seth et al., 2010a), as the Atlantic Subtropical High is displaced polewards, behavior that can be related to the positive trend of the AAO index and poleward shifting of the stormtracks. PSA strengthening in future projections affects the precipitation dipole over South America, increasing the precipitation in the southern center and reducing in the northern center (Junquas et al., 2011a). However, analyses of CMIP3 models by (Menendez and Carril, 2010) show that extreme precipitation over South Hemisphere continents will have little impact from SAM during the last thirty years of 21st century, except in Patagonia and southern Australia.

Amazonia region has a large influence on the global climate, as it has large contribution to the hydrological cycle. It is one of the three regions with maximum tropical precipitation, together with Indonesia and Tropical Africa. The source of humidity to the atmosphere due to evapotranspiration is also large, being responsible for precipitation in other areas of South America. The deforestation in the region has been reduced in recent years, but large areas in the southern sector were already changed to agriculture or pastures areas. Experiments simulating deforestation in Amazonia show strong impacts on several atmospheric variables, including precipitation (Salazar et al., 2007). Extreme droughts in the first decade of 21st century in Amazonia (2005 and 2010) were considered the worst droughts since 1950 (Marengo et al., 2008). Studies on the causes of these droughts indicated the role of North Atlantic warmer than normal SST (Marengo et al., 2008). This condition enhanced ascent motion over North Atlantic and forced subsidence over Amazonia. The north-south SST gradient was favourable for the ITCZ displacement northward, and it was consistent with convection shift to the north and changes in the low level trade winds, which normally brings humidity to the continent in the beginning of the South America Monsoon. Analysis of north-south Atlantic SST gradient in (Good et al., 2008) during the dry season (JJA), showed high negative correlation with precipitation over Amazonia, and also over Northeast Brazil. Relations between this gradient and precipitation in southern Amazonia were also obtained in a CGCM under 1% CO_2 increase, by Good et al. (2008), who suggested that uncertainties in projected changes of the meridional Atlantic SST gradient would be linked to uncertainties in southern Amazonia precipitation during the dry season. This SST gradient also occurs during the rainy season, similar to what occurred in 2005 and 2010 associated with the extreme droughts. AGCM experiments in (Harris et al., 2008) also indicate the influence of Atlantic SST north-south gradient and Pacific SST on Amazonia precipitation. Projections from Regional Models show reduction of rainfall over Northeast Brazil, central-eastern and southern Amazonia, and increase over coast of Peru and Equator, in a warmer climate (Marengo et al., 2010b) .

Other region that is influenced by modes of variability is the La Plata Basin (LPB) region. This is the second largest basin in South America and has the main hydroelectric power plant of this continent. LPB receives large portion of humidity from the Amazon region through the Low Level Jet (LLJ), which feeds mesoescale convective systems frequent in the region and several times responsible for flooding. Higher frequency of LLJ in future model projections was obtained by (Soares and Marengo, 2009). Increased moist flux from the Amazon Basin to the La Plata Basin is consistent with the precipitation increase in the southern regions. Increased precipitation in LPB is projected by CMIP3 models under future global warming scenarios compared to the 20th century (Bombardi and Carvalho, 2009; Marengo et al., 2009; Nunez et al., 2009; Seth et al., 2010b). However, some regional models project less precipitation in the northern sector of the basin.

Atmospheric circulation and precipitation changes over southern South America, in future projections of a regional model, are related to the shifting of Atlantic and Pacific subtropical highs southward and increase of the Chaco low, through a decreased Sea Level Pressure over northern Argentina, an increase in northerly winds over northeastern Argentina, which causes moisture convergence and precipitation in that region (Nunez et al., 2009). The geopotential height increase over southern South America, in projections of JJA, indicates a strengthening of the meridional gradient and stronger westerlies. The changes are consistent with a poleward shifting in the subtropical storm tracks. Another important result is the increase of meridional wind at low levels over the continent, which could represent an increase in the Low Level Jet occurrences. The changes in circulation induce the projected precipitation changes: increased precipitation in central Argentina associated with the enhanced cyclonic circulation of the Chaco low, southward shifting of the Atlantic subtropical high, with humidity advection displaced to that area, in the summer. In the winter, there is reduced precipitation projection over southeastern South America, due to poleward shift of the stormtracks which reduces the cyclonic activity over the region. The shifting of the subtropical high polewards agrees with results of Lu et al. (2007) on the Hadley cell expansion under global warming. This expansion changes the region of subsidence and the subtropical high pressures move southwards. Also, it has an impact on the cyclone and cyclogenesis activity off the Southeast South American coast, where simulations considering future climate scenarios indicate a displacement to the south of their climatological position (Kruger et al., 2011).

Projections of several CMIP3 models and regional models in PRECIS project indicate an increase of southerly winds close to the southwestern South America coast and extension of the upwelling region southward. These changes lead to SST cooling near the coast and reduced temperatures in the coastal areas (Garreaud and Falvey, 2009). The poleward shifting in the stormtracks is consistent with the projected precipitation decrease. Projected precipitation changes in a multi-model analysis of 11 CMIP3 A2 scenario, in the Altiplano region, show an increase in westerly flow at mid and upper levels over central Andes which results in a decrease of moisture transport towards the Altiplano from the interior of the continent during summer, reducing the precipitation between 10% to 30% relative to current values (Minvielle and Garreaud, 2011).

Extreme temperature analysis in regional model projections for future climate indicates increase of warm nights over South America, except in parts of Argentina and reduction of cold nights in the whole continent

(Marengo et al., 2009). Extreme droughts and floods have occurred more frequently in recent years in several regions of SA. These occurrences have contributions from large-scale atmospheric and oceanic features and also from local conditions. Increase in extreme precipitation over La Plata basin region and decrease in central Amazonia and northern South American coast, as well as in number of extremes is projected for the last thirty years of 21st century (Marengo et al., 2009). Number of consecutive dry days increases in northeastern South America in the projections.

14.3.6 Europen and Mediterranean

14.3.6.1 Northern Europe

European climate is heavily influenced by the North Atlantic storm track (especially from October-March) and heat and moisture fluxes from the North Atlantic Ocean. NAO is strongly related to both of these processes and hence has a profound influence on European climate. However, other modes such as ENSO, EAP, AMO etc. as well as ambient conditions are also important in different periods and on different time scales. This section will review recent progress on the relevance of changes in modes for future changes in storminess, precipitation and temperature in Northern Europe.

14.3.6.1.1 Storminess (extreme surface wind speeds)

There remains a lot of uncertainty and model differences in the regional predictions of trends in extra-tropical cyclones (Albrecht et al., 2009; Ulbrich et al., 2009). Several modelling studies suggest that there are likely to be fewer extra-tropical cyclones on average over the hemispheres, associated with a slight poleward shift in the storm track and that the central pressure of these storms will be lower (Meehl et al., 2007b). One source of uncertainty arises from the use of different measures of storminess in different studies: this makes it difficult to cleanly compare conclusions from studies (Ulbrich et al., 2009). More recent studies have involved the use of ensembles of coupled models (Gastineau and Soden, 2009; Leckebusch et al., 2007b; Ulbrich et al., 2008); or the use of high resolution coupled models to look at changes in intensity (Bengtsson et al., 2009); or regional models to look at the local impact of changes in storms (Jiang and Perrie, 2008; Lionello et al., 2008a). Pinto et al. (2006) found a slight poleward shift in deep cyclones and a decrease in the density of all cyclones in a greenhouse gas simulation with ECHAM4/OPYC3. They also found that the changes were not simply related to changes in the mean sea-level pressure. Pinto et al. (2007a) and Pinto et al. (2009) investigated this further and explored the relationship of changes in extreme cyclones with changes in NAO. Donat et al. (2010) found an increased number of European storm days in 9 SRES A1B climate model simulations, and found the increase was more than expected from changes in weather types. Della-Marta and Pinto (2009) explored the uncertainty in winter storm changes over the N. Atlantic and Europe and found a similar result.

14.3.6.1.2 Precipitation (flooding and droughts)

Observational studies have revealed that 20th century winter precipitation trends over Europe are primarily related to changes in atmospheric circulation and the frequency of preferred weather regimes (Boe and Terray, 2008; Pauling and Paeth, 2007). In addition, dynamical meteorology arguments suggest that the intensity of precipitation should multiplicatively depend on the strength of the zonal flow i.e., NAO (Sapiano et al., 2006). Hence, an increase in NAO is likely to increase both the number of wintertime storms heading into N. Europe and also the average intensity of precipitation per storm. In summertime, Folland et al. (2009) found that a positive response in NAO to greenhouse gas concentrations in two climate model simulations resulted in increased summer droughts for northwestern Europe.

14.3.6.1.3 Temperature (heat waves, cold spells, etc.)

A 1000-year climate model simulation showed that the coldest winters in Scandinavia are related to NAO (Gouirand et al., 2007) and unusual temperature extremes were found during the negative NAO event of 2009 (L'Heureux et al., 2010).

14.3.6.2 Mediterranean

The Mediterranean region (MR) here so defined includes the Southern Europe below 45°N latitude along with the North Africa and West Asia rims of the basin. It is generally considered as a transitional region between the mid-latitudes and subtropics with a division line moving seasonally across the area (Lionello et al., 2008b). Hence it is influenced both by extra-tropical and tropical climate dynamics. The most relevant phenomena affecting the region climate variability in diverse periods and time-scales are: the North Atlantic Oscillation (NAO), the European blocking pattern (EB), the Asian Summer Monsoon (ASM) and the Atlantic Multidecadal Oscillation (AMO). Many others modes have been found for the MR but most of them appear as not independent or have a less significant influence.

The cold season precipitation (October to March) interannual variability is mainly controlled by NAO because its influence on the steering of storm tracks paths and the cyclonic storms regionally enhanced or induced in the MR by orography, land-sea distribution and surface conditions. In the negative (positive) phase higher (lower) than normal precipitation prevails in western and European MR. However in the eastern and southeastern rims of the basin an opposite behaviour is attributed to the induced cold air advection over the relatively warm Mediterranean that leads there to instability and rainfall during the positive NAO phase (Feliks et al., 2010). The influence of NAO on winter temperature anomaly patterns is most relevant in the eastern MR likely due to the cold (warm) air advections prevailing over this sector during the positive (negative) phase of the phenomenon (Elmallah and Elsharkawy, 2011; Türkes and Erlat, 2009). In the west and central MR the thermal signature is weaker possibly modulated by radiative and cloud cover influences (Trigo et al., 2004). But the magnitude of regional anomalies associated to NAO depends critically on the location of its centres of action. Thus the observed interdecadal variability in the location of the two NAO centres of action has determined the strengthening of NAO precipitation correlations through the last decades coinciding with a eastward shift of both nodes (Vicente-Serrano and López-Moreno, 2008).

The more northerly position and smaller extent of summertime NAO should imply a weaker influence of this mode on MR sea-level pressure (SLP). Despite that, positive summer NAO phase is associated with enhanced cloudiness and precipitation in central and east European MR and cooler than normal conditions across the eastern sector (Folland et al., 2009; Mariotti and Dell'Aquila, 2011; Zveryaev and Allan, 2010). This opposite signature relative to winter NAO may be attributed to the development of an upper-level cool-air anomaly over the Balkans during positive summer NAO which increases potential instability and rainfall in such MR sector (Bladé et al., 2011).

Other modes have been defined for the MR as the Eastern Atlantic (EA) and the Eastern Atlantic-Western Russian (EA/WR) patterns in the upper-troposphere large-scale circulation (Hatzaki et al., 2009; Krichak and Alpert, 2005). Both resemble the NAO upper-air pattern albeit with its centers of action south-ward or southeast-ward shifted. Accordingly these modes anti-correlate with winter precipitation over the Eastern MR because its negative phase is associated to an enhancing advection of humid and warm air towards that sector combined with local cyclogenesis, while it is related to below-average precipitation in Southwest Europe (Xoplaki et al., 2004). The influence of these "shifted" NAO-like upper-air patterns on winter temperature anomalies is more relevant and positively correlated in the western MR, but negatively correlate in the eastern sector (Hatzaki et al., 2009) with a less clear signature on the south-eastern rim of the Mediterranean basin (Hasanean, 2004). These patterns have not noticeable influence on MR summer climate variability.

Despite the blocking pattern (EB) usually last less than a few weeks, the anomalies induced can be sufficiently intense to lead to significant monthly and seasonal climate anomalies all across the MR. But the anomaly sign and intensity depend critically on the high-pressure blocking position. When it is located over Scandinavia and Northern Russia the pattern resembles the SCAND circulation mode pattern in its positive phase (Bueh and Nakamura, 2007). This tends to be more frequent in winter-spring seasons and is associated to higher than normal precipitation across the MR with extreme rainfall in its central European sector (North Italy and the Balkans) and to colder than normal conditions in Southern Europe (Barriopedro et al., 2006). In contrast to this, a high-pressure blocking over central Europe induces anomalous dry and warm climate over most of the MR. In the summer season the most important warming pattern in western MR is linked to blocking conditions, but no significant signal was detected for the Eastern sector (Xoplaki et al., 2003).

There are evidences of a connection between the ASM and the eastern MR very dry summer climate which is attributed to the air subsidence remotely forced to its west and northwest by the characteristic monsoon upward motions (Ziv et al., 2004). Thus, a southward shift of the monsoon heating may weak the subsidence over eastern European MR and lead to a wetter climate. Alpert et al. (2008) pointed that the onset and latitude of the monsoon determine the summer precipitation patterns in this MR sector. The dry and hot summer climate in the MR presents also significant correlations with West African monsoon albeit current studies seem to attribute this linkage to an influence of MR on such monsoonal phenomenon instead of the opposite way (Mohino et al., 2011; Polo et al., 2011).

Finally, the oceanic mode AMO seems to drive decadal and multidecadal climate variations in the MR, though its influence (positive correlation) is restricted to the air temperature in summertime. A more weak signal has been found in the transition seasons affecting only to the western MR sector, but none AMO signature has been found in winter air temperature nor in the year round precipitation (Mariotti and Dell'Aquila, 2011). The connection mechanisms are still unclear. It is hypothesized that AMO influences on the eastern sub-tropical Atlantic SLP could induce anomalous heat advection over the west MR and other studies show some multidecadal linkages between AMO and ASM (Feng and Hu, 2008a) which could indirectly affect east MR climate as mentioned above.

Since long it is recognized that coarse resolution global models have shortcomings in reproducing realistically cyclones and precipitation patterns in the MR which are highly influenced by complex interactions between large-scale circulations, complex orography, land-sea thermal contrast and surface conditions in the MR. This inconvenience has been partly overcome by new versions of finer resolution global climate coupled models and the more frequent use of regional climate models, some of them air-sea coupled, though quantitative results are quite sensitive to the climate model used (Raible et al., 2010). During winter most of the models project a rainfall decline along this century in most of the MR, albeit some of them show an increase in the north-western sector (Elguindi et al., 2011; Giannakopoulos et al., 2009; Giorgi and Lionello, 2008; Kjellstrom et al., 2011; Raible et al., 2010). This is attributed to a northward shift of the Atlantic storm track and therefore an increase of anticyclonic circulation over the MR and more frequent positive phase NAO events leading to less favorable conditions to storm generation. However some global models with very high vertical resolution in stratosphere do not reproduce such storm track shift resulting in a more noticeable winter precipitation increase in southwestern Europe (Scaife et al., 2011). The patterns of precipitation change in summer season are coincident in all of the current climate model projections leading to a significant rainfall decrease across the MR. Nevertheless this particular agreement among models should not be translated in terms of certainty, because the positive correlation between the summer NAO and precipitation patterns in the MR is not reproduced, and thus the projected upward summer NAO trend do not lead to the associated rainfall enhance in part of the MR on the grounds of current observations (Bladé et al., 2011).

Concerning precipitation extremes, Boberg et al. (2010) analyzed an ensemble of high-resolution RCM simulations driven by diverse GCM of A1B-SRES over Europe to obtain an annual increase of intense precipitation days over the Mediterranean region (with the exception of the Iberian Peninsula) which amplifies with time along the 21st century. However Nikulin et al. (2011), using one RCM driven by six different GCMs, found a great inconsistency in geographical patterns of change among the simulations in summer, while in winter the ensemble average shows small intensification of precipitation extremes over the northern rim of the MR.

There is an almost unanimity in climate change scenarios pointing to a widespread increase of mean temperatures in the MR, being the signal stronger in summer than in winter (Elguindi et al., 2011; Giannakopoulos et al., 2009; Giorgi and Lionello, 2008; Hertig and Jacobeit, 2008; Kjellstrom et al., 2011). The magnitude of warming is in consonance with the intensity of the GHG forcing both across scenarios and future time periods. Differences between the amount of warming projected by the diverse climate models is generally smaller than the mean signal, which gives to these results a rather high confidence level.

Concerning thermal extreme events, diverse regional model projections have identified a tendency toward an increase both in frequency and intensity all across the MR. As an illustrative example, Fisher and Schär (2010) analyzing a set of high-resolution regional climate change simulations showed that for the Iberian Peninsula and the MR the number of heat wave days is projected to increase from an average of about two days per summer for the period 1961–1990 to around 13 days for 2021–2050 and 40 days for 2071–2100. Furthermore since diverse modeling studies have clearly identified a possible amplification of temperature extremes by soil moisture state (Hirschi et al., 2011; Jaeger and Seneviratne, 2010), this mechanism could further magnifies the intensity and frequency of heat waves in the MR given the projected enhance of summer drying conditions in all of the global warming scenarios.

14.3.7 Africa

The African continent encompasses a variety of climatic zones, quite homogeneous in the zonal direction. To the north of the Sahara desert, the Mediterranean coast experiences dry summers and receives its rain from mid-latitude systems during winter. In tropical latitudes, rainfall by and large follows insolation (although this simplified picture is modified by the presence of orography, especially in the Great Horn of Africa, and by the influence of the oceans). Equatorial regions experience rainfall year round, with clear double peaks in correspondence of the equinoctial seasons, when the sun is overhead. Away from the equator, semi-arid regions receive rainfall only during the summer monsoon. Climatic variability is mostly homogeneous within the same separation lines that define the annual cycle and thus we organize this section around the following regions: the Mediterranean rim of North Africa, the Sahel, East Africa, the Congo basin, and Southern Africa.

14.3.7.1 Sahel

Sub-Saharan climate is dominated by the monsoonal system that brings rainfall to the region during only one season. This season, which goes from Mai/June to September, provides all the water needed by the region for the vegetation, agriculture and other human activities. The rainfall during these 4 months is brought by 10 to 20 systems of large extent and very strong intensity that travel from the horn of Africa to the Atlantic Ocean. The timing and sequencing of these systems is thus critical for natural and human systems in the region. The onset of the rainy season is one of the key parameters as it triggers changes in the vegetation and surface properties. The length and frequency of dry spells is another of the critical parameters defining the quality of monsoon season. These parameters, as well as the length or cumulated rainfall of the season, are affected by a large inter-annual variability. As they are intimately linked to the large convective systems bringing the rainfall their variability needs to relate to the large scale conditions and local surface states which govern their life cycle. It is particularly critical when evaluating the sensitivity of models to take into account their ability to reproduce these characteristics of the African Monsoon.

Because of its exceptional magnitude and its clear link to global SST, 20th century decadal rainfall variability in the Sahel is a test of GCMs ability to produce realistic long-term changes in tropical precipitation. Despite substantial biases in the region (Cook and Vizy, 2006) the CMIP3 coupled models overall can capture the observed correlation between Sahel rainfall exhibit and bulk indices of SST variability (Biasutti et al., 2008) even though individual models may fail to capture the details of the SST/rainfall relationship, especially at interannual time-scales (Lau et al., 2006). In response to centennial changes in the tropical Atlantic meridional gradient of SST and in Indo-Pacific SST, the CMIP3 ensemble produces a robust drying of the Sahel in simulations of the 20th century, leading Biasutti and Giannini (2006a) to estimate that at least 30% of the 1930–1999 drying trend in the Sahel could be attributed to anthropogenic forcings. More recently, Ackerley et al. (2011) used a perturbed physics ensemble based on the Hadley center coupled model to examine the trends after 1940 and came to a similar estimate for the role of sulfate (a drying of about 5mm/month per decade, which amount to half of the 1940–1980 trend). These ensemble results confirm previous studies that had simulated drought in the Sahel in response to either just the indirect effect of sulfate aerosols (Rotstayn and Lohmann, 2002) or both historical aerosols and greenhouse gases (Held et al., 2005).

The droughts of the 20th century in West Africa, which were the largest and most intense observed (ref. to other chapter) were characterized by fewer convective systems but systems of the same intensity as during the wet years (LeBarbe and Lebel, 1997; Lebel and Ali, 2009).

A clear attribution of past drought to anthropogenic forcings rests in part on whether the relative cooling of the north compared to the south Atlantic can be ascribed to sulfate aerosols (Chang et al., 2011) or natural variability in the form of the Atlantic Multidecadal Oscillation (Knight et al., 2006; Ting et al., 2009). In any case, a large effect of natural multi-decadal SST and global warming of the oceans on Sahel rainfall seems beyond doubt (Hoerling et al., 2006; Mohino et al., 2011; Rodriguez-Fonseca et al., 2011; Ting et al., 2009, 2011).

A challenge for quantifying the true role played by 20th Century anthropogenic forcings in the Sahel drought is that the amplitude of simulated rainfall anomalies at all timescales is much smaller than observed and that models are unable to reproduce the fact that the droughts were caused by fewer convective systems but with unchanged intensities. This suggests that the current generation of models might be missing some important processes (for example, mesoscale organization of convection or feedbacks between climate, vegetation, and dust) and forcings (for example, aerosols produced by biomass burning, or land use changes). Previous studies have identified West Africa as an area where the feedback between atmospheric and continental processes might be key in the rainfall generating systems (Koster et al., 2004).

In projections of the 21st century, as the effect of anthropogenic aerosols fades and the effect of GHG becomes dominant, changes in annual mean Sahel rainfall become less certain: the CMIP3 models produced both significant drying and significant moistening (Biasutti and Giannini, 2006b; Cook and Vizy, 2006; Held et al., 2005; Lau et al., 2006), and the mechanisms by which a model dries or wets the Sahel are not fully understood (Cook, 2008). Nevertheless the CMIP3 ensemble simulates a more robust response during the pre-onset and the demise portion of the rainy season (Biasutti and Sobel, 2009; Seth et al., 2011). Rainfall is projected to decrease in the early phase of the seasons - implying a delay of about a week in the onset; but is projected to increase at the end of the season - implying an intensification of late-season rains (d'Orgeval et al., 2006). Projections of a change in the timing of the rains is common to other monsoon regions (Biasutti and Sobel, 2009; Li et al., 2006; Seth et al., 2010b) including Southern Africa (Shongwe et al., 2009). Biasutti et al. (2008) have shown that simulated 21st century changes in Sahel rainfall cannot be linearly derived from changes in tropical SST indices in the same way as interannual variations or 20th century trends can. Different patterns of SST change might be responsible for the 21st century trend (some non-stationarity in the Sahel/SST relationship has been noted at interannual time scales (Janicot et al., 2001; Mohino et al., 2011), but local responses to GHG may also affect precipitation independently of SST.

The relevance of a local effect is supported by several lines of evidence. First, since the AMMA experiment there is observational evidence that local soil moisture gradients can trigger convective systems and that these surface contrasts are as important as topography for generating these systems, which bring most of the rain to the region (Taylor et al., 2011a; Taylor et al., 2011b). The second evidence comes from simulations of future rainfall changes in West Africa by regional climate models (RCMs) subject to coupled model-derived boundary conditions. Patricola and Cook (2010) choose one RCM and create an ensemble by running it with boundary conditions from 9 different coupled models from the CMIP3 archive; in a complementary experiment Paeth et al. (2011) compare the projections of different RCMs driven by the same CGCMs. In both cases, the choice of RCM appears crucial: in Patricola and Cook (2010) using the same RCM reduces the spread in projections from that of the original CGCM simulations, in Paeth et al. (2011) different RCMs fundamentally modify the trend seen in the driving CGCM simulation. This behavior indicates that local processes internal to the RCM have enough influence to change the Sahel response to global SST. Patricola and Cook (2011) document a wetting response of the Sahel to increased GHG in the absence of other forcings, but the relative importance of this effect versus the response to SST trends is not well quantified, mostly due to the limitation of using a single RCM. It must be noted that RCM cannot either reproduce the processes that generate the convective systems and thus do not yield a realistic intra-seasonality of the rainfall.

A third line of evidence comes from the analysis of changes in Sahel surface energy budgets in coupled model simulations. Giannini (2010) notes that the surface warms through mostly terrestrial or mostly solar radiation in different models, and interprets this as the result of one of two forcings being dominant. Anthropogenic greenhouse gases increase net terrestrial radiation at the surface, which both warms the land and increases evaporation, favoring low-level vertical instability, near-surface convergence, and increased precipitation (the terrestrial radiation input is amplified via water vapor feedback). Instead, tropical SST warming acts as a source of free-troposphere moist static energy that increases upper level stability, decreasing rainfall and evaporation, and warming the surface through increased net solar radiation. Finally, analysis of a coupled model in which SST has little influence on Sahel rainfall has shown that warming by GHG enhances the development of the Sahara heat low and induces a stronger monsoon (Haarsma et al., 2005). To some degree, this mechanism is present in all CMIP3 models, but while the relationship between a stronger Sahara Low and a stronger monsoon is robust, the relationship between Saharan temperature and the strength of the Sahara Low is not (Biasutti et al., 2009).

Temperature projections are of course more robust than the precipitation projections, although the amount of warming depends in part on whether precipitation will decrease or increase (dryer land would permit less evaporation and lead to warmer surface temperatures). Battisti and Naylor (2009) show that in a middle-of-the-road scenario, the CMIP3 models indicate that by the end of the historical data. Biasutti and Sobel (2009) suggest that the warming will be strongest in early summer, when rainfall anomalies are negative and Patricola and Cook (2010) combine temperature and humidity data to estimate (in the A2 scenario) that the Sahel will see 160 days a year with a high risk of heat stroke (heat index above 314 K).

Finally, we note that it is not clear whether the CMIP3 projections for 2100 can be of guidance for climate change in the Sahel in the next few decades. One reason is the aforementioned large effect of natural variability, the other is the effect of projected land-use changes---which are not included in the CMIP3 integrations but, under the assumption of significant vegetation loss, might be a dominant cause of warming and drying in the near future (Paeth and Thamm, 2007; Paeth et al., 2009). Whether such an assumption is warranted is controversial (Larwanou and Saadou, 2011; Tougiani et al., 2009). Furthermore the coarse resolution of models used for the CMIP simulations do not allow to represent properly the rain generating systems in the Sahel and their interactions with the processes on the continents. For the moment only model running at a few kilometers resolutions could reproduce the atmospheric processes responsible for the life cycle of these convective systems (Kohler et al., 2010).

[PLACEHOLDER FOR SECOND ORDER DRAFT: East Africa, South Africa, Central Africa]

14.3.8 Central Asia and North Asia

Observational temperature records indicate that some of the strongest warming trends during winter (>2°C per 50 years) in the second half of the 20th Century are found in the northern Asian sector (40°–70°N 50°–140°E). The pattern of precipitation trends is less spatially homogeneous, and exhibits both wet and dry tendencies in various locations within this region. The model analysis performed by Knutson et al (2006) suggests that this prominent warming in this region could mostly be attributed to internal variability of the climate system associated with the North Atlantic Oscillation (NAO) and Arctic Oscillation (AO), both of which are known to affect the surface temperature over northern Asia (Sung et al., 2010; Takaya and Nakamura, 2005). A substantial fraction of the recent warming over northern Asia is related to the prominent positive trend of the AO index during the 1980s and early 1990s. Hence model simulations that do not take this natural factor into account are not expected to replicate the full extent of the observed warming in northern Asia. The climate change in this region is likely the consequence of both anthropogenic and natural causes. For Central Asia, observations show no systematic spatially coherent trends in the frequency and duration of extreme precipitation events (Klein Tank and others, 2006).

Climate change hot-spots analysis using the regional climate change index using the mean and interannual variability of temperature and precipitation with the 14 CMIP3 simulations for SRES B1, A1B and A2 scenarios reveals that hot-spots firstly emerges in Northwest China and Mongolia (Xu et al., 2009). The Northeast China hot-spot becomes evident by the mid of the 21st century and it is the most prominent area by the end of the century. They also noted that even in the lowest B1 scenario hot-spots will emerge in the Tibetan Plateau and Northwest China. (Sato et al., 2007) applied two types of dynamical downscaling (DDS) methods with the RCM to investigate the precipitation change over Mongolia in July due to global warming; one is a traditional DDS method in which an RCM is directly nested within a GCM, while the other is a pseudo global warming downscaling method. The two DDS methods show similar results with respect to the changes in precipitation in July where precipitation decreases over northern Mongolia and increases over southern Mongolia. Soil moisture over Mongolia also tend to decrease in July because of the combined effect caused by the decrease of precipitation and the increase of potential evaporation due to rising air temperature, implying more frequent severe droughts in this region by global warming. Future projections by CMIP3 models showed a precipitation decrease in future spring and summer, which is consistent among models (IPCC, 2007), but winter and autumn precipitation tends to increase but with less confidence. Extremes precipitation indices, however, are projected to increase significantly in this region (Kamiguchi et al., 2006).

14.3.9 Eastern Asia

The East Asian summer climate and its variability are associated with water vapour flux along the periphery of the western North Pacific subtropical high (Bonin High). The intensity and poleward extension of the Bonin High is positively correlated with convective activity around the Philippines (Pacific-Japan or PJ pattern) (Kosaka and Nakamura, 2010). The latter is related to tropical cyclone (typhoon) activity. ENSO affects the subtropical high through modulation of convection in the western tropical Pacific (Wang and Zhang, 2002; Wang et al., 2000). The Meiyu-Changma-Baiu rain band appears in early summer season from eastern China through western and central Japan. There is a tight collocation between the rain band and mid-tropospheric warm advection by the SW-NE oriented subtropical jet (Sampe and Xie, 2010). The wintertime circulation is characterized by monsoonal northerlies between the Siberian High and Aleutian Low.

The observations exhibit an overall decreasing tendency in the East Asian summer monsoon rainfall over land in the latter half of the 20th century (Wang and Ding, 2006). The recent warming in the Tropics, which reduces the land-sea temperature contrast represented by the tropospheric mean temperature, is a primary cause for the weakening of the East Asian summer monsoon since the late 1970s (Li et al., 2010; Zhou and Zou, 2010), resulting in increased droughts in northern China and flood in southern China. Qian et al. (2009) found that both the frequency and amount of light rain have decreased in eastern China for 1956–2005 with high spatial coherency. This evidence suggests that the increased aerosol concentrations produced by air pollution have suppressed the light rain events observed in China over the past fifty years. Wang et al. (2006) have examined the long-term precipitation instrumental records for Seoul, Korea for the 1778–2004 period. They reported significant rising trends in summer precipitation amount and an index of precipitation intensity. These investigators further noted that the positive precipitation trends are particularly prominent in the post-1950 era. The annual precipitation in Japan varies largely from year to year, and no clear trends of increases or decreases have been observed (JMA, 2011). However, interannual variability has gradually increased since the 1970s. Daily precipitation observation record over Japan since 1901 indicates that the annual number of days with a heavy precipitation more than 100 mm per day shows a significant long-term increasing trend, a 20% increase from the 30-year period at the beginning of the 20th century to the recent 30-year period. Summer mean precipitation in Korea has been increased by about 15% since 1990s.

Over the Far East region, wintertime storm track activity shows peculiar characteristics, such as midwinter suppression (Nakamura, 1992). In late winter through early spring, events of strong southerlies occur over Japan associated with synoptic cyclones developing to the north. The first of such events is called "Haru-Ichiban", the first storm of the spring. Reanalysis data shows that its early occurrence tends to follow the enhanced winter storm-track activity with less apparent minimum in midwinter, and vice versa, in the course of the seasonal march. (Nishii et al., 2009) indicates that, using the CMIP3 models with the highest reproducibility of the storm-track activity, the future enhancement is likely in the midwinter storm-track activity associated with the weakening of the East Asian winter monsoon, implying that Haru-Ichiban is likely to occur earlier in the late 21st century than in the 20th century.

Unusually cold and cloudy summer is brought about over northeastern Japan by northeasterly winds blowing from the North Pacific ("Yamase" in Japanese). Most of the 18 CMIP3 models project increases of the Yamase frequency in August in future, for which a weakening of mean tropical circulation, including the Walker circulation, is considered to be responsible (Endo, 2012).

The CMIP3 multi-model ensemble scenario projections of future climate indicate an increased summertime rainfall over eastern Asia due to enhanced moisture convergence under the warmer climate, despite a tendency towards weakening of the monsoonal flows themselves. However, large uncertainty exists in the projection of monsoon precipitation (Ding et al., 2007; Kripalani et al., 2007a). CMIP3 models project an intensification of East Asian summer monsoon rainfall interannual variability in the twenty-first century (Lu and Fu, 2010a). Kim and Byun (2009) investigated effective drought index using 15 CMIP3 model results. They found that South Asia and East Asia showed a greater increase in the standard deviation of precipitation than the mean precipitation, with an amplified seasonal precipitation cycle. This amplified seasonal precipitation cycle suggests future drought as well as flood under global warming scenario.
There are dynamical downscaling approaches that better reproduce the Meiyu-Changma-Baiu rain band. By using the pseudo global warming downscaling method, which utilize the multi-model ensemble mean signal of the CMIP3 warming projections over the reanalysis data to minimizes the models' climate bias in simulating the present-day climate, Kawase et al. (2009) showed an increase in precipitation over the Baiu rain band and the southward shift of the Baiu rain band. A combination of a warming projection experiment

with a 20-km mesh AGCM and ensemble simulations with the 60-km resolution model combining four different SSTs and three atmospheric initial conditions is utilized by Kusunoki et al. (2011) to assess the East Asian summer rainfall changes. In the future climate simulation by the 20-km model, precipitation increases over the Yangtze River valley (Meiyu) in May through July, Korean peninsula (Changma) in May, and Japan (Baiu) in July. Simulations by the 20-km and 60-km models consistently show that in the future climate the termination of rainy season over Japan tends to be delayed until August. This is in accord with the CMIP3 multi-model analysis by Kitoh and Uchiyama (2006), who suggested that the El Niño-like SST response in the future tropical Pacific and associated circulation changes are responsible for these late withdrawal of Baiu. Endo (2010) noted a similar observed tendency of delayed Baiu withdrawal from the 109 years station data in eastern and western Japan. Ishizaki et al. (2011), using both the pattern scaling method and the bootstrap method, proposed a method to estimate various sources of uncertainties. They found that the amplitude of uncertainty coming from the RCMs is about the same with that of GCMs or the warming scenarios. From their analysis, the northern city Sapporo's climate moves about 3.5 degrees south in the next 100 years. [PLACEHOLDER FOR SECOND ORDER DRAFT: Results of the RMIP project, or CORDEX-Asia project are yet to come and will be assessed.]

The increase of extreme precipitation over contiguous China projected by CMIP3 models follows the Clausius-Clapeyron relationship and is more homogeneous than total precipitation (Li et al., 2011a, 2011b). Models with higher horizontal resolution are needed to better reproduce extreme rainfall. The change of precipitation intensity projected by a global 40-km mesh AGCM is larger than that of CMIP3 models (Feng et al., 2011a). Kamiguchi et al. (2006), using the MRI-JMA 20-km mesh AGCM, show that heavy precipitation increases notably in Bangladesh and in the Yangtze River basin due to the intensified convergence of water vapour flux in summer at the end of the 21st century. Future projections of heavy precipitation are performed with the 5-km mesh non-hydrostatic regional climate model, embedded within the global 20-km mesh AGCM with CMIP3 models ensemble mean SST changes for the Japanese summer rainy season (Kitoh et al., 2009). They show that the frequency of heavy precipitation will increase in the future for the hourly as well as daily precipitation. In particular, the strong hourly precipitation will increase even in the near future (2030s) when temperature increase is modest: 99.9%-ile value of hourly precipitation increase 7% in the near future and 21% at the end of the 21st century. A southwestward extension of the subtropical anticyclone over the northwestern Pacific Ocean associated with El Niño-like mean state changes and a dry air intrusion at the mid-troposphere from the Asian continent to the northwest Japan gives a favourable condition for intense precipitation in the Baiu season in Japan (Kanada et al., 2010). Future changes in this region depend on changes in the tropical Pacific, i.e., whether precipitation shifts eastward (El Niño-like) or not, and thus models' ability to reproduce the relationship among SST, convection and circulation changes in the tropics.

14.3.10 Middle East and Southern Asia

14.3.10.1 Middle East

The climate in the region varies considerably between a general Mediterranean type (warm and dry summers with some wintertime precipitation) to desert and subtropical climates with virtually no or plenty, but variable amounts of summer monsoon driven precipitation, respectively. The main driver of the annual climate variations comes from the change in the position of the Sun on the sky. During winter, the variability in northern hemisphere atmospheric circulations influence the general position of the storm tracks and the western to central part of the region experience variations in the amount of precipitation received largely govern by the NAO. The eastern part of the region is influenced by the Indian monsoon system, which is largely controlled by the position of the ITCZ and rain is mainly received during the summer months.

An assessment of drought in the Mediterranean region (including substantial parts of Maghreb) for present-day climate and two scenarios, each at two different horizontal resolutions were conducted by (Gao and Giorgi, 2008). Both scenarios show the drought risk around the Mediterranean Sea increasing from west to east. A few recent down scaling results (Dai, 2011; Evans, 2009; Jin et al., 2010; Lionello et al., 2008b) suggest that Eastern Mediterranean will experience a decrease in precipitation during the rainy season due to a northward displacement of the storm tracks. A northward shift in the ITCZ results in more precipitation in the southern part. A moderate change in the annual cycle of precipitation has also been simulated by some models. Precipitation statistics for an area consisting of the western part of the Arab Peninsula was assessed by Black (2009). Most prominent are a (statistically significant) decrease in the number of rainy days, both following a dry or a wet day, and a general decrease of winter rainfall. According to the GCMs in Christensen (2007) and RCM experiments by Onol and Semazzi (2009), temperatures in the region will increase on the order of 2°C in winter and up to 6°C in inland regions in summer for A1B. A reduction in winter precipitation on the order of 25% and an increase of drought duration by up to 60% are expected based also on the A1B scenario (Kim and Byun, 2009). These authors also predict a northward expansion of the Arabian Desert and an increase of autumn precipitation over the Fertile Crescent by up to 50%.

14.3.10.2 Southern Asia

The climate in Southern Asia is predominantly affected by the Indian Monsoon (Section 14.2.2.1). The CMIP3 multi-model ensemble shows an increase in precipitation in summer (Kumar et al., 2011b; May, 2011; Sabade et al., 2011), although there are wide variations among model projections (Annamalai et al., 2007; Kripalani et al., 2007b). Model scatter is larger in winter, and winter precipitation changes are inconclusive. The aerosol indirect effect is not explicitly treated in these models, thus uncertainty related to model physics as well as model resolution remains on the mean precipitation changes. Mandke et al. (2007) investigated changes in active and break spells during the Indian summer monsoon. The emerging picture from 6 models is strengthened break precipitation anomalies, though changes in the timings of active/break spells and duration with climate change are variable among models. It should be noted that the active/break spells of the monsoon are usually related to the tropical intraseasonal oscillation, which are typically poorly represented by models (Lin et al., 2008; Sperber and Annamalai, 2008).

The mean intensity of daily precipitation is found to increase, consistent with fewer wet days, and there are increases to heavy rain events beyond changes in the mean alone (Dash et al., 2009; Goswami et al., 2006b; Kumar et al., 2011a). The chance of reaching particular thresholds of heavy rainfall is found to approximately double over northern India (Turner and Slingo, 2009). Over India, using 50-km resolution regional climate model, (Kumar et al., 2006b) showed substantial increase of extreme precipitation over large area of India, particularly over the west coast of India and west central India. On the other hand, using a 20-km mesh super-high-resolution model, (Rajendran and Kitoh, 2008) obtained an overall increase of precipitation over a large area of peninsula India, but a significant reduction in not only seasonal mean orographic rainfall but also extreme heavy rainfall events over west coasts of Kerala and Karnataka.

Models with high resolution are needed to better resolve features on finer spatial scales. The South Asian summer monsoon rainfall reported by (Rajendran and Kitoh, 2008) who used the MRI/JMA 20-km mesh AGCM shows its fidelity in representing the regional distribution of the present-day monsoon rainfall. Super high-resolution future scenario for the Indian summer monsoon shows wide-spread but spatially varying increase in rainfall over the interior region and significant reduction in orographic rainfall over the west coasts of Kerala. Over this region, the drastic reduction of wind by steep orography predominates over the moisture build-up effect in reducing the rainfall. On the other hand, using the 25-km mesh RegCM3, (Ashfaq et al., 2009) find a suppression of the Indian summer monsoon precipitation, a delay in monsoon onset and an increase in the occurrence of monsoon break periods under the A2 scenario, mainly due to the weakening of the large-scale monsoon flow and suppression of the intraseasonal oscillation. This is in contrast to the CMIP3 multi-model ensemble of shows a significant increase in South Asian summer monsoon precipitation (Kumar et al., 2011b; May, 2011; Sabade et al., 2011).

14.3.11 Southeast Asia

14.3.11.1 Changes on Extremes

With regard to Southeast Asia, annual rainfall decreased between 1961 and 1998, with the number of rainy days decreasing significantly throughout most Southeast Asian countries (Manton et al., 2001). While in Malaysia, the rainfall data indicate that as the total number of dry days, the maximum duration, the mean, and the persistency of dry days are decreased, the trend of the frequency of long dry spells of at least 4 days is also found to decrease in almost all the stations over the Peninsula; however, an increasing trend is observed in the frequency of short spells in these stations during the NE monsoon season. On the other hand, during the southwest monsoon, a positive trend is observed in the characteristics of dry spells including the persistency of two dry days in many stations over the Peninsula (Deni et al., 2010). It was found that there were differences in trend patterns over the Peninsula during both seasons, with a decrease in total rainfall and a significant decrease in frequency of wet days leading to a significant increase in rainfall intensity over the Peninsula, except in eastern areas, during the southwest monsoon. In contrast, a trend of significantly increasing total rainfall and an increase in frequencies of extreme rainfall events during the northeast monsoon caused a significantly increasing trend in rainfall intensity over the Peninsula to be observed. However, no significant trend was observed with respect to extreme intensity during both monsoons over the Peninsula. The findings of this study suggest that rainfall patterns in Peninsular Malaysia are very much affected by the northeast monsoon (Suhaila et al., 2010).

Regions like Vietnam, Laos, Northeast Thailand and Peninsular Malaysia have shown an increasing trend in the frequency of extreme event, while places like archipelago Southeast Asia and Myanmar have shown a decreasing trend (Chang, 2011). For the period between 1979 and 2003, the total accumulated precipitation for the maritime continent region has increased (Lau and Wu, 2007). Further, Lau and Wu (2007) reported that the extreme high (top 10%) and low (bottom 5%) precipitation events are occurring more often than before. During the same period, moderate precipitation events have reduced (Lau and Wu, 2007). The same study also proposed that there is increase in amounts and frequency of high precipitation experienced over the Inter-tropical Convergence Zone, the Indian Ocean and monsoon regions during the 1980s and 1990s (Chang, 2011; Lau and Wu, 2007). For the Western Pacific (East Java region in Indonesia), precipitation data from 1955 to 2005 indicated that there has been an increased ratio of precipitation between the wet and dry season and the signal of monsoon strength weakening (Aldrian and Djamil, 2008). Amounts of heavy rain and their frequency of occurrence were found to be on the rise since the early 1980s in the cores of deep convection in the ITCZ, SPCZ, the Indian Ocean, and monsoon regions, but were found to be reduced over the maritime continent. Intermediate rains reduced over the warm pool regions and the ITCZ and SPCZ adjacent regions, but enhanced over the maritime continent (Lau and Wu, 2007).

Among many previous studies, Alexander et al. (2006) provided the latest, most comprehensive analysis regarding global-scale changes in extreme climate events through combining results obtained by many regional meetings on extreme climates (Choi et al., 2009a). A preliminary investigation of the relationship between the extremes indices and SST indicates that the interannual variability of temperature extremes may be related to local SSTs. However, the inter-annual variability of the regional series also seems to indicate that the peaks in the frequency of 'warm extremes' may coincide with large El Nino events (Caesar et al., 2011) Annual total wet-day precipitation of the Southeast Asia has increase by 21.61 mm/decade, while the extreme rain days has increase by 9.84 mm/decade. There is significant increase of warm night and significant decrease of cool day over the Southeast Asia (Caesar et al., 2011).

14.3.11.2 Climate Phenomena

Multi-scale climate processes contribute to climate variability and change over the Maritime Continent. In the interannual time scale, ENSO affects the intensity of Asian-Australian monsoon (Aldrian and Susanto, 2003), and the monsoon affects the intensity of the local diurnal cycle of land-sea and mountain-valley breezes which the modulate the spatial distribution of precipitation over the islands in the Maritime Continent (Qian et al., 2010; Robertson et al., 2011).

By analyzing satellite and regional climate modeling data, Qian (2008) found that rainfall is concentrated over islands, especially over the mountains, because of sea-breeze convergence, valley-breeze convergence and cumulus-merger processes. Qian et al. (2010) found an inverse relationship between monsoonal wind speed and the amplitude of the local diurnal cycle of precipitation over Java Island, names, strong monsoons disrupt sea-breeze and valley-breeze convergence and reduce rainfall over the mountains, and vise versa for weak monsoons. For example, during warm ENSO years (El Nino), the Walker circulation is weakened and its rising branch is displaced eastward, so that the lower-atmospheric wind anomalies in the Indonesia region are east-south-easterlies, which acts to strengthen the southeasterly monsoonal winds (same direction as the wind anomalies) in the September-November season (SON), but weaken the northwesterly monsoonal winds (opposite direction to the wind anomalies) in the December-February season (DJF). Thus, more rainfall is found over the mountainous south coast of West Java in DJF because of the enhanced sea-breeze plus valley breeze convergence toward the mountains during the weakened northwesterly monsoon in the warm ENSO years.

It is also found that wet monsoon onset is delayed in the warm ENSO years (Moron et al., 2010). In terms of climate change, there are uncertainties about whether the monsoon will be strengthened or the El Nino or La Nina will be more frequent (Paeth et al., 2008), therefore, it is also uncertain how these processes will affected the local rainfall distribution in the Maritime Continent. From the modeling results of (Kitoh et al., 2010) northern Java will likely to be wetter and southern Java with no siginificant change. The monsoon might be slightly stronger in the DJF in Indonesia in the warmer (thus more moisture in the air) future, which produces slightly less or no-significant change of rainfall over the southern mountains but significantly more rainfall over the northern plains of Java.

Recent literature confirms that drought and flooding in the Maritime continent are strongly influenced by rainfall variability, which is closely related to the diurnal change (Qian, 2008; Ward et al., 2011), intraseasonal change like Madden-Julian Oscillation (Hidayat and Kizu, 2010; Salahuddin and Curtis, 2011), annual change like monsoon (Chang et al., 2005; Moron et al., 2009; Moron et al., 2010), and the interannual large-scale climatic phenomena like the El Niño-Southern Oscillation (Aldrian et al., 2007; Juneng et al., 2007; Moron et al., 2010). Complex island topography and local sea-land-air interactions cannot adequately be represented in large scale GCMs or RCMs nor visualized by TRMM (Aldrian and Djamil, 2008; Qian, 2008).

The ENSO has a large impact on the climate variability of the Maritime continent. Warm El Nino Southern Oscillation events usually cause delayed onsets of the austral summer monsoon over Indonesia (Moron et al., 2010) and is associated with an increase in frequency of dry extremes (Curtis et al., 2007). Based simulations with a single GCM (ECHAM5/MPI-OM), Müller and Roeckner (2008) concluded that future changes in the mean state are El Nino-like.

The rainfall diurnal and interannual variability over Indonesia and Malaysia in austral summer (October – April) is significantly affected by the MJO passage (Hidayat and Kizu, 2010; Rauniyar and Walsh, 2011; Salahuddin and Curtis, 2011). Although the impact is largely inhomogeneous over the islands, analysis of precipitation gauges and wind observations suggest that the status of the MJO can be used to forecast climate extremes (dry and wet) in the Maritime continent (Moron et al., 2010; Salahuddin and Curtis, 2011).

14.3.11.3 Climate Modeling Result on Present and Future Climate

Several downscaling simulations over the Maritime continent have been performed at CSIRO, using the Conformal Cubic Atmospheric Model (CCAM). The first series consisted of time-slice simulations at quasi-uniform global resolution of 200 km from 1970–2100 for the A2 emissions scenario, driven by the bias-corrected SSTs of six host coupled GCMs from CMIP3: CSIRO Mk3.5, GFDL 2.0, GFDL 2.1, ECHAM5, HadCM3, and Miroc MedRes (Katzfey et al., 2009). These simulations were followed by downscaled simulations having 60 km resolution over Indonesia. The projections showed a tendency for Java and island to the east to become drier, a tendency for northern Sumatra to become wetter, with mixed results over Kalimantan. The large-scale pattern of change was somewhat similar between the CCAM runs and the host GCMs, although there were significant differences, especially over Irian Jaya (west Papua) and Papua New Guinea, where the GCMs showed rainfall increases while CCAM shows rainfall decreases.

Another large ensemble of CCAM simulations was performed for 1970–2100, consisting of global 60 km time-slice simulations driven by the bias-corrected SSTs of the same six CMIP3 coupled GCMs (Nguyen et al., 2011). These simulations indicated wetter future climates over Sumatra for most seasons. In DJF they indicated wetter conditions over Kalimantan, but drier conditions over Java and south-eastern Indonesia; for other seasons there were mixed results.

Based on projections by 14 CMIP3 models for the end of 21st century under the SRES A1B scenario, the variability of daily and monthly surface air temperature over the Maritime Continent increases for June-August and December-February (Kitoh and Mukano, 2009). In future, the daily temperature variability is projected to increase over land in the Northern Hemisphere summer and in the tropics, and to decrease over the ocean throughout the year, consistent with the projected weakening of cyclonic disturbances.

Based on projections by 18 CMIP3 models for the end of 21st century under the SRES A1B scenario, the models projecting El Niño-like Pacific sea surface temperature changes tend to simulate more future precipitation in the tropical central Pacific and less over the Maritime Continent for June-August (Ose and Arakawa, 2011). The present climate precipitation responses to Niño3 SST variability appear as uncertainty of future regional precipitation changes among the CMIP3 model projections. The present climate model shows active sea air interaction over the maritime continent (Aldrian et al., 2005) that may lead to the role of ocean current such as the Indonesian throughflow in the changing of future climate.

Results of global warming projections by a very high horizontal resolution global atmospheric model with 20-km mesh grid size were analyzed over Asia region including Indonesia (Kitoh et al., 2010). The model well simulates seasonal variation of three Indonesia rainfall pattern, but the model underestimates the total rainfall value for peak of the rainy season over Indonesia. Future projections for the end of 21st century under the SRES A1B scenario show that rainfall increases on the rainy season around 20%. During the dry season, rainfall increases for some area, but decreases for some parts of Java.

14.3.12 Australia and New Zealand

The climate of Australia is a mix of tropical and extra-tropical influences. Northern Australia lies in the tropics and is strongly affected by the monsoon circulation, the MJO and ENSO. Southern Australia extends into the extra-tropical westerly circulation and is also affected by the middle latitude storm track, the SAM, and mid-latitude transient wave propagation. New Zealand lies farther south and is mostly affected by the extra-tropical circulation (Sturman and Tapper, 2006).

14.3.12.1 Australia

Significant trends have been observed in Australian precipitation over recent decades, varying widely between seasons. Especially prominent is a decline in austral winter rainfall in Southwest Western Australia (SWWA) (IOCI, 2001) and autumn to winter rainfall over Southeast Australia (SEA) (Murphy and Timbal, 2008). Both these regions provide a large proportion of Australia's agricultural production, which relies heavily on the predominant cool season rainfall. Climate model simulations under enhanced greenhouse forcing project further reductions in rainfall over much of the country (Hope, 2006). Based on analysis of observed trends, and simulations of future climate change, it is likely that cool season precipitation will continue to decrease over southern Australia. For an arid to semi-arid country such as Australia, this will put further stress on already strained water resources.

Agricultural production in SWWA is heavily dependent on winter rainfall. Since the 1970s, a decrease of about 20% has occurred in autumn and early-winter rainfall. This is associated with an even bigger (~40%) drop in stream inflow into dams (IOCI, 2001). The rainfall decline in SWWA has been linked to changes in large-scale mean SLP (IOCI, 2001), shifts in synoptic systems (Hope et al., 2006), changes in baroclinicity (Frederiksen and Frederiksen, 2007), the SAM (Cai and Cowan, 2006; Hendon et al., 2007b), natural multidecadal variability (Cai et al., 2005), land cover changes (Timbal and Arblaster, 2006), and anthropogenic forcing (Timbal et al., 2006). England et al. (2006) suggested that recent IOD-related warming trends across the eastern Indian Ocean basin bias the SST distribution to a pattern that corresponds to anomalous dry conditions for SWWA.

Recent drought in SEA has been accompanied by sustained long-term declines in precipitation across southern regions of Australia, with the majority of the decrease over SEA occurring during late austral autumn (Murphy and Timbal, 2008). Cai and Cowan (2008a) linked this to an increased (decreased) frequency of El Niño (La Niña) events. This coincided with a reduction in rain-bearing northwest cloud bands, possibly due to long-term Indian Ocean warming (Cai and Cowan, 2008b). Ummenhofer et al. (2009b) associated both the recent drought and many of the eight large historical droughts over SEA with a conspicuous absence of negative IOD events. In contrast, Nicholls (2010) linked the autumn rainfall trend to increases in pressure over Australia, possibly driven by the positive trend in the SAM. Previous studies (Hendon et al., 2007a; Meneghini et al., 2007) also suggested that trends in the SAM could have contributed towards rainfall trends across southern regions of Australia in some seasons. Murphy and Timbal (2008) and Hope et al. (2010) have proposed that the rainfall decline is related to long-term increases in pressure over southern Australia.

Recent drying trends in SEA have been especially pronounced over the Murray-Darling Basin (MDB), with rainfall reductions translating to river system inflows for 2001–2005 being only 40% of the long-term mean (Murphy and Timbal, 2008). Of the total water lost between 2002 and 2006 over SEA, only 3% is related to available surface water, while 83% and 14% was associated with groundwater storage and soil moisture, respectively (Leblanc et al., 2009). Liu et al. (2009) showed that recent deficits in soil moisture across eastern Australia had more robust spatial and temporal signals than did rainfall deficits.

Indisputably, recent higher air temperatures, in addition to substantial rainfall deficits, have exacerbated the drought situation over SEA. Nicholls (2004) found that both the mean maximum and minimum temperatures in this latest drought period are higher than in previous droughts due to continued continental-scale warming since the mid-20th century, almost certainly caused by increased greenhouse gas concentrations (Karoly and Braganza, 2005). Nicholls (2004) raised the possibility that higher temperatures and enhanced evaporation could exacerbate the severity of Australian droughts, even without decreases in rainfall. This is consistent with the marked increases in drought frequency found by Mpelasoka et al. (2008) for future climate projections. Cai and Cowan (2008b) reported a 15% reduction in annual inflow into the MDB associated with a 1°C rise in temperatures.

14.3.12.2 New Zealand

On seasonal to decadal timescales, New Zealand precipitation is modulated by the SAM (Kidston et al., 2009; Renwick and Thompson, 2006), ENSO (Kidson and Renwick, 2002; Ummenhofer and England, 2007), and the Interdecadal Pacific Oscillation (Griffiths, 2007; Salinger et al., 2001) Increased westerly flow across New Zealand, associated with negative SAM and with El Niño events, leads in western regions to increased rainfall and generally lower than normal temperatures. The positive SAM and La Niña conditions are generally associated with increased rainfall in the north and east of the country, and warm conditions.

Ummenhofer et al. (2009a) found the drying trend since 1979 across much of New Zealand during austral summer to be consistent with recent trends in the SAM and to a lesser extent to ENSO. A trend towards increased heavy rainfall in western regions and drying in the east has been linked to an increase in westerly winds over New Zealand (Griffiths, 2007). The increasing westerlies are related largely to ENSO and IPO variability since the mid-20th century.

Temperatures over New Zealand have risen by around 1°C over the past century. The upward trend has been modulated by an increase in the frequency of cool southerly wind flows over the country since the 1950s. Once the southerly trend is taken account of, the warming observed over New Zealand is consistent with large-scale anthropogenic forcing (Dean and Stott, 2009).

Projections of future climate suggest that further increases in the westerlies are likely over New Zealand, especially in winter and spring, over the South Island. In summer and autumn, the increased frequency of the positive SAM, and the influence of poleward expansion of the subtropical high pressure belt, are projected to lead to drier conditions in many parts of the country, and a decrease in westerly wind strength in northern regions. Such climate change projections imply increased seasonality of rainfall in many parts of the country. Drought risk in eastern and northern regions is likely to increase significantly (Clark et al., 2011; Mullan et al., 2008). Temperatures are projected to rise at about 70% of the global rate, because of the buffering effect of the oceans around New Zealand. The median (from a range of SRES emissions scenarios and global models) increase in mean temperatures over New Zealand is expected to be around 2°C for a global rise of around 3°C, compared to the late 20th Century (Mullan et al., 2008). Temperature rises are likely to be smallest in spring (SON) while the season of greatest warming varies by region around the country. Sea level rise is very likely to continue at close to the global rate, as has been observed over the past century (Ministry for the Environment, 2008).

14.3.13 (Pacific) Islands Region

The Pacific basin is home to a large number of small islands, located mostly in the tropics, within 20 degrees latitude of the Equator, from Hawaii in the north to Fiji and Pitcairn in the south. The climates of all tropical Pacific islands are strongly modulated by the trade wind circulation, the major convergence zones (the ITCZ and SPCZ) and ENSO and PDO/IPO cycles. Individual islands and island groups can have widely different climates, depending on the importance or otherwise of local topography and land-sea contrast.

Critical issue for Pacific islands in relation to climate change are associated with changes in sea surface temperatures, ENSO and the major convergence zones, which determine rainfall patterns and the interannual variability of rainfall, and sea level rise. The latter is critical for many island groups, as many are low-lying and are especially prone to inundation and the effects of salination upon fresh water supplies. Other more mesoscale factors include surface winds and humidity, trade-wind inversion height and intensity, the diurnal cycle, and their interaction with orography. Such features are generally poorly represented (if at all) in global models. Combined dynamical and statistical downscaling is necessary, with the former identifying key parameters for the latter (see Working Group II report).

14.3.13.1 North Pacific

Hawaii is an island chain in the subtropics (20°N) over the central Pacific Ocean. The Hawaiian Islands are relatively well studied in terms of climatology and interannual variability, and serve as a good example for discussion of island climate and climate change. The change in its climate is probably affected, but does not simply follow, the ambient change because of strong effects of orography and the diurnal cycle (e.g., Yang et al., 2008). For example, while average rainfall is less than 400 mm yr^{-1} in the ambient subtropical Pacific, annual rainfall at the peak of Kauai Island exceeds 10,000 mm yr^{-1}. Hawaii rainfall is affected by ENSO and PDO, where El Niño events and positive PDO periods tend to be associated with drier than normal conditions, while La Niña and the negative PDO is associated with wetter than normal conditions (Norton et al., 2011).

Statistical downscaling based on global model projections suggests there will be a drying in the regions that are already driest in the Hawaiian Islands. At the same time, there will likely be an increase in the frequency and a decrease in intensity of heavy rainfall events in a warmer climate (Norton et al., 2011) but the change is small and equivocal with large uncertainties resulting from inter-model variability in projection (Elison Timm et al., 2011).

14.3.13.2 South Pacific

The climate of the South Pacific is controlled by the location and variability of the SPCZ, which strongly affects mean rainfall and its interannual variability, as well as modulating local wind regimes and average temperatures. Tropical cyclones are an important feature of South Pacific climate, during the cyclone season from November to April. Cyclones most frequently form over the Coral Sea, to the north of New Caledonia and to the west of Vanuatu.

The ENSO cycle has a significant effect upon the average location of the SPCZ, as discussed in Section 14.2.3. During El Niño events the SPCZ tends to lie northeast of its normal position, leading to below-normal rainfall in southern and western parts of the region, such as New Caledonia and Fiji. During La Niña events, the SPCZ tends to lie southwest of its normal position, leading to below-normal rainfall in northern and eastern parts of the region, such as in Samoa and Tuvalu.

Future projections of climate change do not show a clear trend for the ENSO cycle, hence the future of the SPCZ is uncertain. A warming climate implies a more moist lower atmosphere, suggesting that precipitation within the SPCZ may increase. However, recent work (Widlansky et al., 2011) suggests that rainfall within the SPCZ may weaken because of changes in the atmospheric circulation that could reduce the converge of moisture at low levels into the SPCZ region. Such changes are critically dependent upon how the distribution of sea surface temperatures changes across the tropical Pacific.

Generally, temperatures are likely to rise fastest along the Equator, especially east of the Date Line, in a pattern reminiscent of an El Niño event. Yet, the associated change in east-west SST gradient is less certain and varies between model projections, adding to uncertainty in the future movement and intensity of the SPCZ (see Chapters 11 and 12).

A critical component of climate change for all Pacific islands, and for small islands generally, is sea level rise (see Chapter 13). Many islands in the tropical Pacific are low-lying and could suffer significant inundation, and salination of fresh water supplies, with the rises in sea levels expected this century. However, recent work (Webb and Kench, 2010) shows that changing wave climates can help to build up or to erode low-lying islands in the tropical south Pacific, depending upon location. Hence, the effects of sea-level rise are likely to be felt unequally across the Pacific, in some places exacerbated and in other places mitigated by changes in wind and wave regimes.

14.3.14 Antarctica

Much of the climate variability over the southern oceans and Antarctic coastal regions is modulated by the Southern Annular Mode (SAM, see Section 14.2.10), on top of an ENSO influence across the Pacific sector. Variability in the SAM has an impact on many aspects of the climate of the Antarctic and Southern Ocean, including temperatures, winds and precipitation (Genthon et al., 2003). A more positive SAM results in higher near-surface air temperatures across the Antarctic Peninsula and slightly colder conditions around the coast of East Antarctica (Thompson and Solomon, 2002). Over recent decades the SAM has had a significant positive trend during autumn and summer (Marshall, 2003), associated with an increase in the strength of the westerly circulation over the southern oceans. This is consistent with a warming that has been observed across the northern Peninsula region and a cooling over much the east Antarctic. Recently, the warming the region of the Antarctic peninsula has been shown to extend across much of the west Antarctic, at least since the IGY in 1957 (Steig et al., 2009).

The strength of the circumpolar westerlies is also modulated by the semi-annual oscillation (SAO). During the twenty-first century changes are expected in the SAO as a result of alterations in pressure across the Southern Hemisphere. Bracegirdle et al. (2008) considered modeled circulation changes over the southern oceans and found a more pronounced strengthening of the autumn peak of the SAO compared with the spring peak, implying some change in the seasonality of the mean strength of the SAM.

The strengthening of the circumpolar westerlies has had far-reaching consequences. With stronger winds there has been less ocean uptake of carbon dioxide (Le Quéré et al., 2007). The MSLP field around the Antarctic has a zonal wave number 3 form (especially in winter), with the deepest low being the Amundsen Sea Low (ASL) at around 130°W. The depth of this low is strongly influenced by the strength of the westerlies and as the SAM has become more positive so the ASL has deepened. This has resulted in stronger northerly winds down the Antarctic Peninsula and stronger southerlies over the Ross Sea, giving a reduction (increase) in ice extent over the Bellingshausen Sea (Ross Sea) (Turner et al., 2009). Despite such regional decreases, total Antarctic sea ice extent has been increasing on average over the past few decades, associated with the northward Ekman drift induced by the strengthening SAM (Hall and Visbeck, 2002).

Future trends in the SAM and hence Antarctic climate will be affected by both greenhouse gas increase and by the recovery of the 'ozone hole' (see Section 14.2.10) with a reversal of the positive trend possible in summer, and a continuation of the positive trend more likely in winter (Bracegirdle et al., 2008). The increasing trend in total sea ice extent is likely to stop and then reverse in coming decades, as warming of the water column and the overlying atmosphere override the effects of changing ocean circulation.

A remarkable feature of recent Antarctic environmental change has been the progressive loss of ice shelves down the Antarctic Peninsula. This culminated in the disintegration of the Larsen B Ice Shelf in February 2002 when 500 billion tonnes of ice were released into the Southern Ocean. The recent increase in the strength of the westerlies has resulted in more mild, maritime air masses crossing the Peninsula, especially in summer, when the warming has the greatest impact on the ice shelves. However, the disintegration of the ice shelves started well before the era of stratospheric ozone loss and the more positive SAM, indicating longer term climatic change across the region have been taking place.

ENSO is also known to influence Antarctic climate, especially sea ice and coastal climate across the Pacific sector (Bertler et al., 2006; Guo et al., 2004; Kwok and Comiso, 2002). The ENSO influence tends to result in dipole-like patterns with warming in one sector while there is cooling in another. As the future of the ENSO cycle remains uncertain (see Section 14.2.4), it is unclear what effect ENSO will have on climate changes over Antarctica.

[START BOX 14.3 HERE]

Box 14.3: Tropical Cyclones

The potential for regional changes in future tropical cyclone frequency, track and intensity is of great interest, not just because of the associated risk of damage and loss of life, but also because tropical cyclones can play a significant role in maintaining regional water resources (Jiang and Zipser, 2010). Detection of past trends in various measures of tropical cyclone activity is constrained by the quality of the historical data records and the amplitude of observed natural variability in these measures (Knutson et al., 2010). Consideration of global trends as well as trends in specific regions is further complicated by substantial regional differences in data quality, collection protocols, and record length (Knapp and Kruk, 2010; Song et al., 2010). Annual-mean global tropical cyclone frequency since 1980 (within the geostationary satellite era) has remained roughly steady at about 90 per year, with a standard deviation of about 10% (9 storms). Standard deviations of annual frequency in individual ocean basins, however, can be greater than 40% of the means in those basins, which reduces the signal-to-noise ratio and introduces substantial uncertainty into regional tropical cyclone frequency trend detection.

Attempts to detect trends in even smaller intra-basin regions such as those defined by islands or archipelagos is further constrained by the reduced data sample size associated with acute parsing of the global data. Intra-basin regional trend detection is also substantially challenged by variability in tropical cyclone tracks (Kossin and Camargo, 2009). This variability is driven largely by random fluctuations in atmospheric steering currents, but also is observed in response to more systematic climatic forcings such as the El Niño – Southern Oscillation, North Atlantic Oscillation, Atlantic Meridional Mode, and Madden-Julian Oscillation (Camargo et al., 2008; Camargo et al., 2007; Chand and Walsh, 2009; Kossin et al., 2010). Even modest tropical cyclone track variability can lead to large differences in associated impacts at a specific location. For example, small islands can be impacted by multiple tropical cyclones in one season (e.g., the Philippines in 2009) and then remain largely unaffected for multiple subsequent years even while the total number of storms in the larger, but immediate surrounding region exhibits normal variability.

The combination of data issues (quality and sample size), signal-to-noise issues, and the natural variability of tropical cyclone tracks introduce substantial uncertainties into detection-attribution studies as well as disaster and mitigation planning aimed at specific intra-basin regions. Furthermore, while theoretical underpinnings have been put forward linking tropical cyclone intensity and genesis with anthropogenic climate change (Emanuel, 1987; Rappin et al., 2010), there is little theoretical guidance available to help elucidate the relationships between climate variability and tropical cyclone track variability.

Inter-basin analyses of variability and trends of various measures of tropical cyclone activity provide mixed results from which robust conclusions are difficult to establish. Regional trends in tropical cyclone frequency have been identified in the North Atlantic, but the fidelity of these trends is debated (Holland and Webster, 2007; Landsea, 2007; Mann et al., 2007b). Different methods for estimating undercounts in the earlier part of the North Atlantic tropical cyclone record provide mixed conclusions (Chang and Guo, 2007; Kunkel and al., 2008; Mann et al., 2007a; Vecchi and Knutson, 2008, 2011). Trends have also been identified in the north Indian Ocean and may be due to changes in the tropical easterly jet (Krishna, 2009; Rao et al., 2008) but again uncertainties in the regional tropical cyclone data quality significantly limit reliability. Regional trends have not been detected in other oceans (Chan and Xu, 2009; Kubota and Chan, 2009). Thus there is only *low confidence* that any reported long-term increases in tropical cyclone activity are robust, after accounting for past changes in observing capabilities (Knutson et al., 2010).

While there is evidence that SST in the tropics has increased due to increasing greenhouse gases (Gillett et al., 2008; Karoly and Wu, 2005; Knutson et al., 2006; Santer and al., 2006) and there is a theoretical expectation that increases in potential intensity will lead to stronger tropical cyclones (Elsner et al., 2008; Emanuel, 2000; Wing et al., 2007), the relationship between SST and potential intensity under CO_2 warming has not yet been fully fleshed out. Observations demonstrate a strong positive correlation between SST and the potential intensity. However, there is a growing body of research suggesting that regional potential intensity is controlled by the difference between regional SST and spatially averaged SST in the tropics

(Ramsay and Sobel, 2011; Vecchi and Soden, 2007c; Xie et al., 2010d). Since increases of SST due to global warming are not expected to lead to increasingly large SST gradients, this recent research suggests that increasing SST due to global warming, by itself, does not yet have a fully understood physical link to increasingly strong tropical cyclones.

Inter-basin SST differences may explain the observed inter-basin differences in the variability and trend of tropical cyclone activity. The present period of heightened tropical cyclone activity in the North Atlantic, concurrent with comparative quiescence in other ocean basins (e.g., Maue, 2009), is apparently related to differences in the rate of SST increases, as global SST has been rising steadily but at a slower rate than the Atlantic (Holland and Webster, 2007). The present period of relatively enhanced warming in the Atlantic has been proposed to be due to internal variability (Zhang and Delworth, 2009a), anthropogenic tropospheric aerosols (Mann and Emanuel, 2006b), and mineral (dust) aerosols (Evan et al., 2009). None of these proposed mechanisms provide a clear expectation that North Atlantic SST will continue to increase at a greater rate than the tropical-mean SST, and there is substantial uncertainty in projections of Atlantic tropical cyclone activity based on projected SST increases alone (Vecchi et al., 2008).

Similar to observational analyses, confidence in numerical simulations of tropical cyclone activity is reduced when model spatial scale is reduced from global to region-specific (IPCC SREX Box 3.1). Projections based on the SRES A1B warming scenario through the late 21st century indicate that it is *likely* that the global frequency of tropical cyclones will either decrease or remain essentially unchanged (change of –6 to –34%) while mean intensity increases by +2 to +11% and tropical cyclone rainfall rates increase by about 20% within 100 km of the cyclone centre (Knutson et al., 2010). However, inter-model differences in regional projections lead to lower confidence in basin-specific projections, and confidence is particularly low for projections of frequency within individual basins (Knutson et al., 2010). Still, high-resolution modelling studies typically project substantial increases in the frequency of the most intense cyclones and it is *more likely than not* that this increase will be substantially larger than 10% in some basins (Bender et al., 2010; Knutson et al., 2010).

In addition to greenhouse warming scenarios, tropical cyclones can also respond to anthropogenic forcing via different pathways. For example, increasing human emissions of black carbon and other aerosols in South Asia has affected SST gradients in the Northern Indian Ocean (Chung and Ramanathan, 2006; Meehl et al., 2008), which has in turn led to a weakening of the vertical wind shear in the region. Evan et al. (2011a) linked the reduced wind shear to the observed increase in the number of very intense storms in the Arabian Sea, including five very severe cyclones that have occurred since 1998 killing over 3500 people and causing over $6.5 billion in damages (in 2011 U.S. dollars).

As noted above, ENSO variability is known to modulate the variability of tropical cyclone genesis and track. The details of the relationships vary by region (e.g., El Nino events are related to more western North Pacific typhoons and fewer Atlantic hurricanes). Similarly, tropical cyclones respond to other known modes of variability such as the MJO. It has been demonstrated that skilful deterministic seasonal prediction of the mean location of typhoon formation fundamentally depends on the model's ability to predict the inter-annual variability of the atmospheric circulation in the western North Pacific influenced by ENSO (Takaya et al., 2010). Yokoi and Takayabu (2009) examined the global warming impact on tropical cyclone genesis frequency over the western North Pacific basin. They found that all of five CMIP3 AOGCMs, which exhibit high performance in simulating horizontal distribution of annual mean frequency under the current climate condition, project an increasing trend of the frequency in the eastern part of the domain, especially over the central North Pacific, and a decreasing trend in the western part, with a maximum decrease over the South China Sea.

The increasing trend over the central North Pacific can be interpreted by analogy with inter-annual variability related to ENSO, because models project SST and large-scale circulation field like an El Niño pattern. A 20-km-mesh very-high-resolution AGCM, under the present-day (1979–2003) simulation, yielded reasonably realistic climatology and inter-annual variability of tropical cyclone genesis frequency and tracks. Its future (2075–2099) projection indicates a significant reduction (by about 23%) in frequency of occurrence, which occurs primarily during the late part of the year (September to December), and an eastward shift in the positions of the two prevailing northward re-curving TC tracks during the peak tropical cyclone season (July–October) (Murakami et al., 2011). This eastward shift of typhoon tracks is also suggested by coarse resolution AOGCMs (Yokoi and Takayabu, 2009). These changes are associated with large-scale changes in tropical circulations, and therefore appear to be critically dependent on the spatial pattern of future sea surface temperature. Thus, reliable projections of future tropical cyclone activity, both global and regional, depend critically on reliable projections of the behaviour of ENSO under global warming, as well as an adequate understanding of the physical links with tropical cyclones. At this time, however, there is still uncertainty in the projected behaviour of ENSO (Collins et al., 2010).

The reduction in signal-to-noise ratio that accompanies changing focus from global to regional scales also lengthens the detection time-scale (i.e., the time required for a trend signal to rise above the natural variability in a statistically significant way). Based on changes in tropical cyclone intensity predicted by idealized numerical simulations with CO_2-induced tropical SST warming, Knutson and Tuleya (2004) suggested that clearly detectable increases may not be manifest for decades to come. The more recent high-resolution dynamical downscaling study of Bender et al. (2010) supports this argument and suggests that the predicted increases in the frequency of the strongest Atlantic storms may not emerge as a clear statistically significant signal until the latter half of the 21st century under the SRES A1B warming scenario.

In summary, detection and attribution of trends as well as agreement among numerical simulations is significantly compromised when the scale of focus is reduced from global to regional. This is particularly severe when intra-basin regions, such as island chains or specific sections of coastline, are considered and tropical cyclone track variability plays a larger role. The influence of past and future climate change on tropical cyclones is *likely* to vary by region, but the specific characteristics of the changes are not yet well understood, and the substantial influence of ENSO on global and regional tropical cyclone activity emphasizes the need for more reliable assessments of future changes in ENSO characteristics. Given the uncertainty of the homogeneity of historic regional tropical cyclone records, there is *low confidence* in the fidelity of any reported regional trends in tropical cyclone activity on multidecadal timescales or greater. While projections under 21st century greenhouse warming indicate that it is *likely* that the global frequency of tropical cyclones will either decrease or remain essentially unchanged, concurrent with a *likely* increase in both global mean tropical cyclone maximum wind speed and rainfall rates, there is *lower confidence* in region-specific projections of frequency and intensity. Still, based on high-resolution modeling studies, the frequency of the most intense storms will *more likely than not* increase substantially in some basins under projected 21st century warming.

[END BOX 14.3 HERE]

[START BOX 14.4 HERE]

Box 14.4: Extra-Tropical Cyclones

Background

Extra-tropical cyclones (ETCs) are pervasive features of mid-latitude weather maps, with a typical scale of 1000km and lifetimes of 1–5 days (Hoskins and Hodges, 2002). These storms grow on the baroclinic instability of the large-scale atmospheric flow, extracting potential energy from the meridional temperature gradients that arise from the contrast in solar heating between high and low latitudes. ETCs preferentially occur over the ocean basins where surface friction is low and heat and moisture are readily available, forming the midlatitude storm tracks (Brayshaw et al., 2009; Gerber and Vallis, 2009). ETCs have a dual importance in climate; not only are they responsible for many of the most extreme weather events in the midlatitudes (e.g., Liberato et al., 2011) but they are also key components of the global climate system, acting as eddies which transport heat, momentum and vorticity and shape the large scale atmospheric circulation itself.

In the past there has been little agreement on how ETCs will respond to anthropogenic forcing (Cubasch et al., 2001). The generation of climate models which contributed to the CMIP3 project began to show more agreement, with many models in particular predicting a poleward shift of the storm tracks (Yin, 2005) and an expansion of the tropics (Lu et al., 2007). As stated in AR4 (Meehl et al., 2007a) this response is particularly clear in the Southern Hemisphere, where the poleward jet shift associated with the Southern Annular Mode is more robust (Miller et al., 2006a). In the Northern Hemisphere, however, the poleward shift is less robust.

It is evident to some extent in zonal mean fields (Yin, 2005) but regional responses differ widely from this in many models (Ulbrich et al., 2008). Shifts in the locations of the storm tracks are closely associated with shifts in the westerly jet streams (Athanasiadis et al., 2010). In fact the transient eddies of the storm tracks are increasingly taken as the starting point for theories explaining the variability and change of the jets (e.g., Benedict et al., 2004). However, the coupling between the storm track and the large-scale flow is intrinsically two-way in nature (Gerber and Vallis, 2007; Lorenz and Hartmann, 2003; Robinson, 2006), which often confounds the search for simple chains of cause and effect.

Competing influences on future ETC change

The key challenge in predicting future storm track change is the balancing of several different competing dynamical influences (Held, 1993; O'Gorman, 2010; Woollings, 2010). It is becoming more apparent that the relatively modest storm track response in many models does indeed reflect the partial cancelling of opposing tendencies (Butler et al., 2010; Lim and Simmonds, 2009; Son and Lee, 2005). A key factor that has received much attention is the contrast in the meridional gradient of warming at upper and lower levels. In the upper troposphere the merdional temperature gradient is projected to increase due to both the latent heat-related enhanced warming in the tropics and the stratospheric cooling which extends down to around 200hPa at high latitudes. In the lower troposphere, in contrast, warming is enhanced over the polar regions, in particular over the Arctic in winter, and this corresponds to a decrease in the meridional temperature gradient. In this way the potential energy available for storm growth is expected to increase at upper levels but decrease at lower levels, and it is still unclear whether this will lead to an overall increase or decrease in ETC activity. The outcome can appear as an increase in eddy activity at upper levels and a decrease at lower levels (Hernandez-Deckers and von Storch, 2010), although in other models the low level eddy activity can increase even though the meridional temperature gradient decreases (Wu et al., 2011a). While the influence of the warming pattern is most often described in terms of the associated horizontal gradients, several recent studies have considered the implications of the vertical temperature gradients. These are related to the static stability which also has an important influence on baroclinicity and hence storm growth. The pattern of warming reflects increased stability in the tropics and subtropics and decreased stability at higher latitudes, and there is some modelling evidence that this may be a strong factor in the response (Kodama and Iwasaki, 2009; Lim and Simmonds, 2009; Lu et al., 2008, 2010). The increase in the depth of the troposphere as it warms may also be important (Lorenz and DeWeaver, 2007).

Irrespective of whether the horizontal or vertical gradients dominate it is clear that the considerable uncertainties in the tropical and polar warming lead to uncertainty in the storm track response (Rind, 2008). Given the two-way nature of the coupling between the storm tracks and the large-scale circulation, it is also possible that the storm track response itself is partly responsible for the changes in the large-scale temperature distribution. However, there is some evidence that this is not the case and that the atmospheric poleward heat fluxes are largely determined by local processes which set the amplitude of the tropical and polar warming (Hwang and Frierson, 2011). Several specific mechanisms have been proposed to explain how the storm tracks respond to the large scale changes, including changes in eddy phase speed (Chen et al., 2007; Chen et al., 2008; Lu et al., 2008), eddy source regions (Lu et al., 2010) and eddy length scales (Kidston et al., 2011) with a subsequent effect on wave-breaking characteristics (Riviere, 2011), and the issue is still widely debated.

There are also local processes that could prove very important for the storm track response in certain regions. Sea-ice loss is a particular example that has been shown to influence midlatitude storm activity in some modelling studies (Bader et al., 2011; Deser et al., 2010c; Seierstad and Bader, 2009), and changes in ocean circulation appear to be important in the North Atlantic, as described below. The land-sea contrast in warming also has a local influence on baroclinicity along the eastern continental coastlines (Long et al., 2009; McDonald, 2011). There is some disagreement over whether the storm track response to a combination of forcings combines linearly, with some studies suggesting relatively linear behaviour (Lim and Simmonds, 2009) but others suggesting otherwise (Butler et al., 2010). However, it has been suggested that model simulations are often too short to allow a quantitative assessment of the linearity, especially in idealised models with unrealistically long dynamical timescales (Simpson et al., 2010).

The increase of moisture content in a warmer atmosphere is also likely to have competing effects. Latent heating has been shown to play a role in invigorating individual ETCs, and this may be particularly important for cyclones developing over the eastern ocean basins that are likely to lead to downstream impacts (Dacre and Gray, 2009; Fink et al., 2009). However, there is evidence that the overall effect of moistening is to weaken eddy activity by improving the efficiency of poleward heat transport and hence reducing the dry baroclinicity (Frierson et al., 2007; O'Gorman and Schneider, 2008; Schneider et al., 2010). Consistent with this, Bengtsson et al. (2009) showed that while the precipitation does increase along the storm tracks this does not lead to an increase in cyclone intensity in other measures such as wind speed or vorticity.

Projected ETC changes and their relevance for regional climates

The response of ETCs in the latest projections is described in Section 12.4.4.3. Here we summarise the most robust aspects of this and assess the implications for regional climate change. In general, there remains low confidence in the implications of storm track change for future regional climate. While individual models can show regional storm track changes that are comparable with the natural variability, there is little agreement between models on such changes. It is also apparent that there can be considerable disagreement between different cyclone/storm track identification methods (Raible et al., 2008; Ulbrich et al., 2009), which can lead to different conclusions even when applied to the same data. Conversely, when the same method is applied to different models the spread between the model responses is often larger than the ensemble mean response, especially in the Northern Hemisphere (Laine et al., 2009; Ulbrich et al., 2008).

A poleward shift of the Southern Hemisphere storm track remains one of the most robust projections, yet even here there is considerable quantitative uncertainty associated partly with the varied model biases in jet latitude (Kidston and Gerber, 2010). Many models also predict a similar poleward shift in the North Pacific (Bengtsson et al., 2006; Catto, 2011; Ulbrich et al., 2008), although this is weaker compared to natural variability and often varies considerably between ensemble members (McDonald, 2011; Pinto et al., 2007b). The poleward shifts are generally less clear at the surface than at upper levels (McDonald, 2011; Yin, 2005), reducing the regional impacts. However, Gastineau and Soden (2009) still find a poleward shift in extreme surface wind events in the CMIP3 models, with the strongest changes in the subtropics and the Southern high latitudes. Several models predict a particular weakening of the Mediterranean storm track (Donat et al., 2011; Loeptien et al., 2008; Pinto et al., 2007b; Ulbrich et al., 2009) in which increasing static stability is very important (Raible et al., 2010).

Several studies have noted that the response of the North Atlantic storm track is quite different from a poleward shift in many models, comprising instead a strengthening of the storm track and a downstream extension into Europe (Bengtsson et al., 2006; Catto, 2011; McDonald, 2011; Pinto et al., 2007b; Ulbrich et al., 2008). In some models this regional response is very important (Ulbrich et al., 2009), with storm activity over Western Europe increasing by 50% (McDonald, 2011) or by an amount comparable to the natural variability (Pinto et al., 2007b; Woollings et al., 2011). The return periods of intense cyclones are shortened (Della-Marta and Pinto, 2009) with clear effects on wind damage measures (Donat et al., 2011; Leckebusch et al., 2007a). This response is related to the local minimum in warming in North Atlantic SSTs, which serves to increase the meridional temperature gradient on its southern side (Catto, 2011; Laine et al., 2009). The minimum in warming in turn arises due to the weakening of northward ocean heat transports by the meridional overturning circulation (MOC), and the varying MOC responses of the models can account for a significant fraction of the uncertainty in the Atlantic storm track response (Woollings et al., 2011). While this storm track response is a robust feature of the CMIP3 ensemble, there are some models with very different SST and storm track responses (Laine et al., 2009), so the multi-model ensemble mean response is much weaker (Ulbrich et al., 2008).

Most models and studies are in agreement on a global reduction in ETC numbers (Ulbrich et al., 2009), although only by a few percent which would have little impact. In individual regions there can be much larger changes which are comparable to natural variations, but it is rare that these changes are seen robustly in the majority of models (e.g., Donat et al., 2011). ETC intensities are particularly sensitive to the method and quantity used to define them, so there is little consensus on changes in intensity (Ulbrich et al., 2009). While there are indications that the absolute values of pressure minima deepen in scenario simulations (Lambert and Fyfe, 2006), this is often associated with large-scale pressure changes rather than changes in the pressure gradients or winds associated with ETCs (Bengtsson et al., 2009; McDonald, 2011; Ulbrich et al., 2009).

Some models with improved representation of the stratosphere have shown a markedly different anthropogenic response in the Northern Hemisphere which resembles the negative phase of the Northern Annular Mode (Morgenstern et al., 2010), with consequences for Atlantic / European storm activity in particular (Scaife et al., 2011). Concerns over the skill of CMIP3 models in representing both the stratosphere and the MOC mean that confidence in Northern Hemisphere storm track projections remains low. There are still relatively few high-resolution global models that have been used for storm track projections (Bengtsson et al., 2009; Catto, 2011; Geng and Sugi, 2003). Several studies have used Regional Climate Models (RCMs) to simulate storms at high resolution in particular regions. In multi-model experiments over Europe the storm response is more sensitive to the choice of driving GCM than the choice of RCM (Donat et al., 2011; Leckebusch et al., 2006), highlighting the importance of large-scale circulation uncertainties. There has been little work on potential changes to mesoscale storm systems, although it has been suggested that polar lows may reduce in frequency due to an increase in static stability (Zahn and von Storch, 2010).

[END BOX 14.4 HERE]

[START FAQ 14.1 HERE]

FAQ 14.1: How are Projected Changes in Regional and Global Climate Related?

Regional climates are strongly affected by regional processes and by the effects of climate phenomena which move heat from one region to another. Such natural variations in climate can add to or damp out global-scale trends for years to decades. As the globe warms, climate change is likely to change the way natural phenomena are expressed, which may further affect the rate of change of regional climates around the globe.

Regional climates vary across the world since the sun's energy is not distributed evenly over the globe, and the regional effects of topography, land-sea contrast, and land cover contribute to local climates. So too the effects of climate change are not distributed evenly, but vary by region according to latitude and geographical variation.

Global average climate change is a signature of the overall increase in energy in the climate system, as a result of greenhouse gas increase (which itself is approximately uniform around the globe). Regional climate changes are related to geographical differences and also to the structure of the climate system and the actions of the various climate phenomena (patterns of variability, or regional feedback processes). For example, regions on the poleward edges of the subtropics are likely to experience drying, as the subtropical high pressure belts continue to expand towards the poles. Conversely, more poleward latitudes are likely to experience precipitation increases as the atmosphere warms and its average moisture content increases.

The polar regions provide a good case study of some of the factors at play. Climate change near the poles is currently evolving quite differently in the two hemispheres, because of the influences of different climate patterns. In the Arctic, warming is happening considerably faster than the global average, mostly because the melting of ice and snow produces a regional feedback, allowing more sunlight to be absorbed in the Arctic and thereby giving rise to increased warming (which further encourages ice and snow melt). In the Antarctic, many parts of the continent (especially the east Antarctic) have seen no warming, or even cooling, in recent decades, and Antarctic se-ice extent is increasing gradually. This is largely because the speeding up of the westerly wind belt over the southern oceans in the last few decades has acted to isolate the Antarctic continent and to reduce heat transport from lower latitudes. Moreover, it helps to draw sea ice northwards. The increase in the westerlies comes about from a combination of loss of stratospheric ozone and from changes in the temperature structure of the atmosphere related to greenhouse gas increase. Despite the overall picture for the Antarctic, the Antarctic Peninsula region is warming rapidly, since it is far enough northwards to lie under the westerly wind belt.

Natural climate phenomena such as the El Niño-Southern Oscillation (ENSO) cycle transport heat between one region and another, and between the atmosphere and the oceans. During an El Niño, the eastern tropical Pacific warms while regions in the north and south Pacific tend to cool, for several months at a time (see FAQ14.1 Figure 1). Such natural cycles add a lot of seasonal and annual variability to regional climates, and will continue to do so into the future. Changes in the behaviour of phenomena such as the ENSO cycle would result in changes to this regional heating and cooling, on top of any background warming trend, in some areas helping to reinforce the background global trend and in other areas working to damp it out. The future of the ENSO cycle remains uncertain, as its future behaviour depends upon the details of upper-ocean warming across the tropical Pacific which are not consistently or well represented in the range of current climate models.

Phenomena that operate over longer time frames, such as the Pacific Decadal Oscillation (PDO) and the Atlantic Multi-decadal Oscillation (AMO), play an important role as they can affect climate trends over decades and in different regions can mask or amplify climate change signals for many years at a time. It is critical to understand the details of how such climate phenomena work, and how they are changing in response to anthropogenic warming of the climate system, since they bear directly on regional climates and they are often associated with significant climate extremes (drought, floods, heat waves).

[INSERT FAQ 14.1, FIGURE 1 HERE]

FAQ 14.1, Figure 1: Regional effects of El Niño upon surface temperatures, shown as the average temperature anomaly for an SOI value of -1 standard deviations. The top panel shows the temperature anomalies for December-February (northern winter) and the bottom panel for June-August (northern summer). Colours change every 0.5°C, with values with absolute value less than 0.25°C blanked out.

[END FAQ 14.1 HERE]

[START FAQ 14.2 HERE]

FAQ 14.2: How is Climate Change Affecting Monsoons?

The strength of the monsoons is related to the moisture content of the air, land-sea temperature contrast, land cover/land use, atmospheric aerosol loadings, and other factors. Climate model projections suggest that increases in monsoon intensity and area are likely in many regions, even though the monsoon circulations themselves are likely to weaken. However, because many other factors come in to play regionally, the overall effect of climate change upon monsoon strength and variability remains uncertain.

Model projections of future climate through the 21st century suggest that monsoon precipitation in the tropics, and the area affected by monsoon circulations, is likely to increase as the climate warms. This is consistent with the general principle that warmer air tends to have higher moisture content, so rainfall in a warmer climate tends to be more intense. A number of studies indicate a trend towards heavier monsoon rains in the main tropical monsoon regions, with a large increase in the frequency of extreme rainfalls. However, in some regions where local topography and winds play an important role (e.g., parts of western India), decreases in rainfall are simulated where decreases in local topographic effects on precipitation outweigh the overall increase in atmospheric moisture. Moreover, in some subtropical regions (e.g., northern China), decreases in summer monsoon winds and rainfall have been observed, and are related to changes in the extra-tropical circulation such as the strength and location of the subtropical high pressure belt.

While the tropical rainfall associated with the monsoons may increase in future, model results also suggest that the monsoon circulations may become weaker and more variable. Monsoon systems are very sensitive to land-sea temperature contrast, which can be influenced by natural variability in upper ocean circulation and by regional variation in solar radiation associated with changes in the aerosol loading in the atmosphere.

References

Abram, N. J., M. K. Gagan, J. E. Cole, W. S. Hantoro, and M. Mudelsee, 2008: Recent intensification of tropical climate variability in the Indian Ocean. *Nature Geoscience*, **1**, 849-853.

ACIA, 2005: *Arctic Climate Impact Assessment.* Cambridge University Press, 1042 pp.

Ackerley, D., B. B. B. Booth, S. H. E. Knight, E. J. Highwood, D. J. Frame, M. R. Allen, and D. P. Rowell, 2011: Sensitivity of 20 thCentury Sahel Rainfall to Sulfate Aerosol and CO 2Forcing. *Journal of Climate*, papers2://publication/doi/10.1175/JCLI-D-11-00019.1. 110506142853088.

Albrecht, A., D. Schindler, K. Grebhan, U. Kohnle, and H. Mayer, 2009: Storminess over the North-Atlantic European region under climate change - a review. *Allgemeine Forst Und Jagdzeitung*, **180**, 109-118.

Aldrian, E., and R. D. Susanto, 2003: Identification of three dominant rainfall regions within Indonesia and their relationship to sea surface temperature. *International Journal of Climatology*, **23**, 1435-1452.

Aldrian, E., and Y. S. Djamil, 2008: Spatio-temporal climatic change of rainfall in east Java Indonesia. *International Journal of Climatology*, **28**, 435-448.

Aldrian, E., L. D. Gates, and F. H. Widodo, 2007: Seasonal variability of Indonesian rainfall in ECHAM4 simulations and in the reanalyses: The role of ENSO. *Theoretical and Applied Climatology*, **87**, 41-59.

Aldrian, E., D. Sein, D. Jacob, L. D. Gates, and R. Podzun, 2005: Modelling Indonesian rainfall with a coupled regional model. *Climate Dynamics*, **25**, 1-17.

Alexander, L. V., et al., 2006: Global observed changes in daily climate extremes of temperature and precipitation. *Journal of Geophysical Research-Atmospheres*, **111**.

Alexander, M., D. Vimont, P. Chang, and J. Scott, 2010: The Impact of Extratropical Atmospheric Variability on ENSO: Testing the Seasonal Footprinting Mechanism Using Coupled Model Experiments. *Journal of Climate*, **23**, 2885-2901.

Alexander, M., I. Blade, M. Newman, J. Lanzante, N. Lau, and J. Scott, 2002: The atmospheric bridge: The influence of ENSO teleconnections on air-sea interaction over the global oceans. *Journal of Climate*, **15**, 2205-2231.

Alexander, M. A., 2010: Extratropical air-sea interaction, SST variability and the Pacific Decadal Oscillation (PDO). *Climate Dynamics: Why Does Climate Vary?*, D. S. a. F. Bryan, Ed., American Geophysical Union, 123 - 148.

Alory, G., S. Wijffels, and G. Meyers, 2007: Observed temperature trends in the Indian Ocean over 1960-1999 and associated mechanisms. *Geophysical research Letters*, **34**, -.

Alpert, P., et al., 2008: Relations between climate variability in the Mediterranean region and the tropics: ENSO, South Asian and African monsoons, hurricanes and Saharan dust. *Mediterranean Climate Variability*, M. P. a. B. R. Lionello P, Ed., Elsevier, 149-178.

Amador, J. A., E. J. Alfaro, O. G. Lizano, and V. O. Magana, 2006: Atmospheric forcing of the eastern tropical Pacific: A review. *Progress in Oceanography*, **69**, 101-142.

AMAP, 2011: Snow, Water, Ice and Permafrost in the Arctic., 490pp. pp.

Ambaum, M., B. Hoskins, and D. Stephenson, 2001: Arctic oscillation or North Atlantic oscillation? *Journal of Climate*, **14**, 3495-3507.

An, S.-I., 2008: Interannual variations of the Tropical Ocean instability wave and ENSO. *Journal of Climate*, **21**, 3680-3686.

An, S.-I., J.-W. Kim, S.-H. Im, B.-M. Kim, and J.-H. Park, 2011: Recent and future sea surface temperature trends in the tropical Pacific warm pool and cold tongue regions. *Climate Dynamics*, 10.1007/s00382-011-1129-7.

An, S. I., and F. F. Jin, 2000: An Eigen analysis of the interdecadal changes in the structure and frequency of ENSO mode. *Geophysical research Letters*, **27**, 2573-2576.

An, S. I., and B. Wang, 2000: Interdecadal change of the structure of the ENSO mode and its impact on the ENSO frequency. *Journal of Climate*, **13**, 2044-2055.

An, S. I., J. S. Kug, Y. G. Ham, and I. S. Kang, 2008: Successive modulation of ENSO to the future greenhouse warming. *Journal of Climate*, **21**, 3-21.

Anderson, B. T., 2003: Tropical Pacific sea surface temperatures and preceding sea level pressure anomalies in the subtropical North Pacific. *Journal of Geophysical Research Atmospheres*, **108**.

Anderson, B. T., J. Wang, G. Salvucci, S. Gopal, and S. Islam, 2010a: Observed Trends in Summertime Precipitation over the Southwestern United States, **23**, 1937-1944.

——, 2010b: Observed Trends in Summertime Precipitation over the Southwestern United States. 1937-1944.

Annamalai, H., K. Hamilton, and K. R. Sperber, 2007: The South Asian summer monsoon and its relationship with ENSO in the IPCC AR4 simulations. *Journal of Climate*, **20**, 1071-1092.

Anstey, J. A., and T. G. Shepherd, 2008: Response of the northern stratospheric polar vortex to the seasonal alignment of QBO phase transitions. *Geophysical research Letters*, **35**.

Arblaster, J. M., G. A. Meehl, and D. J. Karoly, 2011: Future climate change in the Southern Hemisphere: Competing effects of ozone and greenhouse gases. *Geophysical research Letters*, **38**, L02701.

Ashfaq, M., S. Ying, T. Wen-wen, R. J. Trapp, G. Xueijie, J. S. Pal, and N. S. Diffenbaugh, 2009: Suppression of South Asian summer monsoon precipitation in the 21st century. *Geophysical research Letters*, 10.1029/2008gl036500. L01704 (01705 pp.).

Ashok, K., Z. Guan, and T. Yamagata, 2001: Impact of the Indian Ocean Dipole on the relationship between the Indian monsoon rainfall and ENSO. *Geophysical research Letters*. 4499-4502.

Ashok, K., S. K. Behera, S. A. Rao, H. Y. Weng, and T. Yamagata, 2007: El Nino Modoki and its possible teleconnection. *Journal of Geophysical Research-Oceans*, **112**.

Athanasiadis, P. J., J. M. Wallace, and J. J. Wettstein, 2010: Patterns of Wintertime Jet Stream Variability and Their Relation to the Storm Tracks. *Journal of the Atmospheric Sciences*, **67**, 1361-1381.

Bader, J., M. D. S. Mesquita, K. I. Hodges, N. Keenlyside, S. Osterhus, and M. Miles, 2011: A review on Northern Hemisphere sea-ice, storminess and the North Atlantic Oscillation: Observations and projected changes. *Atmos. Res.*, **101**, 809-834.

Baines, P. G., and C. K. Folland, 2007: Evidence for a rapid global climate shift across the late 1960s. *Journal of Climate*, **20**, 2721-2744.

Baldwin, M., D. Stephenson, and I. Jolliffe, 2009: Spatial Weighting and Iterative Projection Methods for EOFs. *Journal of Climate*, **22**, 234-243.

Baldwin, M. P., et al., 2001: The quasi-biennial oscillation. *Reviews of Geophysics*, **39**, 179-229.

Barnes, E. A., J. Slingo, and T. Woollings, 2011: A methodology for the comparison of blocking climatologies across indices, models and climate scenarios.

Barnett, T., et al., 2008: Human-induced changes in the hydrology of the western United States. *Science*, DOI 10.1126/science.1152538. 1080-1083.

Barriopedro, D., R. Garcia-Herrera, and R. M. Trigo, 2010: Application of blocking diagnosis methods to General Circulation Models. Part I: a novel detection scheme. *Climate Dynamics*, **35**, 1373-1391.

Barriopedro, D., R. Garcia-Herrera, A. R. Lupo, and E. Hernandez, 2006: A climatology of northern hemisphere blocking. *Journal of Climate*, **19**, 1042-1063.

Battisti, D., and R. L. Naylor, 2009: Historical Warnings of Future Food Insecurity with Unprecedented Seasonal Heat. *Science*, **323**, 240.

Behera, S., J. Luo, and T. Yamagata, 2008: Unusual IOD event of 2007. *Geophysical research Letters*, **35**, -.

Bell, C. J., L. J. Gray, A. J. Charlton-Perez, M. M. Joshi, and A. A. Scaife, 2009: Stratospheric Communication of El Nino Teleconnections to European Winter. *Journal of Climate*, **22**, 4083-4096.

Bender, M. A., T. R. Knutson, R. E. Tuleya, J. J. Sirutis, G. A. Vecchi, S. T. Garner, and I. M. Held, 2010: Modeled impact of anthropogenic warming on the frequency of intense Atlantic hurricanes. *Science*, **327**, 454-458.

Benedict, J., and D. Randall, 2009: Structure of the Madden-Julian Oscillation in the Superparameterized CAM. *Journal of the Atmospheric Sciences*, **66**, 3277-3296.

Benedict, J. J., S. Lee, and S. B. Feldstein, 2004: Synoptic view of the North Atlantic Oscillation. *Journal of the Atmospheric Sciences*, **61**, 121-144.

Bengtsson, L., K. I. Hodges, and E. Roeckner, 2006: Storm tracks and climate change. *Journal of Climate*, **19**, 3518-3543.

Bengtsson, L., K. I. Hodges, and N. Keenlyside, 2009: Will Extratropical Storms Intensify in a Warmer Climate? *Journal of Climate*, **22**, 2276-2301.

Bertler, N., T. Naish, P. Mayewski, and P. Barrett, 2006: Opposing oceanic and atmospheric ENSO influences on the Ross Sea region, Antarctica. *Advances in Geosciences*, **6**, 83-86.

Bhend, J., and H. von Storch, 2008: Consistency of observed winter precipitation trends in northern Europe with regional climate change projections. *Climate Dynamics*, **31**, 17-28.

Biasutti, M., and A. Giannini, 2006a: Robust Sahel drying in response to late 20th century forcings. *Geophysical research Letters*, ARTN L11706, DOI 10.1029/2006GL026067. -.

——, 2006b: Robust Sahel drying in response to late 20th century forcings. *Geophysical Research Letters*, **33**, -.

Biasutti, M., and A. H. Sobel, 2009: Delayed seasonal cycle and African monsoon in a warmer climate. *Geophys Res Lett*, **36**, L23707.

Biasutti, M., A. H. Sobel, and S. J. Camargo, 2009: The role of the Sahara Low in summertime Sahel rainfall variability and change in the CMIP3 models. *Journal of Climate*, **22**, 5755-5771.

Biasutti, M., I. Held, A. Sobel, and A. Giannini, 2008: SST forcings and Sahel rainfall variability in simulations of the twentieth and twenty-first centuries. *Journal of Climate*, **21**, 3471-3486.

Bjerknes, J., 1966: A POSSIBLE RESPONSE OF ATMOSPHERIC HADLEY CIRCULATION TO EQUATORIAL ANOMALIES OF OCEAN TEMPERATURE. *Tellus*, **18**, 820-&.

——, 1969: ATMOSPHERIC TELECONNECTIONS FROM EQUATORIAL PACIFIC. *Monthly Weather Review*, **97**, 163-&.

Black, E., 2009: The impact of climate change on daily precipitation statistics in Jordan and Israel. *Atmospheric Science Letters*, **10**, 192-200.

Bladé, I., B. Liebmann, D. Fortuny, and J. van Oldenborg, 2011: Observed and simulated impacts of the summer NAO in Europe: Implications for projected drying in the Mediterranean region. Climate Dynamics (in press).

Boberg, F., P. Berg, P. Thejll, W. J. Gutowski, and J. H. Christensen, 2010: Improved confidence in climate change projections of precipitation further evaluated using daily statistics from ENSEMBLES models. *Climate Dynamics*, **35**, 1509-1520.

Boe, J., and L. Terray, 2008: A weather-type approach to analyzing winter precipitation in France: Twentieth-century trends and the role of anthropogenic forcing. *Journal of Climate*, **21**, 3118-3133.

Boe, J., L. Terray, C. Cassou, and J. Najac, 2009: Uncertainties in European summer precipitation changes: role of large scale circulation. *Climate Dynamics*, **33**, 265-276.

Boé, J., A. Hall, and X. Qu, 2009: September sea-ice cover in the Arctic Ocean projected to vanish by 2100. *Nature Geoscience*, **2**, 341-343.
Boer, G., and S. Lambert, 2008: Multi-model decadal potential predictability of precipitation and temperature. *Geophysical research Letters*, **35**, -.
Boer, G. J., 2009: Changes in Interannual Variability and Decadal Potential Predictability under Global Warming. *Journal of Climate*, **22**, 3098-3109.
Boer, G. J., and K. Hamilton, 2008: QBO influence on extratropical predictive skill. *Climate Dynamics*, **31**, 987-1000.
Bollasina, M., Y. Ming, and V. Ramaswamy, 2011: Anthropogenic Aerosols and the Weakening of the South Asian Summer Monsoon. *Science*, **334**, 502-505.
Bombardi, R. J., and L. M. V. Carvalho, 2009: IPCC global coupled model simulations of the South America monsoon system. *Climate Dynamics*, **33**, 893-916.
Booth, B., P. Halloran, and N. Dunstone, 2011: External forcing of the North Atlantic sea surface temperatures. *Nature*, **Submitted**.
Boschat, G., P. Terray, and S. Masson, 2011: Interannual relationships between Indian Summer Monsoon and Indo-Pacific coupled modes of variability during recent decades. *Climate Dynamics*, **37**, 1019-1043.
Bracegirdle, T. J., W. M. Connolley, and J. Turner, 2008: Antarctic climate change over the Twenty First Century. *Journal of Geophysical Research*, **113**, 13.
Braconnot, P., et al., 2007: Results of PMIP2 coupled simulations of the Mid-Holocene and Last Glacial Maximum - Part 2: feedbacks with emphasis on the location of the ITCZ and mid- and high latitudes heat budget. *Climate of the Past*, **3**, 279-296.
Brandefelt, J., 2006: Atmospheric modes of variability in a changing climate. *Journal of Climate*, **19**, 5934-5943.
Brandefelt, J., and E. Källén, 2004: The response of the Southern Hemisphere atmospheric circulation to an enhanced greenhouse gas forcing. *Journal of Climate*, **17**, 4425-4442, doi: 4410.1175/3221.4421.
Branstator, G., and F. Selten, 2009: "Modes of Variability" and Climate Change. *Journal of Climate*, **22**, 2639-2658.
Brayshaw, D. J., B. Hoskins, and M. Blackburn, 2009: The Basic Ingredients of the North Atlantic Storm Track. Part I: Land-Sea Contrast and Orography. *Journal of the Atmospheric Sciences*, **66**, 2539-2558.
Breugem, W., W. Hazeleger, and R. Haarsma, 2006: Multimodel study of tropical Atlantic variability and change. *Geophysical research Letters*, ARTN L23706, DOI 10.1029/2006GL027831. -.
——, 2007: Mechanisms of northern tropical Atlantic variability and response to CO2 doubling. *Journal of Climate*, DOI 10.1175/JCLI4137.1. 2691-2705.
Broccoli, A., K. Dahl, and R. Stouffer, 2006: Response of the ITCZ to Northern Hemisphere cooling. *Geophysical research Letters*, **33**, -.
Bronnimann, S., 2007: Impact of El Nino Southern Oscillation on European climate. *Reviews of Geophysics*, **45**.
Brown, J., S. Power, F. Delage, R. Colman, A. Moise, and B. Murphy, 2011: Evaluation of the South Pacific Convergence Zone in IPCC AR4 Climate Model Simulations of the Twentieth Century. *Journal of Climate*, **24**, 1565-1582.
Brown, R., and P. Mote, 2009: The Response of Northern Hemisphere Snow Cover to a Changing Climate. *Journal of Climate*, DOI 10.1175/2008JCLI2665.1. 2124-2145.
Bueh, C., and H. Nakamura, 2007: Scandinavian pattern and its climatic impact. 2117-2131.
Buehler, T., C. C. Raible, and T. F. Stocker, 2011: The relationship of winter season North Atlantic blocking frequencies to extreme cold or dry spells in the ERA-40. *Tellus Series A*, **63**, 212-222.
Bunge, L., and A. J. Clarke, 2009: A Verified Estimation of the El Nino Index Nino-3.4 since 1877. *Journal of Climate*, **22**, 3979-3992.
Butler, A. H., D. W. J. Thompson, and R. Heikes, 2010: The Steady-State Atmospheric Circulation Response to Climate Change-like Thermal Forcings in a Simple General Circulation Model. *Journal of Climate*, **23**, 3474-3496.
Caesar, J., et al., 2011: Changes in temperature and precipitation extremes over the Indo-Pacific region from 1971 to 2005. *International Journal of Climatology*, **31**, 791-801.
Cai, W., and T. Cowan, 2008a: Dynamics of late autumn rainfall reduction over southeastern Australia. *Geophysical research Letters*, **35**, -.
Cai, W., T. Cowan, and A. Sullivan, 2009: Recent unprecedented skewness towards positive Indian Ocean Dipole occurrences and its impact on Australian rainfall. *Geophysical research Letters*, **36**, -.
Cai, W., A. Sullivan, T. Cowan, J. Ribbe, and G. Shi, 2011: Simulation of the Indian Ocean Dipole: A relevant criterion for selecting models for climate projections. *Geophysical research Letters*, **38**, -.
Cai, W. J., and T. Cowan, 2006: SAM and regional rainfall in IPCC AR4 models: Can anthropogenic forcing account for southwest Western Australian winter rainfall reduction? *Geophysical research Letters*, **33**, -.
——, 2008b: Evidence of impacts from rising temperature on inflows to the Murray-Darling Basin. *Geophysical research Letters*, **35**, -.
Cai, W. J., G. Shi, and Y. Li, 2005: Multidecadal fluctuations of winter rainfall over southwest Western Australia simulated in the CSIRO Mark 3 coupled model. *Geophysical research Letters*, **32**, -.
Camargo, S. J., A. W. Robertson, A. G. Barnston, and G. M., 2008: Clustering of eastern North Pacific tropical cyclone tracks: ENSO and MJO effects. *Geochemistry, Geophysics, Geosystems*, **9**.

Camargo, S. J., A. W. Robertson, S. J. Gaffney, P. Smyth, and M. Ghil, 2007: Cluster analysis of typhoon tracks. Part I: General properties. *Journal of Climate*, **20**, 3635-3653.
Cane, M. A., et al., 1997: Twentieth-century sea surface temperature trends. *Science*, **275**, 957-960.
Carvalho, L. M. V., C. Jones, and T. Ambrizzi, 2005: Opposite phases of the antarctic oscillation and relationships with intraseasonal to interannual activity in the tropics during the austral summer. *Journal of Climate*, **18**, 702-718.
Cassou, C., 2008: Intraseasonal interaction between the Madden-Julian Oscillation and the North Atlantic Oscillation. *Nature*, **455**, 523-527.
Cassou, C., and L. Terray, 2001: Dual influence of Atlantic and Pacific SST anomalies on the North Atlantic/Europe winter climate. *Geophysical research Letters*, **28**, 3195–3198.
Casty, C., C. C. Raible, T. F. Stocker, H. Wanner, and J. Luterbacher, 2007: A European pattern climatology 1766-2000. *Climate Dynamics*, **29**, 791-805.
Catto, J. L., Shaffrey, L. C. and Hodges, K. I., 2011: Northern Hemisphere extratropical cyclones in a warming climate in the HiGEM high resolution climate model.
Cavazos, T., C. Turrent, and D. Lettenmaier, 2008: Extreme precipitation trends associated with tropical cyclones in the core of the North American monsoon. *Geophysical research Letters*, **35**, -.
Cayan, D., T. Das, D. W. Pierce, T. P. Barnett, M. Tyree, and A. Gershunov, 2010: Climate Change and Water in Southwestern North America Special Feature: Future dryness in the southwest US and the hydrology of the early 21st century drought. *Proceedings of the National Academy of Sciences*, **107**, 21271-21276.
Cayan, D. R., K. T. Redmond, and L. G. Riddle, 1999: ENSO and hydrologic extremes in the Western United States, **12**, 2881-2893.
Ceballos, L., E. Di Lorenzo, N. Schneider, and B. Taguchi, 2009: North Pacific gyre oscillation synchronizes climate fluctuations in the eastern and western North Pacific. *Journal of Climate*, **22**, 5163-5174.
Chan, J. C. L., and M. Xu, 2009: Inter-annual and inter-decadal variations of landfalling tropical cyclones in East Asia. Part I: Time series analysis. *International Journal of Climatology*, **29**, 1285-1293.
Chand, S. S., and K. J. E. Walsh, 2009: Tropical cyclone activity in the Fiji region: Spatial patterns and relationship to large-scale circulation. *Journal of Climate*, **22**, 3877-3893.
Chang, C.-H., 2011: Preparedness and storm hazards in a global warming world: lessons from Southeast Asia. *Natural Hazards*, **56**, 667-679.
Chang, C., J. Chiang, M. Wehner, A. Friedman, and R. Ruedy, 2011: Sulfate Aerosol Control of Tropical Atlantic Climate over the Twentieth Century. *Journal of Climate*, **24**, 2540-2555.
Chang, C. P., Z. Wang, J. McBride, and C. H. Liu, 2005: Annual cycle of Southeast Asia - Maritime continent rainfall and the asymmetric monsoon transition. *Journal of Climate*, **18**, 287-301.
Chang, E. K. M., and Y. Guo, 2007: Is the number of North Atlantic tropical cyclones significantly underestimated prior to the availability of satellite observations? *Geophysical research Letters*, **34**, L14801.
Chang, P., L. Ji, and H. Li, 1997: A decadal climate variation in the tropical Atlantic Ocean from thermodynamic air-sea interactions. *Nature*. 516-518.
Chang, P., et al., 2008: Oceanic link between abrupt changes in the North Atlantic Ocean and the African monsoon. *Nature Geoscience*, **1**, 444-448.
Chang, P., et al., 2006: Climate fluctuations of tropical coupled systems - The role of ocean dynamics. *Journal of Climate*, **19**, 5122-5174.
Chen, G., I. M. Held, and W. A. Robinson, 2007: Sensitivity of the latitude of the surface westerlies to surface friction. *Journal of the Atmospheric Sciences*, **64**, 2899-2915.
Chen, G., J. Lu, and D. M. W. Frierson, 2008: Phase Speed Spectra and the Latitude of Surface Westerlies: Interannual Variability and Global Warming Trend. *Journal of Climate*, **21**, 5942-5959.
Chen, W., Z. Jiang, L. Li, and P. Yiou, 2011: Simulation of regional climate change under the IPCC A2 scenario in southeast China. *Climate Dynamics*, **36**, 491-507.
Cheng, W., J. C. H. Chiang, and C. M. Bitz, 2007: Adjustment of the global climate to an abrupt slowdown of the Atlantic meridional overturning circulation. American Geophysical Union, 295–314.
Chiang, J., and D. Vimont, 2004: Analogous Pacific and Atlantic meridional modes of tropical atmosphere-ocean variability. *Journal of Climate*. 4143-4158.
Chiessi, C., S. Mulitza, J. Patzold, G. Wefer, and J. Marengo, 2009: Possible impact of the Atlantic Multidecadal Oscillation on the South American summer monsoon. *Geophysical research Letters*, **36**, -.
Choi, D. H., J. S. Kug, W. T. Kwon, F. F. Jin, H. J. Baek, and S. K. Min, 2010: Arctic Oscillation responses to greenhouse warming and role of synoptic eddy feedback. *Journal of Geophysical Research-Atmospheres*, **115**.
Choi, G., et al., 2009a: Changes in means and extreme events of temperature and precipitation in the Asia-Pacific Network region, 1955-2007. *International Journal of Climatology*, **29**, 1906-1925.
Choi, J., S.-I. An, B. Dewitte, and W. W. Hsieh, 2009b: Interactive Feedback between the Tropical Pacific Decadal Oscillation and ENSO in a Coupled General Circulation Model. *Journal of Climate*, **22**, 6597-6611.
Choi, J., S.-I. An, J.-S. Kug, and S.-W. Yeh, 2011: The role of mean state on changes in El Nio's flavor. *Climate Dynamics*, **37**, 1205-1215.
Chowdary, J. S., S.-P. Xie, H. Tokinaga, Y. M. Okumura, H. Kubota, N. C. Johnson, and X.-T. Zheng, 2012: Inter-decadal variations in ENSO teleconnection to the Indo-western Pacific for 1870-2007. *Journal of Climate*, 10.1175/JCLI-D-11-00070.1.

Christensen, J. H., et al., 2007: Regional Climate Projections. *Climate Change 2007: The Physical Science Basis. Contribution of Working Group I to the Fourth Assessment Report of the Intergovernmental Panel on Climate Change*, Cambridge University Press.
Christiansen, B., 2005: The shortcomings of nonlinear principal component analysis in identifying circulation regimes. *Journal of Climate*, **18**, 4814-4823.
Chung, C. E., and V. Ramanathan, 2006: Weakening of North Indian SST gradients and the monsoon rainfall in India and the Sahel. *Journal of Climate*, **19**, 2036-2045.
Clark, A., B. Mullan, and A. Porteous, 2011: Scenarios of regional drought under climate changeWLG2010-32, 135 pp.
Clement, A. C., R. Seager, M. A. Cane, and S. E. Zebiak, 1996: An ocean dynamical thermostat. *Journal of Climate*, **9**, 2190-2196.
Cloern, J., K. A. Hieb, T. Jacobson, B. Sanso, E. Di Lorenzo, and e. al., 2010: Biological communities in San Francisco Bay track a North Pacific climate shift. *Geophysical research Letters*, **37**, 6 pages.
Cobb, K. M., C. D. Charles, H. Cheng, and R. L. Edwards, 2003: El Nino/Southern Oscillation and tropical Pacific climate during the last millennium. *Nature*, **424**, 271-276.
Coelho, C. A. S., and L. Goddard, 2009: El Nino-Induced Tropical Droughts in Climate Change Projections. *Journal of Climate*, **22**, 6456-6476.
Collins, M., et al., 2010: The impact of global warming on the tropical Pacific ocean and El Nino. *Nature Geoscience*, **3**, 391-397.
Comarazamy, D. E., and J. E. Gonzalez, 2011: Regional long-term climate change (1950-2000) in the midtropical Atlantic and its impacts on the hydrological cycle of Puerto Rico. *Journal of Geophysical Research-Atmospheres*, **116**.
Conroy, J., and J. Overpeck, 2011: Regionalization of Present-Day Precipitation in the Greater Monsoon Region of Asia. *Journal of Climate*, **24**, 4073-4095.
Contreras, R. F., 2002: Long-term observations of tropical instability waves. *Journal of Physical Oceanography*, **32**, 2715-2722.
Cook, E. R., K. J. Anchukaitis, B. M. Buckley, R. D. D'Arrigo, G. C. Jacoby, and W. E. Wright, 2010: Asian Monsoon Failure and Megadrought During the Last Millennium. *Science*, **328**, 486-489.
Cook, K., 2008: CLIMATE SCIENCE The mysteries of Sahel droughts. *Nature Geoscience*, **1**, 647-648.
Cook, K. H., and E. K. Vizy, 2006: Coupled model simulations of the west African monsoon system: Twentieth- and Twenty-First-century simulations. *Journal of Climate*, **19**, 3681-3703.
Cook, K. H., and E. K. Vizy, 2010: Hydrodynamics of the Caribbean Low-Level Jet and Its Relationship to Precipitation. *Journal of Climate*, **23**, 1477-1494.
Coppola, E., F. Kucharski, F. Giorgi, and F. Molteni, 2005: Bimodality of the North Atlantic Oscillation in simulations with greenhouse gas forcing. *Geophysical research Letters*, **32**.
Croci-Maspoli, M., C. Schwierz, and H. C. Davies, 2007: Atmospheric blocking: space-time links to the NAO and PNA. *Climate Dynamics*, **29**, 713-725.
Cubasch, U., et al., 2001: Projections of future climate change. Intergovernmental Panel on Climate Change.
Curtis, S., 2008: The Atlantic multidecadal oscillation and extreme daily precipitation over the US and Mexico during the hurricane season. *Climate Dynamics*, **30**, 343-351.
Curtis, S., A. Salahuddin, R. F. Adler, G. J. Huffman, G. Gu, and Y. Hong, 2007: Precipitation extremes estimated by GPCP and TRMM: ENSO relationships. *Journal of Hydrometeorology*, **8**, 678-689.
d'Orgeval, T., J. Polcher, and L. Li, 2006: Uncertainties in modelling future hydrological change over West Africa. *Climate Dynamics*, **26**, 93-108.
Dacre, H. F., and S. L. Gray, 2009: The Spatial Distribution and Evolution Characteristics of North Atlantic Cyclones. *Monthly Weather Review*, **137**, 99-115.
Dai, A., 2006: Precipitation characteristics in eighteen coupled climate models. *Journal of Climate*, **19**, 4605-4630.
Dai, A., 2011: Drought under global warming: a review. *Wiley Interdisciplinary Reviews-Climate Change*, **2**, 45-65.
Das, T., et al., 2009: Structure and Detectability of Trends in Hydrological Measures over the Western United States. *Journal of Hydrometeorology*, DOI 10.1175/2009JHM1095.1. 871-892.
Dash, S. K., M. A. Kulkarni, U. C. Mohanty, and K. Prasad, 2009: Changes in the characteristics of rain events in India. *Journal of Geophysical Research-Atmospheres*, **114**.
De Szoeke, S., and S. Xie, 2008: The tropical eastern Pacific seasonal cycle: Assessment of errors and mechanisms in IPCC AR4 coupled ocean - Atmosphere general circulation models. *Journal of Climate*, **21**, 2573-2590.
Dean, S., and P. Stott, 2009: The Effect of Local Circulation Variability on the Detection and Attribution of New Zealand Temperature Trends. *Journal of Climate*, **22**, 6217-6229.
DeFries, R., L. Bounoua, and G. Collatz, 2002: Human modification of the landscape and surface climate in the next fifty years. *Global Change Biology*. 438-458.
Della-Marta, P. M., and J. G. Pinto, 2009: Statistical uncertainty of changes in winter storms over the North Atlantic and Europe in an ensemble of transient climate simulations. *Geophysical Research Letters*, **36**.
DelSole, T., M. Tippett, and J. Shukla, 2011: A Significant Component of Unforced Multidecadal Variability in the Recent Acceleration of Global Warming. *Journal of Climate*, **24**, 909-926.
Delworth, T., and K. Dixon, 2006: Have anthropogenic aerosols delayed a greenhouse gas-induced weakening of the North Atlantic thermohaline circulation? *Geophysical research Letters*, **33**, -.

DeMott, C., D. A. Randall, and M. Branson, 2012: Response of the Madden-Julian Oscillation to 21st century warming. in draft form.
Deni, S. M., J. Suhaila, W. Z. W. Zin, and A. A. Jemain, 2010: Spatial trends of dry spells over Peninsular Malaysia during monsoon seasons. *Theoretical and Applied Climatology*, **99**, 357-371.
Deser, C., A. Phillips, and J. Hurrell, 2004: Pacific interdecadal climate variability: Linkages between the tropics and the North Pacific during boreal winter since 1900. *Journal of Climate*. 3109-3124.
Deser, C., A. S. Phillips, and M. A. Alexander, 2010a: Twentieth century tropical sea surface temperature trends revisited. *Geophysical research Letters*, **37**.
Deser, C., M. Alexander, S. Xie, and A. Phillips, 2010b: Sea Surface Temperature Variability: Patterns and Mechanisms. *Annual Review of Marine Science*, **2**, 115-143.
Deser, C., R. Tomas, M. Alexander, and D. Lawrence, 2010c: The Seasonal Atmospheric Response to Projected Arctic Sea Ice Loss in the Late Twenty-First Century. *Journal of Climate*, **23**, 333-351.
Deser, C., A. Phillips, V. Bourdette, and H. Teng, 2011: Uncertainty in climate change projections: the role of internal variability. *Climate Dynamics*, DOI 10.1007/s00382-010-0977-x.
Di Lorenzo, E., et al., 2010: Central Pacific El Nino and decadal climate change in the North Pacific Ocean. *Nature Geoscience*, **3**, 762-765.
Di Lorenzo, E., et al., 2009: Nutrient and salinity decadal variations in the central and eastern North Pacific. *Geophysical research Letters*, **36**, -.
DiNezio, P. N., A. C. Clement, G. A. Vecchi, B. J. Soden, and B. P. Kirtman, 2009: Climate Response of the Equatorial Pacific to Global Warming. *Journal of Climate*, **22**, 4873-4892.
Ding, Y., G. Ren, Z. Zhao, Y. Xu, Y. Luo, Q. Li, and J. Zhang, 2007: Detection, causes and projection of climate change over China: An overview of recent progress. *Advances in Atmospheric Sciences*, DOI 10.1007/s00376-007-0954-4. 954-971.
Dole, R., M. Hoerling, J. Perlwitz, J. Eischeid, and P. Pegion, 2011: Was there a basis for anticipating the 2010 Russian heat wave?. doi 10.1029/2010GL046582.
Donat, M. G., G. C. Leckebusch, J. G. Pinto, and U. Ulbrich, 2010: European storminess and associated circulation weather types: future changes deduced from a multi-model ensemble of GCM simulations. *Climate Research*, **42**, 27-43.
Donat, M. G., G. C. Leckebusch, S. Wild, and U. Ulbrich, 2011: Future changes in European winter storm losses and extreme wind speeds inferred from GCM and RCM multi-model simulations. *Natural Hazards and Earth System Sciences*, **11**, 1351-1370.
Dong, B., R. T. Sutton, and T. Woollings, 2011: Changes of interannual NAO variability in response to greenhouse gases forcing. *Climate Dynamics*, **37**, 1621-1641.
Dong, B. W., R. T. Sutton, and A. A. Scaife, 2006: Multidecadal modulation of El Nino-Southern Oscillation (ENSO) variance by Atlantic Ocean sea surface temperatures. *Geophysical research Letters*, **33**.
Dong, L., T. J. Vogelsang, and S. J. Colucci, 2008: Interdecadal trend and ENSO-related interannual variability in Southern Hemisphere blocking. *Journal of Climate*, **21**, 3068-3077.
Drumond, A., R. Nieto, L. Gimeno, and T. Ambrizzi, 2008: A Lagrangian identification of major sources of moisture over Central Brazil and La Plata Basin. *Journal of Geophysical Research-Atmospheres*, **113**.
DU, Y., and S. XIE, 2008: Role of atmospheric adjustments in the tropical Indian Ocean warming during the 20th century in climate models. *Geophysical research Letters*, **35**.
Du, Y., L. Yang, and S. Xie, 2011: Tropical Indian Ocean Influence on Northwest Pacific Tropical Cyclones in Summer following Strong El Nino. *Journal of Climate*, DOI 10.1175/2010JCLI3890.1. 315-322.
Du, Y., S. P. Xie, G. Huang, and K. M. Hu, 2009: Role of Air-Sea Interaction in the Long Persistence of El Nino-Induced North Indian Ocean Warming. *Journal of Climate*, **22**, 2023-2038.
Elguindi, N., S. Somot, M. Dequé, and W. Ludwig, 2011: Climate change evolution of the hydrological balance of the Mediterranean, Black and Caspian Seas:impact of climate model resolution, **36**, 205-228.
Elison Timm, O., H. F. Diaz, T. W. Giambulluca, and M. Takahashi, 2011: Projection of changes in the frequency of heavy rain events over Hawaii based on leading Pacific climate modes. *Journal of Geophysical Research*, **116**.
Elmallah, E. S., and S. G. Elsharkawy, 2011: Influence of circulation indices upon winter temeperature variability in Egypt., 439-448.
Elsner, J. B., J. P. Kossin, and T. H. Jagger, 2008: The increasing intensity of the strongest tropical cyclones. *Nature*, **455**, 92-95.
Emanuel, K., 2007: Environmental factors affecting tropical cyclone power dissipation. *Journal of Climate*, **20**, 5497-5509.
Emanuel, K. A., 1987: Dependence of hurricane intensity on climate. *Nature*, **326**, 483-485.
——, 2000: A statistical analysis of tropical cyclone intensity. *Monthly Weather Review*, **128**, 1139-1152.
Endo, H., 2010: Long-Term Changes of Seasonal Progress in Baiu Rainfall Using 109 Years (1901-2009) Daily Station Data. *Sola*, DOI 10.2151/sola.2011-002. 5-8.
Endo, H., 2012: Future changes of Yamase bringing unusually cold summers over northeastern Japan in CMIP3 multi-models. *Journal of the Meteorological Society of Japan*. (in press).
England, M. H., C. C. Ummenhofer, and A. Santoso, 2006: Interannual rainfall extremes over southwest Western Australia linked to Indian ocean climate variability. *Journal of Climate*, **19**, 1948-1969.

Evan, A., J. Kossin, C. Chung, and V. Ramanathan, 2011a: Arabian Sea tropical cyclones intensified by emissions of black carbon and other aerosols. *Nature*, **To appear 3 November 2011 (to be confirmed)**.
Evan, A. T., J. P. Kossin, C. E. Chung, and V. Ramanathan, 2011b: Arabian Sea tropical cyclones intensified by emissions of black carbon and other aerosols. *Nature*, **479**, 94-97.
Evan, A. T., D. J. Vimont, A. K. Heidinger, J. P. Kossin, and R. Bennartz, 2009: The Role of Aerosols in the Evolution of Tropical North Atlantic Ocean Temperature Anomalies. *Science*, **324**, 778-781.
Evans, J. P., 2009: 21st century climate change in the Middle East. *Climatic Change*, **92**, 417-432.
Fedorov, A. V., and S. G. Philander, 2000: Is El Nino changing? *Science*, **288**, 1997-2002.
Feldstein, S. B., and C. Franzke, 2006: Are the North Atlantic Oscillation and the Northern Annular Mode distinguishable? *Journal of the Atmospheric Sciences*, **63**, 2915-2930.
Feliks, Y., M. Ghil, and A. W. Robertson, 2010: Oscillatory Climate Modes in the Eastern Mediterranean and Their Synchronization with the North Atlantic Oscillation. *Journal of Climate*, **23**, 4060-4079.
Feng, J., and J. P. Li, 2011: Influence of El Nino Modoki on spring rainfall over south China. *Journal of Geophysical Research-Atmospheres*, **116**.
Feng, L., T. J. Zhou, B. Wu, T. Li, and J. J. Luo, 2011a: Projection of Future Precipitation Change over China with a High-Resolution Global Atmospheric Model. *Advances in Atmospheric Sciences*, **28**, 464-476.
Feng, S., and Q. Hu, 2008a: How the North Atlantic Multidecadal Oscillation may have influenced the Indian summer monsoon during the past two millennia? , doi:10.1029/2007GL032484.
Feng, S., and Q. Hu, 2008b: How the North Atlantic Multidecadal Oscillation may have influenced the Indian summer monsoon during the past two millennia. *Geophysical research Letters*, **35**, -.
Feng, S., Q. Hu, and R. Oglesby, 2011b: Influence of Atlantic sea surface temperatures on persistent drought in North America. *Climate Dynamics*, **37**, 569-586.
Fereday, D. R., J. R. Knight, A. A. Scaife, C. K. Folland, and A. Philipp, 2008: Cluster analysis of North Atlantic-European circulation types and links with tropical Pacific sea surface temperatures. *Journal of Climate*, **21**, 3687-3703.
Findell, K. L., and T. L. Delworth, 2010: Impact of Common Sea Surface Temperature Anomalies on Global Drought and Pluvial Frequency. *Journal of Climate*, DOI 10.1175/2009JCLI3153.1. 485-503.
Findell, K. L., A. J. Pitman, M. H. England, and P. J. Pegion, 2009: Regional and Global Impacts of Land Cover Change and Sea Surface Temperature Anomalies. *Journal of Climate*, **22**, 3248-3269.
Fink, A. H., T. Bruecher, V. Ermert, A. Krueger, and J. G. Pinto, 2009: The European storm Kyrill in January 2007: synoptic evolution, meteorological impacts and some considerations with respect to climate change. *Natural Hazards and Earth System Sciences*, **9**, 405-423.
Fischer-Bruns, I., D. F. Banse, and J. Feichter, 2009: Future impact of anthropogenic sulfate aerosol on North Atlantic climate. *Climate Dynamics*, **32**, 511-524.
Fisher, E., and C. Schär, 2010: Consistent geographical patterns of changes in high-impact European heatwaves. 398-403.
Fogt, R. L., and D. H. Bromwich, 2006: Decadal variability of the ENSO teleconnection to the high-latitude South Pacific governed by coupling with the Southern Annular Mode. *Journal of Climate*, **19**, 979–997.
Folland, C., M. Salinger, N. Jiang, and N. Rayner, 2003: Trends and variations in South Pacific island and ocean surface temperatures. *Journal of Climate*, **16**, 2859-2874.
Folland, C. K., J. A. Renwick, M. J. Salinger, and A. B. Mullan, 2002: Relative influences of the Interdecadal Pacific Oscillation and ENSO on the South Pacific Convergence Zone. *Geophysical research Letters*, **29 (13): 10.1029/2001GL014201**, 4pp.
Folland, C. K., J. Knight, H. W. Linderholm, D. Fereday, S. Ineson, and J. W. Hurrell, 2009: The Summer North Atlantic Oscillation: Past, Present, and Future. *Journal of Climate*, **22**, 1082-1103.
Fortin, D., and S. Lamoureux, 2009: Multidecadal hydroclimatic variability in northeastern North America since 1550 AD. *Climate Dynamics*, **33**, 427-432.
Frank, W., and P. Roundy, 2006: The role of tropical waves in tropical cyclogenesis. *Monthly Weather Review*, **134**, 2397-2417.
Frederiksen, J. S., and C. S. Frederiksen, 2007: Interdecadal changes in southern hemisphere winter storm track modes. *Tellus Series a-Dynamic Meteorology and Oceanography*, **59**, 599-617.
Frierson, D. M. W., I. M. Held, and P. Zurita-Gotor, 2007: A gray-radiation aquaplanet moist GCM. Part II: Energy transports in altered climates. *Journal of the Atmospheric Sciences*, **64**, 1680-1693.
Fu, G. B., S. P. Charles, J. J. Yu, and C. M. Liu, 2009: Decadal Climatic Variability, Trends, and Future Scenarios for the North China Plain. *Journal of Climate*, **22**, 2111-2123.
Fu, Y., and R. Lu, 2010: Simulated change in the interannual variability of South Asian summer monsoon in the 21st century. *Advances in Atmospheric Sciences*, **27**, 992-1002.
Furtado, J., E. Di Lorenzo, N. Schneider, and N. A. Bond, 2011: North Pacific Decadal Variability and Climate Change in the IPCC AR4 Models. *Journal of Climate*, **24**, 18.
Gao, X. J., and F. Giorgi, 2008: Increased aridity in the Mediterranean region under greenhouse gas forcing estimated from high resolution simulations with a regional climate model. *Global and Planetary Change*, **62**, 195-209.
Garfinkel, C. I., and D. L. Hartmann, 2011: The Influence of the Quasi-Biennial Oscillation on the Troposphere in Wintertime in a Hierarchy of Models, Part 1: Simplified Dry GCMs. *Journal of the Atmospheric Sciences*, **68**.

Garreaud, R. D., and M. Falvey, 2009: The coastal winds off western subtropical South America in future climate scenarios. *International Journal of Climatology*, **29**, 543-554.

Gastineau, G., and B. J. Soden, 2009: Model projected changes of extreme wind events in response to global warming. *Geophysical research Letters*, **36**.

Geng, Q. Z., and M. Sugi, 2003: Possible change of extratropical cyclone activity due to enhanced greenhouse gases and sulfate aerosols - Study with a high-resolution AGCM. *Journal of Climate*, **16**, 2262-2274.

Genthon, C., G. Krinner, and M. Sacchettini, 2003: Interannual Antarctic tropospheric circulation and precipitation variability. *Climate Dynamics*, **21**, 289-307.

Gerber, E. P., and G. K. Vallis, 2007: Eddy-zonal flow interactions and the persistence of the zonal index. *Journal of the Atmospheric Sciences*, **64**, 3296-3311.

——, 2009: On the Zonal Structure of the North Atlantic Oscillation and Annular Modes. *Journal of the Atmospheric Sciences*, **66**, 332-352.

Gerber, E. P., L. M. Polvani, and D. Ancukiewicz, 2008: Annular mode time scales in the Intergovernmental Panel on Climate Change Fourth Assessment Report models. *Geophysical research Letters*, **35**.

Gerber, E. P., et al., 2010: Stratosphere-troposphere coupling and annular mode variability in chemistry-climate models. *Journal of Geophysical Research*, **115**.

Gergis, J. L., and A. M. Fowler, 2009: A history of ENSO events since AD 1525: implications for future climate change. *Climatic Change*, **92**, 343-387.

Giannakopoulos, C., P. Le Sager, M. Bindi, M. Moriondo, E. Kostopoulou, and C. M. Goodess, 2009: Climatic changes and associated impacts in the Mediterranean resulting from a 2 degrees C global warming. *Global and Planetary Change*, **68**, 209-224.

Giannini, A., 2010: Mechanisms of Climate Change in the Semiarid African Sahel: The Local View. *Journal of Climate*, **23**, 743-756.

Giannini, A., R. Saravanan, and P. Chang, 2003: Oceanic forcing of Sahel rainfall on interannual to interdecadal time scales. *Science*, DOI 10.1126/science.1089357. 1027-1030.

Giannini, A., A. W. Robertson, and J. H. Qian, 2007: A role for tropical tropospheric temperature adjustment to El Nino-Southern Oscillation in the seasonality of monsoonal Indonesia precipitation predictability. *Journal of Geophysical Research-Atmospheres*, **112**.

Gillett, N. P., P. A. Stott, and B. D. Santer, 2008: Attribution of cyclogenesis region sea surface temperature change to anthropogenic influence. *Geophysical research Letters*, **35**, L09707.

Giorgetta, M. A., and M. C. Doege, 2005: Sensitivity of the quasi-biennial oscillation to CO2 doubling. *Geophysical research Letters*, **32**.

Giorgi, F., and R. Francesco, 2000: Evaluating uncertainties in the prediction of regional climate change. *Geophysical research Letters*, **27**, 1295-1298.

Giorgi, F., and P. Lionello, 2008: Climate change projections for the Mediterranean region. *Global and Planetary Change*, **63**, 90-104.

Giorgi, F., et al., 2001: Emerging patterns of simulated regional climatic changes for the 21st century due to anthropogenic forcings. *Geophysical research Letters*, **28**, 3317-3320.

Goldenberg, S. B., C. Landsea, A. M. Mestas-Nunez, and W. M. Gray, 2001: The recent increase in Atlantic hurricane activity: Causes and implications. *Science*. 474-479.

Gong, D. Y., and C. H. Ho, 2002: The Siberian High and climate change over middle to high latitude Asia. *Theoretical and Applied Climatology*, **72**, 1-9.

Good, P., J. A. Lowe, M. Collins, and W. Moufouma-Okia, 2008: An objective tropical Atlantic sea surface temperature gradient index for studies of south Amazon dry-season climate variability and change. *Philosophical Transactions of the Royal Society B-Biological Sciences*, **363**, 1761-1766.

Goswami, B. N., M. S. Madhusoodanan, C. P. Neema, and D. Sengupta, 2006a: A physical mechanism for North Atlantic SST influence on the Indian summer monsoon. *Geophysical research Letters*, **33**.

Goswami, B. N., V. Venugopal, D. Sengupta, M. S. Madhusoodanan, and P. K. Xavier, 2006b: Increasing trend of extreme rain events over India in a warming environment. *Science*, **314**, 1442-1445.

Gouirand, I., A. Moberg, and E. Zorita, 2007: Climate variability in Scandinavia for the past millennium simulated by an atmosphere-ocean general circulation model. *Tellus Series a-Dynamic Meteorology and Oceanography*, **59**, 30-49.

Griffiths, G., M. Salinger, and I. Leleu, 2003: Trends in extreme daily rainfall across the South Pacific and relationship to the South Pacific Convergence Zone. *International Journal of Climatology*, **23**, 847-869.

Griffiths, G. M., 2007: Changes in New Zealand daily rainfall extremes 1930 - 2004. *Weather and Climate*, **27**, 3-44.

Gu, D. F., and S. G. H. Philander, 1995: SECULAR CHANGES OF ANNUAL AND INTERANNUAL VARIABILITY IN THE TROPICS DURING THE PAST CENTURY. *Journal of Climate*, **8**, 864-876.

Guanghua, C., and T. Chi-Yung, 2010: Different impacts of two kinds of Pacific Ocean warming on tropical cyclone frequency over the western North Pacific. *Geophysical research Letters*, **37**.

Guo, Z. C., D. H. Bromwich, and K. M. Hines, 2004: Modeled antarctic precipitation. Part II: ENSO modulation over West Antarctica. *Journal of Climate*, **17**, 448-465.

Gutzler, D. S., 2004: An Index of Interannual Precipitation Variability in the Core of the North American Monsoon Region, **17**, 4473-4480.

Haarsma, R., F. Selten, S. Weber, and M. Kliphuis, 2005: Sahel rainfall variability and response to greenhouse warming. *Geophysical research Letters*, **32**, -.
Hagos, S., and K. Cook, 2008: Ocean warming and late-twentieth-century Sahel drought and recovery. *Journal of Climate*, **21**, 3797-3814.
Hall, A., and M. Visbeck, 2002: Synchronous variability in the Southern Hemisphere atmosphere, sea ice, and ocean resulting from the annular mode. *Journal of Climate*, **15**, 3043-3057.
Han, J., and H. Wang, 2007: Interdecadal variability of the east Asian summer monsoon in an AGCM. *Advances in Atmospheric Sciences*, DOI 10.1007/s00376-007-0808-0. 808-818.
Han, W., et al., 2010: Patterns of Indian Ocean sea-level change in a warming climate. *Nature Geoscience*, **3**, 546-550.
Hansen, J., M. Sato, R. Ruedy, K. Lo, D. W. Lea, and M. Medina-Elizade, 2006: Global temperature change. *Proceedings of the National Academy of Sciences of the United States of America*, **103**, 14288-14293.
Harris, P. P., C. Huntingford, and P. M. Cox, 2008: Amazon Basin climate under global warming: the role of the sea surface temperature. *Philosophical Transactions of the Royal Society B-Biological Sciences*, **363**, 1753-1759.
Hartmann, B., and G. Wendler, 2005: The Significance of the 1976 Pacific Climate Shift in the Climatology of Alaska. *Journal of Climate*, **18**, 4824–4839.
Hasanean, H. M., 2004: Wintertime surface temperature in Egypt in relation to the associated atmospheric circulation. *International Journal of Climatology*, **24**, 985-999.
Hatzaki, M., H. Flocas, C. Giannakopoulos, and P. Maheras, 2009: The Impact of the Eastern Mediterranean Teleconnection Pattern on the Mediterranean Climate. 977-992.
Held, I., T. Delworth, J. Lu, K. Findell, and T. Knutson, 2005: Simulation of Sahel drought in the 20th and 21st centuries. *Proceedings of the National Academy of Sciences of the United States of America*, **102**, 17891-17896.
Held, I. M., 1993: LARGE-SCALE DYNAMICS AND GLOBAL WARMING. *Bulletin of the American Meteorological Society*, **74**, 228-241.
Held, I. M., and B. J. Soden, 2006: Robust responses of the hydrological cycle to global warming. *Journal of Climate*, **19**, 5686–5699.
Hemming, D., C. Buontempo, E. Burke, M. Collins, and N. Kaye, 2010: How uncertain are climate model projections of water availability indicators across the Middle East? *Philosophical Transactions of the Royal Society a-Mathematical Physical and Engineering Sciences*, **368**, 5117-5135.
Hendon, H. H., D. W. J. Thompson, and M. C. Wheeler, 2007a: Australian rainfall and surface temperature variations associated with the Southern Hemisphere annular mode. *Journal of Climate*, **20**, 2452–2467.
Hendon, H. H., D. W. J. Thompson, and M. C. Wheeler, 2007b: Australian rainfall and surface temperature variations associated with the Southern Hemisphere annular mode. *Journal of Climate*, **20**, 2452-2467.
Hernandez-Deckers, D., and J.-S. von Storch, 2010: Energetics Responses to Increases in Greenhouse Gas Concentration. *Journal of Climate*, **23**, 3874-3887.
Hertig, E., and J. Jacobeit, 2008: Assessments of Mediterranean precipitation changes for the 21st century using statistical downscaling techniques. *International Journal of Climatology*, **28**, 1025-1045.
Hidayat, R., and S. Kizu, 2010: Influence of the Madden-Julian Oscillation on Indonesian rainfall variability in austral summer. *International Journal of Climatology*, **30**, 1816-1825.
Hirschi, M., and S. I. Seneviratne, 2010: Intra-annual link of spring and autumn precipitation over France. *Climate Dynamics*, **35**, 1207-1218.
Hirschi, M., et al., 2011: Observational evidence for soil-moisture impact on hot extremes in southeastern Europe. *Nature Geoscience*, **4**, 17-21.
Hoerling, M., J. Hurrell, J. Eischeid, and A. Phillips, 2006: Detection and attribution of twentieth-century northern and southern African rainfall change. *Journal of Climate*, **19**, 3989-4008.
Hoerling, M., J. Hurrell, T. Xu, G. Bates, and A. Phillips, 2004: Twentieth century North Atlantic climate change. Part II: Understanding the effect of Indian Ocean warming. *Climate Dynamics*, DOI 10.1007/s00382-004-0433-x. 391-405.
Hoerling, M. P., A. Kumar, and M. Zhong, 1997: El Nino, La Nina, and the nonlinearity of their teleconnections. *Journal of Climate*, **10**, 1769-1786.
Holland, G. J., and P. J. Webster, 2007: Heightened tropical cyclone activity in the North Atlantic: Natural variability or climate trend? *Philosophical Transactions of the Royal Society A*, **365**, 2695-2716.
Holland, M. M., J. Finnis, A. P. Barrett, and M. C. Serreze, 2007: Projected changes in Arctic Ocean freshwater budgets. *Journal of Geophysical Research*, **112**, G04S55.
Hong, C.-C., Y.-H. Li, T. Li, and M.-Y. Lee, 2011: Impacts of central Pacific and eastern Pacific El Ninos on tropical cyclone tracks over the western North Pacific. *Geophysical research Letters*, **38**.
Hope, P., B. Timbal, and R. Fawcett, 2010: Associations between rainfall variability in the southwest and southeast of Australia and their evolution through time. *International Journal of Climatology*, **30**, 1360-1371.
Hope, P. K., 2006: Projected future changes in synoptic systems influencing southwest Western Australia. *Climate Dynamics*, **26**, 765-780.
Hope, P. K., W. Drosdowsky, and N. Nicholls, 2006: Shifts in the synoptic systems influencing southwest Western Australia. *Climate Dynamics*, **26**, 751-764.
HOREL, J., and J. WALLACE, 1981: PLANETARY-SCALE ATMOSPHERIC PHENOMENA ASSOCIATED WITH THE SOUTHERN OSCILLATION. *Monthly Weather Review*. 813-829.

Hori, M. E., D. Nohara, and H. L. Tanaka, 2007: Influence of Arctic Oscillation towards the Northern Hemisphere surface temperature variability under the global warming scenario. *Journal of the Meteorological Society of Japan*, **85**, 847-859.

Hoskins, B. J., and K. I. Hodges, 2002: New perspectives on the Northern Hemisphere winter storm tracks. *Journal of the Atmospheric Sciences*, **59**, 1041-1061.

Hsu, P.-C., T. Li, and B. Wang, 2011a: Trends in global monsoon area and precipitation in the past 30 years. *Geophysical research Letters*, **38**.

Hsu, P.-C., T. Li, J.-J. Luo, H. Murakami, A. Kitoh, and M. Zhao, 2011b: Increase of global monsoon area and precipitation under global warming: A robust signal? *Nature Geoscience (submitted)*.

Hu, Q., and S. Feng, 2008: Variation of the North American summer monsoon regimes and the Atlantic multidecadal oscillation. *Journal of Climate*, **21**, 2371-2383.

Hu, Z. Z., 1997: Interdecadal variability of summer climate over East Asia and its association with 500 hPa height and global sea surface temperature. *Journal of Geophysical Research-Atmospheres*, **102**, 19403-19412.

Huang, G., K. Hu, and S. Xie, 2010: Strengthening of Tropical Indian Ocean Teleconnection to the Northwest Pacific since the Mid-1970s: An Atmospheric GCM Study. *Journal of Climate*, DOI 10.1175/2010JCLI3577.1. 5294-5304.

Huang, R., W. Chen, B. Yang, and R. Zhang, 2004: Recent advances in studies of the interaction between the east Asian winter and summer monsoons and ENSO cycle. *Advances in Atmospheric Sciences*. 407-424.

Hurrell, J. W., 1996: Influence of variations in extratropical wintertime teleconnections on Northern Hemisphere temperature. *Geophysical research Letters*, **23**, 665-668.

Hurrell, J. W., and C. Deser, 2009: North Atlantic climate variability: The role of the North Atlantic Oscillation. *Journal of Marine Systems*, **78**, 28-41.

Hurrell, J. W., and C. Deser, 2010: North Atlantic climate variability: The role of the North Atlantic Oscillation. *Journal of Marine Systems*, **79**, 231-244.

Hurrell, J. W., Y. Kushnir, M. Visbeck, and G. Ottersen, 2003: An Overview of the North Atlantic Oscillation. *The North Atlantic Oscillation: Climate Significance and Environmental Impact.* Vol. 134, American Geophysical Union.

Huss, M., R. Hock, A. Bauder, and M. Funk, 2010: 100-year mass changes in the Swiss Alps linked to the Atlantic Multidecadal Oscillation. *Geophysical research Letters*, **37**, -.

Hwang, Y.-T., and D. M. W. Frierson, 2011: Increasing atmospheric poleward energy transport with global warming (vol 37, L24807, 2010). *Geophysical research Letters*, **38**.

Ihara, C., Y. Kushnir, M. Cane, and V. de la Pena, 2009: Climate Change over the Equatorial Indo-Pacific in Global Warming. *Journal of Climate*, **22**, 2678-2693.

Ineson, S., and A. Scaife, 2009: The role of the stratosphere in the European climate response to El Nino. *Nature Geoscience*, DOI 10.1038/NGEO381. 32-36.

Ineson, S., A. A. Scaife, J. R. Knight, J. C. Manners, N. J. Dunstone, L. J. Gray, and J. D. Haigh, 2011: Solar forcing of winter climate variability in the Northern Hemisphere. *Nature Geoscience*, DOI: 10.1038/NGEO1282.

Inoue, T., and H. Ueda, 2009: Evaluation for the Seasonal Evolution of the Summer Monsoon over the Asian and Western North Pacific Sector in the WCRP CMIP3 Multi-model Experiments. *Journal of the Meteorological Society of Japan*, DOI 10.2151/jmsj.87.539. 539-560.

——, 2011: Delay of the First Transition of Asian Summer Monsoon under Global Warming Condition. *Scientific Online Letters for the Atmosphere*, **7**, 81-84.

IOCI, 2001: Second research report - towards understanding climate variability in South Western Australia, 204 pp.

IPCC, 2007a: *Climate Change 2007: Impacts, Adaptation and Vulnerability. Contribution of Working Group II to the Fourth Assessment Report of the Intergovernmental Panel on Climate Change (IPCC).* Cambridge University Press, 976 pp. pp.

——, 2007b: *Climate Change 2007: The Physical Science Basis. Contribution of Working Group I to the Fourth Assessment Report of the Intergovernmental Panel on Climate Change (IPCC).* Cambridge University Press, 996 pp pp.

Ishizaki, N. N., et al., 2011: Probabilistic regional climate analogue in the warmer Japan. *Journal of the Meteorological Society of Japan*.

Izumo, T., C. D. Montegut, J. J. Luo, S. K. Behera, S. Masson, and T. Yamagata, 2008: The Role of the Western Arabian Sea Upwelling in Indian Monsoon Rainfall Variability. *Journal of Climate*, **21**, 5603-5623.

J.W., H., K. Y., V. M., and O. G., 2003: An Overview of the North Atlantic Oscillation. *The North Atlantic Oscillation: Climate Significance and Environmental Impact.* Vol. 134, American Geophysical Union.

Jaeger, E. B., and S. I. Seneviratne, 2010: Impact of soil moisture–atmosphere coupling on European climate extremes and trends in a regional climate model.

Janicot, S., S. Trzaska, and I. Poccard, 2001: Summer Sahel-ENSO teleconnection and decadal time scale SST variations. *Climate Dynamics*, **18**, 303-320.

Jiang, H., and E. Zipser, 2010: Contribution of Tropical Cyclones to the Global Precipitation from Eight Seasons of TRMM Data: Regional, Seasonal, and Interannual Variations. *Journal of Climate*, **23**, 1526–1543.

Jiang, J., and W. Perrie, 2008: Climate change effects on North Atlantic cyclones. *Journal of Geophysical Research-Atmospheres*, **113**.

Jin, F., A. Kitoh, and P. Alpert, 2010: Water cycle changes over the Mediterranean: a comparison study of a super-high-resolution global model with CMIP3. *Philosophical Transactions of the Royal Society a-Mathematical Physical and Engineering Sciences*, **368**, 5137-5149.
JMA, 2011: Climate Change Monitoring Report 2010. Japan Meteorological Agency, 98.
Joshi, M. M., A. J. Charlton, and A. A. Scaife, 2006: On the influence of stratospheric water vapor changes on the tropospheric circulation. *Geophysical research Letters*, **33**.
Juneng, L., F. T. Tangang, and C. J. C. Reason, 2007: Numerical case study of an extreme rainfall event during 9-11 December 2004 over the east coast of Peninsular Malaysia. *Meteorology and Atmospheric Physics*, **98**, 81-98.
Junquas, C., C. Vera, L. Li, and H. Le Treut, 2011a: Summer precipitation variability over Southeastern South America in a global warming scenario. Springer-Verlag 2011.
Junquas, C., C. Vera, L. Li, and H. Le Treut, 2011b: Summer precipitation variability over Southeastern South America in a global warming scenario. *Climate Dynamics*, **doi: 10.1007/s00382-011-1141-y**.
Kamiguchi, K., A. Kitoh, T. Uchiyama, R. M. and, and A. Noda, 2006: Changes in precipitation-based extremes indices due to global warming projected by a global 20-km-mesh atmospheric model, **2**, 64-67.
Kanada, S., M. N. and, and T. Kato, 2010: Changes in mean atmospheric structures around Japan during July due to global warming in regional climate experiments using a cloud resolving model, **4**, 11-14.
Kang, S., I. Held, D. Frierson, and M. Zhao, 2008: The response of the ITCZ to extratropical thermal forcing: Idealized slab-ocean experiments with a GCM. *Journal of Climate*, **21**, 3521-3532.
Kao, H. Y., and J. Y. Yu, 2009: Contrasting Eastern-Pacific and Central-Pacific Types of ENSO. *Journal of Climate*, **22**, 615-632.
Kapnick, S., and A. Hall, 2011: Causes of recent changes in western North American snowpack.
Karmalkar, A. V., R. S. Bradley, and H. F. Diaz, 2011: Climate change in Central America and Mexico: regional climate model validation and climate change projections. *Climate Dynamics*, **37**, 605-629.
Karnauskas, K. B., R. Seager, A. Kaplan, Y. Kushnir, and M. A. Cane, 2009: Observed Strengthening of the Zonal Sea Surface Temperature Gradient across the Equatorial Pacific Ocean. *Journal of Climate*, **22**, 4316-4321.
Karoly, D. J., and Q. G. Wu, 2005: Detection of regional surface temperature trends. *Journal of Climate*, **18**, 4337-4343.
Karoly, D. J., and K. Braganza, 2005: Attribution of recent temperature changes in the Australian region. *Journal of Climate*, **18**, 457-464.
Karpechko, A. Y., 2010: Uncertainties in future climate attributable to uncertainties in future Northern Annular Mode trend. *Geophysical research Letters*, **37**.
Kattsov, V. M., J. E. Walsh, W. L. Chapman, V. A. Govorkova, T. V. Pavlova, and X. D. Zhang, 2007: Simulation and projection of arctic freshwater budget components by the IPCC AR4 global climate models. *Journal of Hydrometeorology*, **8**, 571-589.
Katzfey, J. J., J. McGregor, K. Nguyen, and M. Thatcher, 2009: Dynamical downscaling techniques: Impacts on regional climate change signals. *18th World Imacs Congress and Modsim09 International Congress on Modelling and Simulation: Interfacing Modelling and Simulation with Mathematical and Computational Sciences*. 3942-3947.
Kaufman, D. S., et al., 2009: Recent warming reverses long-term Arctic cooling. *Science*, **325**, 1236-1239.
Kawase, H., et al., 2009: Intermodel variability of future changes in the Baiu rainband estimated by the pseudo global warming downscaling method. *Journal of Geophysical Research-Atmospheres*, ARTN D24110, DOI 10.1029/2009JD011803. -.
Kawatani, Y., K. Hamilton, and S. Watanabe, 2011: The Quasi-Biennial Oscillation in a double CO2 climate. *Journal of the Atmospheric Sciences*, **68**, 265–283.
Kay, J. E., T. L'Ecuyer, A. Gettelman, G. Stephens, and C. O'Dell, 2008: The contribution of cloud and radiation anomalies to the 2007 Arctic sea ice extent minimum. *Geophysical research Letters*, **35**, L08503.
Keenlyside, N., M. Latif, J. Jungclaus, L. Kornblueh, and E. Roeckner, 2008: Advancing decadal-scale climate prediction in the North Atlantic sector. *Nature*, **453**, 84-88.
Kidson, J. W., and J. A. Renwick, 2002: Patterns of convection in the tropical Pacific and their influence on New Zealand weather. *International Journal of Climatology*, **22**, 151-174.
Kidston, J., and E. P. Gerber, 2010: Intermodel variability of the poleward shift of the austral jet stream in the CMIP3 integrations linked to biases in 20th century climatology. *Geophysical research Letters*, **37**.
Kidston, J., J. A. Renwick, and J. McGregor, 2009: Hemispheric-scale seasonality of the Southern Annular Mode and impacts on the climate of New Zealand. *Journal of Climate*, **22**, 4759-4770.
Kidston, J., G. K. Vallis, S. M. Dean, and J. A. Renwick, 2011: Can the Increase in the Eddy Length Scale under Global Warming Cause the Poleward Shift of the Jet Streams? *Journal of Climate*, **24**, 3764-3780.
Kiehl, J. T., 2007: Twentieth century climate model response and climate sensitivity. *Geophysical research Letters*, **34**, L22710, doi:22710.21029/22007GL031383.
Kim, B. M., and S. I. An, 2011: Understanding ENSO Regime Behavior upon an Increase in the Warm-Pool Temperature Using a Simple ENSO Model. *Journal of Climate*, **24**, 1438-1450.
Kim, D., and H. Byun, 2009: Future pattern of Asian drought under global warming scenario. *Theoretical and Applied Climatology*, DOI 10.1007/s00704-008-0100-y. 137-150.

Kim, H. J., B. Wang, and Q. H. Ding, 2008: The Global Monsoon Variability Simulated by CMIP3 Coupled Climate Models. *Journal of Climate*, **21**, 5271-5294.
Kim, H. M., P. J. Webster, and J. A. Curry, 2009: Impact of Shifting Patterns of Pacific Ocean Warming on North Atlantic Tropical Cyclones. *Science*, **325**, 77-80.
——, 2011: Modulation of North Pacific Tropical Cyclone Activity by Three Phases of ENSO. *Journal of Climate*, **24**, 1839-1849.
Kitoh, A., and T. Uchiyama, 2006: Changes in onset and withdrawal of the East Asian summer rainy season by multi-model global warming experiments. *Journal of the Meteorological Society of Japan*. 247-258.
Kitoh, A., and T. Mukano, 2009: Changes in Daily and Monthly Surface Air Temperature Variability by Multi-Model Global Warming Experiments. *Journal of the Meteorological Society of Japan*, **87**, 513-524.
Kitoh, A., S. Kusunoki, and T. Nakaegawa, 2011: Climate change projections over South America in the late 21st century with the 20 and 60 km mesh Meteorological Research Institute atmospheric general circulation model (MRI-AGCM). *Journal of Geophysical Research-Atmospheres*, **116**, -.
Kitoh, A., T. Ose, K. Kurihara, S. Kusunoki, M. S. and, and K. T.-M. Group, 2009: Projection of changes in future weather extremes using super-high-resolution global and regional atmospheric models in the KAKUSHIN Program: Results of preliminary experiments, **3**, 49-53.
Kitoh, A., et al., 2010: Climate Change Projections in Some Asian Countries. *Climate Change Adaptation and International Development*, R. Fujikura, and M. Kawanishi, Eds., Earthscan Taylor & Francis Groups, 416.
Kjellstrom, E., G. Nikulin, U. Hansson, G. Strandberg, and A. Ullerstig, 2011: 21st century changes in the European climate: uncertainties derived from an ensemble of regional climate model simulations., 24-40.
Klein, S., B. Soden, and N. Lau, 1999: Remote sea surface temperature variations during ENSO: Evidence for a tropical atmospheric bridge. *Journal of Climate*. 917-932.
Klein Tank, A. M. G., and a. others, 2006: Changes in daily temperature and precipitation extremes in central and south Asia. *J. Geophys. Res.*, **111**.
Klingaman, N., S. Woolnough, H. Weller, and J. Slingo, 2011: The Impact of Finer-Resolution Air-Sea Coupling on the Intraseasonal Oscillation of the Indian Monsoon. *Journal of Climate*, **24**, 2451-2468.
Knapp, K. R., and M. C. Kruk, 2010: Quantifying inter-agency differences in tropical cyclone best track wind speed estimates. *Monthly Weather Review*, **138**, 1459-1473.
Knight, J., 2009: The Atlantic Multidecadal Oscillation Inferred from the Forced Climate Response in Coupled General Circulation Models. *Journal of Climate*, **22**, 1610-1625.
Knight, J., C. Folland, and A. Scaife, 2006: Climate impacts of the Atlantic Multidecadal Oscillation. *Geophysical research Letters*, ARTN L17706, DOI 10.1029/2006GL026242. -.
Knight, J., R. Allan, C. Folland, M. Vellinga, and M. Mann, 2005: A signature of persistent natural thermohaline circulation cycles in observed climate. *Geophysical research Letters*, **32**, -.
Knutson, T. R., and R. E. Tuleya, 2004: Impact of CO2-Induced Warming on Simulated Hurricane Intensity and Precipitation: Sensitivity to the Choice of Climate Model and Convective Parameterization. *Journal of Climate*, **17**, 3477-3495.
Knutson, T. R., J. J. Sirutis, S. T. Garner, G. A. Vecchi, and I. M. Held, 2008: Simulated reduction in Atlantic hurricane frequency under twenty-first-century warming conditions. *Nature Geoscience*, **1**, 359-364.
Knutson, T. R., et al., 2006: Assessment of twentieth-century regional surface temperature trends using the GFDL CM2 coupled models. *Journal of Climate*, **19**, 1624-1651.
Knutson, T. R., et al., 2010: Tropical cyclones and climate change. *Nature Geoscience*, **3**, 157-163.
Kodama, C., and T. Iwasaki, 2009: Influence of the SST Rise on Baroclinic Instability Wave Activity under an Aquaplanet Condition. *Journal of the Atmospheric Sciences*, **66**, 2272-2287.
Kodera, K., M. E. Hori, S. Yukimoto, and M. Sigmond, 2008: Solar modulation of the Northern Hemisphere winter trends and its implications with increasing CO2. *Geophysical research Letters*, **35**.
Kohler, M., N. Kalthoff, and C. Kottmeier, 2010: The impact of soil moisture modifications on CBL characteristics in West Africa: A case-study from the AMMA campaign. *Quarterly Journal of the Royal Meteorological Society*, **136**, 442-455.
Koldunov, N. V., D. Stammer, and J. Marotzke, 2010: Present-Day Arctic Sea Ice Variability in the Coupled ECHAM5/MPI-OM Model. *Journal of Climate*, **23**, 2520-2543.
Kosaka, Y., and H. Nakamura, 2010: Mechanisms of meridional teleconnection observed between a summer monsoon system and a subtropical anticyclone. Part I: The Pacific-Japan pattern. *J.Climate*, **23**, 5085-5108.
Kossin, J. P., and S. J. Camargo, 2009: Hurricane track variability and secular potential intensity trends. *Climatic Change*, **97**, 329-337.
Kossin, J. P., S. J. Camargo, and M. Sitkowski, 2010: Climate Modulation of North Atlantic Hurricane Tracks. *Journal of Climate*, **23**, 3057-3076.
Koster, R., et al., 2004: Regions of strong coupling between soil moisture and precipitation. *Science*, **305**, 1138-1140.
Kravtsov, S., and C. Spannagle, 2008: Multidecadal climate variability in observed and modeled surface temperatures. *Journal of Climate*, **21**, 1104-1121.
Krichak, S. O., and P. Alpert, 2005: Decadal trends in the east Atlantic-west Russia pattern and Mediterranean precipitation. *International Journal of Climatology*, **25**, 183-192.

Kripalani, R., J. Oh, and H. Chaudhari, 2007a: Response of the East Asian summer monsoon to doubled atmospheric CO2: Coupled climate model simulations and projections under IPCC AR4. *Theoretical and Applied Climatology*, DOI 10.1007/s00704-006-0238-4. 1-28.

Kripalani, R. H., J. H. Oh, A. Kulkarni, S. S. Sabade, and H. S. Chaudhari, 2007b: South Asian summer monsoon precipitation variability: Coupled climate model simulations and projections under IPCC AR4. *Theoretical and Applied Climatology*, **90**, 133-159.

Krishna, K. M., 2009: Intensifying tropical cyclones over the North Indian Ocean during summer monsoon – Global warming. *Global and Planetary Change*, **65**, 12-16.

Krishnamurti, T. N., A. Thomas, A. Simon, and V. Kumar, 2010: Desert Air Incursions, an Overlooked Aspect, for the Dry Spells of the Indian Summer Monsoon. *Journal of the Atmospheric Sciences*, **67**, 3423-3441.

Kruger, L. F., R. P. da Rocha, M. S. Reboita, and T. Ambrizzi, 2011: RegCM3 nested in the HadAM3 scenarios A2 and B2: projected changes in cyclogeneses, temperature and precipitation over South Atlantic Ocean. *Climatic Change*.

Kubota, H., and J. C. L. Chan, 2009: Interdecadal variability of tropical cyclone landfall in the Philippines from 1902 to 2005. *Geophysical research Letters*, **36**, L12802.

Kucharski, F., F. Molteni, and J. Yoo, 2006: SST forcing of decadal Indian Monsoon rainfall variability. *Geophysical research Letters*, **33**, -.

Kucharski, F., I. Kang, R. Farneti, and L. Feudale, 2011: Tropical Pacific response to 20th century Atlantic warming. *Geophysical research Letters*, ARTN L03702, DOI 10.1029/2010GL046248. -.

Kucharski, F., A. Bracco, J. Yoo, A. Tompkins, L. Feudale, P. Ruti, and A. Dell'Aquila, 2009a: A Gill-Matsuno-type mechanism explains the tropical Atlantic influence on African and Indian monsoon rainfall. *Quarterly Journal of the Royal Meteorological Society*, **135**, 569-579.

Kucharski, F., et al., 2009b: The CLIVAR C20C project: skill of simulating Indian monsoon rainfall on interannual to decadal timescales. Does GHG forcing play a role? *Climate Dynamics*, **33**, 615-627.

Kug, J.-S., F.-F. Jin, and S.-I. An, 2009: Two Types of El Nino Events: Cold Tongue El Nino and Warm Pool El Nino. *Journal of Climate*, **22**, 1499-1515.

Kug, J.-S., S.-I. An, Y.-G. Ham, and I.-S. Kang, 2010a: Changes in El Nio and La Nia teleconnections over North Pacific-America in the global warming simulations. *Theoretical and Applied Climatology*, **100**, 275-282.

Kug, J. S., S. I. An, Y. G. Ham, and I. S. Kang, 2010b: Changes in El Nio and La Nia teleconnections over North Pacific-America in the global warming simulations. *Theoretical and Applied Climatology*, **100**, 275-282.

Kug, J. S., J. Choi, S. I. An, F. F. Jin, and A. T. Wittenberg, 2010c: Warm Pool and Cold Tongue El Nino Events as Simulated by the GFDL 2.1 Coupled GCM. *Journal of Climate*, **23**, 1226-1239.

Kumar, K., S. Patwardhan, A. Kulkarni, K. Kamala, K. Rao, and R. Jones, 2011a: Simulated projections for summer monsoon climate over India by a high-resolution regional climate model (PRECIS). *Current Science*, **101**, 312-326.

Kumar, K., et al., 2011b: The once and future pulse of Indian monsoonal climate. *Climate Dynamics*, **36**, 2159-2170.

Kumar, K. K., B. Rajagopalan, and M. A. Cane, 1999: On the weakening relationship between the Indian monsoon and ENSO. *Science*, **284**, 2156-2159.

Kumar, K. K., B. Rajagopalan, M. Hoerling, G. Bates, and M. Cane, 2006a: Unraveling the mystery of Indian monsoon failure during El Nino. *Science*, **314**, 115-119.

Kumar, K. R., et al., 2006b: High-resolution climate change scenarios for India for the 21st century. *Current Science*, **90**, 334-345.

Kunkel, K. E., and e. al., 2008: Observed Changes in Weather and Climate Extremes. In: Weather and Climate Extremes in a Changing Climate. Regions of Focus: North America,

Hawaii, Caribbean, and U.S. Pacific Islands., 222 pp. pp.

Kuzmina, S. I., L. Bengtsson, O. M. Johannessen, H. Drange, L. P. Bobylev, and M. W. Miles, 2005: The North Atlantic Oscillation and greenhouse-gas forcing. *Geophysical research Letters*, **32**.

Kvamsto, N., P. Skeie, and D. Stephenson, 2004: Impact of labrador sea-ice extent on the North Atlantic oscillation. *International Journal of Climatology*, **24**, 603-612.

Kwok, R., and J. C. Comiso, 2002: Southern ocean climate and sea ice anomalies associated with the Southern Oscillation. *Journal of Climate*, **15**, 487-501.

L'Heureux, M., and R. Higgins, 2008: Boreal winter links between the Madden-Julian oscillation and the Arctic oscillation. *Journal of Climate*, **21**, 3040-3050.

L'Heureux, M., A. Butler, B. Jha, A. Kumar, and W. Q. Wang, 2010: Unusual extremes in the negative phase of the Arctic Oscillation during 2009. *Geophysical research Letters*, **37**.

L'Heureux, M. L., and D. W. J. Thompson, 2006: Observed relationships between the El Niño–Southern Oscillation and the extratropical zonal-mean circulation. *Journal of Climate*, **19**, 276-287.

Laine, A., M. Kageyama, D. Salas-Melia, G. Ramstein, S. Planton, S. Denvil, and S. Tyteca, 2009: An Energetics Study of Wintertime Northern Hemisphere Storm Tracks under 4 x CO(2) Conditions in Two Ocean-Atmosphere Coupled Models. *Journal of Climate*, **22**, 819-839.

Lambert, S. J., and J. C. Fyfe, 2006: Changes in winter cyclone frequencies and strengths simulated in enhanced greenhouse warming experiments: results from the models participating in the IPCC diagnostic exercise. *Climate Dynamics*, **26**, 713-728.

Landsea, C. W., 2007: Counting Atlantic tropical cyclones back to 1900. *Eos Transactions (AGU)*, **88**, 197-202.

Landsea, C. W., R. A. Pielke, A. Mestas-Nunez, and J. A. Knaff, 1999: Atlantic basin hurricanes: Indices of climatic changes. *Climatic Change*. 89-129.

Lapp, S. L., J. M. St. Jacques, E. M. Barrow, and D. J. Sauchyn, 2011: GCM projections for the Pacifi Decadal Oscillation under greenhouse forcing for the early 21st century. *International Journal of Climatology*, DOI: 10.1002/joc.2364.

Larkin, N. K., and D. E. Harrison, 2005: On the definition of El Nino and associated seasonal average US weather anomalies. *Geophysical research Letters*, **32**.

Larwanou, M., and M. Saadou, 2011: The role of human interventions in tree dynamics and environmental rehabilitation in the Sahel zone of Niger. *Journal of Arid Environments*, **75**, 194-200.

Latif, M., N. Keenlyside, and J. Bader, 2007: Tropical sea surface tempera- ture, vertical wind shear, and hurricane development. *Geophysical research Letters*, **34**, L01710.

Lau, K., S. Shen, K. Kim, and H. Wang, 2006: A multimodel study of the twentieth-century simulations of Sahel drought from the 1970s to 1990s. *Journal of Geophysical Research-Atmospheres*, **111**, -.

Lau, K., et al., 2008: The Joint Aerosol-Monsoon Experiment - A new challenge for monsoon climate research. *Bulletin of the American Meteorological Society*, DOI 10.1175/BAMS-89-3-369. 369-+.

Lau, K. M., and H. T. Wu, 2007: Detecting trends in tropical rainfall characteristics, 1979-2003. *International Journal of Climatology*, **27**, 979-988.

——, 2010: Characteristics of Precipitation, Cloud, and Latent Heating Associated with the Madden-Julian Oscillation. *Journal of Climate*, **23**, 504-518.

Lau, N.-C., and M.-J. Nath, 2012: A model study of heat waves over North America: Meteorological aspects and projections for the 21st century. *Journal of Climate*, **25**.

Lau, W. K. M., and K. M. Kim, 2010: Fingerprinting the impacts of aerosols on long-term trends of the Indian summer monsoon regional rainfall. *Geophysical research Letters*, **37**.

Lawrence, D., and P. Webster, 2002: The boreal summer intraseasonal oscillation: Relationship between northward and eastward movement of convection. *Journal of the Atmospheric Sciences*, **59**, 1593-1606.

Le Quéré, C., et al., 2007: Saturation of the Southern Ocean CO_2 sink due to recent climate change. *Science*, **316**, 1735-1738.

LeBarbe, L., and T. Lebel, 1997: Rainfall climatology of the HAPEX-Sahel region during the years 1950-1990. *Journal of Hydrology*, **189**, 43-73.

Lebel, T., and A. Ali, 2009: Recent trends in the Central and Western Sahel rainfall regime (1990-2007). *Journal of Hydrology*, **375**, 52-64.

Leblanc, M. J., P. Tregoning, G. Ramillien, S. O. Tweed, and A. Fakes, 2009: Basin-scale, integrated observations of the early 21st century multiyear drought in southeast Australia. *Water Resources Research*, **45**, -.

Leckebusch, G. C., U. Ulbrich, L. Froehlich, and J. G. Pinto, 2007a: Property loss potentials for European midlatitude storms in a changing climate. *Geophysical Research Letters*, **34**.

Leckebusch, G. C., U. Ulbrich, L. Frohlich, and J. G. Pinto, 2007b: Property loss potentials for European midlatitude storms in a changing climate. *Geophysical research Letters*, **34**.

Leckebusch, G. C., B. Koffi, U. Ulbrich, J. G. Pinto, T. Spangehl, and S. Zacharias, 2006: Analysis of frequency and intensity of European winter storm events from a multi-model perspective, at synoptic and regional scales. *Climate Research*, **31**, 59-74.

Lee, J. N., S. Hameed, and D. T. Shindell, 2008: The northern annular mode in summer and its relation to solar activity variations in the GISS ModelE. *Journal of Atmospheric and Solar-Terrestrial Physics*, **70**, 730-741.

Lee, S.-K., C. Wang, and D. B. Enfield, 2010: On the impact of central Pacific warming events on Atlantic tropical storm activity. *Geophysical research Letters*, **37**.

Lee, T., and M. J. McPhaden, 2010: Increasing intensity of El Nino in the central-equatorial Pacific. *Geophysical research Letters*, **37**.

Lengaigne, M., and G. Vecchi, 2010: Contrasting the termination of moderate and extreme El Nio events in coupled general circulation models. *Climate Dynamics*, **35**, 299-313.

Levine, R. C., and A. G. Turner, 2011: Dependence of Indian monsoon rainfall on moisture fluxes across the Arabian Sea and the impact of coupled model sea surface temperature biases.

Levitus, S., G. Matishov, D. Seidov, and I. Smolyar, 2009: Barents Sea multidecadal variability. *Geophysical research Letters*, **36**, L19604.

Li, G., and B. Ren, 2011: Evidence for strengthening of the tropical Pacific ocean surface wind speed during 1979-2001. *Theoretical Applied Climatology*, 10.1007/s00704-011-0463-3.

Li, H. M., L. Feng, and T. J. Zhou, 2011a: Multi-model Projection of July-August Climate Extreme Changes over China under CO2 Doubling. Part I: Precipitation. *Advances in Atmospheric Sciences*, **28**, 433-447.

——, 2011b: Multi-Model Projection of July-August Climate Extreme Changes over China under CO2 Doubling. Part II: Temperature. *Advances in Atmospheric Sciences*, **28**, 448-463.

Li, H. M., A. G. Dai, T. J. Zhou, and J. Lu, 2010: Responses of East Asian summer monsoon to historical SST and atmospheric forcing during 1950-2000. *Climate Dynamics*, **34**, 501-514.

Li, J. B., et al., 2011c: Interdecadal modulation of El Nino amplitude during the past millennium. *Nature Climate Change*, **1**, 114-118.

Li, S., J. Perlwitz, X. Quan, and M. Hoerling, 2008: Modelling the influence of North Atlantic multidecadal warmth on the Indian summer rainfall. *Geophysical research Letters*, **35**, -.
Li, W., R. Fu, and R. Dickinson, 2006: Rainfall and its seasonality over the Amazon in the 21st century as assessed by the coupled models for the IPCC AR4. *Journal of Geophysical Research-Atmospheres*, **111**, -.
Li, Y., and N.-C. Lau, 2011: Impact of ENSO on the atmospheric variability over the North Atlantic in late winter-Role of transient eddies. *Journal of Climate*, **24**.
——, 2012: Contributions of downstream eddy development to the teleconnection between ENSO and atmospheric circulation over the North Atlantic. *Journal of Climate*, **25**.
Liberato, M. L. R., J. G. Pinto, I. F. Trigo, and R. M. Trigo, 2011 Klaus – an exceptional winter storm over northern Iberia and southern France.
Liebmann, B., et al., 2007: Onset and end of the rainy season in South America in observations and the ECHAM 4.5 atmospheric general circulation model. *Journal of Climate*, **20**, 2037-2050.
Lienert, F., J. C. Fyfe, and W. J. Marryfield, 2011: Do Climate Models Capture the Tropical Influences on North Pacific sea surface temperature variability? *Journal of Climate*, **in press**.
Lim, E.-P., and I. Simmonds, 2009: Effect of tropospheric temperature change on the zonal mean circulation and SH winter extratropical cyclones. *Climate Dynamics*, **33**, 19-32.
Lin, H., G. Brunet, and J. Derome, 2009: An Observed Connection between the North Atlantic Oscillation and the Madden-Julian Oscillation. *Journal of Climate*, **22**, 364-380.
Lin, J., 2007: The double-ITCZ problem in IPCC AR4 coupled GCMs: Ocean-atmosphere feedback analysis. *Journal of Climate*, **20**, 4497-4525.
Lin, J., et al., 2006: Tropical intraseasonal variability in 14 IPCC AR4 climate models. Part I: Convective signals. *Journal of Climate*, **19**, 2665-2690.
Lin, J. L., et al., 2008: Subseasonal variability associated with Asian summer monsoon simulated by 14 IPCC AR4 coupled GCMs. *Journal of Climate*, **21**, 4541-4567.
Linkin, M., and S. Nigam, 2008: The north pacific oscillation-west Pacific teleconnection pattern: Mature-phase structure and winter impacts. *Journal of Climate*, **21**, 1979-1997.
Lintner, B., and J. Neelin, 2008: Eastern margin variability of the South Pacific Convergence Zone. *Geophysical research Letters*, **35**.
Lionello, P., U. Boldrin, and F. Giorgi, 2008a: Future changes in cyclone climatology over Europe as inferred from a regional climate simulation. *Climate Dynamics*, **30**, 657-671.
Lionello, P., S. Platon, and X. Rodo, 2008b: Preface: Trends and climate change in the Mediterranean region. *Global and Planetary Change*, **63**, 87-89.
Liu, J. P., and J. A. Curry, 2006: Variability of the tropical and subtropical ocean surface latent heat flux during 1989-2000. *Geophysical research Letters*, **33**.
Liu, Y. Y., A. I. J. M. van Dijk, R. A. M. de Jeu, and T. R. H. Holmes, 2009: An analysis of spatiotemporal variations of soil and vegetation moisture from a 29-year satellite-derived data set over mainland Australia. *Water Resources Research*, **45**, -.
Liu, Z., S. Vavrus, F. He, N. Wen, and Y. Zhong, 2005: Rethinking tropical ocean response to global warming: The enhanced equatorial warming. *Journal of Climate*, **18**, 4684-4700.
Lockwood, M., R. G. Harrison, T. Woollings, and S. K. Solanki, 2010: Are cold winters in Europe associated with low solar activity? *Environmental Research Letters*, **5**.
Loeptien, U., O. Zolina, S. Gulev, M. Latif, and V. Soloviov, 2008: Cyclone life cycle characteristics over the Northern Hemisphere in coupled GCMs. *Climate Dynamics*, **31**, 507-532.
Long, Z., W. Perrie, J. Gyakum, R. Laprise, and D. Caya, 2009: Scenario changes in the climatology of winter midlatitude cyclone activity over eastern North America and the Northwest Atlantic. *Journal of Geophysical Research-Atmospheres*, **114**.
Lorenz, D. J., and D. L. Hartmann, 2003: Eddy-zonal flow feedback in the Northern Hemisphere winter. *Journal of Climate*, **16**, 1212-1227.
Lorenz, D. J., and E. T. DeWeaver, 2007: Tropopause height and zonal wind response to global warming in the IPCC scenario integrations. *Journal of Geophysical Research-Atmospheres*, **112**.
Lu, J., 2009: The dynamics of the Indian Ocean sea surface temperature forcing of Sahel drought. *Climate Dynamics*, **33**, 445-460.
Lu, J., G. A. Vecchi, and T. Reichler, 2007: Expansion of the Hadley cell under global warming. *Geophysical research Letters*, **34**.
Lu, J., G. Chen, and D. M. W. Frierson, 2008: Response of the Zonal Mean Atmospheric Circulation to El Nino versus Global Warming. *Journal of Climate*, **21**, 5835-5851.
——, 2010: The Position of the Mid latitude Storm Track and Eddy-Driven Westerlies in Aquaplanet AGCMs. *Journal of the Atmospheric Sciences*, **67**, 3984-4000.
Lu, R., and Y. Fu, 2010a: Intensification of East Asian Summer Rainfall Interannual Variability in the Twenty-First Century Simulated by 12 CMIP3 Coupled Models. *Journal of Climate*, DOI 10.1175/2009JCLI3130.1. 3316-3331.
——, 2010b: Intensification of East Asian Summer Rainfall Interannual Variability in the Twenty-First Century Simulated by 12 CMIP3 Coupled Models. *Journal of Climate*, **23**, 3316-3331.

Luo, D. H., W. Zhou, and K. Wei, 2010: Dynamics of eddy-driven North Atlantic Oscillations in a localized shifting jet: zonal structure and downstream blocking. *Climate Dynamics*, **34**, 73-100.
Luo, F., S. Li, and T. Furevik, 2011: The connection between the Atlantic Multidecadal Oscillation and the Indian Summer Monsoon in Bergen Climate Model Version 2.0. *J. Geophys. Res.*, **116**, D19117.
Luo, Y., and L. M. Rothstein, 2011: Response of the Pacific ocean circulation to climate change. *Atmosphere-ocean*, **49**, 235-244.
MADDEN, R., and P. JULIAN, 1994: OBSERVATIONS OF THE 40-50-DAY TROPICAL OSCILLATION - A REVIEW. *Monthly Weather Review*, **122**, 814-837.
Maloney, E. D., and J. Shaman, 2008: Intraseasonal variability of the West African monsoon and Atlantic ITCZ. *Journal of Climate*, **21**, 2898-2918.
Mandke, S. K., A. K. Sahai, M. A. Shinde, S. Joseph, and R. Chattopadhyay, 2007: Simulated changes in active/break spells during the Indian summer monsoon due to enhanced CO2 concentrations: assessment from selected coupled atmosphere-ocean global climate models. *International Journal of Climatology*, **27**, 837-859.
Mann, M. E., and K. A. Emanuel, 2006a: Atlantic hurricane trends linked to climate change. *Eos Transactions (AGU)*, **87**, 233-241.
Mann, M. E., and K. A. Emanuel, 2006b: Atlantic hurricane trends linked to climate change. *Eos Transactions (AGU)*, **87**, 233-241.
Mann, M. E., T. A. Sabbatelli, and U. Neu, 2007a: Evidence for a modest undercount bias in early historical Atlantic tropical cyclone counts. *Geophysical research Letters*, **34**, L22707.
Mann, M. E., K. A. Emanuel, G. J. Holland, and P. J. Webster, 2007b: Atlantic tropical cyclones revisited. *Eos Transactions (AGU)*, **88**, 349-350.
Manton, M. J., et al., 2001: Trends in extreme daily rainfall and temperature in Southeast Asia and the South Pacific: 1961-1998. *International Journal of Climatology*, **21**, 269-284.
Mantua, N., and S. Hare, 2002: The Pacific decadal oscillation. *Journal of Oceanography*, **58**, 35-44.
Mantua, N. J., S. R. Hare, Y. Zhang, J. M. Wallace, and R. C. Francis, 1997: A Pacific interdecadal climate oscillation with impacts on salmon production. *Bulletin of the American Meteorological Society*. 1069-1079.
Marengo, J. A., R. Jones, L. M. Alves, and M. C. Valverde, 2009: Future change of temperature and precipitation extremes in South America as derived from the PRECIS regional climate modeling system. *International Journal of Climatology*, **29**, 2241-2255.
Marengo, J. A., M. Rusticucci, O. Penalba, and M. Renom, 2010a: An intercomparison of observed and simulated extreme rainfall and temperature events during the last half of the twentieth century: part 2: historical trends. *Climatic Change*, **98**, 509-529.
Marengo, J. A., et al., 2008: The drought of Amazonia in 2005. *Journal of Climate*, **21**, 495-516.
Marengo, J. A., et al., 2010b: Future change of climate in South America in the late twenty-first century: intercomparison of scenarios from three regional climate models. *Climate Dynamics*, **35**, 1089-1113.
Mariotti, A., and A. Dell'Aquila, 2011: Decadal climate variability in the Mediterranean region: roles of large-scale forcings and regional processes., doi 10.1007/s00382-00011-01056-00387.
Marshall, A. G., and A. A. Scaife, 2009: Impact of the QBO on surface winter climate. *Journal of Geophysical Research*, **114**.
Marshall, A. G., and A. A. Scaife, 2010: Improved predictability of stratospheric sudden warming events in an atmospheric general circulation model with enhanced stratospheric resolution. *Journal of Geophysical Research-Atmospheres*, **115**.
Marshall, G. J., 2003: Trends in the southern annular mode from observations and reanalyses. *Journal of Climate*, **16**, 4134-4143.
Marshall, G. J., 2007: Half-century seasonal relationships between the Southern Annular Mode and Antarctic temperatures. *International Journal of Climatology*, **27**, 373–383.
Marshall, G. J., S. di Battista, S. S. Naik, and M. Thamban, 2011: Analysis of a regional change in the sign of the SAM-temperature relationship in Antarctica. *Climate Dynamics*, **36**, 277–287.
Marullo, S., V. Artale, and R. Santoleri, 2011: The SST Multidecadal Variability in the Atlantic-Mediterranean Region and Its Relation to AMO. *Journal of Climate*, **24**, 4385-4401.
Matsueda, M., H. Endo, and R. Mizuta, 2010: Future change in Southern Hemisphere summertime and wintertime atmospheric blockings simulated using a 20-km-mesh AGCM. *Geophysical research Letters*, **37**, L02803.
Maue, R. N., 2009: Northern Hemisphere tropical cyclone activity. *Geophysical research Letters*, **36**, -.
May, W., 2011: The sensitivity of the Indian summer monsoon to a global warming of 2A degrees C with respect to pre-industrial times. *Climate Dynamics*, **37**, 1843-1868.
McCabe, G., and D. Wolock, 2010: Long-term variability in Northern Hemisphere snow cover and associations with warmer winters. *Climatic Change*, DOI 10.1007/s10584-009-9675-2. 141-153.
McCabe, G. J., and M. M. Dettinger, 2002: Primary modes and predictability of year-to-year snowpack variations in the western United States from teleconnections with Pacific Ocean Climate. *Journal of Hydrometeorology*, **3**, 13.
McDonald, R. E., 2011 Understanding the impact of climate change on Northern Hemisphere extra-tropical cyclones. 1399-1425
McKee, D. C., X. Yuan, A. L. Gordon, B. A. Huber, and Z. Dong, 2011: Climate impact on interannual variability of Weddell Sea Bottom Water. *Journal of Geophysical Research*, **116**.

McPhaden, M. J., T. Lee, and D. McClurg, 2011: El Nino and its relationship to changing background conditions in the tropical Pacific Ocean. *Geophysical research Letters*, **38**.
Meehl, G., J. Arblaster, and W. Collins, 2008: Effects of Black Carbon Aerosols on the Indian Monsoon. *Journal of Climate*, **21**, 2869-2882.
Meehl, G. A., and A. X. Hu, 2006: Megadroughts in the Indian monsoon region and southwest North America and a mechanism for associated multidecadal Pacific sea surface temperature anomalies. *Journal of Climate*, **19**, 1605-1623.
Meehl, G. A., J. M. Arblaster, D. M. Lawrence, A. Seth, E. K. Schneider, B. P. Kirtman, and D. Min, 2006: Monsoon regimes in the CCSM3. *Journal of Climate*, **19**, 2482-2495.
Meehl, G. A., et al., 2007a: Global climate projections. Contribution of Working Group I to the Fourth Assessment Report of the Intergovernmental Panel on Climate Change
Meehl, G. A., et al., 2007b: Global Climate Projections. *Climate Change 2007: The Physical Science Basis. Contribution of Working Group I to the Fourth Assessment Report of the Intergovernmental Panel on Climate Change*, Cambridge University Press.
Mendez, M., and V. Magana, 2010: Regional Aspects of Prolonged Meteorological Droughts over Mexico and Central America. *Journal of Climate*, **23**, 1175-1188.
Mendoza, B., V. Garcia-Acosta, V. Velasco, E. Jauregui, and R. Diaz-Sandoval, 2007: Frequency and duration of historical droughts from the 16th to the 19th centuries in the Mexican Maya lands, Yucatan Peninsula. *Climatic Change*, **83**, 151-168.
Meneghini, B., I. Simmonds, and I. N. Smith, 2007: Association between Australian rainfall and the Southern Annular Mode. *International Journal of Climatology*, **27**, 109-121.
Menendez, C. G., and A. F. Carril, 2010: Potential changes in extremes and links with the Southern Annular Mode as simulated by a multi-model ensemble. *Climatic Change*, **98**, 359-377.
Miller, R. L., G. A. Schmidt, and D. T. Shindell, 2006a: Forced annular variations in the 20th century intergovernmental panel on climate change fourth assessment report models. *Journal of Geophysical Research-Atmospheres*, **111**, 17.
——, 2006b: Forced annular variations in the 20th century intergovernmental panel on climate change fourth assessment report models. *Journal of Geophysical Research-Atmospheres*, **111**.
Ming, Y., and V. Ramaswamy, 2009: Nonlinear Climate and Hydrological Responses to Aerosol Effects. *Journal of Climate*, DOI 10.1175/2008JCLI2362.1. 1329-1339.
Ministry for the Environment, 2008: Coastal hazards and climate change. A guidance manual for local Government in New Zealand, viii+127 pp.
Minvielle, M., and R. D. Garreaud, 2011: Projecting Rainfall Changes over the South American Altiplano. *Journal of Climate*, **24**, 4577-4583.
Mitas, C. M., and A. Clement, 2005: Has the Hadley cell been strengthening in recent decades? *Geophysical research Letters*, **32**.
——, 2006: Recent behavior of the Hadley cell and tropical thermodynamics in climate models and reanalyses. *Geophysical research Letters*, **33**.
Mitchell, D. L., D. Ivanova, R. Rabin, T. J. Brown, and K. Redmond, 2002a: Gulf of California Sea Surface Temperatures and the North American Monsoon: Mechanistic Implications from Observations, **15**, 2261-2281.
——, 2002b: Gulf of California Sea Surface Temperatures and the North American Monsoon: Mechanistic Implications from Observations. 2261-2281.
Mitchell, T. P., and J. M. Wallace, 1996: ENSO seasonality: 1950-78 versus 1979-92. *Journal of Climate*, **9**, 3149-3161.
Mo, K. C., 2010: Interdecadal Modulation of the Impact of ENSO on Precipitation and Temperature over the United States. *Journal of Climate*, **23**, 3639-3656.
Mohino, E., S. Janicot, and J. Bader, 2011: Sahel rainfall and decadal to multi-decadal sea surface temperature variability. *Climate Dynamics*, **37**, 419-440.
Monahan, A. H., L. Pandolfo, and J. C. Fyfe, 2001: The preferred structure of variability of the Northern Hemisphere atmospheric circulation. *Geophysical research Letters*, **28**, 1019–1022.
Monahan, A. H., J. C. Fyfe, M. H. P. Ambaum, D. B. Stephenson, and G. R. North, 2009: Empirical Orthogonal Functions: The Medium is the Message. *Journal of Climate*, **22**, 6501-6514.
Morgenstern, O., et al., 2010: Anthropogenic forcing of the Northern Annular Mode in CCMVal-2 models. *Journal of Geophysical Research-Atmospheres*, **115**.
Moron, V., A. W. Robertson, and R. Boer, 2009: Spatial Coherence and Seasonal Predictability of Monsoon Onset over Indonesia. *Journal of Climate*, **22**, 840-850.
Moron, V., A. W. Robertson, and J.-H. Qian, 2010: Local versus regional-scale characteristics of monsoon onset and post-onset rainfall over Indonesia. *Climate Dynamics*, **34**, 281-299.
Moum, J. N., R. C. Lien, A. Perlin, J. D. Nash, M. C. Gregg, and P. J. Wiles, 2009: Sea surface cooling at the Equator by subsurface mixing in tropical instability waves. *Nature Geoscience*, **2**, 761-765.
Mpelasoka, F., K. Hennessy, R. Jones, and B. Bates, 2008: Comparison of suitable drought indices for climate change impacts assessment over Australia towards resource management. *International Journal of Climatology*, **28**, 1283-1292.

Msadek, R., K. Dixon, T. Delworth, and W. Hurlin, 2010: Assessing the predictability of the Atlantic meridional overturning circulation and associated fingerprints (vol 37, L19608, 2010). *Geophysical research Letters*, **37**, -.
Mueller, W. A., and E. Roeckner, 2008: ENSO teleconnections in projections of future climate in ECHAM5/MPI-OM. *Climate Dynamics*, **31**, 533-549.
Mullan, B., et al., 2008: Climate change effects and impacts assessment: A guidance manual for Local Government in New Zealand. 2nd Edition, xviii + 149 pp.
Muller, W. A., and E. Roeckner, 2006: ENSO impact on midlatitude circulation patterns in future climate change projections. *Geophysical research Letters*, **33**.
——, 2008: ENSO teleconnections in projections of future climate in ECHAM5/MPI-OM. *Climate Dynamics*, **31**, 533-549.
Murakami, H., B. Wang, and A. Kitoh, 2011: Future change of western North Pacific typhoons: Projections by a 20-km-mesh global atmospheric model.
Murphy, B. F., and B. Timbal, 2008: A review of recent climate variability and climate change in southeastern Australia. *International Journal of Climatology*, **28**, 859-879.
Nakamura, H., 1992: Midwinter Suppression of Baroclinic Wave Activity in the Pacific, **49 (17)**, 1629-1642.
Naylor, R. L., D. S. Battisti, D. J. Vimont, W. P. Falcon, and M. B. Burke, 2007: Assessing risks of climate variability and climate change for Indonesian rice agriculture. *Proceedings of the National Academy of Sciences of the United States of America*, **104**, 7752-7757.
Neelin, J., C. Chou, and H. Su, 2003: Tropical drought regions in global warming and El Nino teleconnections. *Geophysical research Letters*, **30**, -.
Newton, A., R. Thunell, and L. Stott, 2006: Climate and hydrographic variability in the Indo-Pacific Warm Pool during the last millennium. *Geophysical research Letters*, **33**, -.
Nguyen, K., J. Katzfey, and J. McGregor, 2011: Global 60 km simulations with CCAM: evaluation over the tropics. *Climate Dynamics*, 10.1007/s00382-011-1197-8. in press.
Nicholls, N., 2004: The changing nature of Australian droughts. *Climatic Change*, **63**, 323-336.
——, 2010: Local and remote causes of the southern Australian autumn-winter rainfall decline, 1958-2007. *Climate Dynamics*, **34**, 835-845.
Nigam, S., 2003a: *Teleconnections.* Vol. 6, Academic Press, 2243–2269 pp.
——, 2003b: Teleconnections. *Encyclopedia of Atmospheric Sciences,*, J. A. P. J. R. Holton, and J. A. Curry, Eds., Ed., Academic Press, 2243–2269.
Nigam, S., M. Barlow, and E. H. Berbery, 1999: Analysis links Pacific decadal variability to drought and streamflow in United States. 621.
Nikulin, G., E. Kjellstrom, U. Hansson, G. Strandberg, and A. Ullerstig, 2011: Evaluation and future projections of temperature, precipitation and wind extremes over Europe in an ensemble of regional climate simulations. 41-55.
Nishii, K., T. Miyasaka, Y. Kosaka, and H. Nakamura, 2009: Reproducibility and Future Projection of the Midwinter Storm-Track Activity over the Far East in the CMIP3 Climate Models in Relation to "Haru-Ichiban" over Japan. *Journal of the Meteorological Society of Japan*, DOI 10.2151/jmsj.87.581. 581-588.
Norton, C. W., P. S. Chu, and T. A. Schroeder, 2011: Projecting changes in future heavy rainfall events for Oahu, Hawaii: A statistical downscaling approach. *Journal of Geophysical Research*, **116**.
Nunez, M. N., S. A. Solman, and M. F. Cabre, 2009: Regional climate change experiments over southern South America. II: Climate change scenarios in the late twenty-first century. *Climate Dynamics*, **32**, 1081-1095.
O'Gorman, P. A., 2010: Understanding the varied response of the extratropical storm tracks to climate change. *Proceedings of the National Academy of Sciences of the United States of America*, **107**, 19176-19180.
O'Gorman, P. A., and T. Schneider, 2008: Energy of Midlatitude Transient Eddies in Idealized Simulations of Changed Climates. *Journal of Climate*, **21**, 5797-5806.
Onol, B., and F. H. M. Semazzi, 2009: Regionalization of Climate Change Simulations over the Eastern Mediterranean. *Journal of Climate*, **22**, 1944-1961.
Ose, T., and O. Arakawa, 2011: Uncertainty of Future Precipitation Change Due to Global Warming Associated with Sea Surface Temperature Change in the Tropical Pacific. *Journal of Meteorological Society of Japan*, **89**, 539-552.
Ouzeau, G., J. Cattiaux, H. Douville, A. Ribes, and D. Saint-Martin, 2011: European cold winter 2009-2010: How unusual in the instrumental record and how reproducible in the ARPEGE-Climat model? *Geophysical research Letters*, **38**, 6.
Overland, J. E., and M. Y. Wang, 2005: The third Arctic climate pattern: 1930s and early 2000s. *Geophysical research Letters*, **32**, L23808.
Overland, J. E., M. Wang, and S. Salo, 2008: The recent Arctic warm period. *Tellus Series A*, **60**, 589-597.
Paeth, H., and H. Thamm, 2007: Regional modelling of future African climate north of 15 degrees S including greenhouse warming and land degradation. *Climatic Change*, **83**, 401-427.
Paeth, H., A. Scholten, P. Friederichs, and A. Hense, 2008: Uncertainties in climate change prediction: El Nino-Southern Oscillation and monsoons. *Global and Planetary Change*, **60**, 265-288.
Paeth, H., K. Born, R. Girmes, R. Podzun, and D. Jacob, 2009: Regional Climate Change in Tropical and Northern Africa due to Greenhouse Forcing and Land Use Changes. *Journal of Climate*, **22**, 114-132.

Paeth, H., et al., 2011: Progress in regional downscaling of west African precipitation. *Atmospheric Science Letters*, **12**, 75-82.
Palmer, T. N., 1999: A nonlinear dynamical perspective on climate prediction. *Journal of Climate*, **12**, 575–591.
Patricola, C., and K. Cook, 2010: Northern African climate at the end of the twenty-first century: an integrated application of regional and global climate models. *Climate Dynamics*, **35**, 193-212.
——, 2011: Sub-Saharan Northern African climate at the end of the twenty-first century: forcing factors and climate change processes. *Climate Dynamics*, **37**, 1165-1188.
Pauling, A., and H. Paeth, 2007: On the variability of return periods of European winter precipitation extremes over the last three centuries. *Climate of the Past*, **3**, 65-76.
Perlwitz, J., S. Pawson, R. L. Fogt, J. E. Nielsen, and W. D. Neff, 2008: Impact of stratospheric ozone hole recovery on Antarctic climate. *Geophysical research Letters*, **35**.
Pierce, D., et al., 2008: Attribution of Declining Western US Snowpack to Human Effects. *Journal of Climate*, DOI 10.1175/2008JCLI2405.1. 6425-6444.
Pinto, J. G., T. Spangehl, U. Ulbrich, and P. Speth, 2006: Assessment of winter cyclone activity in a transient ECHAM4-OPYC3 GHG experiment. *Meteorol. Z.*, **15**, 279-291.
Pinto, J. G., E. L. Frohlich, G. C. Leckebusch, and U. Ulbrich, 2007a: Changing European storm loss potentials under modified climate conditions according to ensemble simulations of the ECHAM5/MPI-OM1 GCM. *Natural Hazards and Earth System Sciences*, **7**, 165-175.
Pinto, J. G., S. Zacharias, A. H. Fink, G. C. Leckebusch, and U. Ulbrich, 2009: Factors contributing to the development of extreme North Atlantic cyclones and their relationship with the NAO. *Climate Dynamics*, **32**, 711-737.
Pinto, J. G., U. Ulbrich, G. C. Leckebusch, T. Spangehl, M. Reyers, and S. Zacharias, 2007b: Changes in storm track and cyclone activity in three SRES ensemble experiments with the ECHAM5/MPI-OM1 GCM. *Climate Dynamics*, **29**, 195-210.
Plumb, R. A., 1977: The interaction of two internal waves with the mean flow: Implications for the theory of the quasi-biennial oscillation. *Journal of the Atmospheric Sciences*, **34**, 1847-1858.
Pohlmann, H., et al., 2011: Skillful predictions of the mid-latitude Atlantic meridional overturning circulation in a multi-model system. *Geophys. Res. Lett.*, **Submitted**.
Polo, I., A. Ullmann, P. Roucou, and B. Fontain, 2011: Weather Regimes in the Euro-Atlantic and Mediterranean Sector, and Relationship with West African Rainfall over the 1989-2008 Period from a Self-Organizing Maps Approach . 3423-3432.
Polvani, L. M., M. Previdi, and C. Deser, 2011: Large cancellation, due to ozone recovery, of future Southern Hemisphere atmospheric circulation trends. *Geophysical research Letters*, **38**.
Polyakov, I., V. Alexeev, U. Bhatt, E. Polyakova, and X. Zhang, 2010: North Atlantic warming: patterns of long-term trend and multidecadal variability. *Climate Dynamics*, **34**, 439-457.
Polyakov, I. V., et al., 2003: Variability and Trends of Air Temperature and Pressure in the Maritime Arctic, 1875–2000. *Journal of Climate*, **16**, 2067-2077.
Power, S. B., T. Caey, C. Folland, A. Colman, and V. Mehta, 1999: Interdecadal modulation of the Impact of ENSO on Australia. *Climate Dynamics*, **15**, 5.
Qian, J.-H., 2008: Why precipitation is mostly concentrated over islands in the Maritime Continent. *Journal of the Atmospheric Sciences*, **65**, 1428-1441.
Qian, J.-H., A. W. Robertson, and V. Moron, 2010: Interactions among ENSO, the Monsoon, and Diurnal Cycle in Rainfall Variability over Java, Indonesia. *Journal of the Atmospheric Sciences*, **67**, 3509-3524.
Qian, Y., D. Kaiser, L. Leung, and M. Xu, 2006: More frequent cloud-free sky and less surface solar radiation in China from 1955 to 2000. *Geophysical research Letters*, ARTN L01812, DOI 10.1029/2005GL024586. -.
Qian, Y., W. Wang, L. Leung, and D. Kaiser, 2007: Variability of solar radiation under cloud-free skies in China: The role of aerosols. *Geophysical research Letters*, ARTN L12804, DOI 10.1029/2006GL028800. -.
Qian, Y., D. Gong, J. Fan, L. Leung, R. Bennartz, D. Chen, and W. Wang, 2009: Heavy pollution suppresses light rain in China: Observations and modeling. *Journal of Geophysical Research-Atmospheres*, ARTN D00K02, DOI 10.1029/2008JD011575. -.
Quadrelli, R., and J. M. Wallace, 2004: A simplified linear framework for interpreting patterns of Northern Hemisphere wintertime climate variability. *Journal of Climate*, **17**, 3728-3744.
Raia, A., and I. F. D. Cavalcanti, 2008: The Life Cycle of the South American Monsoon System. *Journal of Climate*, **21**, 6227-6246.
Raible, C. C., B. Ziv, H. Saaroni, and M. Wild, 2010: Winter synoptic-scale variability over the Mediterranean Basin under future climate conditions as simulated by the ECHAM5. *Climate Dynamics*, **35**, 473-488.
Raible, C. C., P. M. Della-Marta, C. Schwierz, H. Wernli, and R. Blender, 2008: Northern hemisphere extratropical cyclones: A comparison of detection and tracking methods and different reanalyses. *Monthly Weather Review*, **136**, 880-897.
Rajendran, K., and A. Kitoh, 2008: Indian summer monsoon in future climate projection by a super high-resolution global model, **95**, 1560-1569.
Ramanathan, V., and G. Carmichael, 2008: Global and regional climate changes due to black carbon. *Nature Geoscience*, **1**, 221-227.

Ramesh, K. V., and P. Goswami, 2007: Reduction in temporal and spatial extent of the Indian summer monsoon. *Geophysical research Letters*, **34**.
Ramsay, H. A., and A. H. Sobel, 2011: The effects of relative and absolute sea surface temperature on tropical cyclone potential intensity using a single column model. *Journal of Climate*, **24**, 183-193.
Rao, V. B., C. C. Ferreira, S. H. Franchito, and S. S. V. S. Ramakrishna, 2008: In a changing climate weakening tropical easterly jet induces more violent tropical storms over the north Indian Ocean. *Geophysical research Letters*, **35**, L15710.
Rappin, E. D., D. S. Nolan, and K. A. Emanuel, 2010: Thermodynamic control of tropical cyclogenesis in environments of radiative-convective equilibrium with shear. *Quarterly Journal of the Royal Meteorological Society*, **136**, 1954-1971.
Rauniyar, S. P., and K. J. E. Walsh, 2011: Scale Interaction of the Diurnal Cycle of Rainfall over the Maritime Continent and Australia: Influence of the MJO. *Journal of Climate*, **24**, 325-348.
Rauscher, S. A., F. Giorgi, N. S. Diffenbaugh, and A. Seth, 2008: Extension and Intensification of the Meso-American mid-summer drought in the twenty-first century. *Climate Dynamics*, **31**, 551-571.
Rawlins, M. A., and Coauthors, 2010: Analysis of the Arctic System for Freshwater Cycle Intensification: Observations and Expectations. *Journal of Climate*, **23**, 5715-5737.
Rayner, N., Parker, D., Horton, E., Folland, C., Alexander, L., Rowell, D., Kent, E. and Kaplan, A., 2003. Global analyses of sea surface temperature, sea ice, and night marine air temperature since the late nineteenth century. Journal of Geophysical Research-Atmospheres, 108(D14): -.
Reboita, M. S., T. Ambrizzi, and R. P. da Rocha, 2009: Relationship between the southern annular mode and southern hemisphere atmospheric systems. *Revista Brasileira de Meteorologia*.
Ren, H. L., and F. F. Jin, 2011: Nino indices for two types of ENSO. *Geophysical research Letters*, **38**.
Renwick, J. A., 2005: Persistent positive anomalies in the Southern Hemisphere circulation. *Monthly Weather Review*, **133**, 977-988.
Renwick, J. A., and D. W. J. Thompson, 2006: The Southern Annular Mode and New Zealand climate. *Water & Atmosphere*, **14**, 24-25.
Richter-Menge, J., and J. E. Overland, 2009: Arctic Report Card 2009. NOAA, 103.
Rigor, I. G., J. M. Wallace, and R. L. Colony, 2002: Response of Sea Ice to the Arctic Oscillation. *Journal of Climate*, **15**, 2648-2663.
Rind, D., 2008: The consequences of not knowing low-and high-latitude climate sensitivity. *Bulletin of the American Meteorological Society*, **89**, 855-864.
Ring, M. J., and R. A. Plumb, 2007: Forced annular mode patterns in a simple atmospheric general circulation model. *Journal of the Atmospheric Sciences*, **64**, 3611-3626.
Riviere, G., 2011: A Dynamical Interpretation of the Poleward Shift of the Jet Streams in Global Warming Scenarios. *Journal of the Atmospheric Sciences*, **68**, 1253-1272.
Robertson, A., et al., 2011: The Maritime Continent monsoon. *The Global Monsoon System: Research and Forecast*, *C. Chang*, *Y. Ding*, *N.* L*au*, *R. J*ohn*son*, B. *Wan*g, and T. *Yasuna*ri, Eds., *World Scientific Publication Company*, 594.
Robinson, W. A., 2006: On the self-maintenance of midlatitude jets. *Journal of the Atmospheric Sciences*, **63**, 2109-2122.
Rodriguez-Fonseca, B., I. Polo, J. Garcia-Serrano, T. Losada, E. Mohino, C. Mechoso, and F. Kucharski, 2009: Are Atlantic Ninos enhancing Pacific ENSO events in recent decades? *Geophysical research Letters*, ARTN L20705, DOI 10.1029/2009GL040048. -.
Rodriguez-Fonseca, B., et al., 2011: Interannual and decadal SST-forced responses of the West African monsoon. *Atmospheric Science Letters*, **12**, 67-74.
Rogers, J. C., 1981: The North Pacific Oscillation. *Journal of Climatology*, **1**, 19.
Rotstayn, L., and U. Lohmann, 2002: Tropical rainfall trends and the indirect aerosol effect. *Journal of Climate*. 2103-2116.
Ruiz-Barradas, A., and S. Nigam, 2006: IPCC's twentieth-century climate simulations: Varied representations of north American hydroclimate variability. *Journal of Climate*. 4041-4058.
——, 2010: Great Plains Precipitation and Its SST Links in Twentieth-Century Climate Simulations, and Twenty-First-and Twenty-Second-Century Climate Projections. *Journal of Climate*, DOI 10.1175/2010JCLI3173.1. 6409-6429.
Ruosteenoja, K., T. R. Carter, K. Jylha, and H. Tuomenvirta, 2003: Future climate in world regions: and intercomparison of model-based projections for the new IPCC emissions scenarios, 83 pp.
S, K., M. R, and M. M, 2011: Future changes in the East Asian rain band projected by global atmospheric models with 20-km and 60-km grid size.
Sabade, S., A. Kulkarni, and R. Kripalani, 2011: Projected changes in South Asian summer monsoon by multi-model global warming experiments. *Theoretical and Applied Climatology*, DOI 10.1007/s00704-010-0296-5. 543-565.
Saenger, C., A. Cohen, D. Oppo, R. Halley, and J. Carilli, 2009: Surface-temperature trends and variability in the low-latitude North Atlantic since 1552. *Nature Geoscience*, **2**, 492-495.
Saji, N., Xie, S. and Yamagata, T., 2006: Tropical Indian Ocean variability in the IPCC twentieth-century climate simulations. Journal of Climate, 19(17): 4397-4417.

Saji, N. H., B. N. Goswami, P. N. Vinayachandran, and T. Yamagata, 1999: A dipole mode in the tropical Indian Ocean. *Nature*, **401**, 360-363.
Salahuddin, A., and S. Curtis, 2011: Climate extremes in Malaysia and the equatorial South China Sea. *Global and Planetary Change*, **78**, 83-91.
Salazar, L. F., C. A. Nobre, and M. D. Oyama, 2007: Climate change consequences on the biome distribution in tropical South America. *Geophysical research Letters*, **34**.
Salinger, M. J., J. A. Renwick, and A. B. Mullan, 2001: Interdecadal Pacific Oscillation and South Pacific climate. *International Journal of Climatology*, **21**, 1705-1722.
Sampe, T., and S.-P. Xie, 2010: Large-scale dynamics of the Meiyu-Baiu rainband: Environmental forcing by the westerly jet. *J. Climate*, **23**, 113-134.
Santer, B. D., and e. al., 2006: Forced and unforced ocean temperature changes in Atlantic and Pacific tropical cyclogenesis regions. *Proceedings of the National Academy of Sciences*, **103**, 13905-13910.
Sapiano, M. R. P., D. B. Stephenson, H. J. Grubb, and P. A. Arkin, 2006: Diagnosis of variability and trends in a global precipitation dataset using a physically motivated statistical model. *Journal of Climate*, **19**, 4154-4166.
Sato, T., F. Kimura, and A. Kitoh, 2007: Projection of global warming onto regional precipitation over Mongolia using a regional climate model. *Journal of Hydrology*, DOI 10.1016/j.jhydrol.2006.07.023. 144-154.
Scaife, A., et al., 2011: Climate change projections and stratosphere–troposphere interaction. *Climate Dynamics*, DOI 10.1007/s00382-011-1080-7.
Scaife, A. A., J. R. Knight, G. K. Vallis, and C. K. Folland, 2005: A stratospheric influence on the winter NAO and North Atlantic surface climate. *Geophysical research Letters*, **32**.
Scaife, A. A., C. K. Folland, L. V. Alexander, A. Moberg, and J. R. Knight, 2008: European climate extremes and the North Atlantic Oscillation. *Journal of Climate*, **21**, 72-83.
Scaife, A. A., T. Woollings, J. Knight, G. Martin, and T. Hinton, 2010: Atmospheric blocking and mean biases in 18 climate models. *Journal of Climate*, **23**, 6143-6152.
Schimanke, S., J. Koerper, T. Spangehl, and U. Cubasch, 2011: Multi-decadal variability of sudden stratospheric warmings in an AOGCM. *Geophysical research Letters*, **38**.
Schneider, D., C. Deser, and Y. Okumura, 2011: An assessment and interpretation of the observed warming of West Antarctica in the austral spring. *Climate Dynamics*, 10.1007/s00382-010-0985-x. 1-25.
Schneider, N., and B. Cornuelle, 2005: The forcing of the Pacific decadal oscillation. *Journal of Climate*, **18**, 4355-4373.
Schneider, T., P. A. O'Gorman, and X. J. Levine, 2010: WATER VAPOR AND THE DYNAMICS OF CLIMATE CHANGES. *Reviews of Geophysics*, **48**.
Schott, F., S. Xie, and J. McCreary, 2009: INDIAN OCEAN CIRCULATION AND CLIMATE VARIABILITY. *Reviews of Geophysics*, ARTN RG1002, DOI 10.1029/2007RG000245. -.
Seager, R., and R. Murtugudde, 1997: Ocean dynamics, thermocline adjustment, and regulation of tropical SST. *Journal of Climate*, **10**, 521-534.
Seager, R., and G. Vecchi, 2010: Greenhouse warming and the 21st century hydroclimate of southwestern North America. *Proceedings of the National Academy of Sciences*, **107**, 21277-21282.
Seager, R., A. Tzanova, and J. Nakamura, 2009a: Drought in the Southeastern United States: Causes, Variability over the Last Millennium, and the Potential for Future Hydroclimate Change. *Journal of Climate*, DOI 10.1175/2009JCLI2683.1. 5021-5045.
Seager, R., Y. Kushnir, M. Ting, M. Cane, N. Naik, and J. Miller, 2008: Would advance knowledge of 1930s SSTs have allowed prediction of the dust bowl drought? *Journal of Climate*, **21**, 3261-3281.
Seager, R., et al., 2009b: Mexican drought: an observational modeling and tree ring study of variability and climate change. *Atmosfera*, **22**, 1-31.
Seierstad, I., D. Stephenson, and N. Kvamsto, 2007: How useful are teleconnection patterns for explaining variability in extratropical storminess ? *Tellus Series a-Dynamic Meteorology and Oceanography*, **59**, 170-181.
Seierstad, I. A., and J. Bader, 2009: Impact of a projected future Arctic Sea Ice reduction on extratropical storminess and the NAO. *Climate Dynamics*, **33**, 937-943.
Semenov, V., M. Latif, D. Dommenget, N. Keenlyside, A. Strehz, T. Martin, and W. Park, 2010: The Impact of North Atlantic-Arctic Multidecadal Variability on Northern Hemisphere Surface Air Temperature. *Journal of Climate*, **23**, 5668-5677.
Semenov, V. A., 2007: Structure of temperature variability in the high latitudes of the Northern Hemisphere. *Izvestiya Atmospheric and Oceanic Physics*, **43**, 687-695.
Servain, J., I. Wainer, J. McCreary, and A. Dessier, 1999: Relationship between the equatorial and meridional modes of climatic variability in the tropical Atlantic. *Geophysical research Letters*. 485-488.
Seth, A., M. Rojas, and S. Rauscher, 2010a: CMIP3 projected changes in the annual cycle of the South American Monsoon. *Climatic Change*, **98**, 331-357.
Seth, A., M. Rojas, and S. A. Rauscher, 2010b: CMIP3 projected changes in the annual cycle of the South American Monsoon. *Climatic Change*, **98**, 331-357.
Seth, A., S. A. Rauscher, M. Rojas, A. Giannini, and S. J. Camargo, 2011: Enhanced spring convective barrier for monsoons in a warmer world? *Climatic Change*, **104**, 403-414.
Shanahan, T., et al., 2009: Atlantic Forcing of Persistent Drought in West Africa. *Science*, **324**, 377-380.

Shongwe, M. E., G. J. van Oldenborgh, B. van den Hurk, B. de Boer, C. A. S. Coelho, and M. K. van Aalst, 2009: Projected Changes in Mean and Extreme Precipitation in Africa under Global Warming. Part I: Southern Africa. *Journal of Climate*, **22**, 3819-3837.
Silvestri, G., and C. Vera, 2009: Nonstationary Impacts of the Southern Annular Mode on Southern Hemisphere Climate. *Journal of Climate*, **22**, 6142-6148.
Simpson, I. R., M. Blackburn, J. D. Haigh, and S. N. Sparrow, 2010: The Impact of the State of the Troposphere on the Response to Stratospheric Heating in a Simplified GCM. *Journal of Climate*, **23**, 6166-6185.
Sinha, A., et al., 2011: A global context for megadroughts in monsoon Asia during the past millennium. *Quaternary Science Reviews*, **30**, 47-62.
Smedsrud, L. H., A. Sorteberg, and K. Kloster, 2008: Recent and future changes of the Arctic sea-ice cover. *Geophysical research Letters*, **35**, L20503.
Smirnov, D., and D. Vimont, 2011: Variability of the Atlantic Meridional Mode during the Atlantic Hurricane Season. *Journal of Climate*, **24**, 1409-1424.
Smith, D., S. Cusack, A. Colman, C. Folland, G. Harris, and J. Murphy, 2007: Improved surface temperature prediction for the coming decade from a global climate model. *Science*, **317**, 796-799.
Soares, W. R., and J. A. Marengo, 2009: Assessments of moisture fluxes east of the Andes in South America in a global warming scenario. *International Journal of Climatology*, **29**, 1395-1414.
Sobel, A., and S. Camargo, 2011: Projected Future Seasonal Changes in Tropical Summer Climate. *Journal of Climate*, **24**, 473-487.
Son, S.-W., et al., 2008: The impact of stratospheric ozone recovery on the southern hemisphere westerly jet. *Science*, **320**, 1486-1489.
Son, S. W., and S. Y. Lee, 2005: The response of westerly jets to thermal driving in a primitive equation model. *Journal of the Atmospheric Sciences*, **62**, 3741-3757.
Song, J.-J., Y. Wang, and L. Wu, 2010: Trend discrepancies among three best track data sets of western North Pacific tropical cyclones. *Journal of Geophysical Research*, **115**.
Souza, P., and I. F. A. Cavalcanti, 2009: Atmospheric centres of action associated with the Atlantic ITCZ position. *International Journal of Climatology*, **29**, 2091-2105.
Sperber, K., and H. Annamalai, 2008: Coupled model simulations of boreal summer intraseasonal (30-50 day) variability, Part 1: Systematic errors and caution on use of metrics. *Climate Dynamics*, **31**, 345-372.
Steffensen, J., et al., 2008: High-resolution Greenland Ice Core data show abrupt climate change happens in few years. *Science*, **321**, 680-684.
Steig, E. J., D. P. Schneider, S. D. Rutherford, M. E. Mann, J. C. Comiso, and D. T. Shindell, 2009: Warming of the Antarctic ice-sheet surface since the 1957 International Geophysical Year. *Nature*, **457**, 459-462.
Stephenson, D., A. Hannachi, and A. O'Neill, 2004: On the existence of multiple climate regimes. *Quarterly Journal of the Royal Meteorological Society*, **130**, 583-605.
Stephenson, D., V. Pavan, M. Collins, M. Junge, and R. Quadrelli, 2006: North Atlantic Oscillation response to transient greenhouse gas forcing and the impact on European winter climate: a CMIP2 multi-model assessment. *Climate Dynamics*, **27**, 401-420.
Stoner, A. M. K., K. Hayhoe, and D. J. Wuebbles, 2009: Assessing General Circulation Model Simulations of Atmospheric Teleconnection Patterns. *Journal of Climate*, **22**, 4348-4372.
Stouffer, R., et al., 2006: Investigating the causes of the response of the thermohaline circulation to past and future climate changes. *Journal of Climate*, **19**, 1365-1387.
Straus, D., and J. Shukla, 2002: Does ENSO force the PNA? *Journal of Climate*. 2340-2358.
Stroeve, J., M. M. Holland, W. Meier, T. Scambos, and M. Serreze, 2007: Arctic sea ice decline: Faster than forecast. *Geophysical research Letters*, **34**, L09501.
Sturman, A. P., and N. J. Tapper, 2006: *The Weather and Climate of Australia and New Zealand.* 2nd ed. Oxford University Press, 541 pp.
Sud, Y. C., G. K. Walker, Y. P. Zhou, G. A. Schmidt, K. M. Lau, and R. F. Cahalan, 2008: Effects of doubled CO2 on tropical sea surface temperatures (SSTs) for onset of deep convection and maximum SST: Simulations based inferences (vol 35, artn no L18708, 2008). *Geophysical research Letters*, **35**.
Suhaila, J., S. M. Deni, W. Z. W. Zin, and A. A. Jemain, 2010: Spatial patterns and trends of daily rainfall regime in Peninsular Malaysia during the southwest and northeast monsoons: 1975-2004. *Meteorology and Atmospheric Physics*, **110**, 1-18.
Sung, M.-K., G.-H. Lim, and J.-S. Kug, 2010: Phase asymmetric downstream development of the North Atlantic Oscillation and its impact on the East Asian winter monsoon. *J. Geophys. Res.*, **115**.
Sutton, R., and D. Hodson, 2007: Climate response to basin-scale warming and cooling of the North Atlantic Ocean. *Journal of Climate*, **20**, 891-907.
Takahashi, K., and D. S. Battisti, 2007: Processes Controlling the Mean Tropical Pacific Precipitation Pattern. Part II: The SPCZ and the Southeast Pacific Dry Zone. *Journal of Climate*, **20**, 5696-5706.
Takahashi, K., A. Montecinos, K. Goubanova, and B. Dewitte, 2011: ENSO regimes: Reinterpreting the canonical and Modoki El Nino. *Geophysical research Letters*, **38**.
Takaya, K., and H. Nakamura, 2005: Mechanisms of intraseasonal amplification of the cold Siberian high. *J. Atmos. Sci.*, **62**, 4423-4440.

Takaya, Y., T. Yasuda, T. Ose, and T. Nakaegawa, 2010: Predictability of the Mean Location of Typhoon Formation in a Seasonal Prediction Experiment with a Coupled General Circulation Model. *Journal of the Meteorological Society of Japan*, DOI 10.2151/jmsj.2010-502. 799-812.
Taschetto, A. S., and M. H. England, 2009: El Nino Modoki Impacts on Australian Rainfall. *Journal of Climate*, **22**, 3167-3174.
Taschetto, A. S., C. C. Ummenhofer, A. Sen Gupta, and M. H. England, 2009: Effect of anomalous warming in the central Pacific on the Australian monsoon. *Geophysical research Letters*, **36**.
Taylor, C., A. Gounou, F. Guichard, P. Harris, R. Ellis, F. Couvreux, and M. De Kauwe, 2011a: Frequency of Sahelian storm initiation enhanced over mesoscale soil-moisture patterns. *Nature Geoscience*, **4**, 430-433.
Taylor, C., et al., 2011b: New perspectives on land-atmosphere feedbacks from the African Monsoon Multidisciplinary Analysis. *Atmospheric Science Letters*, **12**, 38-44.
Teng, H. Y., W. M. Washington, G. A. Meehl, L. E. Buja, and G. W. Strand, 2006: Twenty-first century Arctic climate change in the CCSM3 IPCC scenario simulations. *Climate Dynamics*, **26**, 601-616.
Thompson, D. W. J., and J. M. Wallace, 1998: The Arctic Oscillation signature in the wintertime geopotential height and temperature fields. *Geophysical research Letters*, **25**, 1297-1300.
——, 2000: Annular modes in the extratropical circulation. Part I: Month-to-month variability. *Journal of Climate*, **13**, 1000-1016.
Thompson, D. W. J., and S. Solomon, 2002: Interpretation of recent Southern Hemisphere climate change. *Science*, **296**, 895-899.
Thompson, D. W. J., S. Solomon, P. J. Kushner, M. H. England, K. M. Grise, and D. J. Karoly, 2011: Signatures of the Antarctic ozone hole in Southern Hemisphere surface climate change. *Nature Geoscience*, **4**, 741-749.
Timbal, B., and J. M. Arblaster, 2006: Land cover change as an additional forcing to explain the rainfall decline in the south west of Australia. *Geophysical research Letters*, **33**, -.
Timbal, B., J. M. Arblaster, and S. Power, 2006: Attribution of the late-twentieth-century rainfall decline in southwest Australia. *Journal of Climate*, **19**, 2046-2062.
Timmermann, A., F. F. Jin, and J. Abshagen, 2003: A nonlinear theory for El Nino bursting. *Journal of the Atmospheric Sciences*, **60**, 152-165.
Timmermann, A., S. McGregor, and F. Jin, 2010a: Wind Effects on Past and Future Regional Sea Level Trends in the Southern Indo-Pacific. *Journal of Climate*, **23**, 4429-4437.
Timmermann, A., et al., 2010b: Towards a quantitative understanding of millennial-scale Antarctic warming events. *Quaternary Science Reviews*, **29**, 74-85.
Timmermann, A., et al., 2007: The influence of a weakening of the Atlantic meridional overturning circulation on ENSO. *Journal of Climate*, **20**, 4899-4919.
Ting, M., Y. Kushnir, R. Seager, and C. Li, 2009: Forced and Internal Twentieth-Century SST Trends in the North Atlantic. *Journal of Climate*, **22**, 1469-1481.
——, 2011: Robust features of Atlantic multi-decadal variability and its climate impacts. *Geophysical research Letters*, **38**, -.
Tokinaga, H., and S. Xie, 2011: Weakening of the equatorial Atlantic cold tongue over the past six decades. *Nature Geoscience*, **4**, 222-226.
Tokinaga, H., S.-P. Xie, A. Timmermann, S. McGregor, T. Ogata, H. Kubota, and Y. M. Okumura, 2012a: Regional patterns of tropical Indo-Pacific climate change: Evidence of the Walker Circulation weakening. *J. Climate*.
——, **2012b**: Regional patterns of tropical Indo-Pacific climate change: Evidence of the Walker Circulation weakening. *Journal of Climate*, 10.1175/JCLI-D-11-00263.1.
Tougiani, A., C. Guero, and T. Rinaudo, 2009: Community mobilisation for improved livelihoods through tree crop management in Niger. *GeoJournal*, **74**, 377-389.
Trenberth, K. E., and J. W. Hurrell, 1994: Decadal atmosphere-ocean vairations in the Pacific. *Climate Dynamics*, **9**, 17.
Trenberth, K. E., and D. P. Tepaniak, 2001: Indices of El Nino evolution. *Journal of Climate*, **14**, 1697-1701.
Trenberth, K. E., D. P. Stepaniak, and L. Smith, 2005: Interannual variability of patterns of atmospheric mass distribution. *Journal of Climate*, **18**, 2812-2825.
Trigo, R. M., I. F. Trigo, C. C. DaCamara, and T. J. Osborn, 2004: Climate impact of the European winter blocking episodes from the NCEP/NCAR Reanalyses. *Climate Dynamics*, **23**, 17-28.
Türkes, M., and E. Erlat, 2009: Winter mean temperature variability in Turkey associated with the North Atlantic Oscillation . 211-225.
Tung, K. K., and J. S. Zhou, 2010: The Pacific's Response to Surface Heating in 130 Yr of SST: La Nina-like or El Nino-like? *Journal of the Atmospheric Sciences*, **67**, 2649-2657.
Turner, A. G., and J. M. Slingo, 2009: Subseasonal extremes of precipitation and active-break cycles of the Indian summer monsoon in a climate-change scenario. *Quarterly Journal of the Royal Meteorological Society*, **135**, 549-567.
Turner, A. G., P. M. Inness, and J. M. Slingo, 2007a: The effect of doubled CO2 and model basic state biases on the monsoon-ENSO system. I: Mean response and interannual variability. *Quarterly Journal of the Royal Meteorological Society*, **133**, 1143-1157.
Turner, J., J. E. Overland, and J. E. Walsh, 2007b: An Arctic and Antarctic perspective on recent climate change. *International Journal of Climatology*, **27**, 277-293.

Turner, J., et al., 2009: Non-annular atmospheric circulation change induced by stratospheric ozone depletion and its role in the recent increase of Antarctic sea ice extent. *Geophys. Res. Lett.*, **36**, L08502, doi:08510.01029/02009GL037524.
Tyrlis, E., and B. J. Hoskins, 2008: Aspects of a Northern Hemisphere atmospheric blocking climatology. *Journal of the Atmospheric Sciences*, **65**, 1638-1652.
Ueda, H., M. Ohba, and S. P. Xie, 2009: Important Factors for the Development of the Asian-Northwest Pacific Summer Monsoon. *Journal of Climate*, **22**, 649-669.
Ulbrich, U., G. C. Leckebusch, and J. G. Pinto, 2009: Extra-tropical cyclones in the present and future climate: a review. *Theoretical and Applied Climatology*, **96**, 117-131.
Ulbrich, U., J. G. Pinto, H. Kupfer, G. C. Leckebusch, T. Spangehl, and M. Reyers, 2008: Changing northern hemisphere storm tracks in an ensemble of IPCC climate change simulations. *Journal of Climate*, **21**, 1669-1679.
Ummenhofer, C. C., and M. H. England, 2007: Interannual extremes in New Zealand precipitation linked to modes of Southern Hemisphere climate variability. *Journal of Climate*, **20**, 5418-5440.
Ummenhofer, C. C., A. Sen Gupta, and M. H. England, 2009a: Causes of Late Twentieth-Century Trends in New Zealand Precipitation. *Journal of Climate*, **22**, 3-19.
Ummenhofer, C. C., et al., 2009b: What causes southeast Australia's worst droughts? *Geophysical research Letters*, **36**, -.
Vasconcellos, F. C., and I. F. A. Cavalcanti, 2010: Extreme precipitation over Southeastern Brazil in the austral summer and relations with the Southern Hemisphere annular mode. *Atmospheric Science Letters*, **11**, 21-26.
Vecchi, G. A., and B. J. Soden, 2007a: Global warming and the weakening of the tropical circulation. *Journal of Climate*, **20**, 4316-4340.
Vecchi, G. A., and B. J. Soden, 2007b: Increased tropical Atlantic wind shear in model projections of global warming. *Geophysical research Letters*, **34**.
Vecchi, G. A., and B. J. Soden, 2007c: Effect of remote sea surface temperature change on tropical cyclone potential intensity. *Nature*, **450**, 1066-U1069.
Vecchi, G. A., and T. R. Knutson, 2008: On Estimates of Historical North Atlantic Tropical Cyclone Activity. *Journal of Climate*, **21**, 3580-3600.
——, 2011: Estimating annual numbers of Atlantic hurricanes missing from the HURDAT database (1878-1965) using ship track density. *Journal of Climate*, **24**, 1736-1746.
Vecchi, G. A., K. L. Swanson, and B. J. Soden, 2008: Whither hurricane activity. *Science*, **322**.
Vecchi, G. A., B. J. Soden, A. T. Wittenberg, I. M. Held, A. Leetmaa, and M. J. Harrison, 2006: Weakening of tropical Pacific atmospheric circulation due to anthropogenic forcing. *Nature*, **441**, 73-76.
Vergara, 2007: Visualizing Future Climate in Latin America: Results from the application of the Earth Simulator.
Vicente-Serrano, S., and J. López-Moreno, 2008: Nonstationary influence of the North Atlantic Oscillation on European precipitation., doi 10.1029/2008JD010382.
Vicente-Serrano, S. M., and J. I. Lopez-Moreno, 2008: Differences in the non-stationary influence of the North Atlantic Oscillation on European precipitation under different scenarios of greenhouse gas concentrations. *Geophysical research Letters*, **35**.
Vimont, D., and J. Kossin, 2007: The Atlantic Meridional Mode and hurricane activity. *Geophysical research Letters*, ARTN L07709, DOI 10.1029/2007GL029683. -.
Vimont, D., M. Alexander, and A. Fontaine, 2009: Midlatitude Excitation of Tropical Variability in the Pacific: The Role of Thermodynamic Coupling and Seasonality. *Journal of Climate*, **22**, 518-534.
Vincent, D., 1994: The South Pacific Convergence Zone (SPCZ): A review. *Monthly Weather Review*, **122**, 1949-1970.
Vincent, E., M. Lengaigne, C. Menkes, N. Jourdain, P. Marchesiello, and G. Madec, 2011: Interannual variability of the South Pacific Convergence Zone and implications for tropical cyclone genesis. *Climate Dynamics*, **36**, 1881-1896.
Walker, G. T., 1923: Correlation in seasonal variations of weather VIII. A preliminary study of world-weather, 75-131 pp.
——, 1924: Correlation in seasonal variations of wether. IX. A further study of world weather, 275-332 pp.
Wallace, J. M., and D. S. Gutzler, 1981: Teleconnections in the geopotential height field during the Northern Hemisphere winter. *Monthly Weather Review*, **109**, 784-812.
Wang, B., 1995: INTERDECADAL CHANGES IN EL-NINO ONSET IN THE LAST 4 DECADES. *Journal of Climate*, **8**, 267-285.
Wang, B., and Y. Wang, 1996: Temporal structure of the Southern Oscillation as revealed by waveform and wavelet analysis. *Journal of Climate*, **9**, 1586-1598.
Wang, B., and S. I. An, 2001: Why the properties of El Nino changed during the late 1970s. *Geophysical research Letters*, **28**, 3709-3712.
Wang, B., and Q. Zhang, 2002: Pacific-east Asian teleconnection. Part II: How the Philippine Sea anomalous anticyclone is established during El Nino development. *Journal of Climate*, **15**, 3252-3265.
Wang, B., and S. I. An, 2002: A mechanism for decadal changes of ENSO behavior: roles of background wind changes. *Climate Dynamics*, **18**, 475-486.

Wang, B., and Q. Ding, 2006: Changes in global monsoon precipitation over the past 56 years. *Geophysical research Letters*, **33**, L06711.

Wang, B., and Q. Ding, 2008: Global monsoon: Dominant mode of annual variation in the tropics. *Dynamics of Atmospheres and Oceans*, **44**, 165-183.

Wang, B., R. G. Wu, and X. H. Fu, 2000: Pacific-East Asian teleconnection: how does ENSO affect East Asian climate? *Journal of Climate*, **13**, 1517-1536.

Wang, B., R. G. Wu, and T. Li, 2003: Atmosphere-warm ocean interaction and its impacts on Asian-Australian monsoon variation. *Journal of Climate*, **16**, 1195-1211.

Wang, B., Q. Ding, and J. Jhun, 2006: Trends in Seoul (1778-2004) summer precipitation. *Geophysical research Letters*, ARTN L15803, DOI 10.1029/2006GL026418. -.

Wang, B., J. Yang, and T. J. Zhou, 2008a: Interdecadal changes in the major modes of Asian-Australian monsoon variability: Strengthening relationship with ENSO since the late 1970s. *Journal of Climate*, **21**, 1771-1789.

Wang, B., Z. W. Wu, J. P. Li, J. Liu, C. P. Chang, Y. H. Ding, and G. X. Wu, 2008b: How to measure the strength of the East Asian summer monsoon. *Journal of Climate*, **21**, 4449-4463.

Wang, C., 2006: An overlooked feature of tropical climate: Inter-Pacific-Atlantic variability. *Geophysical research Letters*, ARTN L12702, DOI 10.1029/2006GL026324. -.

Wang, C., S. K. Lee, and D. B. Enfield, 2007: Impact of the Atlantic warm pool on the summer climate of the Western Hemisphere. *Journal of Climate*, **20**, 5021-5040.

——, 2008c: Climate response to anomalously large and small Atlantic warm pools during the summer. *Journal of Climate*, **21**, ***2437–2450***.

Wang, C., F. Kucharski, R. Barimalala, and A. Bracco, 2009: Teleconnections of the tropical Atlantic to the tropical Indian and Pacific Oceans: A review of recent findings. *Meteorol. Z.*, DOI 10.1127/0941-2948/2009/0394. 445-454.

Wang, G., and H. H. Hendon, 2007: Sensitivity of Australian rainfall to inter-El Nino variations. *Journal of Climate*, **20**, 4211-4226.

Wang, H., 2001: The weakening of the Asian monsoon circulation after the end of 1970's. *Advances in Atmospheric Sciences*. 376-386.

Wang, M., and J. E. Overland, 2009: A sea ice free summer Arctic within 30 years? *Geophysical research Letters*, **36**, L07502.

Wang, X., C. Wang, W. Zhou, D. Wang, and J. Song, 2011: Teleconnected influence of North Atlantic sea surface temperature on the El Nio onset. *Climate Dynamics*, **37**, 663-676.

Wanner, H., et al., 2001: North Atlantic Oscillation - Concepts and studies. *Surveys in Geophysics*, **22**, 321-382.

Ward, P., M. Marfai, Poerbandono, and E. Aldrian, 2011: Climate adaptation in the city of Jakarta. *Climate Adaptation and Flood Risk in Coastal Cities*, J. Aerts, W. Botzen, M. Bowman, P. Ward, and P. Dircke, Eds., Routledge - Earthscan, 352.

Webb, A. P., and P. S. Kench, 2010: The dynamic response of reef islands to sea-level rise: Evidence from multi-decadal analysis of island change in the Central Pacific. *Global and Planetary Change*, **72**, 234-246.

Webster, P. J., A. M. Moore, J. P. Loschnigg, and R. R. Leben, 1999: Coupled ocean-atmosphere dynamics in the Indian Ocean during 1997-98. *Nature*, **401**, 356-360.

Widlansky, M., P. Webster, and C. Hoyos, 2011: On the location and orientation of the South Pacific Convergence Zone. *Climate Dynamics*, **36**, 561-578.

Wiedenmann, J. M., A. R. Lupo, I. I. Mokhov, and E. A. Tikhonova, 2002: The climatology of blocking anticyclones for the Northern and Southern Hemispheres: Block intensity as a diagnostic. *Journal of Climate*, **15**, 3459-3473.

Williams, K., A. Jones, D. Roberts, C. Senior, and M. Woodage, 2001: The response of the climate system to the indirect effects of anthropogenic sulfate aerosol. *Climate Dynamics*. 845-856.

Wing, A. A., A. H. Sobel, and S. J. Camargo, 2007: Relationship between the potential and actual intensities of tropical cyclones on interannual time scales. *Geophysical research Letters*, **34**, L08810.

Wittenberg, A. T., 2009: Are historical records sufficient to constrain ENSO simulations? *Geophysical research Letters*, **36**.

Woollings, T., 2008: Vertical structure of anthropogenic zonal-mean atmospheric circulation change. *Geophysical research Letters*, **35**.

Woollings, T., 2010: Dynamical influences on European climate: an uncertain future. *Philosophical Transactions of the Royal Society a-Mathematical Physical and Engineering Sciences*, **368**, 3733-3756.

Woollings, T., B. Hoskins, M. Blackburn, and P. Berrisford, 2008: A new Rossby wave-breaking interpretation of the North Atlantic Oscillation. *Journal of the Atmospheric Sciences*, **65**, 609-626.

Woollings, T., A. Hannachi, B. Hoskins, and A. Turner, 2010: A Regime View of the North Atlantic Oscillation and Its Response to Anthropogenic Forcing. *Journal of Climate*, **23**, 1291-1307.

Woollings, T., J. M. Gregory, M. Reyers, and J. G. Pinto, 2011 Ocean-atmosphere interaction in the Atlantic storm track response to climate change.

Wu, B. Y., J. Wang, and J. E. Walsh, 2006: Dipole anomaly in the winter Arctic atmosphere and its association with sea ice motion. *Journal of Climate*, **19**, 210-225.

Wu, Q. G., and D. J. Karoly, 2007: Implications of changes in the atmospheric circulation on the detection of regional surface air temperature trends. *Geophysical research Letters*, **34**.

Wu, R., B. Kirtman, and V. Krishnamurthy, 2008: An asymmetric mode of tropical Indian Ocean rainfall variability in boreal spring. *Journal of Geophysical Research-Atmospheres*, **113**, -.
Wu, Y., M. Ting, R. Seager, H.-P. Huang, and M. A. Cane, 2011a: Changes in storm tracks and energy transports in a warmer climate simulated by the GFDL CM2.1 model. *Climate Dynamics*, **37**, 53-72.
Wu, Z., N. Huang, J. Wallace, B. Smoliak, and X. Chen, 2011b: On the time-varying trend in global-mean surface temperature. *Climate Dynamics*, **37**, 759-773.
Xie, S.-P., C. Deser, G. A. Vecchi, J. Ma, H. Teng, and A. T. Wittenberg, 2010a: Global Warming Pattern Formation: Sea Surface Temperature and Rainfall. *Journal of Climate*, **23**, 966-986.
XIE, S., and S. PHILANDER, 1994: A COUPLED OCEAN-ATMOSPHERE MODEL OF RELEVANCE TO THE ITCZ IN THE EASTERN PACIFIC. *Tellus Series a-Dynamic Meteorology and Oceanography*. 340-350.
Xie, S., C. Deser, G. Vecchi, J. Ma, H. Teng, and A. Wittenberg, 2010b: Global Warming Pattern Formation: Sea Surface Temperature and Rainfall. *Journal of Climate*, **23**, 966-986.
Xie, S., K. Hu, J. Hafner, H. Tokinaga, Y. Du, G. Huang, and T. Sampe, 2009: Indian Ocean Capacitor Effect on Indo-Western Pacific Climate during the Summer following El Nino. *Journal of Climate*, **22**, 730-747.
Xie, S. P., and J. A. Carton, 2004: Tropical Atlantic variability: Patterns, mechanisms, and impacts. American Geophysical Union, 121–142.
Xie, S. P., Y. Du, G. Huang, X. T. Zheng, H. Tokinaga, K. M. Hu, and Q. Y. Liu, 2010c: Decadal Shift in El Nino Influences on Indo-Western Pacific and East Asian Climate in the 1970s. *Journal of Climate*, **23**, 3352-3368.
Xie, S. P. D., C. Deser, G. A. Vecchi, J. Ma, H. Teng, and A. T. Wittenberg, 2010d: Global Warming Pattern Formation: Sea Surface Temperature and Rainfall. *Journal of Climate*, **23**, 966-986.
Xoplaki, E., J. F. Gonzalez-Rouco, J. Luterbacher, and H. Wanner, 2003: Mediterranean summer air temperature variability and its connection to the large-scale atmospheric circulation and SSTs. *Climate Dynamics*, **20**, 723-739.
——, 2004: Wet season Mediterranean precipitation variability: influence of large-scale dynamics and trends. *Climate Dynamics*, **23**, 63-78.
Xu, M., C. Chang, C. Fu, Y. Qi, A. Robock, D. Robinson, and H. Zhang, 2006: Steady decline of east Asian monsoon winds, 1969-2000: Evidence from direct ground measurements of wind speed. *Journal of Geophysical Research-Atmospheres*, ARTN D24111, DOI 10.1029/2006JD007337. -.
Xu, Y., X.-J. Gao, and F. Giorgi, 2009: Regional variability of climate change hot-spots in East Asia. *Adv. Atmos. Sci.*, **26**, 783-792.
Xue, Y., and others, 2010: Intercomparison and analyses of the climatology of the West African Monsoon in the West African Monsoon Modeling and Evaluation project (WAMME) first model intercomparison experiment. *Climate Dynamics*, **35**, 3-27.
Yamagata, T., S. K. Behera, J.-J. Luo, S. Masson, M. Jury, and S. A. Rao, 2004: Coupled ocean-atmosphere variability in the tropical Indian Ocean. American Geophysical Union, 189–212.
Yan, H., L. G. Sun, Y. H. Wang, W. Huang, S. C. Qiu, and C. Y. Yang, 2011: A record of the Southern Oscillation Index for the past 2,000 years from precipitation proxies. *Nature Geoscience*, **4**, 611-614.
Yang, Y., S.-P. Xie, and J. Hafner, 2008: Cloud patterns lee of Hawaii Island: A synthesis of satellite observations and numerical simulation. *Journal of Geophysical Research*, **113**.
Ye, Z. Q., and W. W. Hsieh, 2008: Changes in ENSO and Associated Overturning Circulations from Enhanced Greenhouse Gases by the End of the Twentieth Century. *Journal of Climate*, **21**, 5745-5763.
Yeh, S.-W., B. P. Kirtman, J.-S. Kug, W. Park, and M. Latif, 2011: Natural variability of the central Pacific El Nino event on multi-centennial timescales. *Geophysical research Letters*, **38**.
Yeh, S. W., and B. P. Kirtman, 2005: Pacific decadal variability and decadal ENSO amplitude modulation. *Geophysical research Letters*, **32**.
Yeh, S. W., J. S. Kug, B. Dewitte, M. H. Kwon, B. P. Kirtman, and F. F. Jin, 2009: El Nino in a changing climate. *Nature*, **461**, 511-U570.
Yin, J. H., 2005: A consistent poleward shift of the storm tracks in simulations of 21st century climate. *Geophysical research Letters*, **32**, 4.
Yokoi, S., and Y. Takayabu, 2009: Multi-model Projection of Global Warming Impact on Tropical Cyclone Genesis Frequency over the Western North Pacific. *Journal of the Meteorological Society of Japan*, DOI 10.2151/jmsj.87.525. 525-538.
Yu, B., and F. W. Zwiers, 2010: Changes in equatorial atmospheric zonal circulations in recent decades. *Geophysical research Letters*, **37**.
Yu, J. Y., H. Y. Kao, and T. Lee, 2010: Subtropics-Related Interannual Sea Surface Temperature Variability in the Central Equatorial Pacific. *Journal of Climate*, **23**, 2869-2884.
Yu, J. Y., H. Y. Kao, T. Lee, and S. T. Kim, 2011: Subsurface ocean temperature indices for Central-Pacific and Eastern-Pacific types of El Nio and La Nia events. *Theoretical and Applied Climatology*, **103**, 337-344.
Yu, R. C., and T. J. Zhou, 2007: Seasonality and three-dimensional structure of interdecadal change in the East Asian monsoon. *Journal of Climate*, **20**, 5344-5355.
Yu, R. C., B. Wang, and T. J. Zhou, 2004: Tropospheric cooling and summer monsoon weakening trend over East Asia. *Geophysical research Letters*, **31**, 4.

Zahn, M., and H. von Storch, 2010: Decreased frequency of North Atlantic polar lows associated with future climate warming. *Nature*, **467**, 309-312.

Zanchettin, D., A. Rubino, and J. Jungclaus, 2010: Intermittent multidecadal-to-centennial fluctuations dominate global temperature evolution over the last millennium. *Geophysical research Letters*, **37**, -.

Zhang, C., 2005: Madden-Julian oscillation. *Reviews of Geophysics*, **43**, -.

Zhang, C., and J. Gottschalck, 2002: SST anomalies of ENSO and the Madden-Julian oscillation in the equatorial Pacific. *Journal of Climate*, **15**, 2429-2445.

Zhang, C., et al., 2006a: Simulations of the Madden-Julian oscillation in four pairs of coupled and uncoupled global models. *Climate Dynamics*, **27**, 573-592.

Zhang, L., L. Wu, and L. Yu, 2011: Oceanic origin of a recent La Nia-like trend in the tropical Pacific. *Advances in Atmospheric Sciences*, **28**, 1109-1117.

Zhang, M. H., and H. Song, 2006: Evidence of deceleration of atmospheric vertical overturning circulation over the tropical Pacific. *Geophysical research Letters*, **33**.

Zhang, Q., Y. Guan, and H. Yang, 2008a: ENSO amplitude change in observation and coupled models. *Advances in Atmospheric Sciences*, DOI 10.1007/s00376-008-0361-5. 361-366.

Zhang, R., and T. Delworth, 2007: Impact of the Atlantic Multidecadal Oscillation on North Pacific climate variability. *Geophysical research Letters*, **34**, -.

Zhang, R., and T. L. Delworth, 2009a: A new method for attributing climate variations over the Atlantic Hurricane Basin's main development region. *Geophysical Research Letters*, **36**, -.

Zhang, R., and T. L. Delworth, 2009b: A new method for attributing climate variations over the Atlantic Hurricane Basin's main development region. *Geophysical research Letters*, **36**, L06701.

Zhang, R., T. Delworth, and I. Held, 2007a: Can the Atlantic Ocean drive the observed multidecadal variability in Northern Hemisphere mean temperature? *Geophysical research Letters*, **34**, -.

Zhang, R., S. Kang, and I. Held, 2010: Sensitivity of Climate Change Induced by the Weakening of the Atlantic Meridional Overturning Circulation to Cloud Feedback. *Journal of Climate*, **23**, 378-389.

Zhang, X., W. Lin, and M. Zhang, 2007b: Toward understanding the double Intertropical Convergence Zone pathology in coupled ocean-atmosphere general circulation models. *Journal of Geophysical Research-Atmospheres*, **112**, -.

Zhang, X. B., F. W. Zwiers, and P. A. Stott, 2006b: Multimodel multisignal climate change detection at regional scale. *Journal of Climate*, **19**, 4294-4307.

Zhang, X. D., A. Sorteberg, J. Zhang, R. Gerdes, and J. C. Comiso, 2008b: Recent radical shifts of atmospheric circulations and rapid changes in Arctic climate system. *Geophysical research Letters*, **35**, L22701.

Zhang, Y. C., X. Y. Kuang, W. D. Guo, and T. J. Zhou, 2006c: Seasonal evolution of the upper-tropospheric westerly jet core over East Asia. *Geophysical research Letters*, **33**, 4.

Zheng, X.-T., S.-P. Xie, and Q. Liu, 2011: Response of the Indian Ocean basin mode and its capacitor effect to global warming. *Journal of Climate*, **24**.

Zheng, X., S. Xie, G. Vecchi, Q. Liu, and J. Hafner, 2010: Indian Ocean Dipole Response to Global Warming: Analysis of Ocean-Atmospheric Feedbacks in a Coupled Model. *Journal of Climate*, DOI 10.1175/2009JCLI3326.1. 1240-1253.

Zhou, T., and J. Zhang, 2009: Harmonious Inter-decadal Changes of July-August Upper Tropospheric Temperature Across the North Atlantic, Eurasian Continent, and North Pacific. *Advances in Atmospheric Sciences*, **26**, 656-665.

Zhou, T. J., and L. W. Zou, 2010: Understanding the Predictability of East Asian Summer Monsoon from the Reproduction of Land-Sea Thermal Contrast Change in AMIP-Type Simulation. *Journal of Climate*, **23**, 6009-6026.

Zhou, T. J., L. X. Zhang, and H. M. Li, 2008: Changes in global land monsoon area and total rainfall accumulation over the last half century. *Geophysical research Letters*, **35**, 6.

Zhou, T. J., D. Y. Gong, J. Li, and B. Li, 2009a: Detecting and understanding the multi-decadal variability of the East Asian Summer Monsoon - Recent progress and state of affairs. *Meteorol. Z.*, **18**, 455-467.

Zhou, T. J., et al., 2009b: Why the Western Pacific Subtropical High Has Extended Westward since the Late 1970s. *Journal of Climate*, **22**, 2199-2215.

Zhou, T. J., et al., 2009c: The CLIVAR C20C project: which components of the Asian-Australian monsoon circulation variations are forced and reproducible? *Climate Dynamics*, **33**, 1051-1068.

Zhu, Y. L., and H. J. Wang, 2010: The Arctic and Antarctic Oscillations in the IPCC AR4 Coupled Models. *Acta Meteorologica Sinica*, **24**, 176-188.

Ziv, B., H. Saaroni, and P. Alpert, 2004: The factors governing the summer regime of the eastern Mediterranean., 1859-1871.

Zubair, L., and C. F. Ropelewski, 2006: The strengthening relationship between ENSO and northeast monsoon rainfall over Sri Lanka and southern India. *Journal of Climate*, **19**, 1567-1575.

Zveryaev, I., and R. Allan, 2010: Summertime precipitation variability over Europe and its links to atmospheric dynamics and evaporation., doi 10.1029/2008JD011213.

Tables

Table 14.1: Temperature and precipitation projections by the AR4 global models. Original Table 11.1 from AR4. [PLACEHOLDER FOR SECOND ORDER DRAFT: AR5 models will be summarized]. Averages over a number regions of the projections by a set of 21 AR4 global models for the A1B scenario. The mean temperature and precipitation responses are first averaged for each model over all available realizations of the 1980–1999 period from the 20C3M simulations and the 2080–2099 period of A1B. Computing the difference between these two periods, the table shows the minimum, maximum, median (50%), and 25% and 75% quartile values among the 21 models, for temperature in degrees Celsius and precipitation as a fractional change. Regions in which the middle half (25–75%) of this distribution is all of the same sign in the precipitation response are colored light brown for decreasing and light green for increasing precipitation. Signal-to-noise ratio for these values is indicated by first computing a consensus standard deviation of 20 year means, using those models that have at least 3 realizations of the 20C3M simulations. The signal is assumed to increase linearly in time, and the time required for the median signal to reach 2.88 times the standard deviation is displayed as an estimate of when this signal is clearly discernable. The probability of extremely warm, wet, and dry seasons is also presented, as described in the text (in Christensen et al. (2007)). For definitions of the regions see Giorgi et al. (2001) [to be considered for Supplementary Material].

		Temperature Response		% Precipitation Response		Extreme Seasons		
REGION	SEASON	MIN 25 50 75 MAX	T YRS	MIN 25 50 75 MAX	T YRS	WARM	WET	DRY
Africa								
WAF	DJF	2.3 2.7 3.0 3.5 4.6	10	-16 -2 6 13 23	115	100	24	5
	MAM	1.7 2.8 3.5 3.6 4.8	10	-11 -7 -3 5 11	175	100	8	9
	JJA	1.5 2.7 3.2 3.7 4.7	10	-18 -2 2 7 16	>200	100	21	9
	SON	1.9 2.5 3.3 3.7 4.7	10	-12 0 1 10 15	>200	100	14	5
	ANN	1.8 2.7 3.3 3.6 4.7	10	-9 -2 2 7 13	170	100	25	9
EAF	DJF	2.0 2.6 3.1 3.4 4.2	10	-3 6 13 16 33	55	100	24	1
	MAM	1.7 2.7 3.2 3.5 4.5	10	-9 2 6 9 20	130	100	14	5
	JJA	1.6 2.7 3.4 3.6 4.7	10	-18 -2 4 7 16	150	100	9	6
	SON	1.9 2.6 3.1 3.6 4.3	10	-10 3 7 13 38	95	100	21	3
	ANN	1.8 2.5 3.2 3.4 4.3	10	-3 2 7 11 25	60	100	32	1
SAF	DJF	1.8 2.7 3.1 3.4 4.7	10	-6 -3 0 5 10	>200	100	8	6
	MAM	1.7 2.9 3.1 3.8 4.7	10	-25 -8 0 4 12	>200	98	3	8
	JJA	1.9 3.0 3.4 3.6 4.8	10	-43 -27 -22 -7 -3	70	100	1	21
	SON	2.1 3.0 3.7 4.0 5.0	10	-43 -20 -13 -8 3	90	100	2	19
	ANN	1.9 2.9 3.4 3.7 4.8	10	-12 -9 -4 2 6	115	100	2	13
SAH	DJF	2.4 2.9 3.2 3.5 5.0	15	-47 -31 -18 -12 31	>200	97	3	11
	MAM	2.3 3.3 3.6 3.8 5.2	10	-42 -37 -18 -10 13	190	100	3	21
	JJA	2.6 3.6 4.1 4.4 5.8	10	-53 -28 -5 16 74	>200	100	13	10
	SON	2.8 3.4 3.7 4.3 5.4	10	-52 -15 6 23 64	>200	100	5	6
	ANN	2.6 3.2 3.6 4.0 5.4	10	-44 -24 -6 3 57	>200	100	7	15
Europe								
NEU	DJF	2.6 3.6 4.3 5.5 8.1	40	9 13 15 22 25	50	82	44	0
	MAM	2.1 2.4 3.1 4.3 5.3	35	0 8 12 15 21	60	81	31	1
	JJA	1.4 1.9 2.7 3.3 5.0	25	-21 -5 2 7 16	>200	89	10	10
	SON	1.9 2.6 2.9 4.2 5.4	30	-5 4 8 11 13	80	86	20	2
	ANN	2.3 2.7 3.2 4.5 5.3	25	0 6 9 11 16	45	97	47	1
SEU	DJF	1.7 2.5 2.6 3.3 4.6	25	-16 -10 -6 -1 6	155	93	3	12
	MAM	2.0 3.0 3.2 3.5 4.5	20	-24 -17 -16 -8 -2	60	99	1	28
	JJA	2.7 3.7 4.1 5.0 6.5	15	-53 -35 -24 -14 -3	55	100	1	41
	SON	2.3 2.8 3.3 4.0 5.2	15	-29 -15 -12 -9 -2	90	99	1	21
	ANN	2.2 3.0 3.5 4.0 5.1	15	-27 -16 -12 -9 -4	45	100	0	45
Asia								

REGION	SEASON	Temperature Response MIN 25 50 75 MAX	T YRS	% Precipitation Response MIN 25 50 75 MAX	T YRS	Extreme Seasons WARM	WET	DRY
NAS	DJF	2.9 4.8 6.0 6.6 8.7	20	12 20 26 37 55	30	90	69	0
	MAM	2.0 2.9 3.7 5.0 6.8	25	2 16 18 24 26	30	88	65	1
	JJA	2.0 2.7 3.0 4.9 5.6	15	-1 6 9 12 16	40	100	53	1
	SON	2.8 3.6 4.8 5.8 6.9	15	7 15 17 19 29	30	99	63	0
	ANN	2.7 3.4 4.3 5.3 6.4	15	10 12 15 19 25	20	100	90	0
CAS	DJF	2.2 2.6 3.2 3.9 5.2	25	-11 0 4 9 22	>200	83	9	2
	MAM	2.3 3.1 3.9 4.5 4.9	20	-26 -14 -9 -5 3	140	91	3	17
	JJA	2.7 3.7 4.1 4.9 5.7	10	-58 -28 -13 -5 21	140	100	3	20
	SON	2.5 3.2 3.8 4.1 4.9	15	-18 -4 3 9 24	>200	99	9	10
	ANN	2.6 3.2 3.7 4.4 5.2	10	-18 -6 -3 2 6	>200	100	4	12
TIB	DJF	2.8 3.7 4.1 4.9 6.9	20	1 12 19 26 36	45	95	38	0
	MAM	2.5 2.9 3.6 4.3 6.3	15	-3 4 10 14 34	70	94	35	2
	JJA	2.7 3.2 4.0 4.7 5.4	10	-11 0 4 10 28	>200	100	27	3
	SON	2.7 3.3 3.8 4.6 6.2	15	-8 -4 8 14 21	100	100	20	4
	ANN	2.8 3.2 3.8 4.5 6.1	10	-1 2 10 13 28	45	100	46	2
EAS	DJF	2.1 3.1 3.6 4.4 5.4	20	-4 6 10 17 42	105	95	19	1
	MAM	2.1 2.6 3.3 3.8 4.6	15	0 7 11 14 20	55	97	36	2
	JJA	1.9 2.5 3.1 3.9 5.0	10	-2 5 9 11 17	45	100	34	1
	SON	2.2 2.7 3.3 4.2 5.0	15	-13 -1 9 15 29	95	100	20	2
	ANN	2.3 2.8 3.3 4.1 4.9	10	2 4 9 14 20	40	100	48	1
SAS	DJF	2.7 3.2 3.6 3.9 4.8	10	-35 -9 -5 1 15	>200	99	5	7
	MAM	2.1 3.0 3.5 3.8 5.3	10	-30 -2 9 18 26	150	100	13	5
	JJA	1.2 2.2 2.7 3.2 4.4	15	-3 4 11 16 23	45	96	31	0
	SON	2.0 2.5 3.1 3.5 4.4	10	-12 8 15 20 26	50	100	27	3
	ANN	2.0 2.7 3.3 3.6 4.7	10	-15 5 11 15 20	40	100	38	3
SEA	DJF	1.6 2.1 2.5 2.9 3.6	10	-4 3 6 10 12	80	99	24	3
	MAM	1.5 2.2 2.7 3.1 3.9	10	-4 2 7 9 17	75	100	26	2
	JJA	1.5 2.2 2.4 2.9 3.8	10	-3 3 7 9 17	70	100	25	1
	SON	1.6 2.2 2.4 2.9 3.6	10	-2 2 6 10 21	85	99	26	2
	ANN	1.5 2.3 2.5 3.0 3.7	10	-2 3 7 8 15	40	100	44	1
North America								
ALA	DJF	4.4 5.6 6.3 7.5 11.0	30	6 20 28 34 56	40	80	40	0
	MAM	2.3 3.2 3.5 4.7 7.7	35	3 13 17 23 38	40	64	44	0
	JJA	1.3 1.8 2.4 3.8 5.7	25	1 8 14 20 30	45	87	45	1
	SON	2.3 3.6 4.5 5.3 7.4	25	6 14 19 31 36	40	86	53	0
	ANN	3.0 3.7 4.5 5.2 7.4	20	6 13 21 25 32	25	97	82	0
CGI	DJF	3.3 5.2 5.9 7.2 8.5	20	6 15 26 32 42	30	93	60	0
	MAM	2.4 3.2 3.8 4.6 7.2	20	4 13 17 20 34	35	96	52	1
	JJA	1.5 2.1 2.8 3.7 5.6	15	0 8 11 12 19	35	100	49	1
	SON	2.7 3.4 4.0 5.7 7.3	20	7 14 16 22 37	35	100	60	0
	ANN	2.8 3.5 4.3 5.0 7.1	15	8 12 15 20 31	25	100	89	0
WNA	DJF	1.6 3.1 3.6 4.4 5.8	25	-4 2 7 11 36	105	79	17	2
	MAM	1.5 2.4 3.1 3.4 6.0	20	-7 2 5 8 14	130	86	13	4
	JJA	2.3 3.2 3.8 4.8 5.7	10	-18 -10 -1 2 10	>200	100	2	13
	SON	2.0 2.8 3.1 4.5 5.3	20	-3 3 6 12 18	105	94	18	2
	ANN	2.1 2.9 3.4 4.1 5.7	15	-3 0 5 9 14	70	100	20	2
CNA	DJF	2.0 2.9 3.5 4.2 6.1	30	-18 0 5 8 14	>200	74	6	5

REGION	SEASON	Temperature Response MIN 25 50 75 MAX	T YRS	% Precipitation Response MIN 25 50 75 MAX	T YRS	Extreme Seasons WARM	WET	DRY
	MAM	1.9 2.8 3.3 3.9 5.7	25	-17 2 7 12 17	125	83	18	4
	JJA	2.4 3.1 4.1 5.1 6.4	20	-31 -15 -3 4 20	>200	92	6	16
	SON	2.4 3.0 3.5 4.6 5.8	20	-17 -4 4 11 24	>200	92	11	8
	ANN	2.3 3.0 3.5 4.4 5.8	15	-16 -3 3 7 15	>200	98	12	6
ENA	DJF	2.1 3.1 3.8 4.6 6.0	25	2 9 11 19 28	85	82	24	3
	MAM	2.3 2.7 3.5 3.9 5.9	20	-4 7 12 16 23	60	86	22	2
	JJA	2.1 2.6 3.3 4.3 5.4	15	-17 -3 1 6 13	>200	99	9	10
	SON	2.2 2.8 3.5 4.4 5.7	20	-7 4 7 11 17	150	95	20	5
	ANN	2.3 2.8 3.6 4.3 5.6	15	-3 5 7 10 15	55	100	32	1
Central and South America								
CAM	DJF	1.4 2.2 2.6 3.5 4.6	15	-57 -18 -14 -9 0	105	96	2	25
	MAM	1.9 2.7 3.6 3.8 5.2	10	-46 -25 -16 -10 15	75	100	1	20
	JJA	1.8 2.7 3.4 3.6 5.5	10	-44 -25 -9 -4 12	90	100	5	24
	SON	2.0 2.7 3.2 3.7 4.6	10	-45 -10 -4 7 24	>200	100	7	16
	ANN	1.8 2.6 3.2 3.6 5.0	10	-48 -16 -9 -5 9	65	100	3	35
AMZ	DJF	1.7 2.4 3.0 3.7 4.6	10	-13 0 4 11 17	130	93	27	5
	MAM	1.7 2.5 3.0 3.7 4.6	10	-13 -1 1 4 14	>200	100	16	5
	JJA	2.0 2.7 3.5 3.9 5.6	10	-38 -10 -3 2 13	170	100	7	16
	SON	1.8 2.8 3.5 4.1 5.4	10	-35 -12 -2 8 21	>200	100	15	14
	ANN	1.8 2.6 3.3 3.7 5.1	10	-21 -3 0 6 14	>200	100	21	9
SSA	DJF	1.5 2.5 2.7 3.3 4.3	10	-16 -2 1 7 10	>200	100	13	4
	MAM	1.8 2.3 2.6 3.0 4.2	15	-11 -2 1 5 7	>200	98	9	7
	JJA	1.7 2.1 2.4 2.8 3.6	15	-20 -7 0 3 17	>200	95	8	11
	SON	1.8 2.2 2.7 3.2 4.0	15	-20 -12 1 6 11	>200	99	7	11
	ANN	1.7 2.3 2.5 3.1 3.9	10	-12 -1 3 5 7	125	100	10	9
Australia and New Zealand								
NAU	DJF	2.2 2.6 3.1 3.7 4.6	20	-20 -8 1 9 27	>200	87	7	4
	MAM	2.1 2.7 3.1 3.3 4.3	20	-24 -12 1 15 40	>200	91	12	2
	JJA	2.0 2.7 3.0 3.3 4.3	25	-54 -20 -14 3 26	>200	95	4	10
	SON	2.5 3.0 3.2 3.8 5.0	20	-58 -32 -12 2 20	>200	98	5	10
	ANN	2.3 2.8 3.0 3.5 4.5	15	-25 -8 -4 8 23	>200	99	9	5
SAU	DJF	2.0 2.4 2.7 3.2 4.2	20	-23 -12 -2 12 30	>200	95	9	6
	MAM	2.0 2.2 2.5 2.8 3.9	20	-31 -9 -5 13 32	>200	89	7	7
	JJA	1.7 2.0 2.3 2.5 3.5	15	-37 -20 -11 -4 9	120	96	4	18
	SON	2.0 2.6 2.8 3.0 4.1	20	-42 -27 -14 -5 4	140	94	5	14
	ANN	1.9 2.4 2.6 2.9 3.9	15	-27 -13 -4 3 12	>200	100	5	7
Polar Region								
ARC	DJF	4.3 6.0 6.9 8.4 11.4	15	11 19 26 29 39	25	100	89	0
	MAM	2.4 3.7 4.4 4.9 7.3	15	9 14 16 21 32	25	100	74	0
	JJA	1.2 1.7 2.1 3.0 5.3	15	4 10 14 17 20	25	100	83	0
	SON	2.9 4.8 6.0 7.2 8.9	15	9 17 21 26 35	20	100	95	0
	ANN	2.8 4.0 4.9 5.6 7.8	15	10 15 18 22 28	20	100	100	0
ANT	DJF	0.8 2.2 2.6 2.9 4.6	20	-11 5 9 14 31	50	84	32	2
	MAM	1.3 2.2 2.6 3.3 5.3	20	1 8 12 19 40	40	89	52	0
	JJA	1.4 2.3 2.8 3.3 5.2	25	5 14 19 24 41	30	82	60	0
	SON	1.3 2.1 2.3 3.2 4.8	25	-2 9 12 18 36	45	77	42	0

REGION	SEASON	Temperature Response MIN 25 50 75 MAX	T YRS	% Precipitation Response MIN 25 50 75 MAX	T YRS	Extreme Seasons WARM	WET	DRY
	ANN	1.4 2.3 2.6 3.0 5.0	15	-2 9 14 17 35	25	98	81	1
Small Islands								
CAR	DJF	1.4 1.8 2.1 2.4 3.2	10	-21 -11 -6 0 10	185	100	3	10
	MAM	1.3 1.8 2.2 2.4 3.2	10	-28 -20 -13 -6 6	115	100	3	18
	JJA	1.3 1.8 2.0 2.4 3.2	10	-57 -35 -20 -6 8	60	100	2	40
	SON	1.6 1.9 2.0 2.5 3.4	10	-38 -18 -6 1 19	180	100	5	21
	ANN	1.4 1.8 2.0 2.4 3.2	10	-39 -19 -12 -3 11	60	100	2	37
IND	DJF	1.4 2.0 2.1 2.4 3.8	10	-4 2 4 9 20	135	100	19	2
	MAM	1.5 2.0 2.2 2.5 3.8	10	0 3 5 6 20	80	100	24	1
	JJA	1.4 1.9 2.1 2.4 3.7	10	-3 -1 3 5 20	165	100	19	4
	SON	1.4 1.9 2.0 2.3 3.6	10	-5 2 4 7 21	110	100	19	2
	ANN	1.4 1.9 2.1 2.4 3.7	10	-2 3 4 5 20	65	100	29	2
NPA	DJF	1.5 1.9 2.4 2.5 3.6	10	-5 1 3 6 17	130	100	17	1
	MAM	1.4 1.9 2.3 2.5 3.5	10	-17 -1 1 3 17	>200	100	14	8
	JJA	1.4 1.9 2.3 2.7 3.9	10	1 5 8 14 25	55	100	42	0
	SON	1.6 1.9 2.4 2.9 3.9	10	1 5 6 13 22	50	100	32	0
	ANN	1.5 1.9 2.3 2.6 3.7	10	0 3 5 10 19	60	100	36	1
SPA	DJF	1.4 1.7 1.8 2.1 3.2	10	-6 1 4 7 15	80	100	20	4
	MAM	1.4 1.8 1.9 2.1 3.2	10	-3 3 6 8 17	35	100	36	1
	JJA	1.4 1.7 1.8 2.0 3.1	10	-2 1 3 5 12	70	100	29	3
	SON	1.4 1.6 1.8 2.0 3.0	10	-8 -2 2 4 5	135	100	14	15
	ANN	1.4 1.7 1.8 2.0 3.1	10	-4 -3 3 6 11	40	100	38	2

Notes:
ARC = land + ocan
ANT = land only

Chapter 14: Climate Phenomena and their Relevance for Future Regional Climate Change

Coordinating Lead Authors: Jens Hesselbjerg Christensen (Denmark), Kanikicharla Krishna Kumar (India)

Lead Authors: Edvin Aldrian (Indonesia), Soon-Il An (Korea), Iracema Cavalcanti (Brazil), Manuel de Castro (Spain), Wenjie Dong (China), Prashant Goswami (India), Alex Hall (USA), Joseph Katongo Kanyanga (Zambia), Akio Kitoh (Japan), James Kossin (USA), Ngar-Cheung Lau (USA), James Renwick (New Zealand), David Stephenson (UK), Shang-Ping Xie (USA), Tianjun Zhou (China)

Contributing Authors: Tercio Ambrizzi, Mark Baldwin, Michela Biasutti, Josephine Brown, Ping Chang, Clara Deser, David Enfield, Alessandra Giannini, Ashok Karumuri, Jeff Knight, Thomas Knutson, Ashwini Kulkarni,Victor Magnana, Gareth Marshall, Jan Polcher, Yun Qian, Izuru Takayabu, John Turner, Caroline Ummenhofer, Bin Wang, Chunzai Wang, Matthew Widlansky, Tim Woollings, Chidong Zhang

Review Editors: John Fyfe (Canada), Won-Tae Kwon (Korea), Kevin Trenberth (USA), David Wratt (New Zealand)

Date of Draft: 16 December 2011

Notes: TSU Compiled Version

Figures

Box 14.2 Figure 1: [PLACEHOLDER FOR THE SECOND ORDER DRAFT: A synthesis figure to complement the information about main phenomena that shows a global map marking all the phenomena and also boxes showing the regions to be used in Section 14.3.]

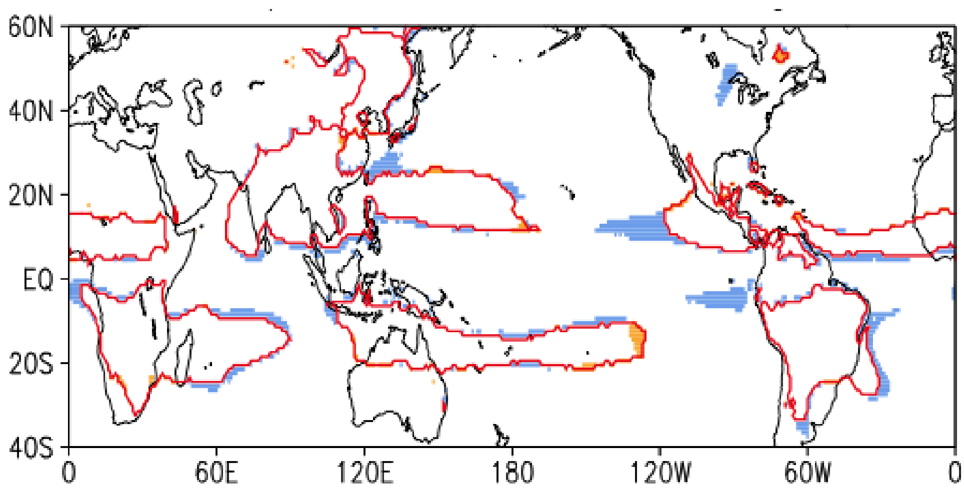

Figure 14.1: Changes in global monsoon area (GMA) under global warming. Difference of the GMA between the global warming and present-day simulations derived from the composite of five high-resolution model experiments, Red contours denote the composite GMA in the present-day simulations. Blue (orange) shading indicates the increase (decrease) of the GMA.

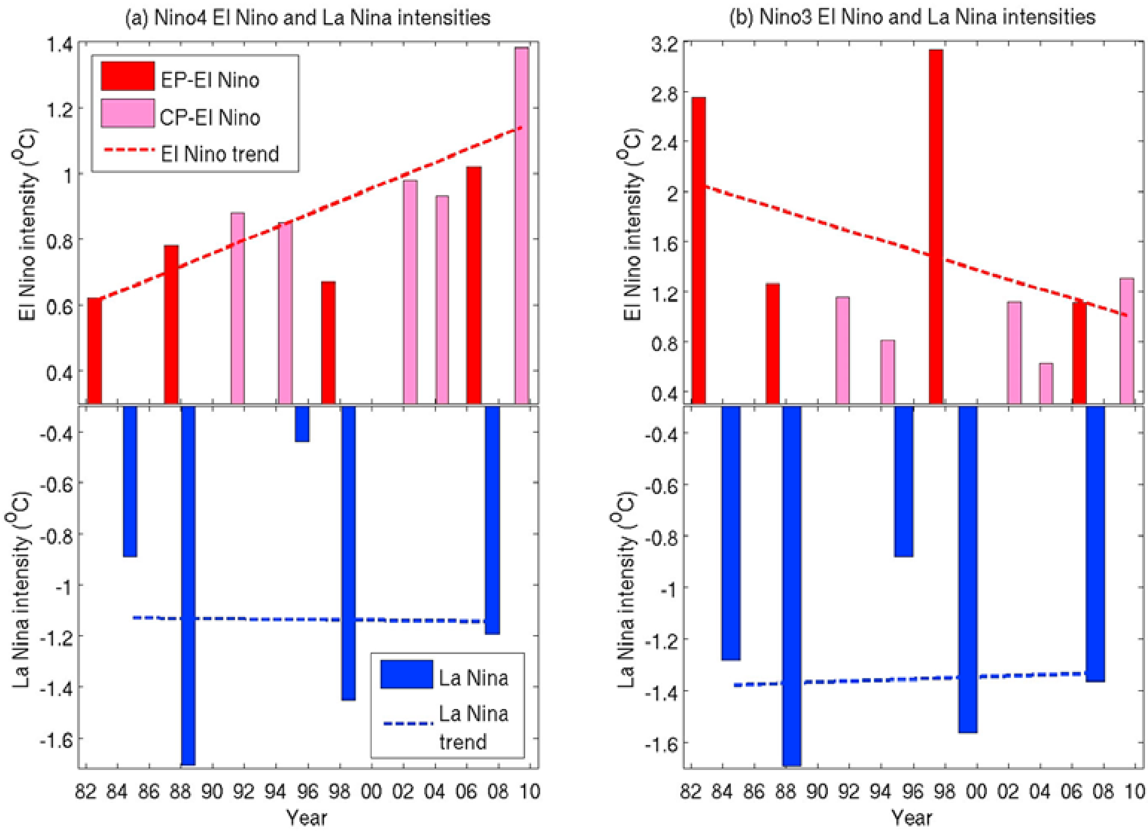

Figure 14.2: (a) Intensities of El Niño and La Niña events in the central equatorial Pacific (Niño4 region) and the estimated linear trends, which is 0.20(±0.18)°C/decade for El Niño and −0.01(±0.75)°C/decade for La Niña events. (b) Intensities of El Niño and La Niña events in the eastern equatorial Pacific (Niño3 region) and the estimated linear trends, which is 0.39(±0.71)°C/decade for El Niño and 0.02(±0.47)°C/decade for La Niña events. The uncertainty ranges reflect the 90% confidence intervals estimated from a Student's t-test. Note that the vertical scales start from ±0.3°C and that the scales are different for the Niño3 and Niño4 time series (Lee and McPhaden, 2010).

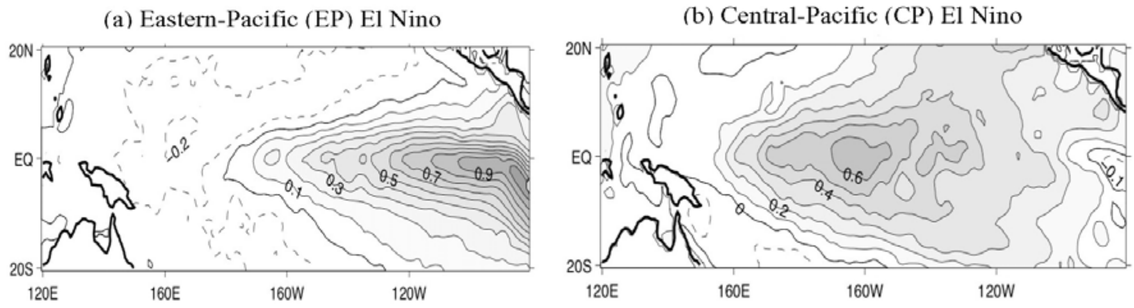

Figure 14.3: Leading EOF patterns of SST anomalies obtained from a combined EOF-regression analysis of Kao and Yu (2009) for (a) the eastern-Pacific type of El Niño and (b) the central Pacific type of El Niño. Contour intervals are 0.1 (Courtesy from Jin-Yi Yu).

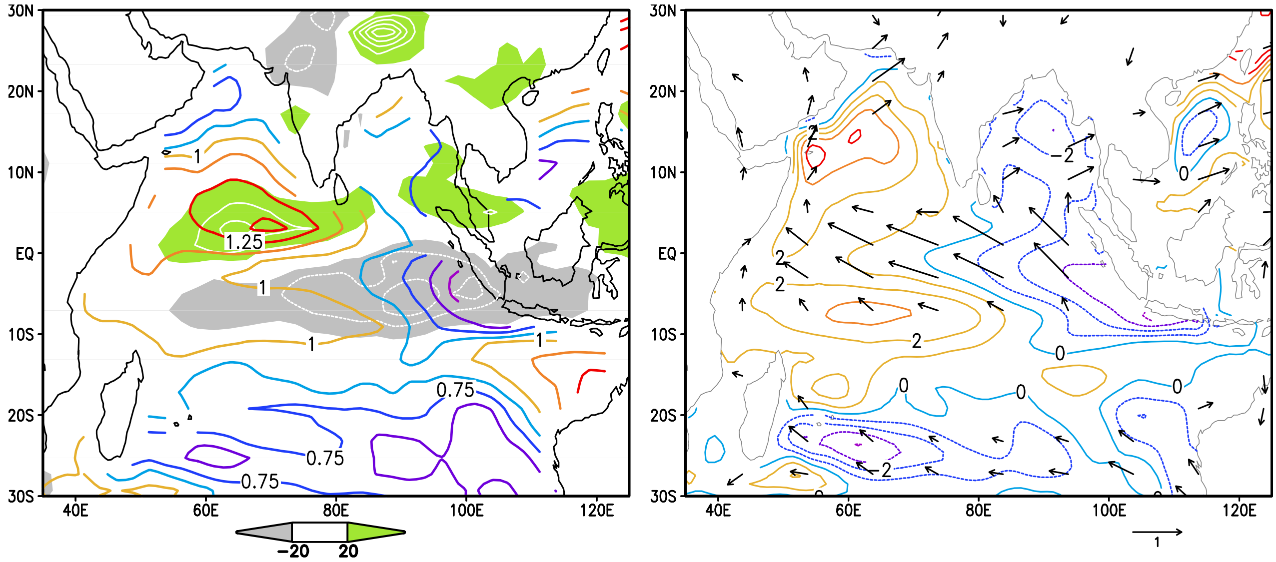

Figure 14.4: August-October changes in CM2.1 A1B: (a) SST (color CI=0.125°C) and precipitation (green/gray shade and white contours at CI=20 mm/month); (b) sea surface height (CI=1 cm) and surface wind velocity (m/s). [PLACEHOLDER FOR SECOND ORDER DRAFT: to be replaced with a CMIP5 RCP6.0 ensemble mean.]

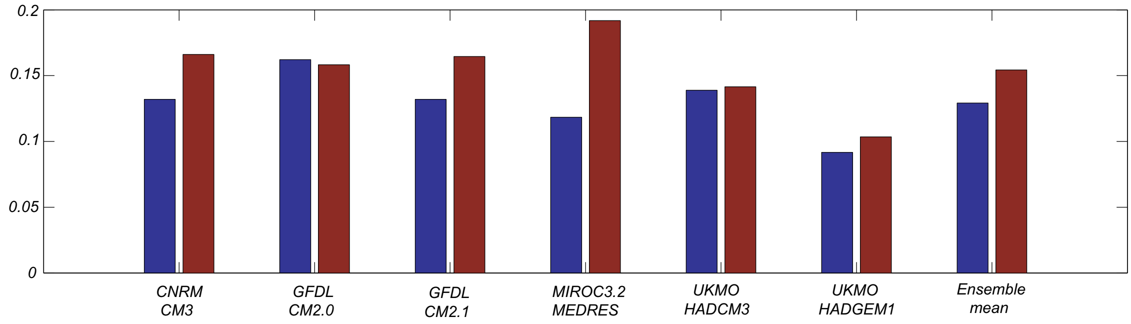

Figure 14.5: IOB persistence in the A1B projections by six CMIP3 models with good skills in the IOB simulation (Saji et al., 2006) he JAS(1) North Indian Ocean SST regression upon the Nino3.4 SST index in the 20th (1901–2000, blue bars) and 21st (2001–2100, brown bars) centuries. JAS(1) denotes the July-August-September season in the ENSO decay year. The IOB persistence increases in four and decreases in one model. [PLACEHOLDER FOR SECOND ORDER DRAFT: to be updated with CMIP5 RCP6.0 results.]

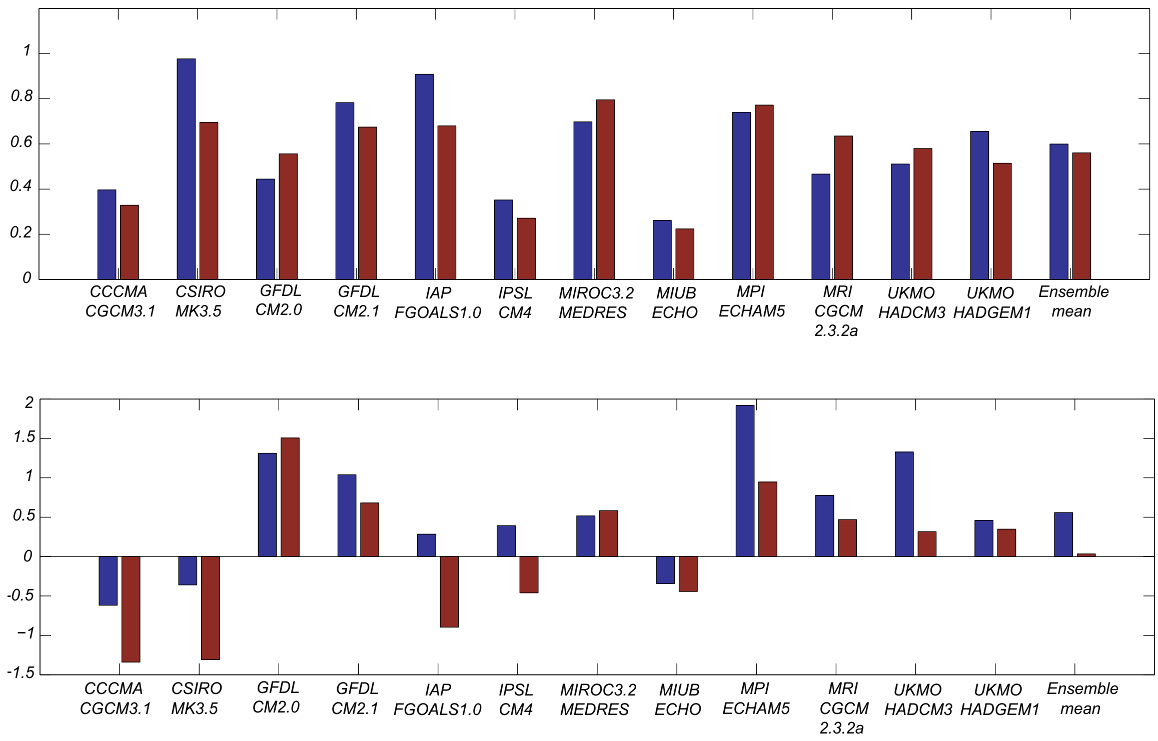

Figure 14.6: IOD change between the 20th century (1901–2000, blue bars) simulations and 21st century (2001–2100, brown bars) A1B projections by 12 CMIP3 models: (a) standard deviation, and (b) skewness of the September-November IOD index of (Saji et al., 1999). The amplitude change is small and inconsistent among models, increasing in five and decreasing in seven. The skewness decreases in nearly all the models. [PLACEHOLDER FOR SECOND ORDER DRAFT: to be updated with CMIP5 RCP6.0 results.]

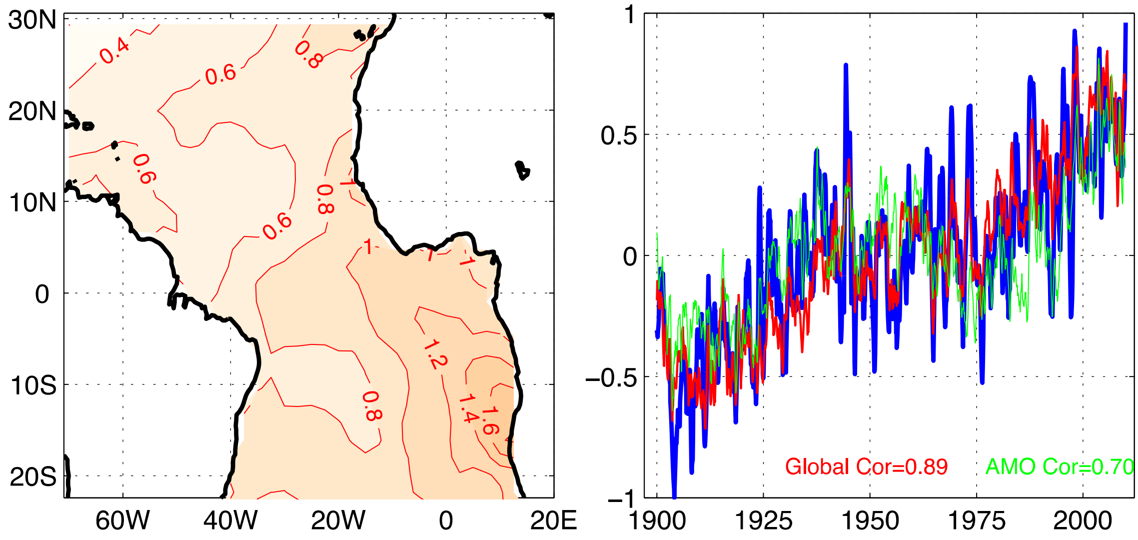

Figure 14.7: The leading EOF (left) of a gridded observed SST record from Hadley Centre sea ice and SST version 1 (HadISST1) data set (Rayner et al., 2003), which explains 36% of the SST variance, and the associated time series (right) normalized by its maximum absolute value (blue) overlaid by the globally averaged SST (red) and an AMO index derived by averaging the SST over the entire North Atlantic Ocean (green).

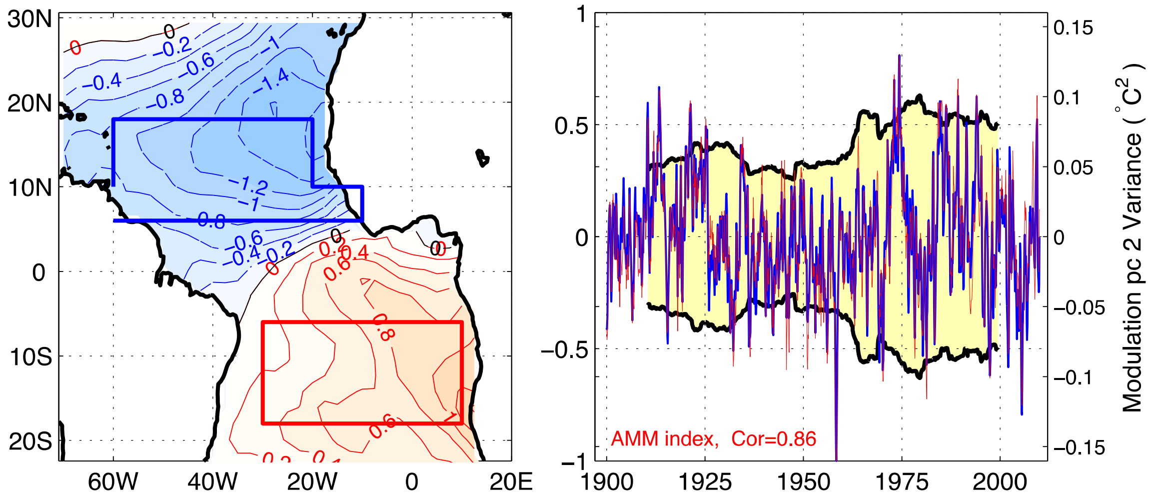

Figure 14.8: Same as Figure 14.7, except for the 2nd EOF (left), which explains 14% of the SST variance. The associated time series (blue in right panel) is overlaid by a detrended interhemispheric SST gradient index derived by differencing the SSTs averaged in the two boxes shown in the left panel. The two time series are correlated at r=0.86. The yellow shade and black lines show the amplitude modulation of the PC time series using a 21-year moving window.

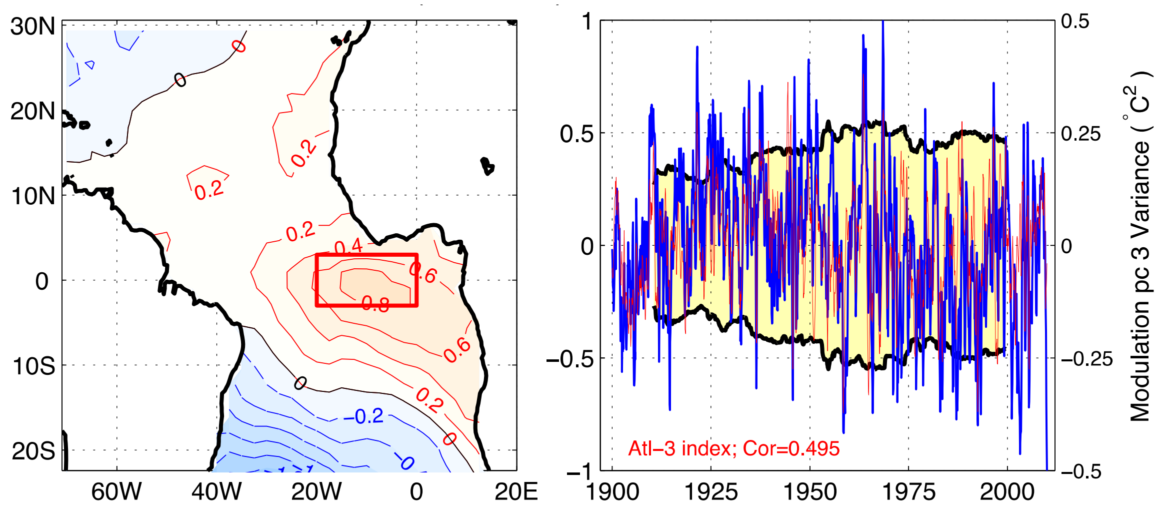

Figure 14.9: Same as Figure 14.7, except for the 3rd EOF (left), which explains 9% of the SST variance. The associated time series (blue in right panel) is overlaid by a detrended Atl-3 index derived by averaging the SST in the box shown in the left panel. The two time series are correlated at r=0.5. The yellow shade and black lines show the amplitude modulation of the Atl-3 index using a 21-year moving window.

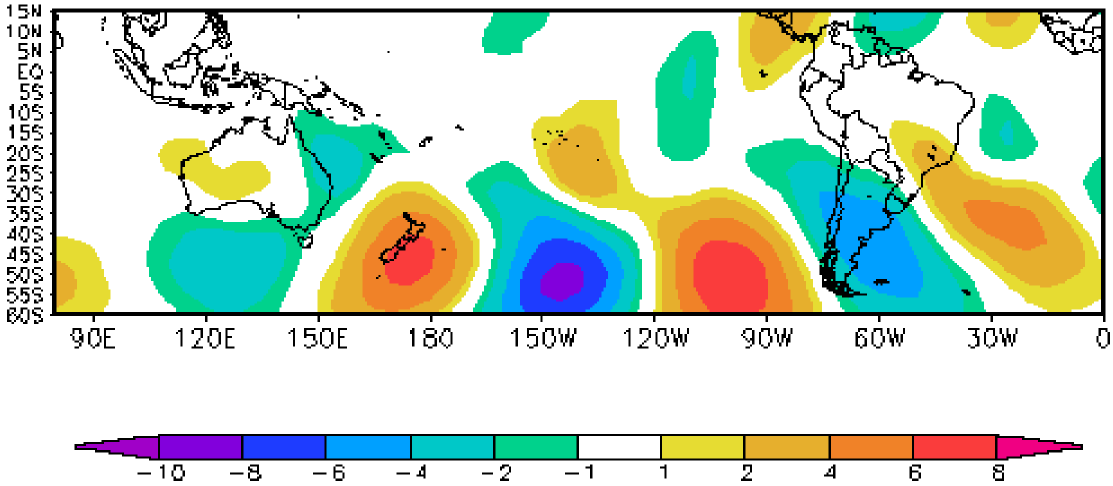

Figure 14.10: PSA pattern obtained from the First EOF of meridional wind, filtered in the 30–90 days band, period of November to March.

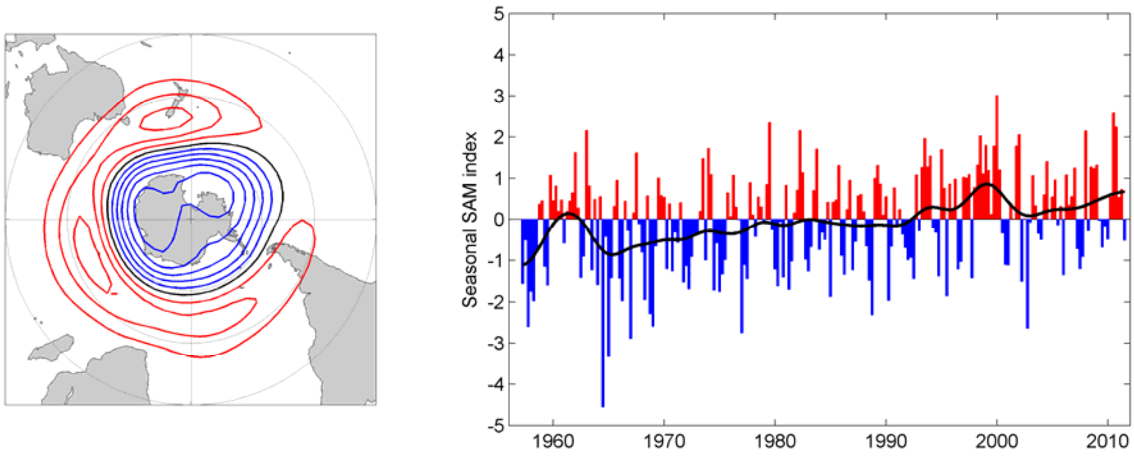

Figure 14.11: Left – the pattern of the positive SAM in the 500 hPa monthly height anomaly field (average height anomalies when the amplitude time series is +1 standard deviation). Positive contours are red, negative are blue and zero is black. The contour interval is 7.5 m. Right – the seasonal-mean amplitude of the SAM pattern, taken from station data (courtesy G. Marshall, British Antarctic Survey, www.nerc-bas.ac.uk/public/icd/gjma/newsam.1957.2007.txt). The black line illustrates the long-term trend.

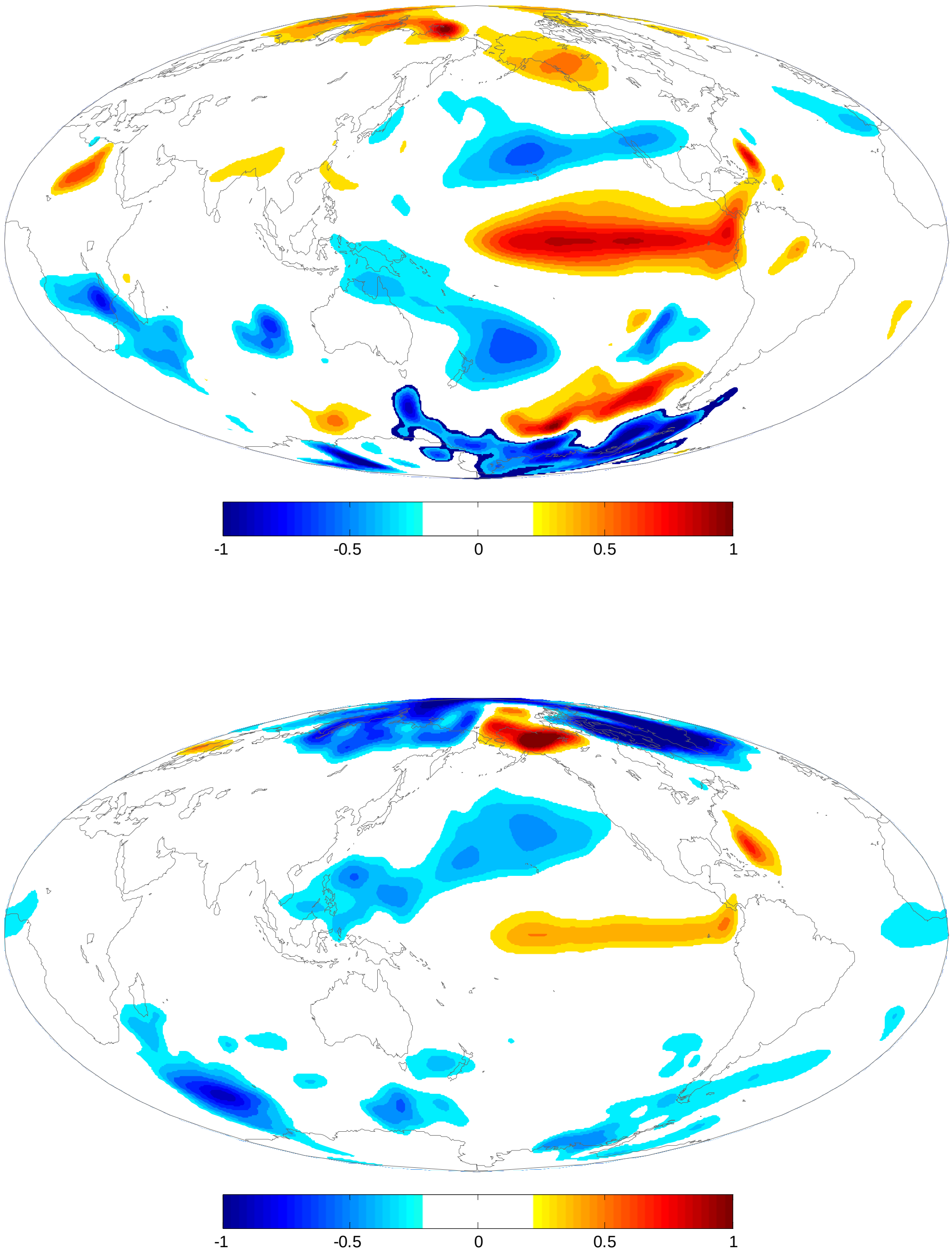

FAQ 14.1, Figure 1: Regional effects of El Niño upon surface temperatures, shown as the average temperature anomaly for an SOI value of -1 standard deviations. The top panel shows the temperature anomalies for December-February (northern winter) and the bottom panel for June-August (northern summer). Colours change every 0.5°C, with values with absolute value less than 0.25°C blanked out.